Journal of Advanced Transportation

Road Traffic Research in Smart City Transport Systems and Networks 2022

Lead Guest Editor: Elżbieta Macioszek
Guest Editors: Anna Granà, Chmielewski Jacek, and Tullio Giuffrè

Road Traffic Research in Smart City Transport Systems and Networks 2022

Journal of Advanced Transportation

Road Traffic Research in Smart City Transport Systems and Networks 2022

Lead Guest Editor: Elżbieta Macioszek
Guest Editors: Anna Granà, Chmielewski Jacek, and Tullio Giuffrè

Copyright © 2022 Hindawi Limited. All rights reserved.

This is a special issue published in "Journal of Advanced Transportation." All articles are open access articles distributed under the Creative Commons Attribution License, which permits unrestricted use, distribution, and reproduction in any medium, provided the original work is properly cited.

Associate Editors

Juan C. Cano, Spain
Steven I. Chien, USA
Antonio Comi, Italy
Zhi-Chun Li, China
Jinjun Tang, China

Academic Editors

Kun An, China
Shriniwas Arkatkar, India
José M. Armingol, Spain
Socrates Basbas, Greece
Francesco Bella, Italy
Abdelaziz Bensrhair, France
Hui Bi, China
María Calderon, Spain
Tiziana Campisi, Italy
Giulio E. Cantarella, Italy
Maria Castro, Spain
Mei Chen, USA
Maria Vittoria Corazza, Italy
Andrea D'Ariano, Italy
Stefano De Luca, Italy
Rocío De Oña, Spain
Luigi Dell'Olio, Spain
Cédric Demonceaux, France
Sunder Lall Dhingra, India
Roberta Di Pace, Italy
Dilum Dissanayake, United Kingdom
Jing Dong, USA
Yuchuan Du, China
Juan-Antonio Escareno, France
Domokos Esztergár-Kiss, Hungary
Saber Fallah, United Kingdom
Gianfranco Fancello, Italy
Zhixiang Fang, China
Francesco Galante, Italy
Yuan Gao, China
Laura Garach, Spain
Indrajit Ghosh, India
Rosa G. González-Ramírez, Chile
Ren-Yong Guo, China
Yanyong Guo, China
Jérôme Ha#rri, France
Hocine Imine, France
Umar Iqbal, Canada
Rui Jiang, China
Peter J. Jin, USA
Sheng Jin, China
Victor L. Knoop, The Netherlands
Eduardo Lalla, The Netherlands
Michela Le Pira, Italy
Jaeyoung Lee, USA
Seungjae Lee, Republic of Korea
Ruimin Li, China
Zhenning Li, China
Christian Liebchen, Germany
Tao Liu, China
Chung-Cheng Lu, Taiwan
Filomena Mauriello, Italy
Luis Miranda-Moreno, Canada
Rakesh Mishra, United Kingdom
Tomio Miwa, Japan
Andrea Monteriù, Italy
Sara Moridpour, Australia
Giuseppe Musolino, Italy
Jose E. Naranjo, Spain
Mehdi Nourinejad, Canada
Eneko Osaba, Spain
Dongjoo Park, Republic of Korea
Luca Pugi, Italy
Alessandro Severino, Italy
Nirajan Shiwakoti, Australia
Michele D. Simoni, Sweden
Ziqi Song, USA
Amanda Stathopoulos, USA
Daxin Tian, China
Alejandro Tirachini, Chile
Long Truong, Australia
Avinash Unnikrishnan, USA
Pascal Vasseur, France
Antonino Vitetta, Italy
S. Travis Waller, Australia
Bohui Wang, China
Jianbin Xin, China

Hongtai Yang, China
Vincent F. Yu, Taiwan
Mustafa Zeybek, Turkey
Jing Zhao, China
Ming Zhong, China
Yajie Zou, China

Contents

Hindawi
Journal of Advanced Transportation
Volume 2022, Article ID 7071279, 11 pages
https://doi.org/10.1155/2022/7071279

Research Article

A Fuzzy Ecosystem Benchmarking for Crowdfunding in Transport Sector

Gargi Pant Shukla,[1] Santosh Kumar,[2] Mukesh Kumar,[3] Ankit Kumar,[4] and Manoj Chhetri[5]

[1]*Doon Business School, Dehradun, India*
[2]*Jaipuria Institute of Management, Jaipur, India*
[3]*Institute of Business Management, GLA University, Mathura, India*
[4]*GLA University, Mathura, India*
[5]*Royal University of Bhutan, Phuntsholing, Chukha, Bhutan*

Correspondence should be addressed to Manoj Chhetri; manoj_chhetri.cst@rub.edu.bt

Received 12 May 2022; Revised 19 May 2022; Accepted 1 August 2022; Published 16 September 2022

Academic Editor: Elżbieta Macioszek

Copyright © 2022 Gargi Pant Shukla et al. This is an open access article distributed under the Creative Commons Attribution License, which permits unrestricted use, distribution, and reproduction in any medium, provided the original work is properly cited.

The global crowdfunding (CF) market was valued at 10.2 billion US$ in 2018 and is expected to almost triple in size by 2025. The CF is evolving as a major and easy source of fundraising methods for various industries. Still, this acceptability is not widely accepted in transportation activities due to various limitations and low awareness among policymakers. The present research analyzes the factors contributing to the growth of market acceptability of CF, divided into three different research phases: identifying barriers from the literature, interviews with transport industry experts at two stages, and designing an ISM model in a fuzzy environment. The identification phase led to selecting 16 factors from the past literature and suggesting industrial experts. The Interpretive Structural Modelling (ISM) analysis was used to understand the impact and linkage of identified barriers on seven levels of the fuzzy scale. The factors are classified into four major categories based on the fuzzy matrix's drive and dependence power using Fuzzy MICMAC. The sixteen identified growth factors for CF have been distributed in 5 levels in the ISM designed model. All the factors had fallen in only two quadrants of MICMAC based on the fuzzy scale matrix. Except for No or Low in regulation, the selected fifteen factors fall in the linkage quadrant, with high dependency and driving power. Such relation of all variables is the precise reason for storm growth in the field. "No or Low in regulation" is one of the most significant factors to the growth and acceptance of this innovative fundraising method by common investors but cannot be controlled directly by the associated crowdfunding members in the transport industry.

1. Introduction

In recent years, crowdfunding has become an important elective funding source looking for outside financing. Crowdfunding is a term portraying a new twist on generally old fundraising methods. Existing empirical investigations report huge growth in fundraising volume through crowdfunding (CF) worldwide. The success story of CF in the transportation industry is well known; in a recent year, a Germany based start-up launched a high-speed train, Locomore, with the help of CF sources. The company sourced over €231,000 in the first phase and €460,000 in the second phase of fund sourcing in 2016 to launch its Stuttgart-Berlin rail service. Through crowdsourcing, Commuter Club, UK's independent train season ticket retailer and finance provider, has raised more than £2.2 m in 2019 (source: rail technology). The current condition of the COVID pandemic has created a very conducive environment for the growth of CF. Many of us used the CF platform for help with medical bills, funeral expenses, lost wages, small business support, food assistance, and other needs. COVID-related fundraising activities increased exponentially after March

2020 on platforms such as GoFundMe [1]. The Ph.D. thesis work of Soto [2] highlights various aspects of crowdfunding-based transportation infrastructural projects along with their implementation and policies.

Crowdfunding is an umbrella term that refers to an increasingly widespread form of fundraising where individuals pool their money, usually smaller contributions by individuals to achieve a particular goal. However, attention toward crowdfunding by many investors, policymakers, founders, and regulators has increased its mechanisms and dynamics in general, and equity crowdfunding, in particular, is not yet well understood [3].

The concept of crowdfunding can be traced back to the nearer broader concept of crowdsourcing, which uses the crowd to get the solution, ideas, and feedback concerning the progress of corporate activities [4, 5]. The primary motive of crowdfunding is to collect funds for some specific projects or functions, typically by using social networks online, usually, a small sum of individual contributions, to provide financial support to an effort by a fundraiser to attain a specific goal. Such investment may create different forms of obligations, like equity, loan, donation, and even advance payment of an order for future buying [6–9]. Crowdfunding provides unparalleled efficiency of capital creation, mainly to start-ups.

Because CF differs from standard fund sourcing methods, it can help businesses raise financing at an early stage of development. Even if the company is liquidated, CF creates a differential right on its assets. Unlike traditional fundraising approaches, even very successful crowdfunding fundraising does not necessitate the involvement of a financial institution as underwriters, which further reduces the related fees involved in the fundraising. Therefore, fundraising expenses in CF become lower than conventional fundraising methods in the absence of cumbersome regulatory procedures, constraints, and paperwork. The crowdfunding market is relatively new and complex for average business houses. The global crowdfunding market was valued at $12.27 billion in 2021 and is expected to almost triple in size by 2025. Possibly, the crowdfunding approach is going to be the future of fundraising in finance markets. Also, the cost of raising funds through IPOs is comparatively much higher. It differs from other funding sources due to varied relationships between funders and fundraisers by goals, context, and fundraising efforts [10].

Although CF has piqued the interest of academics and professionals, there are relatively few structural works of the literature on the subject, primarily to examine the facilitators and determinants in the rise of CF in the transportation industry. This paper is one of the early attempts to investigate growth determinants and the different fundamental features of the potential underlying structure of CFs, known as their "detailed investment realities." Developing economies, such as India, are still battling to recover from the financial shocks caused by the 2008 global crisis. Any errors in fundraising methods such as crowdfunding may raise concerns about sustainability. Sustainability is one of the major areas of concern in such a high growth economy. An increasing flow of finance from national and foreign sources is the key to achieving such economic sustainability. Crowdfunding (CFs) is evolving as one of the most preferred vehicles of fund mobilization.

It becomes crucial to study the factors and their importance contributing to the growth of CF. Many of these factors and their association with management education have been studied mainly in isolation. The research methodology is the backbone of a research study; the methodology explains the structured way of solving problems, achieving objectives and the validity of the result. The current study falls under the quantitative domain of research [11]. Hence, this study is designed to determine the factors affecting the growth of CF in the long run. This paper is one of the preliminary attempts to study the mutual relationship among all the elements in the development of CF. The primary objective of this paper is to rank the barriers based on their dominance. Then, an analysis would attempt to understand the mutual imperative relationship of all selected factor barriers to developing a sustainable market for CF. The Interpretive Structural Modelling (ISM) model in the FUZZY environment designed on expert opinions has been used as a research methodology. The study is an attempt to make some incremental contributions which are as follows:

(i) Defines the impact of each factor in the system of elements on CF.

(ii) Applies the in-depth understanding of the judgmental sample of experts and generates an acceptable framework for the academics, policymakers, and industry.

(iii) Uses the mathematical explanation of Interpretive Structural Modelling (ISM) and "Matrices d'Impacts Croises Multiplication. Appliqué a UN Classement" (cross-impact matrix multiplication applied to classification) (MICMAC) in a fuzzy environment to attain new perceptions about the factors on CF.

Accordingly, the research objectives (RO) and research questions of this study are as follows:

RO1: to explore and identify the enablers of crowdfunding (CF), mainly in the transport sector

RO2: to propose an integrated fuzzy ISM-MICMAC decision-making framework to assess and benchmark the CF

The following research questions (RQ) have been framed to achieve the above-cited objectives:

RQ1: what are the critical dimensions and enablers of the CF?

RQ2: how does the mutual interaction of enablers of CF play a significant role in industry and business houses?

RQ3: how can a systematic framework help assess the severity of each enabler in a fuzzy environment?

The main purpose of the research is to highlight the factors of CF, a technology-driven financing activity, in the growth of the transportation industry. The CF is evolving as

a major and easy source of fundraising methods for various industries. Still, this acceptability is not widely accepted in transportation activities due to various limitations and low awareness among policymakers.

The paper is divided into the following sections: Section 1 provides an introduction and understanding of crowdfunding, including the risk and economy of CF, Section 2 provides a review of previously published literature related to the study, and Sections 3 and 4 provide an outline of the research structure. Sections 5 and 6 describe the questionnaire and ISM application construction, followed by fuzzy computation. Section 7 has a discussion of the findings. Section 8 addresses recommendations and applications, while Section 9 discusses limitations and future research opportunities.

2. Literature Review

2.1. Literature on the Enablers of CF. The study domain of CF is relatively new in finance, so it is no surprise that the associated literature is only in the emerging stage. The government's lack of support and incentives is the main reason behind the lack of awareness about crowdfunding in India. Mass research, transparency, feasibility, convenience, goal orientation, and reward lead to investment in crowdfunding [12]. Non-investor-friendly, low trust, credibility, transparency, and awareness are some challenges for crowdfunding in India [13]. Underlying project quality and personal networks are the critical components associated with the success of crowdfunding and the projects which are geographically related to both types and have successfully raised funds [14]. Investors who have a personal connection with friends and family have more driven the geographic effect. However, the online platform has eliminated the distance-related problems like data gathering information, and the social-related frictions are still not eliminated by the technology [15]. Referring to the economic model of "multi-side platforms," a theoretical framework for crowdfunding websites was proposed, classifying projects according to the objectives of crowd funder and initiator. Four different typologies such as business, cooperation, patronage, and donation were pointed out by them [16]. Three types of investment opportunities, that is, donations, passive investment, and active investment, are offered to potential investors to finance a project under crowdfunding. Active investments are more related to equity than passive investments related to debt [17].

The early schema of the inner working of crowdfunding is presented, and the social entrepreneurship context was discussed, which shows the matchmaking process between the venture, offering debt or equity investments, and the crowd [18]. Currently, crowdfunding is an infant [9].

To reach the target fund, individual social capital has a significant positive effect, whereas geolocalized capital has no significant effect [19]. Portals prefer fewer disclosure requirements and fewer restrictions on the free trading of crowdfunded shares, whereas start-ups prefer fewer restrictions on the ability to crowdfund. However, more disclosure, limits on amounts entrepreneurs can raise, and lower thresholds for audited financial statements are demanded by investors [20]. The entrepreneur's reputation affects capital formation outcomes favourably in terms of both degree and speed. The capital formation depends on the entrepreneur's reputation rather than on funder characteristics, project characteristics, or timing of backing. This becomes important as more financial institutions rely on nontraditional social media data to make funding decisions [21]. Projects in the field of transport and transport support are creating huge funds by CF across the globe, which is better than other traditional sources of funds [2]. Crowdfunding is becoming an easier source of fundraising for big and capital intensive transport-related projects and infrastructure [22].

2.2. Literature on the Traditional Fundraising Methods. IPOs investment is generally treated as low-hanging fruits by the investors. If investors get allotment in IPOs and sell these stocks on the listing, they get returns better than the going market. Generally, IPOs are underpriced compared to their listed peer group companies [23]. The uninformed retail investors might undergo a winner's curse problem" by making all their allocation in IPOs [24]. IPOs are used as a short-term investment avenue to get maximum return, as they are generally available at a comparatively low price [25]. IPOs can be a good source of return, as generally, they are underpriced, as observed using a signalling model with two signals and attributes [26, 27]. Investment in IPOs in the period 1970-1990 failed to give an expected return in the long run [28]. IPOs are preferred investment tools due to their guideline and transparency of book building [29].

Many kinds of literature support different reasons for IPO pricing under various market conditions (Baron [30]; Muscarella and Vetsuypens [14]; Welch [31, 32]; Allen and Faulhaber [33]; Chemmanur [34]; Michael and Shaw [35]; Koh and Walter [36] Hughes and Thakor [37]; Drake and Vetsuypens [38]; Lowry and Shu [39]; Boehmer and Raymond Fisher [40]; Krigman et al. [41]; Ellis et al. [42]; Booth and Chua [43]; Bubna and Prabhala [44]; and many more).

3. Literature on the Suitability of Methodology

Interpretive Structural Modelling (ISM) is a ranking system of directly or indirectly connected factors in a complete methodical model. The model shows the systematic ranking of factors in a multilevel structured pattern of graphs and statements using opinions from various experts. The structural model inflicts relative direction and ranking of selected factors even for a multifarious system to provide a clear insight to regulators and policymakers [45, 46].

The ISM technique is used to study inter-relationships among identified factors on vendor selection in supply chain management [47–49]. The ISM ranking method has been used to classify factors to execute knowledge management schemes in manufacturing and other production-based industries [50]. The study used the ISM technique to form a multilevel, hierarchy process model for factors required to implement an optimal waste management project [51]. The

concept of ISM methodology has been used to establish a relationship matrix of selected elements for the conservation and management of energy in the cement manufacturing plants [52]. The ISM methodology is used to select and offer a relative position of the factors for the reverse logistics selection process in SCM of the hardware business. The study suggested a relative ranking of barriers [53]. The ISM technique has been used to rank 11 selected key barriers and establish a relative matrix in the implementation of reverse logistics in the automotive industry [54]. The hybrid ISM and ANP are used to find interdependence and feedback relationships in subsystems by multidimensions and scaling techniques in the Chinese industry [55]. The ISM methodology has been used to address issues in green suppliers in the automobile sector [56, 57]. The ISM was applied to established relations among the elements influencing the supplier selection for the built-in-order industry [58]. Further, the ISM ranking model is upgraded by an amalgamation of fuzzy TOPSIS (the Technique for Order of Preference by Similarity to Ideal Solution) as a fusion approach for ranking factors in the area to identify the third-party reverse logistics suppliers [59]. The ISM is also used to sort out problems in the knowledge management system [60]. The ISM is also used to sort out problems in the healthcare sector [61]. The research-based is on a structured ISM method to get the mutual involvement of identified enablers in implementing a flexible manufacturing process [62]. The ISM is also used in finance and investment decisions, an article to sort out problems in retirement planning [63]. ISM model is used to identify the factors of knowledge management [50, 60, 64], literature surveys, [65–67], and many more that have summarised the works of literature published based on ISM model and other hybrid ISM models in different industries.

Many kinds of literature studies based on ISM and hybrid ISM are available related to the studies in different disciplines. However, there is a lack of work carried out on applying this method to evaluate crowdfunding enablers. With the growth of CF and other similar fundraising methods, the industry's sustainability and transparency are critical issues before regulators. The regulators have to understand the factors of the growth of such a new virtual financial system for the betterment and safety of the investors. Very few pieces of the literature have studied accelerators in the area. This study aims to fill the gap and analyze mutual relationships among all the factors in the way of the growth of the CF market. The sixteen factors based on available literature and views from the experts from industry and academia are found as shown in Table 1. The selected decision-making methodology has been used on these identified factors to rank them as per their importance.

4. Research Methodology

The current section is based on paradigm, sampling, and instrument development process to solve the identified problem in a structured way [72]. Due to start-ups' high demand for capital in recent years, CF has received a high concentration level in the last few years. Many existing companies have also joined the race of CF to raise additional funds for their running business. Dint of not much support from regulatory bodies of many countries, the growth rate in the segment has been more than 80% in the last 4 years. Identification and ranking of factors in the growth of CF are the study's central problems.

The ISM in a fuzzy environment has been used to rank the identified accelerating factors. Below mentioned steps are involved in the ISM methodology as explained by Reference [59].

The following steps are shown in the form of the flow chart in Figure 1. The growth of CF involves factors of micro as well as macro levels. The major factors include no geographic restrictions, low cost of issue, high finance literacy, and many more. As shown in Table 1, sixteen factors for study are gathered from past published works of the literature and opinions from experts; Algorithm 1 shows the ISM in a fuzzy environment.

5. Formation of the Questionnaire

The growth path of CF is way different from other traditional capital market tools, as they have different mechanisms from traditional funding. The major objective of the study is achieved by ISM, a tool for better communication in such complex situations. We have selected 12 factors from previous works of the literature, and 4 are added by discussion from the experts. These experts are senior professionals and persons in academia from various colleges with expertise in technology-driven fundraising activities in the capital market. These experts were chosen in the individual capacity of researchers from various locations across India with a minimum experience of 10 years in academics and at least 7 years in the industry. Initially, 35 experts were selected and approached, but only twenty participated after regular communication. The twelve experts were from academia, and eight experts were from the transportation and logistics industry.

All individual responses were collected from experts at two stages and sent to two experts, one from academia and the other from industry, in a consolidated form to get the final response. Finally, one consolidated response matrix has been formed based on all these collected responses and brainstorming sessions.

6. Application of ISM

The ISM methodology starts with creating SSIM (structural selfinteraction matrix). This matrix is a planned presentation of contextual connection of selected factors based on expert opinion.

We use four symbols to show the pairwise directional relationship between the factors, say I and j; symbol "V" is used to indicate factor I will support to achieve factor j, symbol "A" indicates factor j will support in the achievement of factor I, symbol "x" indicates factor j and I will help to achieve each other, and "o" symbol indicates no relation between both factors. The SSIM for the selected factors in the growth of CF is given in Table 2.

The reach-ability matrix is formed from data collected in SSIM, by changing the information of each cell into either 1 or 0 in the matrix, according to the rules as follows:

Table 1: Description of CF barriers.

Sr.no.	Barrier	Description	Supported pieces of the literature
1	No or Low time requirement	CF can collect money in less time, even less than an hour, in many cases	By expert
2	No or Low in regulation (NLR)	CF neither fall under income tax law nor the security act in most of the countries	[13]
3	Low in cost	Issue costs are significantly less in comparison to traditional fundraising methods	[13]
4	No geographic restrictions	There is no restriction on a country as work on the digital platform. CF can get investment from anywhere	Agrawal et al. [68]
5	Usage of unaccounted money	Some platforms do allow investing unaccounted money into the cryptocurrency channel	By expert
6	Lack of access to funding for start-ups	Start-ups cannot raise funds in the form of an IPO	Sanchez [69]; Cumming et al. [70]
7	Inability to generate funds through IPOs or any other traditional route	Many companies and firms are not fit for generating funds through IPOs because of their long business history	Cumming et al. [70]
8	High level of competition in the traditional financial market	Traditional markets are well known to everyone, so there is a massive rush in the market for fundraising	Cumming et al. [70]
9	Heavy dependence on banks and other investment bankers to raise funds from public	Banks and networks of financial institutions dominate the traditional method of fundraising	Kuppuswamy and Bayus Barry [9]
10	High growth of IT and digital awareness	Digital awareness acts as a platform for the spread of such avenues	Sanchez [69]; Cumming et al. [70]
11	Supportive external environment	Current external factors are supportive enough to digest such innovative ideas	Sanchez [69]; Cumming et al. [70]
12	High level of financial literacy	Financial literacy has increased by many folds in the last few years, mainly in the urban population	Sanchez [69]; Turan [71]
13	The innovative structure of CF	CF under a regulatory environment is backed by certain tangible assets and increases the confidence of investors	Sanchez [69]; Cumming et al. [70] https://www.fundstiger.com
14	The greediness of investors for more return	Investors always look to get more and more returns in a short period	By expert
15	A small amount of investment (even US$ 1 can be invested)	Even a small amount, as low as 100 US$, can be invested through the CF platform	Sanchez [69]; Cumming et al. [70]; Turan [71]
16	Lack of developed stock exchanges or other fundraising infrastructure	Many countries are lacking in the infrastructure of fundraising, where CF is the only option to raise fund	By expert

(i) if the cell value in the SSIM is V, it converts into 1 and 0 in the reach-ability matrix for the (i, j) and the (j, i), respectively

(ii) If the cell value in the SSIM is A, then it converts into 0 and 1 in the reach-ability matrix for the (i, j) and the (j, i), respectively

(iii) If the cell value in the SSIM is X, then it converts into 1 and 1 in the reach-ability matrix for the (i, j) and the (j, i), respectively

(iv) If the cell value in the SSIM is O, then it converts into 0 and 0 in the reach-ability matrix for the (i, j) and the (j, i), respectively

The reach-ability matrix after required transitivity is formed and shown as BDRM (binary direct relationship matrix) is presented in Table 3.

The reach-ability and antecedent set for each factor are considered from the final reach-ability matrix, as shown in Table 3 (Warfield, 1974). The reach-ability set of an element consists of the factor itself and the other elements which may support achieving, that is, all factors with value 1 in the row. Correspondingly, the antecedent set of an element is a combination of the element itself and the other elements, which facilitate achieving it, that is, all factors with value 1 in the column. The intersections of both reach-ability and antecedent sets are calculated, and factors with equal intersection values are ranked at the top in the hierarchical model of ISM. Afterwards, the levelled factors are eliminated from another remaining set of factors. Level identification processes of all sixteen considered factors are completed in five iterations, given in Table 4. The calculated hierarchy levels of these selected factors form the digraph as the final level of ISM. The structural digraph is created from the iterations, as shown in the figure. Arrowheads show the connection between the factors, from factor I to heading towards j.

MICMAC, that is, (Matrices d'Impacts Croises Multiplication. Appliqué a UN Classement) "cross-impact matrix multiplication applied to classification," is calculated on the

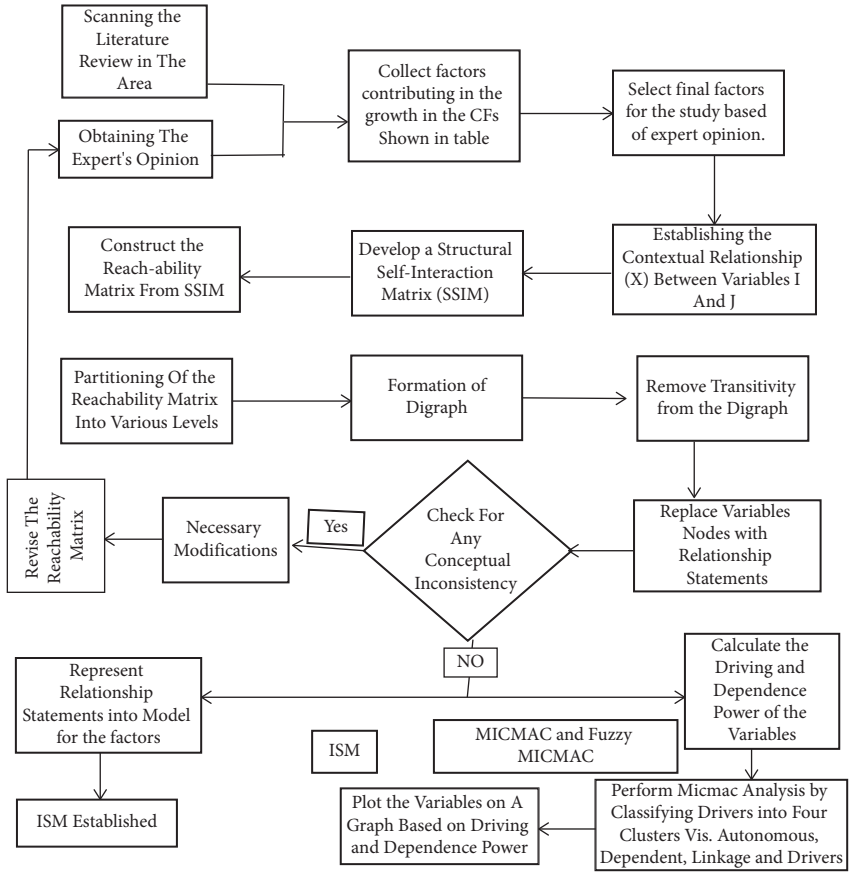

Figure 1: Flow diagram for preparing the ISM model.

Input. List of all the factors.
Output. ISM structure for crowdfunding.
Step 1. List out all the factors to be considered in the study.
Step 2. A contextual connection is recognized among all the identified variables in step 1 for pairwise examination.
Step 3. An SSIM, structural selfinteraction matrix for pairwise relationships among variables, is developed.
Step 4. A reach-ability matrix is developed and checked for transitivity. The transitivity relation among variables is a fundamental hypothesis made in ISM. If element A is associated with element B and B is connected to C, then A is linked to C.
Step 5. The reach-ability matrix is partitioned into different levels to form initial relationship matrix (IRM).
Step 6. A directed graph is drawn by the removal of transitive links based on association found in the reach-ability matrix to form final relationship matrix (FRM).
Step 7. The resulting digraph is transformed into an ISM.
Step 8. The developed ISM model of the previous step is reviewed and checked for "conceptual inconsistency." Some essential modifications can be made as required.
Step 9. The MICMAC and Fuzzy MICMAC analyses are performed to classify all factors in four broad clusters to check the consistent association.

Algorithm 1: ISM in a fuzzy environment.

principle of matrices multiplication [49]. A fuzzy set theory is being used to enhance the responsiveness of MICMAC analysis to come out from the limitations of the ISM model. This technique is called Fuzzy MICMAC, where an additional input for the dependencies between relationships of barriers is being introduced [73]. Further, to draw Fuzzy MICMAC (FMICMAC), data from the same selected expert should be recollected to convert data of BDRM into FDRM (fuzzy direct relationship matrix). FDRM has been derived from the final BDRM, and the used fuzzy sets are described as membership functions with an actual unit interval [0, 1]. A 7-point scale has been used for this fuzzy evaluation, as shown in Table 4.

The expert opinion has been gathered from the same expert panel with ratings for obtaining a direct reach-ability matrix. A triangular fuzzy number "U" is represented as a triplet set (x, y, and z). The triangular fuzzy function is

Table 2: Structural selfinteraction matrix (SSIM).

	16	15	14	13	12	11	10	9	8	7	6	5	4	3	2	1
1	O	O	V	V	O	X	A	A	O	O	A	O	A	O	O	X
2	V	V	V	V	O	X	O	V	V	V	V	X	O	V	X	
3	A	X	V	A	O	O	A	X	V	O	O	X	O	X		
4	O	O	O	A	O	A	A	X	V	V	V	V	X			
5	A	O	V	A	O	A	A	O	O	O	V	X				
6	X	O	O	V	O	A	O	V	O	X	X					
7	X	O	O	A	A	V	O	V	X	X						
8	X	O	O	X	O	O	X	V	X							
9	X	A	O	O	O	X	O	X								
10	O	O	O	X	O	X	X									
11	V	A	O	X	O	X										
12	X	O	O	V	X											
13	O	V	X	X												
14	O	A	X													
15	O	X														
16	X															

Table 3: Reach-ability matrix after transitivity.

	1	2	3	4	5	6	7	8	9	10	11	12	13	14	15	16
1	1	0	1	1	0	0	0	0	0	0	0	0	0	0	1	1
2	0	1	0	1	1	0	0	1	0	1	0	0	0	1	0	0
3	0	0	1	1	1	0	0	0	0	0	0	0	0	0	1	0
4	0	0	0	1	1	0	0	0	0	0	0	0	1	1	0	0
5	0	1	0	1	1	1	0	1	0	1	1	0	0	1	0	0
6	0	0	1	0	1	1	1	1	0	1	0	0	0	1	1	0
7	1	0	1	1	0	1	1	0	1	0	0	0	0	0	0	0
8	0	0	0	1	1	0	0	1	0	0	1	0	0	1	0	0
9	1	0	1	0	1	0	0	1	1	0	1	0	1	0	1	1
10	0	0	0	1	1	0	0	1	0	1	1	1	1	1	0	0
11	1	0	1	1	1	0	0	1	0	1	1	0	0	1	0	0
12	0	0	0	1	0	0	0	0	0	1	1	1	0	0	0	0
13	1	0	0	1	1	0	0	1	0	1	1	0	1	0	0	0
14	0	0	0	1	1	1	0	1	0	1	1	1	1	1	0	0
15	1	1	1	1	1	1	0	1	1	1	1	1	0	1	1	0
16	1	0	1	0	0	0	0	0	0	0	0	0	1	1	0	1

Table 4: 7-point fuzzy scale used in the calculation.

Possibility of reachability	No	Negligible	Low	Medium	High	Very high	Full
Triangular value	(0, 0, 0)	(0, 0.1, 0.3)	(0, 0.3, 0.5)	(0.3, 0.5, 0.7)	(0.5, 0.7, 0.9)	(0.7, 0.9, 1)	(1, 1, 1)

expanded by using a lower limit value (x), a median value (y), and an upper limit value (z), where $x < y < z$. These points signify the coordinates of three vertices of μ (U) in fuzzy set U. For better representation, defuzzification of the collected result on the fuzzy scale is to be performed to get a crisp number for the FDRM. The best nonfuzzy performance (BNP) value has been achieved by using the parameters of

$$\mathbf{BNP_{ij}} = \left[\frac{(\mathbf{z}-\mathbf{a}) * (\mathbf{z}-\mathbf{b})}{3}\right] + \mathbf{z}. \quad (1)$$

The FDRM's power is calculated by using principle-based on fuzzy matrix repeatedly multiplication rule, ($C = \max k \{\min (i, j)\}$) till it is converged. The convergence point can be determined where the driving and dependence powers of selected factors are stabilized or cyclic in their variation with a certain periodicity.

The main idea of FMICMAC is to find the driving and the dependence power of barriers selected in the study by plotting a graph with driving power along the Y-axis and dependence power along the X-axis. The barriers have been categorized into four different categories based on their power; the different categories are as follows:

(i) quadrant I: autonomous category: these factors are weak in both dependence and driving powers, and they usually are disjointed from the structure.

(ii) Quadrant II: dependent category: these factors have high dependence power but low driving power.

Table 5: Dependence power and driving power for factors based on stabilized FDRM.

Factor	Dependence power	Driving power	Factor	Dependence power	Driving power
1	14.2	10.3	9	13.3	11.4
2	2.5	13.9	10	8.6	12.7
3	12.5	8.5	11	9.1	12
4	12.2	11.6	12	8.5	12.1
5	11.3	10.3	13	11	11
6	13.4	10	14	11.7	12.3
7	13.4	11.5	15	9	8.5
8	13.3	11	16	13.3	11.3

(iii) Quadrant III: linkage category: these factors are weak in both dependence and driving powers. They are the most critical factors and have a very high impact on the system. A slight change in these factors has a direct impact on others.

(iv) Quadrant IV: independent category: factors of this quadrant have high driving power but less dependence power.

The categorization of factors used in the study was carried out by using MICMAC and FMICMAC analyses. The analyses are performed based on driving and dependence powers calculated based on expert opinion. All factors' driving and dependence power after stabilization in a fuzzy environment are given in Table 5. A complete integrated model for ISM of these identified factors with 5 levels is given in Figure 2, with factor number 2, that is, "No or Low in regulation," at the base level. Factors 13 and 14, "Innovative structure of CFs" and "Greediness of investors for more returns," are on the top level in a hierarchy with maximum dependency power. These identified factors are distributed in only two quadrants of the FMICMAC graph. The explanations of the outcome are discussed in Section 6; as a result, discussion. Figure 3 shows the diagram of Fuzzy MICMAC on dependence and driving powers of factors.

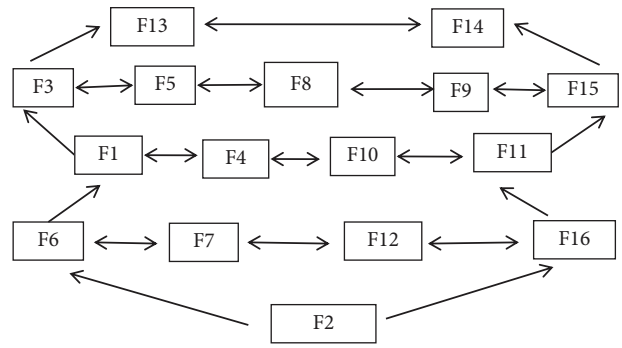

Figure 2: ISM-based model for barriers.

7. Result Discussion

While the growth of CF is undeniably rapid, their lack of recognition among ordinary investors is a major source of concern for their long-term viability. Closing such gaps is crucial if crowdfunding is considered a credible alternative to traditional fundraising methods for larger transportation infrastructure projects. The market's recent exponential growth has created strong connections with other economic sectors, especially start-ups. These organisations exert pressure on regulators to enact the proper legal frameworks to guarantee long-term viability. It is not easy to create such a legal structure; many factors affect how it is integrated into day-to-day business operations. Without first learning the facts about these variables, no one can guarantee a sustainable structure. The objective of the current work was to identify parameters related to CF in a fuzzy environment using a well-established ranking technique. The components used in this study were taken from published literature and expert input and are based on the ISM modelling approach in a fuzzy environment. In order to show how the variables relate to one another, a structure based on the ISM model is developed. Then, a description of the goal is given before inputs from the chosen experts are gathered in two stages, initially on a binary scale and then on a fuzzy scale. Finally, MICMAC developed a graph based on driving power on the y-axis and dependence power on the x-axis. Fuzzy MICMAC analysis elucidates elements' relative meaning and interdependence in great detail.

Although the study is unique in various aspects and seems to be a primary attempt by authors to highlight CF in transportation, still the finding has some similarities with past research conducted in different industries; Agrawal et al. [6] explained the geographical factor of CF and Aitamurto [74] judged CF in journalism and Brabham [75] in public arts. All variables that accept "No" or "Low" as regulatory thresholds fall within quadrant III. There are linkage variables with a high degree of dependant power and a high degree of driving power. These elements exert a significant influence on the system. They significantly impact the system, as each act directly affects others. The fact that most elements fall into this group helps explain the meteoric rise in the popularity of CF. All of these aspects contribute to the acceptance of CF as a novel and unique technique of fundraising. Regulation is the only factor in quadrant IV; it generally moves independently of other system elements. The industry's players have no direct control over the factor.

Although the lack of or low regulation is crucial in the growth and adoption of this novel way of fundraising by regular investors, it cannot be managed directly by the CF industry's connected members. Certain elements, such as "high financial literacy," maybe a positive force in some regions of the world while functioning as an opposing force in a sizable portion of the emerging economy.

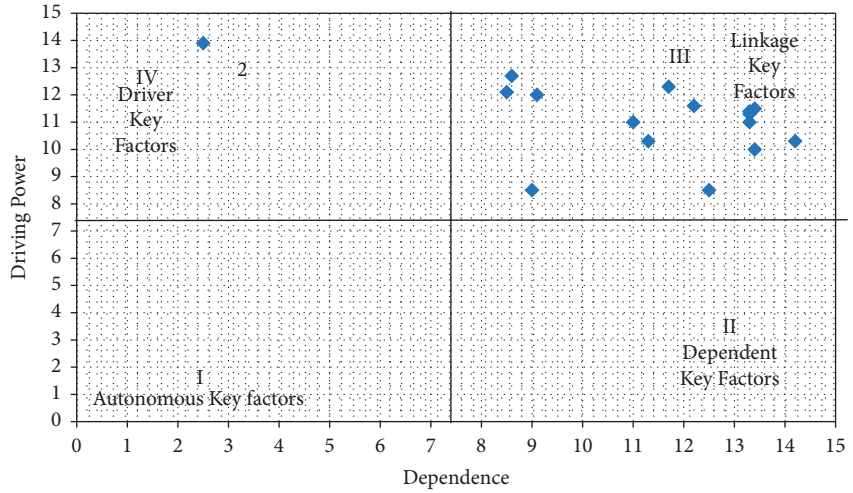

Figure 3: Diagram of Fuzzy MICMAC on dependence and driving powers of factors.

8. Recommendation and Policy Implication

The financial system is important for the country's economic progress and its long-term viability. CF is becoming one of the most popular ways of capital creation, even for large projects in the transportation sector, because of rising digitalization. Investors, particularly those from emerging nations, are growing increasingly interested in the operation, regulation, and understanding of CF. Investment objectives can be addressed by understanding the CF leading factors. Decision-makers should pay less attention to the independent category of elements when making any decision because none of the chosen parameters falls within the autonomous quadrant. All of them should be considered during the CF selection process and at frequent intervals to verify that targeted financial goals are met. Except for "No or Low," all factors in regulation fall into a quadrant's linkage category, which is important for decision-making because their values might reflect changes in other aspects. Without a doubt, the literature findings offer regulators valuable information. Market regulators should ensure that the financial industry as a whole is secure and supported.

9. Limitations and Scope of Future Research

For the purposes of this investigation, the framework built using the ISM and MICMAC models was tested in a nonlinear setting with sixteen variables that influence the growth of the CF market. Certain variables were not included in the framework because they were deemed insufficient for the study's goals and were restricted to the transportation industry. Investors can utilize a model developed as part of this research to assess the strength of CF and make investment decisions as a result of the model's development.

Data Availability

The data used to support the findings of this study are available from the corresponding author upon request.

Conflicts of Interest

The authors declare no conflicts of interest.

References

[1] S. N. Saleh, C. U. Lehmann, and R. J. Medford, "Early crowdfunding response to the COVID-19 pandemic: cross-sectional study," *Journal of Medical Internet Research*, vol. 23, no. 2, p. e25429, 2021.

[2] E. G. Soto, *Built by the Crowd, Crowdfunding Transport Infrastructure Projects*, Vol. 4, PhD work from university of Tilburg, the Netherlands, 2017.

[3] Z. J. Griffin, "Crowdfunding: fleecing the American masses," *Journal of Law, Technology & the Internet*, vol. 4, no. 2, pp. 375–410, 2013.

[4] B. L. Bayus, "Crowdsourcing new product ideas over time an analysis of the dell IdeaStorm community," *Management Science*, vol. 59, no. 1, pp. 226–244, 2013.

[5] F. G. Kleemann, G. Voss, and K. Rieder, "Un(der)paid Innovators: the Commercial Utilization of Consumer Work through Crowdsourcing," *Science, Technology & Innovation Studies*, vol. 4, no. 1, pp. 5–26, 2008.

[6] A. K. Agrawal, C. Christian, and A. Goldfarb, *The Geography of Crowdfunding & Quot; NBER Working Papers 16820*, Vol. 1, National Bureau of Economic Research, Inc, Cambridge, Massachusetts, 2011.

[7] A. K. Agrawal, C. Catalini, and A. Goldfarb, "The Geography of Crowdfunding. National Bureau of Economic Research working paper series no. 16820," vol. 1, 2011, http://www.nber.org/papers/w16820.

[8] G. Ahlers, D. Cumming, C. Guenther, and D. Schweizer, "Equity Crowdfunding," *SSRN Electronic Journal*, vol. 1, 2013.

[9] V. Kuppuswamy and A. Bayus Barry, "Review of crowdfunding research and findings," in *Handbook of New Product Development Research*, P. N. Golder and D. Mitra, Eds., pp. 361–373, Edward Elgar Publishing, Cheltenham UK and Northampton, MA, USA, 2018.

[10] E. R. Mollick, "The dynamics of crowdfunding: an exploratory study," *Journal of Business Venturing*, vol. 29, no. 1, pp. 1–16, 2014.

[11] S. Rahi, *Research Design and Methods*, Create Space Independent Publishing Platform, Scotts Valley, California, 2018.

[12] G. , V. , M. Sharma, A. S. Yadav, and P. N. Udupa, "Crowdfunding in India: an empirical study," *International Journal of Advanced Research*, vol. 7, no. 3, pp. 935–942, 2019.

[13] Sarkar and Abhrajit, "crowd funding in India: issues & challenges (february 27, 2016)," https://ssrn.com/abstract=2739008%20or%20http://dx.doi.org/10.2139/ssrn.2739008.

[14] C. J. Muscarella and M. R. Vetsuypens, "A simple test of Baron's model of IPO underpricing," *Journal of Financial Economics*, vol. 24, no. 1, pp. 125–135, 1989.

[15] R. Agarwal, G. Gao, C. DesRoches, and A. K. Jha, *Research Commentary: The Digital*, vol. 21, no. 4, p. 14, 2010.

[16] G. Giudici, R. Nava, C. Rossi-Lamastra, and C. Verecondo, "Crowdfunding: the new Frontier for financing entrepreneurship?," 2012, http://ssrn.com/abstract=2157429.

[17] B. J. Rubinton, *Crowdfunding: disintermediated investment banking*, University Library of Munich, vol. 1, Germany, Article ID 31649, 2011.

[18] O. Lehner, *Manfred, Crowdfunding Social Ventures: A Model and Research Agenda*, , p. 22, Routledge Handbook of Social and Sustainable Finance, 2016.

[19] G. Giudici, M. Guerini, C. Rossi-Lamastra, and Cristina, "Crowdfunding in Italy: state of the art and future prospects," *Journal of Industrial and Business Economics*, vol. 40, no. 4, pp. 173–188, 2014.

[20] D. J. Cumming and S. A. Johan, "Demand-driven securities regulation: evidence from crowdfunding," *Venture Capital*, vol. 15, no. 4, pp. 361–379, 2013.

[21] E. Li and J. S. Martin, "capital formation and financial intermediation: the role of entrepreneur reputation formation," *Journal of Corporate Finance; FIRN Research*, 2016, https://ssrn.com/abstract=2517273%20or%20http://dx.doi.org/10.2139/ssrn.2517273, Article ID 2517273.

[22] "SEB1, a Consultation Paper on Crowdfunding in India," https://www.sebi.gov.in/sebi_data/attachdocs/1403005615257.pdf.

[23] J. R. Ritter, "The 'hot issue' market of 1980," *Journal of Business*, vol. 57, no. 2, pp. 215–240, 1984.

[24] K. Rock, "Why new issues are underpriced," *Journal of Financial Economics*, vol. 15, no. 1-2, pp. 187–212, 1986.

[25] S. Johan and Y. Zhang, "Quality revealing versus overstating in equity crowdfunding," *Journal of Corporate Finance*, vol. 65, Article ID 101741, 2020.

[26] M. Grinblatt and C.-Y. Hwang, "Signalling and the pricing of new issues," *The Journal of Finance*, vol. 44, no. 2, pp. 393–420, 1989.

[27] N. Jegadeesh, M. Weinstein, and I. Welch, "An empirical investigation of IPO returns and subsequent equity offerings," *Journal of Financial Economics*, vol. 34, no. 2, pp. 153–175, 1993.

[28] J. R. Ritter and T. Loughran, "The new issue puzzle," *The Journal of Finance*, vol. 50, pp. 23–51, 1995.

[29] A. Khurshed, S. Paleari, A. Pande, and S. Vismara, "Transparent book building, certification and initial public offerings," *Journal of Financial Markets*, vol. 19, pp. 154–169, 2014.

[30] D. P. Baron, "A model of the demand for investment banking advising and distribution services for new issues," *The Journal of Finance*, vol. 37, no. 4, pp. 955–976, 1982.

[31] I. Welch, "Seasoned offerings, imitation costs and the underpricing of initial public offerings," *The Journal of Finance*, vol. 44, no. 2, pp. 421–449, 1989.

[32] I. Welch, "Sequential sales, learning and cascades," *The Journal of Finance*, vol. 47, no. 2, pp. 695–732, 1992.

[33] F. Allen and G. R. Faulhaber, "Signalling by underpricing in the IPO market," *Journal of Financial Economics*, vol. 23, no. 2, pp. 303–323, 1989.

[34] T. J. Chemmanur, "The pricing of initial public offerings: a dynamic model with information production," *The Journal of Finance*, vol. 48, no. 1, pp. 285–304, 1993.

[35] R. Michael and W. H. Shaw, "The pricing of initial public offerings: tests of adverse selection and signalling theories," *Review of Financial Studies*, vol. 7, pp. 279–319, 1994.

[36] F. Koh and T. Walter, "A direct test of Rock's model of the pricing of unseasoned issues," *Journal of Financial Economics*, vol. 23, no. 2, pp. 251–272, 1989.

[37] P. J. Hughes and A. V. Thakor, "Litigation risk, intermediation and the underpricing of initial public offerings," *Review of Financial Studies*, vol. 5, no. 4, pp. 709–742, 1992.

[38] P. D. Drake and M. R. Vetsuypens, "IPO underpricing and insurance against legal liability," *Financial Management*, vol. 22, no. 1, pp. 64–73, 1993.

[39] M. Lowry and S. Shu, "Litigation risk and IPO underpricing," *Journal of Financial Economics*, vol. 65, no. 3, pp. 309–335, 2002.

[40] E. Boehmer and P. Raymond Fisher, *Equilibrium Rationing in Initial Public Offerings of Equity, Working Paper*, University of Miami, Coral Gables, USA, 2001.

[41] L. Krigman, W. H. Shaw, and K. L. Womack, "The persistence of IPO mispricing and the predictive power of flipping," *The Journal of Finance*, vol. 54, no. 3, pp. 1015–1044, 1999.

[42] K. Ellis, R. Michaely, and M. O'Hara, "When the underwriter is the market maker: an examination of trading in the IPO aftermarket," *The Journal of Finance*, vol. 55, no. 3, pp. 1039–1074, 2000.

[43] J. R. Booth and L. Chua, "Ownership dispersion, costly information, and IPO underpricing," *Journal of Financial Economics*, vol. 41, no. 2, pp. 291–310, 1996.

[44] A. Bubna and N. R. Prabhala, "IPOs with and without allocation discretion: empirical evidence," *Journal of Financial Intermediation*, vol. 20, no. 4, pp. 530–561, 2011.

[45] J. N. Warfield, "Developing subsystems matrices in structural modelling," *IEEE Trans Syst*, Man and Cybern, vol. 14, no. 1, pp. 18–24, 1974.

[46] A. P. Sage, *Interpretive Structural Modeling: Methodology for Large-Scale Systems*, McGraw-Hill, New York, NY, 1977.

[47] R. Illyas, R. S. Mohammed, and D. K. Banwet, "Creating a flex-lean-agile value chain by outsourcing: an ISM based interventional road map," *Business Process Management Journal*, vol. 14, no. 3, 2008.

[48] A. Mandal and S. G. Deshmukh, "Vendor selection using interpretive structural modelling (ISM)," *International Journal of Operations & Production Management*, vol. 14, no. 6, pp. 52–59, 1994.

[49] Y. Dong and K. Xu, "A supply chain model of vendor managed inventory," *Transportation Research Part E: Logistics and Transportation Review*, vol. 38, no. 2, pp. 75–95, 2002.

[50] M. D. Singh, R. Shankar, R. Narain, and A. Agarwal, "An interpretive structural modeling of knowledge management in engineering industries," *Journal of Advances in Management Research*, vol. 1, no. 1, pp. 28–40, 2003.

[51] H. D. Sharma, A. D. Gupta, and Sushil, "The objectives of waste management in India: a futures inquiry," *Technological Forecasting and Social Change*, vol. 48, no. 3, pp. 285–309, 1995.

[52] J. P. Saxena, P. Sushil, and P. Vrat, "Impact of indirect relationships in classification of variables-a micmac analysis for energy conservation," *Systems Research*, vol. 7, no. 4, pp. 245–253, 1990.

[53] V. Ravi, R. Shankar, and M. K. Tiwari, "Analyzing alternatives in reverse logistics for end-of-life computers: ANP and balanced scorecard approach," *Computers & Industrial Engineering*, vol. 48, no. 2, pp. 327–356, 2005.

[54] V. Ravi and R. Shankar, "Analysis of interactions among the barriers of reverse logistics," *Technological Forecasting and Social Change*, vol. 72, no. 8, pp. 1011–1029, 2005.

[55] J. J. Huang, G. H. Tzeng, and C. S. Ong, "Multidimensional data in multidimensional scaling using the analytic network process," *Pattern Recognition Letters*, vol. 26, no. 6, pp. 755–767, 2005.

[56] G. Kannan, A. N. Haq, P. Sasikumar, and S. Arunachalam, "Analysis and selection of green suppliers using interpretative structural modelling and analytic hierarchy process," *International Journal of Management and Decision Making*, vol. 9, no. 2, pp. 163–182, 2008.

[57] K. Mathiyazhagan, K. Govindan, A. NoorulHaq, and Y. Geng, "An ISM approach for the barrier analysis in implementing green supply chain management," *Journal of Cleaner Production*, vol. 47, pp. 283–297, 2013.

[58] G. Kannan and A. N. Haq, "Analysis of interactions of criteria and sub-criteria for the selection of supplier in the built-in-order supply chain environment," *International Journal of Production Research*, vol. 45, no. 17, pp. 3831–3852, 2007.

[59] G. Kannan, S. Pokharel, and P. Sasi Kumar, "A hybrid approach using ISM and fuzzy TOPSIS for the selection of reverse logistics provider," *Resources, Conservation and Recycling*, vol. 54, no. 1, pp. 28–36, 2009.

[60] M. D. Singh and R. Kant, "Knowledge management barriers: an interpretive structural modeling approach," *International Journal of Management Science and Engineering Management*, vol. 3, no. 2, pp. 141–150, 2008.

[61] S. Kumar and R. Sharma, "Key barriers in the growth of rural health care: an ISM-MICMAC approach," *Benchmarking: An International Journal*, vol. 25, no. 7, pp. 2169–2183, 2018.

[62] T. Raj, R. Shankar, and M. Suhaib, "An ISM approach for modelling the enablers of flexible manufacturing system: the case for Indiaflexible manufacturing system: the case for India," *International Journal of Production Research*, vol. 46, no. 24, pp. 6883–6912, 2008.

[63] S. Kumar, G. P. Shukla, and R. Sharma, "Analysis of key barriers in retirement planning: an approach based on interpretive structural modelling," *Journal of Modelling in Management*, vol. 14, no. 4, pp. 972–986, 2019.

[64] S. Reza, P. F. Yeap, and E. Nazli, "Using interpretive structural modelling to determine the relationships among knowledge management criteria inside Malaysian organizations," *World Academy of Science- Engineering and Technology*, vol. 72, 2010.

[65] K. H. Lai, Y. Bao, and X. Li, "Channel relationship and business uncertainty: evidence from the Hong Kong market," *Industrial Marketing Management*, vol. 37, no. 6, pp. 713–724, 2008.

[66] P. Shahabadkar, S. S. Hebbal, and S. Prashant, "Deployment of interpretive structural modeling methodology in supply chain management –an overview," *Intternattiionall Journal off Industrial Engineering & Production Research*, vol. 23, no. 3, pp. 195–205, 2012.

[67] Q. Zhu, J. Sarkis, and K. H. Lai, "Green supply chain management innovation diffusion and its relationship to organizational improvement: an ecological modernization perspective," *Journal of Engineering and Technology Management*, vol. 29, no. 1, pp. 168–185, 2012.

[68] A. Agrawal, C. Catalini, and A. Goldfarb, "Some simple economics of crowdfunding," *Innovation Policy and the Economy*, vol. 14, no. 1, pp. 63–97, 2014.

[69] D. C. Sanchez, "An optimal ICO mechanism," 2017, https://mpra.ub.uni-muenchen.de/81285/.

[70] D. J. Cumming, S. A. Johan, and Y. Zhang, "The role of due diligence in crowdfunding platforms," *Journal of Banking & Finance*, vol. 108, Article ID 105661, 2019.

[71] S. S. Turan, "Financial innovation - crowdfunding: friend or Foe?" *Procedia - Social and Behavioral Sciences*, vol. 195, pp. 353–362, 2015.

[72] S. Rahi, "Research design and methods: a systematic review of research paradigms, sampling issues and instruments development," *International Journal of Economics and Management Sciences*, vol. 06, no. 02, p. 403, 2017.

[73] D. S. Arya and S. A. Abbasi, "Identification and classification of key variables and their role in environmental impact assessment: methodology and software package INTRA," *Environmental Monitoring and Assessment*, vol. 72, no. 3, pp. 277–296, 2001.

[74] T. Aitamurto, "The impact of crowdfunding on journalism," *Journalism Practice*, vol. 5, no. 4, pp. 429–445, 2011.

[75] D. C. Brabham, "How crowdfunding discourse threatens public arts," *New Media & Society*, vol. 19, no. 7, pp. 983–999, 2016.

Hindawi
Journal of Advanced Transportation
Volume 2022, Article ID 6458371, 12 pages
https://doi.org/10.1155/2022/6458371

Research Article

Exploring Transit Use during COVID-19 Based on XGB and SHAP Using Smart Card Data

Eun Hak Lee

Multimodal Planning & Environment Division, Texas A&M Transportation Institute, 1111 Rellis Pkwy, Bryan, TX 77807, USA

Correspondence should be addressed to Eun Hak Lee; e-lee@tti.tamu.edu

Received 5 May 2022; Revised 15 July 2022; Accepted 30 July 2022; Published 9 September 2022

Academic Editor: Elżbieta Macioszek

Copyright © 2022 Eun Hak Lee. This is an open access article distributed under the Creative Commons Attribution License, which permits unrestricted use, distribution, and reproduction in any medium, provided the original work is properly cited.

As the coronavirus (COVID-19) pandemic continues, many protective measures have been taken in Seoul, Korea, and around the world. This situation has drastically changed lifestyle and travel behavior. An important issue concerns understanding the reasons for giving up transit use and the potential impact on travel patterns during the COVID-19 pandemic. To shed light on these issues that are essential for transit policy, this study explores transit use choice, such as whether users have given-up transit use or not, during the COVID-19 pandemic. Two days of smart card data, before and during the COVID-19 pandemic, were used to look at users who gave up transit use during the COVID-19 pandemic. The choice set of the dataset includes two alternatives, for example, transit use and given-up transit use. An extreme gradient boosting (XGB) model was used to estimate the transit use behavior. Shapley additive explanations were performed to interpret the estimation results of the XGB model. The results for the overall specificity, sensitivity, and balanced accuracy of the proposed XGB model were estimated to be 0.909, 0.953, and 0.931, respectively. The feature analysis based on the Shapley value shows that the number of origin-to-destination trip feature substantially impacts transit use. As such, users tend to avoid transit use as travel time increased during the COVID-19 pandemic. The proposed model shows remarkable performance in accuracy and provided an understanding of the estimated results.

1. Introduction

The global coronavirus (COVID-19) pandemic has profoundly impacted all areas of people's lives around the world. Unlike conventional viruses, the spread of COVID-19 has been difficult to contain, and it is expected to change the appearance of our society permanently rather than temporarily. The first COVID-19 case in Seoul, Korea was reported on January 20, 2020. A year and three months later, in April 2021, 106,898 confirmed cases and 1,756 deaths have been reported in Seoul. To decelerate the spread of COVID-19, the government of Seoul implemented protective measures such as interpersonal distance. The interpersonal distance policy consists of 1~2.5 levels connected with the severity of the spread of COVID-19. Currently, the government of Seoul has announced a 2.5 level which is the strictest lockout measure. This policy significantly changed the lifestyle and travel behavior of local residents in Seoul. The protective measures implemented by the government included closing all facilities, for example, restaurants or gyms, at 10 P.M. and prohibiting gatherings of more than four people. Furthermore, public transport reduced fleet operations by 30% after 9 P.M. According to statistical analysis using smart card data in Seoul, the number of transit trips in 2020 decreased by about 27% compared with the previous year. However, descriptive statistics from smart card data do not provide information on how or why people change their travel behavior, such as given-up transit use. Due to the specificity of the current pandemic situation, little is known about the changes in transit user travel behavior. It is important to understand the reasons for changing travel behavior and the potential impact on transit use during the COVID-19 pandemic.

Early studies addressed the impacts of the COVID-19 pandemic on travel behavior, mode choice, and other activities in different countries worldwide [1–9]. Many studies have focused on travel pattern changes considering work and shopping behaviors. Due to the COVID-19 pandemic, the proportions of telecommuting usage and online

shopping have increased, resulting in a decrease in overall transit and auto trips [10]. To understand this phenomenon, survey and mobile application data were used, however, little work has been published about the change in travel behavior during the interpersonal distance policy period with large-scale data such as smart card data. Many researchers have sought to estimate users' mode choice behavior using smart card data due to its quality and quantity. For example, Kim et al. [11] proposed an express train choice model based on smart card data, and the results of the model showed notable performance in exploring user choice behavior. Lee et al. [12] identified user preference of urban transit modes with the smart card data. Similarly, Jánošíková et al. [13] developed a transit route choice model based on the multinomial logit model (MNL) using smart card data. These previous studies implied that the smart card data was very useful for analyzing mode choice behavior since it accurately provides all transit trip information.

As various data on transit systems are being collected, some studies have explored transit user travel behavior based on a data-driven approach and machine learning techniques [14]. The choice model based on machine learning techniques has an advantage with high accuracy compared to conventional choice models such as the MNL model [15]. One of the major drawbacks of machine learning techniques is the difficulty in interpreting the impact of the inputs on the outputs. However, it has become possible to accurately estimate and analyze various individual travel behaviors with the advent of interpretable machine learning (IML) techniques. For example, Lee et al. [14] used the IML approach to analyze train choice, for example, local and express train, and interpret user preferences. Similarly, Wang and Ross [15] developed an IML-based transit mode choice model and compared it to the MNL model. These studies mentioned that IML provided a more accurate estimation and a better understanding of user preference than other conventional models.

To shed light on these matters that are essential for analysis and transit policy, this study explores transit user's travel behavior, specifically whether or not transit use is given-up, during the COVID-19 pandemic. Two days of smart card data, before and during the COVID-19 pandemic, are used to estimate trips that gave up transit use during the COVID-19 pandemic. The choice set of the dataset includes two alternatives, given-up transit use due to COVID-19 pandemic and transit use. The extreme gradient boosting (XGB) model is used to estimate the transit user's travel behavior. Shapley additive explanations (SHAP) are performed to explain the estimation results of the transit use choice model. Feature importance and relationships between features are investigated by a SHAP summary and dependence plot, respectively. Also, the O-D pairs where the potential for high given-up of transit use were identified in terms of policy implementation.

2. Data Description

2.1. Description of Smart Card Data. The government of Seoul has operated an integrated automatic fare collection system since 2004. The transit fare from the origin to the destination station is charged based on the total distance traveled by transit modes, for example, bus, subway, or both modes (transfer between bus and subway). With a smart card, users can use any combination of transit modes for free up to four transfers. The transit network in Seoul is operated with only a 100% smart card system without any other payment method, for example, cash and ticket, and the smart card data in Seoul provides 99% of transit users' trip information. Thus, it is widely used for microscopic user behavior analysis [16–18].

One of the biggest advantages of the smart card system in Seoul is that users must tap their smart card in or out when they get in or out of transit mode, respectively. If users do not tap in or out their smart card, a double fee will be charged on the next trip as a fine. Thus, the smart card data in Seoul is considered complete and reliable data that records complete transit user information. However, behind these advantages lies the disadvantage of privacy. If someone knows when and where an individual has used transit mode, even roughly, their trip information can be tracked in smart card data. Thus, the government of Seoul implemented a privacy protection policy for smart card data in 2020. The identification of the individual user was deleted to protect the identification of the user's trip sequence and chain. Also, travel time information is recorded every 5 minutes unit, and locations are encrypted with codes that are not identifiable by the general public. Through this privacy protection policy, smart card data has been advanced by recording transit users' information while protecting personal information.

Although the AFC system provides high-quality trip information, limitations of smart card data remain. For example, smart card data typically underestimate ridership owing to possible fare evaders [19, 20]. There also can be anomalies in smart card data due to software problems with the AFC system. These limitations are common that can occur in transit systems around the world. The smart card data used in Seoul also faced this problem, and the government of Seoul estimates anomalies in smart card data to be about 1%. Thus, this study assumed that the smart card data in Seoul contained 99% of transit trips in Seoul without anomalies.

The smart card data from November 14, 2019 and December 10, 2020 were used to analyze the impact of the COVID-19 pandemic on transit mode choice. The smart card data of November 14, 2019 was used as data before the COVID-19 pandemic, and the smart card data of December 10, 2020 was used as data during the COVID-19 pandemic. According to the smart card data, the number of trips before COVID-19 and during the COVID-19 pandemic were 8,196,311 and 4,780,953, respectively. This smart card data indicates that the spread of COVID-19 in Seoul decreased the number of transit trips by about 43% per day. The information for each trip is classified into 16 categories in the smart card data. The description of smart card data and transit network in Seoul is shown in Table 1 and Figure 1, respectively.

2.2. Data Preprocessing. The smart card data of November 14, 2019 and December 10, 2020 were used to estimate the impact of the COVID-19 pandemic on given-up transit use. There are two choice alternatives for transit use, for example, given-up and transit use. However, it is necessary to add

Table 1: Description of the smart card data.

No.	Categories	Description
1	Transaction ID	Unique ID for each transaction
2	Mode code	1: subway, 2: bus, 3: both modes (bus + subway)
3	Line ID	Unique ID for each line
4	Vehicle ID	Unique ID for each bus vehicle (not for subway)
5	Boarding station ID	Unique ID for each station (max five stations are recorded for a trip)
6	Alighting station	Unique ID for each station (max five stations are recorded for a trip)
7	Boarding date/time	Year/month/day/hour/minute/seconds
8	Alighting date/time	Year/month/day/hour/minute/seconds
9	Total travel time	Seconds
10	Total travel distance	Kilometer
11	Number of transfers	0~4 (max four transfers available for a trip)
12	User group	1: general, 2: student, 3: elderly
13	User count	The number of boarding users (for bus trip)
14	Boarding fare	The basic fare for boarding
15	Alighting fare	Additional fare based on the travel distance
16	Zone code	Administrative unit code

Figure 1: Transit network in Seoul.

alternatives such as given-up transit use to take into account the 30% change representing reduced transit trips due to the emergence of the COVID-19 pandemic. Since smart card data only contains the revealed trip information, there is no information about given-up trips due to COVID-19. To obtain information regarding given-up trips, data preprocessing was performed to combine two smart card data sets before and during the COVID-19 pandemic.

Before preprocessing data to obtain the given-up trips for 2020, the data for 2018 and 2019 were compared to identify the yearly change in travel patterns. The results of the comparison showed that the number of trips on November 15, 2018 and November 14, 2019 were 8,268,438 and 8,196,311, respectively. The average travel time and the number of transfers were the same as 30 minutes and 0.24 transfers, respectively. Overall, the difference in travel behavior between November 15, 2018 and November 14, 2019 was less than 0.9%. Thus, the data preprocessing was performed, assuming that the travel pattern in 2019 and 2020 would be the same in the absence of COVID-19. Since the travel time information of smart card data in 2020 is recorded every 5 minutes due to the privacy policy, the travel time information of smart card data in 2019 was also recalculated from seconds unit to 5 minutes unit.

The data preprocessing was performed in two stages. The first stage selected O-D pairs containing given-up trips in 2020. The second stage is to filter the number of given-up trips from the 2019 data and fill it into the 2020 data. Each trip of 2020 was compared to that of 2019 based on departure time, arrival time, mode, number of transfers, and travel time. Departure time, arrival time, and travel time were aggregated by the units of hours when compared for each trip. As a result of the comparison, only trips that existed in the 2019 data were selected as given-up trips.

Figure 2 shows an example of the data preprocessing performed in this study. Firstly, the number of trips of O-D pairs by travel modes was calculated in stage 1. Five O-D pairs were selected as the O-D pairs of trips that are reduced during the COVID-19 pandemic. For the O-D pair from station 1 to station 2, the number of subway trips decreased from 100 to 70. In stage 2, 100 trips from 2019 data and 70 trips from 2020 data were compared based on the departure time, arrival time, mode, number of transfers, and travel time. Among the trips that existed only in the 2019 data, 30 trips were selected as given-up trips. The mode code of a filled trip was set to 0 which refers to the trip that was given-up in the transit use of 2020.

The number of given-up trips was estimated to be 3,415,358. By adding information of trips that were given-up in the transit use of 2020 data, 8,196,311 trips were obtained as the sample. With the preprocessed data, seven features were calculated for each trip to explore changes in transit use choice. The number of O-D trips and the difference between the number of O-D trips were 63.6 and 44.7 trips, respectively, on average. The number of transfers was 0.35 times, on average. The travel time and fare were 27.5 minutes and 1,111 KRW, respectively, on average. The average departure and arrival times were 13:46 and 14:14, respectively. A description and descriptive statistics of the preprocessed data are shown in Table 2.

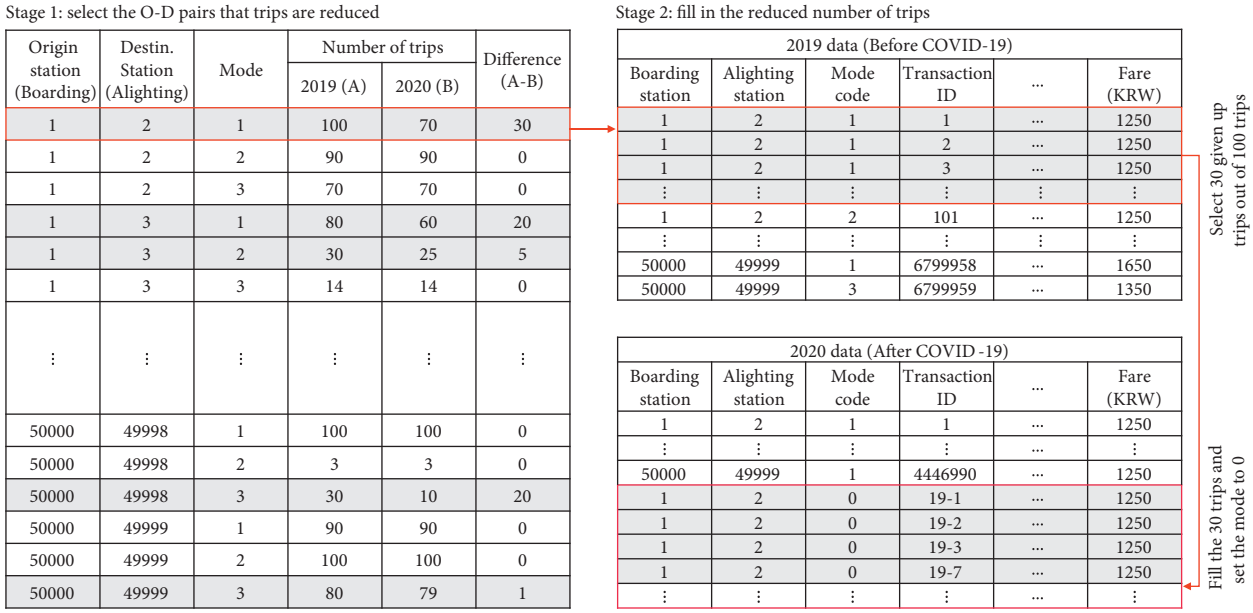

Figure 2: Conceptual illustration of data preprocessing.

Table 2: Description and descriptive statistics of the preprocessed data.

Variable	Category	Count (ratio, %)	Mean
Transit use (choice)	0: given-up transit use	3,415,358 (42.7)	—
	1: transit use	4,780,953 (58.3)	—
	Total	8,196,311 (100.0)	—
Number of O-D trips	Number of trips from origin to destination	—	63.6
Difference between the number of O-D trips	Difference between number of O-D trips before and during COVID-19 pandemic	—	44.7
Number of transfers	Number of transfers from origin to destination	—	0.35
Travel time (minutes)	Travel time from the origin station to the destination station	—	27.5
Fare (KRW)	Fare from origin station to destination station	—	1,111
Departure time (hour)	User's first tap-in time	—	13:46
Arrival time (hour)	User's final tap-out time	—	14:14

3. Methodology

3.1. Extreme Gradient Boosting. Extreme gradient boosting (XGB) proposed by Tianqi Chen and Carlos Guestrin refers to an ensemble machine learning algorithm used for classification or regression predictive modeling problems [21]. XGB is regarded as the most efficient decision tree-based algorithm for data analysis competitions due to its speed and scalability [22]. XGB constructs a sequence of the low-depth decision tree, and each tree is trained to give more weight on the incorrect output of the previous trees. Also, XGB provides parallel tree boosting to solve large-scale problems in a fast and accurate way.

The dataset with 8,196,311 samples includes independent variables x_i and dependent variables y_i, for example, 0 for given-up transit use trip and 1 for transit use trip, $(D = \{(x_i, y_i)\}, |D| = 8,196,311)$. Each x_i has m features therefore $x_i \in \mathcal{R}^m$ ($m = 1$: number of O-D trips, 2: difference between number of trips before and during COVID-19, 3: number of transfers, 4: travel time, 5: fare, 6: arrival time, 7: departure time). These features have corresponding dependent variables such as transit use or given-up ($x_i \in \mathcal{R}^m$, $y_i \in \mathcal{R}$). The tree ensemble model estimates the target value $(\hat{y}_i)$ using f_k which is an Kth independent tree structure with leaf scores as shown in the following equation:.

$$\hat{y} = \phi(x_i) = \sum_{k=1}^{K} f_k(x_i), f_k \in F, \tag{1}$$

where f_k is an independent tree structure with leaf scores and F represent the space of trees. The objective of the model is to minimize $\mathcal{L}(\phi)$ with the loss function l and the mathematical expression of the objective is shown in the following equation:.

$$\mathcal{L}(\phi) = \sum_{i} l(y_i, \hat{y}_i) + \sum_{k} \Omega(f_k). \tag{2}$$

Here, Ω is the term which penalizes the complexity of the model calculated and the mathematical expression of the objective is shown in the following equation:

$$\Omega(f_k) = \gamma T + \frac{1}{2}\lambda w_i^2. \tag{3}$$

In equation (3), w_i is the score of the leaf i and T is the number of leaves. By solving equations (1)–(3), the optimal weight w_i^* and the corresponding value $\widetilde{\mathscr{L}}^t(q)$ are shown the following equations:

$$w_i^* = -\frac{\sum_{i\in I_j}\partial_{\hat{y}^{t-1}} l\left(y_i, \hat{y}^{t-1}\right)}{\sum_{i\in I_j}\partial^2_{\hat{y}^{t-1}} l\left(y_i, \hat{y}^{t-1}\right) + \lambda}, \tag{4}$$

$$g_i = \partial_{\hat{y}^{(t-1)}} l\left(y_i, \hat{y}^{t-1}\right), \tag{5}$$

$$h_i = \partial^2_{\hat{y}^{(t-1)}} l\left(y_i, \hat{y}^{t-1}\right), \tag{6}$$

$$\widetilde{\mathscr{L}}^t(q) = -\frac{1}{2}\sum_{j=1}^{T}\frac{\left(\sum_{i\in I_j} g_i\right)^2}{\sum_{i\in I_j} h_i + \lambda} + \gamma T. \tag{7}$$

It is generally difficult to enumerate all possible tree structures of q. Thus, the greedy algorithm, which branches out a single leaf to many branches iteratively, is used to estimate the optimal solution. The greedy algorithm is usually used to evaluate spilled candidates. $I = I_L \cup I_R$, I_L is the instance set of left nodes after split and I_R is the instance set of right nodes after the split. The mathematical expression is shown in the following equation:

$$\mathscr{L}_s = -\frac{1}{2}\left[\frac{\left(\sum_{i\in I_L} g_i\right)^2}{\sum_{i\in I_L} h_i + \lambda} + \frac{\left(\sum_{i\in I_R} g_i\right)^2}{\sum_{i\in I_R} h_i + \lambda} - \frac{\left(\sum_{i\in I} g_i\right)^2}{\sum_{i\in I} h_i + \lambda}\right] - \gamma. \tag{8}$$

The additional advantage of XGB is that it is not affected by multicollinearity. Thus, several variables can be kept, even if these variables capture the same phenomenon in the same system. This is even desirable since feature analysis using SHAP is conducted in this study.

3.2. Hyperparameter Tuning for XGB. There are several hyperparameters related to the XGB model. Hyperparameter tuning XGB is necessary to avoid the overfitting problem and heavy complexity of the model. A grid search based on cross-validation was performed to set the optimal six hyperparameters, for example, number of iterations, learning rate, subsample, colsample_bytree, alpha, and lambda. The learning rate refers to the scale of the weights of each tree, and it changes the impact of each tree to make a robust model. There are two hyperparameters related to preventing the overfitting problem of the model. The first one is the subsample, which stands for the ratio of randomly selected observations for training instances. The other one is the colsample_bytree parameter which is the fraction of columns when constructing each tree. The alpha parameter is the regulation term on weights of $L1$, and lambda is the regulation term on weights of $L2$. As a result of the grid search based on cross-validation analysis, the hyperparameters of XGB in this study were selected as 622 for the number of iterations, 0.3 for learning rate, 0.9 for subsample, 0.9 for colsample_bytree, 0.4 for an alpha, and 0.3 for lambda, respectively.

3.3. Performance Measures for XGB. Three performance measures, for example, specificity, sensitivity, and balanced accuracy, were selected to evaluate the model performance. These measures are well-known composite classification metrics-based methods for evaluating a multiclass classification model.

Specificity is the number of true-negatives from among the true-negatives and false-positives. Sensitivity stands for the true-positives from among the true-positives and false-negatives. Balanced accuracy is the average of sensitivity and specificity. Balanced accuracy is great for the classification problem when the difference between negative and positive samples is large. In this study, true-positive and false-positive stand that the model estimated transit user as transit use (correct) and given-up (incorrect), respectively. The true-negative and false-negative mean that the model estimated given-up user as given-up (correct) and transit use (incorrect), respectively, where TP is true-positive, FP is false-positive, TN is true-negative, and FN is false-negative. The mathematical expressions of three performance measures are shown in the following equations:

$$\text{specificity} = \frac{\text{TN}}{\text{TN} + \text{FP}}, \tag{9}$$

$$\text{sensitivity} = \frac{\text{TP}}{\text{TP} + \text{FN}}, \tag{10}$$

$$\text{balanced accuracy} = \frac{\text{specificity} + \text{sensitivity}}{2}. \tag{11}$$

3.4. Shapley Additive Explanations for Model Interpretation. SHAP was used to interpret the results of the transit use choice model proposed in this study. The objective of SHAP is to interpret the contribution of each feature to the output [23, 24]. The Shapley values are estimated based on cooperative game theory. The feature values of each sample act as players in a coalition. The Shapley value helps distribute a payoff for all features when each feature might have contributed more or less than the others. The algorithm repeatedly asks the impact of the feature on each output, and the answer is computed as the Shapley value. With the Shapley value, it is possible to interpret the contribution of each feature [25]. To develop an interpretable mode, SHAP uses an additive feature attribution method, for example, an output model is defined as a linear addition of input features. Assuming a model with input features $x_i = (x_1, x_2, \ldots, x_i, x_m)$, where i is the number of input features (e.g., 1: number of O-D trips, 2: difference between number of trips before and during COVID-19, 3: number of transfers, 4: travel time, 5: fare, 6: arrival time, 7: departure time) and the explanation model $g(z')$ with simplified input z'. For transit use subset $S \subseteq N$ (where N stands for the set of all samples), two models are trained to estimate the effect of feature i. The first model $v(S \cup \{i\})$ is trained with feature i

while the other model $v(S)$ is trained without feature i, where $S \cup \{i\}$ and S are the values of input transit use features. The difference in model outputs $v(S \cup \{i\}) - v(S)$ is estimated for each possible subset $S \subseteq N\{i\}$, equation (12) shows the linear function g which is defined by the additive feature function, and equation (13) shows the mathematical expression of the SHAP.

$$g(x') = \theta_0 + \sum_{i=1}^{m} \theta_i X_i', \tag{12}$$

$$\theta_i = \sum_{S \subseteq N\{i\}} \frac{|S|!\,(n - |S| - 1)!}{n!} [v(S \cup \{i\}) - v(S)]. \tag{13}$$

4. Application

4.1. Feature Selection for XGB Model. With data preprocessing, 13 features were gathered to develop the transit use behavior model during COVID-19. The features related to user behavior and sociodemographics were obtained from the smart card data and the open data portal, respectively. With these datasets, the naïve XGB model was developed to select meaningful features to interpret transit users' behavior. The feature selection process consisted of three steps. Firstly, the features were ranked by importance and frequency scores computed from the naïve XGB model. Then, the importance and frequency scores were clustered by the k-means clustering method. Finally, the features were selected based on the significance of the cluster at 99%.

As a result of feature selection analysis, seven features included in four clusters were selected as significant to the model. Specifically, the number of O-D trips feature was estimated to be the most significant feature, with the highest importance and frequency scores of 0.68 and 0.28, respectively. The difference between the number of O-D trips, number of transfers, travel time, arrival time, and departure time features were analyzed to have a significant impact on the output. However, the six sociodemographic-related features, fo example, population, density, number of households and companies, land-use, and average land price, were estimated to have little impact on output with both importance and frequency scores less than 0.5. The results of the feature selection analysis are shown in Figure 3.

4.2. Performance of the Proposed XGB Model. XGB was trained on 85% of the preprocessed dataset and tested on the remaining 15%. The training and test samples were obtained randomly. The training data included 6,966,864 of 8,196,311 trips, and the test data comprised 1,229,447. The performances of the model were estimated to be over 90% in all measures.

The proposed model was designed as a binary problem to classify given-up or transit use trips. However, three measures were classified by transit modes to identify model performance in detail. For subway users, specificity, sensitivity, and balanced accuracy were estimated to be 0.902, 0.903, and 0.903, respectively. The number of true-positives was 179,611 and the number of true-negatives was 310,191. The number of false-positives was 33,610 and the number of false-negatives was 19,209. For bus users, specificity, sensitivity, and balanced accuracy were estimated to be 0.907, 0.987, and 0.947, respectively. The number of true-positives was 193,715 and the number of true-negatives was 230,070. The number of false-positives was 23,501 and the number of false-negatives was 2,484. For both modes (subway + bus) users, specificity, sensitivity, and balanced accuracy were estimated to be 0.932, 0.980, and 0.956, respectively. The number of true-positives was 114,677 and the number of true-negatives was 111,895. The number of false-positives was 8,185 and the number of false-negatives was 2,299.

Overall, specificity, sensitivity, and balanced accuracy were 0.909, 0.953, and 0.931, respectively. These results indicate that the proposed model showed notable performance with an accuracy of over 93.1%. Moreover, the proposed model was found to be suitable for exploring the impact of COVID-19 on transit mode choice. The performance of the proposed model is shown in Table 3.

To compare the results of XGB with the parametric model, the transit use choice model was developed with the MNL model, the method most widely used for modeling choice behavior [14, 15]. The parameters were estimated with 85% of the dataset and validation was performed with 15% of the dataset. Since a multicollinearity problem between variables, three variables, for example, number of O-D trips, number of transfers, and arrival time, were used to develop the MNL model. The result of the MNL model is shown in Table 4. As a result of estimating MNL, the constants of given-up, subway, bus, and both modes were estimated to be 1.095, 0.434, and 0.673, respectively. These results indicated that many people preferred to use transit even during the COVID-19 pandemic. The parameters of the number of O-D trips, the number of transfers, and arrival time were estimated to be 0.0019, −0.1518, and −0.0299, respectively. These parameters indicated that people preferred to give up transit use as the number of trips, the number of transfers increased, and arrival time increased. The F1 score of MNL was estimated to be about 0.706, which is relatively low compared with that of XGB of 0.931. Specifically, the F1 score of MNL tends to be low, in the order of given-up, subway, bus, and both modes. The MNL model could not estimate users' transit use preferences accurately, with a low F1 score of 0.706. This result implied that the MNL model was suitable for simple problems due to the low flexibility of data distribution assumptions. Also, MNL had a limitation in not being able to interpret the relationship between features. However, the XGB model had high flexibility without distribution assumption and the ability to interpret the relationship between features. Thus, the proposed XGB model accurately estimated the transit use behavior, with a high F1 score of 0.931.

4.3. Feature Analysis of the Transit Mode Choice. Shapley values of seven features of the XGB model are illustrated in Figure 4. The features used in the modeling are ordered by their importance in estimating transit use. If the Shapley value is negative, the preference for transit use is low, and if

Figure 3: Results of feature selection analysis: (a) importance score; (b) frequency score.

the Shapley value is positive, the preference for transit use is high.

The results of the feature analysis showed that the number of O-D trips and the difference between the number of O-D trips had the greatest impact on the transit use choice model. The Shapley values of the number of O-D trips showed that the probability of transit use increased as the number of O-D trips increased. Conversely, the Shapley

Table 3: Performance of proposed XGB model.

Modes	Test set			Performance measure		
	Given-up (trips)	Use (trips)	Total	Specificity	Sensitivity	Balanced accuracy
Subway	198,820	343,801	542,621	0.902	0.903	0.903
Bus	196,199	253,571	449,770	0.907	0.987	0.947
Both modes (bus + subway)	116,976	120,080	237,056	0.932	0.980	0.956
Total	511,995	717,452	1,229,447	0.909	0.953	0.931

Table 4: Results of multinomial logit model.

Variable	Constant	Variable			F1 score
		Number of O-D trips	Number of transfers	Arrive time (minutes)	
Given-up	—	−0.0019***	−0.1518***	−0.0299***	0.785
Subway	1.095***	−0.0019***	−0.1518***	−0.0299***	0.717
Bus	0.434***	−0.0019***	−0.1518***	−0.0299***	0.702
Both modes (bus + subway)	0.673***	−0.0019***	−0.1518***	−0.0299***	0.668
Total	—	—	—	—	0.706

Pseudo R^2: 0.48: **represent $p < 0.05$; ***represent $p < 0.01$.

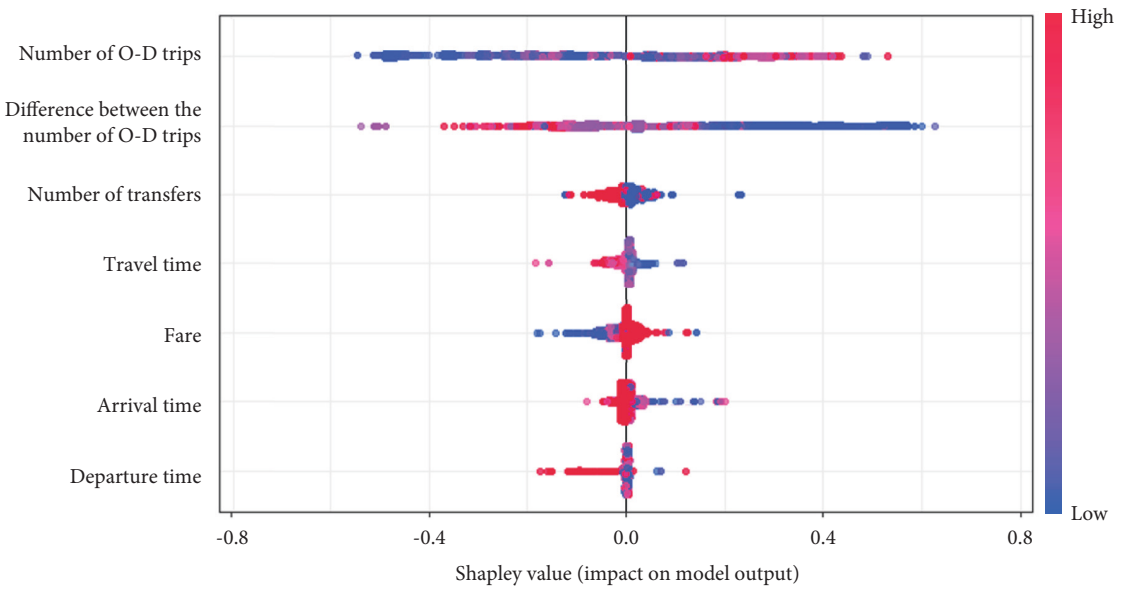

Figure 4: Results of the Shapley values of nine features.

values of the difference between the number of O-D trips indicated that the probability of transit use decreased as the difference between the number of O-D trips increased. The O-D pairs with a high number of transit trips and a low difference between the number of O-D trips had well-equipped transit facilities and had a high level of service (LOS). Thus, users who traveled these O-D pairs did not easily give up their transit use [26].

Among the features related to transit service, for example, number of transfers, travel time, and fare, the number of transfers was found to have the largest impact on transit use behavior. The Shapley value of the number of transfers indicated that the probability of transit use increased as the number of transfers decreased. These results indicated that the users who used both modes gave up transit use since contact with other people could increase as the number of transfers increased. Especially, contact with people was related to the concerns about COVID-19 infection during the pandemic [27]. In the case of the travel time feature, the Shapley value showed that the probability of transit use increased as travel time decreased. The result of the Shapley value for travel time indicated that users avoided long transit times due to concerns about COVID-19 infection [27]. The Shapley value for fare feature showed that users did not prefer transit use as the fare decreased. This result explained that users who use the transit service at a discounted rate, that is, the elderly, disabled, and students, tended to give up transit use during COVID-19. Users who use the transit service at a discounted rate tended to be more health conscious than general users [28]. Thus, elderly, disabled, and student users tended to give up transit use more than general users during the COVID-19 pandemic. The Shapley

values for arrival time and departure time were found to have the least impact on the transit mode choice. These results indicated that the user's departure or arrival time did not significantly affect transit use.

Overall, transit mode preferences were analyzed using eight features, and the impact of each feature was explained. Especially, the presence of COVID-19 had the greatest impact on users that gave up transit use. The impacts of the number of transfers, travel time, and fare on the transit use were also derived from the results, which were consistent with common sense.

4.4. Feature Dependency Analysis of Transit Mode Choice. Travel time was selected as a feature to interpret its impact on transit use since it is one of the most important features to analyze user behavior [1]. Travel time was also the most persuasive to compare the Shapley value by transit modes, since other variables, that is, number of transfers and fare, could vary depending on the modes. The results of feature dependency analysis with travel time and transit use choices, given-up, and transit use were drawn in Figure 5.

In Figure 5(a), subway travel time was selected as a feature to interpret its impact on users who gave up or used the subway during the COVID-19 pandemic. The red points within Circle (1) represent users that gave up transit during the COVID-19 pandemic, and the blue points within Circle (2) represent transit users. Circle (1) described that the Shapley values decreased as subway travel time decreased. The red trips within Circle (1) show the relationship between subway travel time and the Shapley value of subway travel time during the COVID-19 pandemic. The trend for the impact of travel time on subway users was illustrated by a red line. During the COVID-19 pandemic, users tended to give up the subway trip as the travel time increased. The sensitivity of travel time for subway use was estimated to be the highest among that of the transit modes, for example, bus and both modes. The difference between sensitivities of given-up users and transit users was estimated to be the lowest among that of the other modes.

In Figure 5(b), bus travel time was selected as a feature to interpret its impact on users who gave up or used the bus during the COVID-19 pandemic. Circle (3) illustrates the relationship between the travel time of given-up users and Shapley value of travel time. Circle (4) illustrates the relationship between the travel time of transit users and the Shapley value of the travel time. The Shapley value of bus travel time showed that the Shapley value decreased as travel time increased. The trend of the impact of travel time on bus users was illustrated by a red line. During the COVID-19 pandemic, users also tended to give up bus trips as travel time increased. The sensitivity of the travel time for bus use was estimated to be the second-highest among that of the transit modes, for example, subway and both modes.

In Figure 5(c), the travel time of both modes (bus + subway) was selected as a feature to interpret its impact on users who gave up or used both modes during the COVID-19 pandemic. Circle (5) illustrates the relationship between the travel time of given-up users and Shapley value of the travel time. Circle (6) illustrates the relationship between the travel time of transit users and Shapley value of the travel time. Circles (5) and (6) illustrate that the Shapley values decreased as the travel time of both modes increased. The trend of the impact of travel time on both modes users was illustrated by a red line. This result indicated that users did not prefer both modes during the COVID-19 pandemic. However, the sensitivity of the travel time of both modes use was estimated to be very low compared to that of subway and bus.

The overall impact of travel time on transit users is shown in Figure 5(d). Circle (7) illustrates the relationship between the travel time of given-up users and Shapley value of the travel time. Circle (8) illustrates the relationship between the travel time of transit users and Shapley value of travel time. The result of the dependency analysis with the travel time feature indicated that the probability of transit use decreased as travel time increased. Especially, these tendencies in travel time were shown to be more evident for the users that gave up use. Travel time sensitivity was estimated to be high in the order of subway, bus and both modes use. The difference between the sensitivity of given-up and transit users was estimated to be 1.34, 1.69, and 1.88 times, respectively, using linear regression. The difference between the sensitivity of given-up and transit users was high in the order of both modes, bus and subway use. The slopes of the trend line of bus and both modes decreased sharply. These results reflect the behavior of users avoiding spending long travel times in a transit mode due to concerns about infection during the COVID-19 pandemic [5]. These results also implied that the users more easily give up the use of a bus or both modes compared to subway use as travel time increased.

4.5. Discussion. Many countries around the world have implemented policies for the public transportation system as the demand for transit decreased during the COVID-19 pandemic. Specifically, the transit demand in Seoul has been reduced by about 30% during the COVID-19 pandemic. Thus, the government of Seoul considered shortening and reducing the hours of service and dispatching of transit services, respectively. In terms of these practical issues in Seoul, the O-D pairs where the potential for high given-up of transit use was explored using the proposed XGB model. The demand estimation during COVID-19 was performed, and the given-up ratio was calculated for each administrative unit, such as Dong unit. Here, the given-up ratio means a reduction ratio of estimated number of O-D trips during COVID-19 pandemic compared to O-D trips in 2019.

Figure 6 shows the results of the O-D pairs where the potential for high given-up of transit use. The results showed that Jongro and Gangnam areas were the most potential for high given-up of transit use. Specifically, the number of O-D trips between Jongro and Gangnam significantly decreased with a given-up ratio of 0.7~1.0. However, the number of trips from suburban to Jongro or Gangnam was not decreased with a given-up ratio of 0.0~0.2. These results implied that transit use was mostly given-up in the O-D pairs

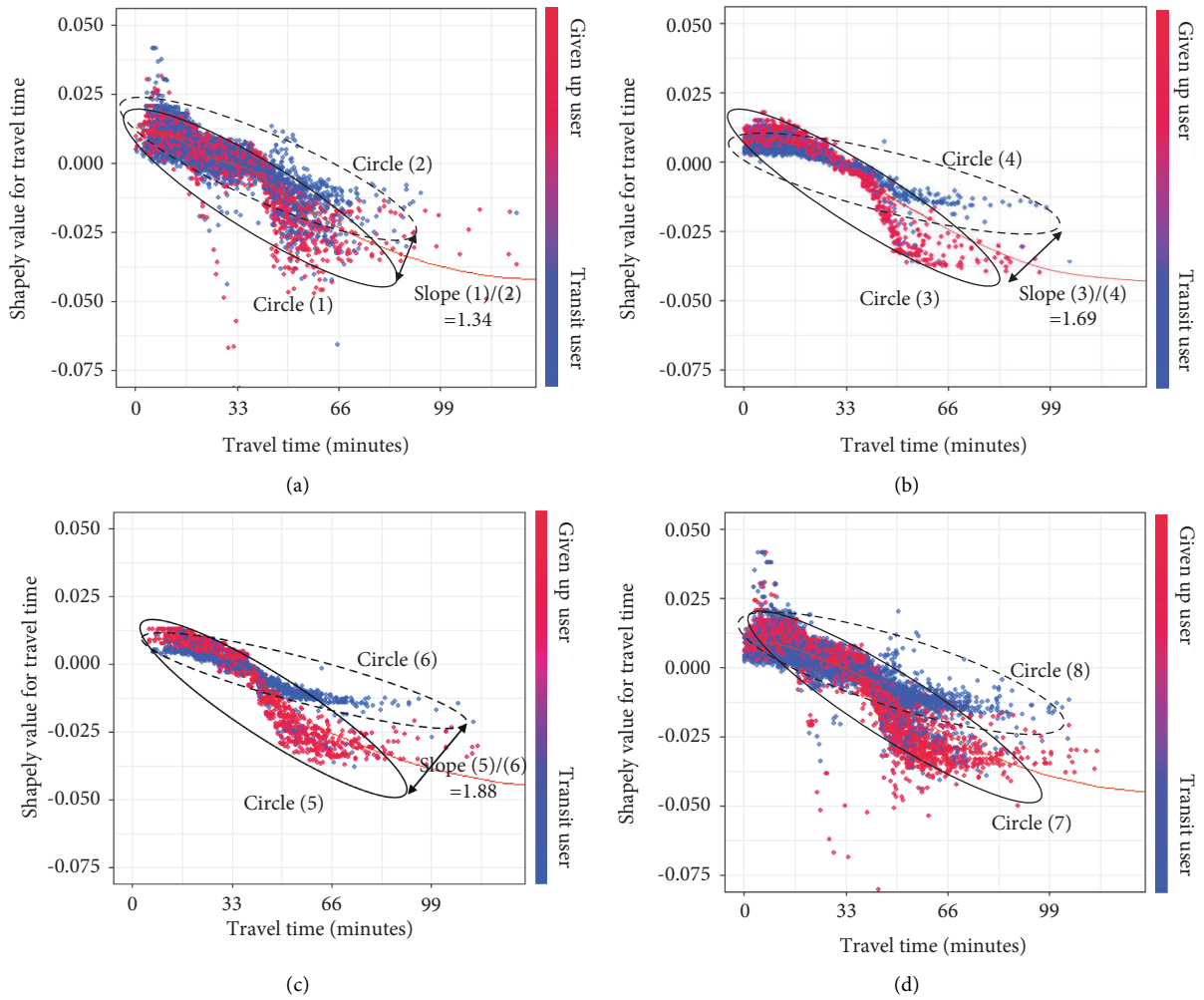

Figure 5: Result of feature dependency analysis. (a) Impact of travel time on subway users during COVID-19 pandemic. (b) Impact of travel time on bus users during COVID-19 pandemic. (c) Impact of travel time on both modes users during COVID-19 pandemic. (d) Overall impact of travel time on transit users during COVID-19 pandemic.

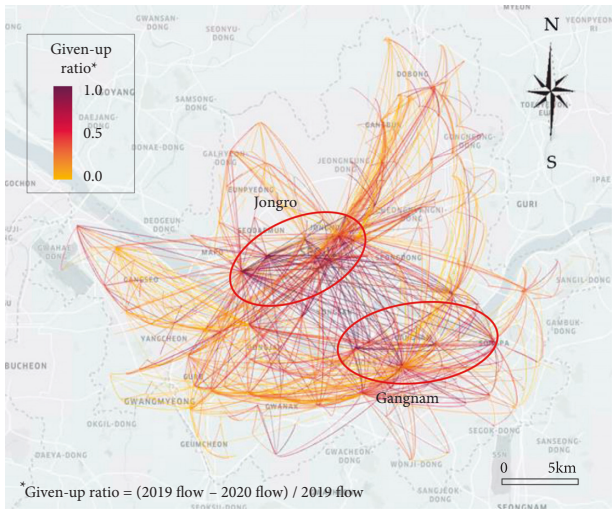

Figure 6: O-D pairs where the potential for high given-up of transit use.

connecting central areas, for example, Jongro and Gangnam, but users still used transit from residential areas to the central areas. From this implication, it could be inferred that users maintain single-purpose trips, such as work trips, but do not have additional business or leisure trips. In terms of transit operation, it is reasonable to reduce hours of service and dispatches of transit services in central areas. Specifically, the transit policies, for example, reduction of hours of service and dispatches of transit services, could be implemented regarding feeder buses in Gangnam and Jongro to improve the operation efficiency. Conversely, the main routes, for example, subway and trunk bus route, connecting the central areas and the suburban areas is not essential to be reduced since the number of trips was not decreased much as inner trips in the central area.

Overall, users tended to give up using transit services when they traveled within the central areas. Thus, it is reasonable to implement transit policies targeting feeder bus routes in central areas to improve operational efficiency.

5. Conclusion

This study aimed to understand the impact of COVID-19 on transit use. Analysis was conducted using two days of smart card data on days, for example, before and during COVID-19 pandemic. With data preprocessing, two alternatives, for example, given-up transit use during the COVID-19 pandemic and transit use, were considered in the choice set. The XGB model was used to train transit preference. Feature analysis based on SHAP was performed to interpret the estimation results from the proposed model. XGB was trained on 6,966,864 of 8,196,311 trips from smart card data and tested on the remaining 1,229,447 trips. The specificity, sensitivity, and balanced accuracy of the proposed model were 0.909, 0.953, and 0.931, respectively. The proposed model was found to be suitable for exploring the impact of COVID-19 on transit use. Feature analysis was performed to explore the impacts of the features on transit use with Shapley values. The number of O-D trips feature was found to impact substantially influence users that gave up transit. Feature dependency analysis was also performed, and the impacts of travel time of the model were identified and interpreted by transit modes. The dependency analysis showed that users gave up transit use as travel time increased. These tendencies in travel time were more evident during the COVID-19 pandemic.

The remarkable performance of XGB supported its ability to estimate the impact of the COVID-19 on transit use. The hyperparameters obtained by the cross-validation conserved the steady low learning error rates in the training of the model. It also derived robust results in estimating transit use. Feature analysis with SHAP provided insights for the proposed model. The Shapley value estimated feature importance and the direction of the impacts. The Shapley value also identified the nonlinear joint impacts of features of the proposed model. There were several interesting findings, such as the COVID-19 pandemic impact on transit use could not be identified by other machine learning techniques. The findings of this study could potentially be helpful and provide implications for policymakers both in mitigating the spread of the disease and establishing appropriate policy that considers travel behavior during the pandemic. With the proposed XGB model, O-D pairs where the potential for high given-up of transit use was identified in terms of policy implementation. As a result, transit use was mostly given-up in the O-D pairs connecting central areas, for example, Jongro and Gangnam. This result implied that it is desirable to implement transit policies targeting feeder bus routes in central areas to improve operational efficiency.

Although the proposed model established notable performance on the estimation of transit use considering users that gave up transit during the COVID-19 pandemic, it would be desirable to consider other external attributes or variables, for example, land-use and sociodemographic features. Understanding additional features would provide a variety of perspectives regarding the impact of the COVID-19 pandemic.

Data Availability

The data used in this research are provided by the Trlab research program conducted at the Seoul National University, Seoul, Republic of Korea. The data are available when readers ask the authors for academic purposes.

Conflicts of Interest

The author declares that there are no conflicts of interest regarding the publication of this article.

Authors' Contributions

Eun Hak Lee conceptualized the study, provided software, wrote the original draft, investigated the study, visualized the study, and validated the study.

References

[1] M. Abdullah, C. Dias, D. Muley, and M. Shahin, "Exploring the impacts of COVID-19 on travel behavior and mode preferences," *Transportation Research Interdisciplinary Perspectives*, vol. 8, p. 100255, 2020.

[2] C. Eisenmann, C. Nobis, V. Kolarova, B. Lenz, and C. Winkler, "Transport mode use during the COVID-19 lockdown period in Germany: the car became more important, public transport lost ground," *Transport Policy*, vol. 103, pp. 60–67, 2021.

[3] N. Askitas, K. Tatsiramos, and B. Verheyden, "Lockdown strategies, mobility patterns and covid-19," 2020, http://arxiv.org/abs/2006.0053.

[4] M. U. G. Kraemer, C. H. Yang, B. Gutierrez et al., "The effect of human mobility and control measures on the COVID-19 epidemic in China," *Science*, vol. 368, no. 6490, pp. 493–497, 2020.

[5] G. Parady, A. Taniguchi, and K. Takami, "Travel behavior changes during the COVID-19 pandemic in Japan: analyzing the effects of risk perception and social influence on going-out self-restriction," *Transportation Research Interdisciplinary Perspectives*, vol. 7, p. 100181, 2020.

[6] J. De Vos, "The effect of COVID-19 and subsequent social distancing on travel behavior," *Transportation Research Interdisciplinary Perspectives*, vol. 5, p. 100121, 2020.

[7] M. de Haas, R. Faber, M. Hamersma, and M. Hamersma, "How COVID-19 and the Dutch 'intelligent lockdown'change activities, work and travel behaviour: evidence from longitudinal data in The Netherlands," *Transportation Research Interdisciplinary Perspectives*, vol. 6, p. 100150, 2020.

[8] A. Shamshiripour, E. Rahimi, R. Shabanpour, and A. K. Mohammadian, "How is COVID-19 reshaping activity-travel behavior? Evidence from a comprehensive survey in Chicago," *Transportation Research Interdisciplinary Perspectives*, vol. 7, p. 100216, 2020.

[9] X. Qu and K. Gao, "Impacts of COVID-19 on the transport sector and measures as well as recommendations of policies and future research: a report on sig-C1 transport theory and modelling," *SSRN Electronic Journal*, pp. 1–12, 2020.

[10] S. Hu, C. Xiong, M. Yang, H. Younes, W. Luo, and L. Zhang, "A big-data driven approach to analyzing and modeling human mobility trend under non-pharmaceutical interventions during COVID-19 pandemic," *Transportation Research Part C: Emerging Technologies*, vol. 124, p. 102955, 2021.

[11] K. M. Kim, S. P. Hong, S. J. Ko, and J. H. Min, "Predicting express train choice of metro passengers from smart card data," *Transportation Research Record*, vol. 2544, no. 1, pp. 63–70, 2016.

[12] E. H. Lee, I. Lee, S. H. Cho, S. Y. Kho, and D. K. Kim, "A travel behavior-based skip-stop strategy considering train choice behaviors based on smartcard data," *Sustainability*, vol. 11, no. 10, p. 2791, 2019.

[13] L. Jánošíková, J. Slavík, and M. Kohání, "Estimation of a route choice model for urban public transport using smart card data," *Transportation Planning and Technology*, vol. 37, no. 7, pp. 638–648, 2014.

[14] E. H. Lee, K. Kim, S. Y. Kho, D. K. Kim, and S. H. Cho, "Estimating express train preference of urban railway passengers based on extreme gradient boosting (XGBoost) using smart card data," *Transportation Research Record*, vol. 34, p. 213214, 2021.

[15] F. Wang and C. L. Ross, "Machine learning travel mode choices: comparing the performance of an extreme gradient boosting model with a multinomial logit model," *Transportation Research Record*, vol. 2672, no. 47, pp. 35–45, 2018.

[16] E. H. Lee, H. Lee, S. Y. Kho, and D. K. Kim, "Evaluation of transfer efficiency between bus and subway based on data envelopment analysis using smart card data," *KSCE Journal of Civil Engineering*, vol. 23, no. 2, pp. 788–799, 2019.

[17] E. H. Lee, H. Shin, S. H. Cho, S. Y. Kho, and D. K. Kim, "Evaluating the efficiency of transit-oriented development using network slacks-based data envelopment analysis," *Energies*, vol. 12, no. 19, p. 3609, 2019.

[18] E. H. Lee, K. Kim, S. Y. Kho, D. K. Kim, and S. H. Cho, "Exploring for route preferences of subway passengers using smart card and train log data," *Journal of Advanced Transportation*, pp. 1–14, 2022.

[19] B. Barabino, C. Lai, and A. Olivo, "Fare evasion in public transport systems: a review of the literature," *Public Transport*, vol. 12, no. 1, pp. 27–88, 2020.

[20] B. Barabino, S. Salis, and B. Useli, "Fare evasion in proof-of-payment transit systems: deriving the optimum inspection level," *Transportation Research Part B: Methodological*, vol. 70, pp. 1–17, 2014.

[21] T. Chen and C. G. Xgboost, "A scalable tree boosting system," in *Proceedings of the 22nd acm sigkdd international conference on knowledge discovery and data mining*, pp. 785–794, New York, NY ACM 2016, 2016.

[22] A. B. Parsa, A. Movahedi, H. Taghipour, S. Derrible, and A. K. Mohammadian, "Toward safer highways, application of XGBoost and SHAP for real-time accident detection and feature analysis," *Accident Analysis & Prevention*, vol. 136, p. 105405, 2020.

[23] S. M. Lundberg and S. I. Lee, "A unified approach to interpreting model predictions," in *Advances in Neural Information Processing Systems*, pp. 4765–4774, 2017.

[24] E. Štrumbelj and I. Kononenko, "Explaining prediction models and individual predictions with feature contributions," *Knowledge and Information Systems*, vol. 41, no. 3, pp. 647–665, 2014.

[25] L. S. Shapley, "A value for n-person games," *Contributions to the Theory of Games*, vol. 2, no. 28, pp. 307–317, 1953.

[26] S. Hu and P. Chen, "Who left riding transit? Examining socioeconomic disparities in the impact of COVID-19 on ridership," *Transportation Research Part D: Transport and Environment*, vol. 90, p. 102654, 2021.

[27] S. H. Cho and H. C. Park, "Exploring the behaviour change of crowding impedance on public transit due to COVID-19 pandemic: before and after comparison," *Transportation Letters*, vol. 13, no. 5-6, pp. 367–374, 2021.

[28] C. Guida and G. Carpentieri, "Quality of life in the urban environment and primary health services for the elderly during the Covid-19 pandemic: an application to the city of Milan (Italy)," *Cities*, vol. 110, p. 103038, 2021.

Hindawi
Journal of Advanced Transportation
Volume 2022, Article ID 7239464, 17 pages
https://doi.org/10.1155/2022/7239464

Review Article

Analytical Methods and Determinants of Frequency and Severity of Road Accidents: A 20-Year Systematic Literature Review

Carlos M. Ferreira-Vanegas, Jorge I. Vélez, and Guisselle A. García-Llinás

Universidad Del Norte, Barranquilla, Colombia

Correspondence should be addressed to Carlos M. Ferreira-Vanegas; ferreirac@uninorte.edu.co and Guisselle A. García-Llinás; gagarcia@uninorte.edu.co

Received 7 April 2022; Accepted 10 June 2022; Published 8 July 2022

Academic Editor: Elżbieta Macioszek

Copyright © 2022 Carlos M. Ferreira-Vanegas et al. This is an open access article distributed under the Creative Commons Attribution License, which permits unrestricted use, distribution, and reproduction in any medium, provided the original work is properly cited.

In this systematic literature review (SLR), we use a series of quantitative bibliometric analyses to (1) identify the main papers, journals, and authors of the publications that make use of statistical analysis (SA) and machine learning (ML) tools as well as technological elements of smart cities (TESC) and Geographic Information Systems to predict road traffic accidents (RTAs); (2) determine the extent to which the identified methods are used for the analysis of RTAs and current trends regarding their use; (3) establish the relationship between the set of variables analyzed and the frequency and severity of RTAs; and (4) identify gaps in method use to highlight potential areas for future research. A total of 3888 papers published between January 2000 and June 2021, distributed in four clusters—RTA + HA + SA (SA, $n = 399$); RTA + HA + ML (ML, $n = 858$); RTA + HA + SC (TESC, $n = 2327$); and RTA + HA + GIS (GIS, $n = 304$)—were analyzed. We identified *Accident Analysis and Prevention* as the most important journal, Fred Mannering as the main author, and The Statistical Analysis of Crash-Frequency Data: A Review and Assessment of Methodological Alternatives as the most cited publication. Although the negative binomial regression method was used for several years, we noticed that other regression models as well as methods based on deep learning, convolutional neural networks, transfer learning, 5G technology, Internet of Things, and intelligent transport systems have recently emerged as suitable alternatives for RTA analysis. By introducing a new approach based on computational algorithms and data visualization, this SLR fills a gap in the area of RTA analysis and provides a clear picture of the current scientific production in the field. This information is crucial for projecting further research on RTA analysis and developing computational and data visualization tools oriented to the automation of RTA predictions based on intelligent systems.

1. Introduction

Road traffic accidents (RTAs) are one of the leading causes of death in all age groups and the first cause in people aged 15–29 years. About 1.3 million people die annually on the world's roads as a result of road traffic accidents [1]. According to a report published by the World Health Organization in December 2018 [2], progress has been insufficient in addressing the lack of safety on the world's roads. The Americas account for 11% of global road deaths, and the death rate is 15.6 per 100,000 people annually. In the last decade, the trend in Africa and Southeast Asia is incremental, while in Europe, America, and Oceania is stable [2]. After Brazil, Colombia is the South American country with the highest number of road accident fatalities; 3629 people died in traffic accidents between January and July 2019 [3].

There is a current trend in several cities around the world to take advantage of technology to develop and monitor their daily activities, from which the term "intelligent city" derives. According to the European Union smart city model [4], a city is considered intelligent if it has at least one initiative that addresses one or more of the following characteristics: smart economy, smart people, smart mobility, smart environment, smart governance, and/or smart living. These characteristics, especially smart mobility, can provide data that facilitates the analysis of RTAs [5].

Since 2009, the interest of researchers in this area to comprehensively analyze, predict, and prevent RTAs has led

to the use of various statistical models, including the logit, probit, Poisson, and Binomial Negative Regression models [6]. These statistical models have good theoretical interpretability, which allow a direct and clear understanding of the relationship between the frequency and/or severity of accidents and the variables analyzed. However, their main drawback is that they consider a linear relationship between risk factors and accident frequency, which may not be suitable in most cases [7]. Other assumptions of these models are very specific such independence between variables and normal distribution of the data, which are also difficult to satisfy in the real world [8].

Recently, models based on machine learning (ML), which include classification models, deep learning, artificial neural networks, random forest, and support vector machines (SVMs), have also been used for this purpose [9, 10]. ML-based models require no assumptions or prior knowledge, can automatically extract useful information from the dataset, and systematically deal with process outliers and missing values [8]. One of the main disadvantages of ML models is their "black box" approach nature, which limits their direct and clear interpretation of the results compared to statistical models [7].

At present, it is possible to analyze large amounts of publications related to RTAs using several bibliometric tools such as VOSviewer® [11]. Through text mining and mapping, VOSviewer allows to build and visualize bibliometric networks, which include individual journals, researchers, or publications, built on the basis of the number of citations each publication has [11]. Another approach is the use of R [12], one of the most powerful and flexible statistical software environments, jointly with the Bibliometrix [13] and causalizeR [14] packages, which facilitate a comprehensive bibliometric analysis using quantitative research. Via word processing algorithms, it is possible to extract causal links within a group of papers of interest based on simple grammar rules, which can subsequently be used to synthesize evidence in unstructured texts in a structured way [14]. These tools allow to perform analyzes based on the title, author, abstract, keywords, and references of the set of publications of interest.

In this SLR, we use quantitative bibliometric analysis to (1) identify the most cited research papers, journals, authors, and methods that contribute to the state of the art of RTA analysis based on statistical techniques, ML, technological elements of smart cities, and geographic information systems, such that they can be referred to new research related to RTA; (2) determine to what extent the methods identified for the analysis of RTAs and the variables included in the main publications are used to recognize current trends regarding their use; (3) establish the relationship between the set of variables analyzed and the methods applied and hence determine the variables with the highest incidence in the frequency and severity of RTAs so that it can be specified in what type of studies these critical variables have been analyzed; and (4) identify gaps, that is, methods and/or variables that have not been sufficiently scrutinized, with the aim of raising possible problems and areas of further research. In Section 2, we describe the methods and infometric tools used to analyze the selected literature, and in Section 3, the main results are presented. Finally, we discuss our findings and identify promising lines of research.

2. Materials and Methods

2.1. Searching for Publications. A search for publications on the Web of Science (WOS, URL: https://www.webofknowledge.com) was conducted. WOS is an online platform that contains databases of bibliographic information and resources for obtaining and analyzing such information, in order to study the performance of research, and whose purpose is to provide analysis tools that allow the assessment of its scientific quality. Through WOS, it is possible to have access to one or several databases simultaneously. The content of WOS is wide, and its high quality allows it to be a reference in the academic and scientific field [10].

After accessing WOS, we generated the search in the "Web of Science Core Collection" in the categories "Road Traffic Accident or Highway Accident and Statistical Analysis," "Road Traffic Accident or Highway Accident and Machine Learning," "Road Traffic Accident or Highway Accident and Smart Cities," and "Road Traffic Accident or Highway Accident and Technological Elements of Smart Cities (TESC)." Each of these terms corresponds to the consulted categories or *clusters* in this document. For each cluster, a new search was made by cluster, which groups the publications of the corresponding consulted categories. The result of each search was exported to text files using the "Full Record and References Cited" option. These files were exported without format and BibTeX as required by VOSviewer® [15] and the Bibliometrix [13] package of R [16], respectively.

2.2. Definition of Clusters. A total of 3888 papers published between January 1, 2000 and June 30, 2021 related to road traffic accidents or highway accident (RTA + HA) were identified after using the string "road traffic accident" or "highway accident" or "road safety" or "road crash" or "crash injury." After adding the terms "statistical analysis" or "Poisson regression" or "negative binomial regression" or "ordered probit regression" or "tobit regression" or "kernel density estimation" or "Bayesian networks," publications were filtered and included as part of the RTA + HA + SA cluster ($n = 399$, 10,26%). Similarly, publications in the RTA + HA + ML cluster ($n = 858$, 22,06%) were included after adding the terms "machine learning" or "classification model" or "regression model" or "data mining" or "support vector machine" or "svm" or "neural networks" or "neural network" or "ann" or "deep learning" or "Big data" or "Decision Tree" or "random forest" or "supervised learning" or "regression analysis." Publications in the RTA + HA + SC cluster ($n = 2327$, 59,85%) were filtered after adding the terms "smart city" or "smart cities" or "intelligent transportation systems" or "its" or "vehicular ad hoc networks" or

"vanets" or "wireless sensor networks" or "wsn" or "internet of things" or "iot." Finally, filtering the original search by adding the terms "gis" or "geographic information system" or "geographic information systems" led to the identify publications in the RTA + HA + GIS ($n = 304$, 7,81%) cluster.

2.3. Bibliometric Analysis. The bibliometric analysis was performed using VOSviewer® [11], and the Bibliometrix [13] and causalizeR [14] packages for R [16]. VOSviewer® are a tool that uses the results of WOS searches to build and visualize bibliometric networks based on number of citations, bibliographic linkage, cocitations, or authorship relationships [17]. This procedure allows you to generate visualizations, using networks, of the most important publications, journals, and authors in the categories described above. With the information extracted from VOSviewer®, a graph is constructed that illustrates the number of publications in the last 20 years in each cluster, in addition to the graphical representation of the top 20 publications and the top 10 authors, journals, and methods through the use of R statistical software packages.

The Bibliometrix package provides several functions that allow to perform advanced bibliometric analysis using bibliographic data obtained from WOS [13]. Such analyses include the identification of countries with higher scientific production, authors with more experience, and the construction of dendrograms for statistical analysis methods and variables used to analyze RTA data.

Bibliometric information was graphically represented using a Sankey diagram [18], which helps to explore the relationship between publications, the methods used, and the variables analyzed. We considered variables related to road and environment factors (i.e., "ramps," "curve," "pavement," "visibility," "weather," "rain," "snow," and "traffic volume"), human factors (i.e., "gender," "age," "sex," "alcohol," "cell," "phone," and "seat belt"), characterization of the crash (i.e., "injury," "fatal," "severity," "week," "hour," "peak," and "year"), and vehicle's factors (i.e., "motorcycle," "truck," "car," and "pedestrian") as defined by Mannering et al. [19]. In addition, we included the following statistical methods widely used in RTA analysis: "Poisson Models" [20], "Binomial Negative Models" [21], "Kernel Functions" [22], "Probit Models," "Logit Models," [23], "Hotspot" [24], "Spatial Model," "Temporal Model" [25] "Regression Model," "Classification Model," "Neural Network" [26], "Clustering," "Bayesian Methods" [27], "Likert Scale" [28], "Image" [29], "Lidar," "GIS" [30], "Markov" [31], "GPS," "IoT" [32], and "Unobserved Heterogeneity" [33]. Based on the aforementioned categories, we used the causalizeR [14] package for R with the keywords "accident" and "severity" with the purpose of generating a diagram that synthesizes the grammatical rules creating causal links around the keywords, that is, identifying the variables that affect the frequency and severity of accidents. To the best of the authors' knowledge, this is the first study making use of methods implemented in the Bibliometrix and causalizeR packages to explore RTA-related publications.

3. Results

3.1. Scientific Production per Cluster. Figure 1 shows the number of publications per year for each cluster between January 2000 and June 2021. Our results suggest a similarity between the RTA + HA + SA and RTA + HA + GIS clusters. In particular, these clusters present a linear trend between 2000 and 2010, and a slightly incremental trend between 2010 and 2021. On the other hand, the number of publications in the RTA + HA + SC cluster increases exponentially from 2007, while those in the RTA + HA + ML cluster present the exponential trend from 2014. Interestingly, the peak in the number of publications occurred in 2020 for all clusters, except in RTA + HA + SC, which had it in 2018.

3.2. Bibliometric Analysis Based on Citations Ranking. Table 1 shows the top-20 most cited papers in each cluster, which are shown in Figure 2, where the journals in which they were published and the number of citations that each publication has is illustrated; Figure 2 also shows the main authors of each cluster, that is, the most cited. In the RTA + HA + SA cluster, the most cited papers are *The statistical analysis of crash-frequency data: A review and assessment of methodological alternatives* ($n = 885$, 22,13%) [33], *The statistical analysis of highway crash-injury severities: A review and assessment of methodological alternatives* ($n = 487$, 12,17%) [36], and *Unobserved heterogeneity and the statistical analysis of highway accident data* ($n = 468$, 11,7%) [19]. Regarding the most cited authors, these are *Fred Mannering* ($n = 2593$, 35,6%), *Dominique Lord* ($n = 1408$, 19,32%), and *Mohammed A. Quddus* ($n = 578$, 7,93%). On the other hand, the most cited journals are *Accident Analysis and Prevention* with 89 documents and 3513 (56,87%) citations, *Transportation Research Part A-Policy and Practice* with 4 documents and 915 (14,81%) citations, and *Analytic Methods in Accident Research* with 13 documents and 833 (13,48%) citations.

In the RTA + HA + ML cluster, the most cited papers are *Multilevel data and Bayesian analysis in traffic safety* ($n = 151$, 7,22%) [100], *A study of factors affecting highway accident rates using the random-parameters Tobit Model* ($n = 145$, 6,93%) [37], and *The red-light running behavior of electric bike riders and cyclists at urban intersections in China: An observational study* ($n = 128$, 6,12%) [40]. As for the most cited authors, these are *Helai Huang* ($n = 383$, 17,26%), *Mohammed Abdel* ($n = 340$, 15,32%), and *Mohammed A. Quddus* ($n = 298$, 13,42%). Similarly, the most cited journals are *Accident Analysis and Prevention* with 91 documents and 2735 (56,90%) citations; *Safety Science* with 12 documents and 413 (8,59%) citations, and *Journal of Safety Research* with 16 documents and 356 (7,4%) citations.

In the RTA + HA + SC cluster, the most cited papers are *A comprehensive survey on vehicular Ad Hoc network* ($n = 633$, 13,61%) [34], *Vehicular ad hoc networks (VANETS): status, results, and challenges* ($n = 475$, 10,21%) [38], and *Unobserved heterogeneity and the statistical analysis of highway accident data* ($n = 468$, 10,06%) [41].

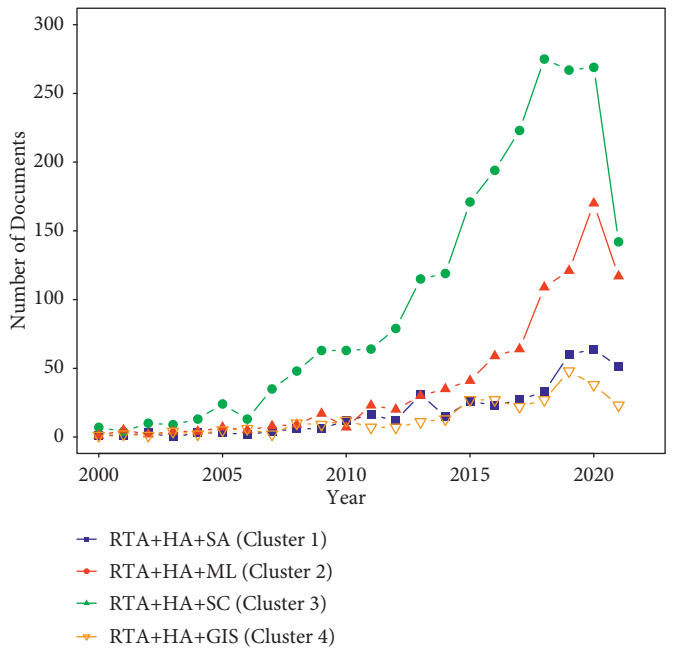

Figure 1: Time series of the scientific production of each cluster.

Table 1: Top 20 most cited papers in the clusters RTA + HA + SA, RTA + HA + ML, RTA + HA + SC, and RTA + HA + GIS.

Position	RTA + HA + SA	RTA + HA + ML	RTA + HA + SC	RTA + HA + GIS
1	Lord and Mannering [33], ($n = 885$)	Huang and Abdel-Aty [31], ($n = 151$)	Al-sultan et al. [34], ($n = 633$)	Anderson [35], ($n = 303$)
2	Savolainen et al. [36], ($n = 487$)	Anastasopoulos et al. [37], ($n = 145$)	Zeadally et al. [38], ($n = 475$)	Pu et al. [39], ($n = 205$)
3	Mannering et al. [19], ($n = 468$)	Wu et al. [40], ($n = 128$)	Mannering et al. [41], ($n = 468$)	Crawford et al. [42], ($n = 105$)
4	Anderson [35], ($n = 296$)	Mannering [43], ($n = 127$)	Whaiduzzaman et al. [44], ($n = 412$)	Plug et al. [45], ($n = 82$)
5	Anastasopoulos and Mannering [46], ($n = 187$)	Yan et al. [47], ($n = 126$)	Abboud et al. [48], ($n = 230$)	Betaille and Toledo-Moreo [49], ($n = 82$)
6	Bella [50], ($n = 164$)	Li et al. [51], ($n = 122$)	Hameed Mir and Filali [52], ($n = 210$)	Erdogan [5], ($n = 75$)
7	Jones et al. [53], ($n = 160$)	Kononen et al. [54], ($n = 118$)	Engoulou et al. [55], ($n = 209$)	Ng et al. [56], ($n = 74$)
8	Anastasopoulos et al. [37], ($n = 145$)	Cheng et al. [57], ($n = 114$)	Lei et al. [58], ($n = 199$)	Zou et al. [59], ($n = 66$)
9	de Ona et al. [27], ($n = 144$)	Kashani and Mohaymany [60], ($n = 107$)	Lal et al. [61], ($n = 199$)	Panter et al. [62], ($n = 62$)
10	Mannering [43], ($n = 127$)	Deck and Willinger [63], ($n = 103$)	Ibanez et al. [64], ($n = 168$)	Carver et al. [65], ($n = 52$)
11	Anastasopoulos et al. [66], ($n = 119$)	Schepers et al. [67], ($n = 98$)	Lin et al. [68], ($n = 166$)	Marshall and Garrick [69], ($n = 42$)
12	Martin [70], ($n = 113$)	Abellan et al. [71], ($n = 93$)	Wang et al. [72], ($n = 163$)	Mandic et al. [28], ($n = 41$)
13	Al-Sultan et al. [73], ($n = 102$)	Yu and Abdel-Aty [74], ($n = 91$)	Bitam et al. [75], ($n = 154$)	Soilan et al. [76], ($n = 41$)
14	Schepers et al. [77], ($n = 92$)	Zhang et al. [78], ($n = 91$)	Hadded et al. [79], ($n = 147$)	Lee et al. [80], ($n = 40$)
15	Wong et al. [81], ($n = 91$)	Montella et al. [82], ($n = 89$)	Anastasopoulos et al. [37], ($n = 145$)	Dissanayake et al. [83], ($n = 39$)
16	Al-Sultan et al. [84], ($n = 91$)	Montella [85], ($n = 84$)	Chen et al. [86], ($n = 142$)	Zhai et al. [87], ($n = 38$)
17	Zheng et al. [88], ($n = 89$)	Sohn and Lee [89], ($n = 80$)	Cheng et al. [90], ($n = 137$)	Yadav et al. [91], ($n = 35$)
18	Zheng et al. [88], ($n = 80$)	Erdogan [5], ($n = 75$)	Wang and Abdel-Aty [92], ($n = 135$)	Greasley [93], ($n = 33$)
19	Plug et al. [45], ($n = 80$)	Stallard and Smith [94], ($n = 74$)	Cailean and Dimian [95], ($n = 130$)	Eksler et al. [96], ($n = 33$)
20	Bella [97], ($n = 79$)	Ng et al. [56], ($n = 74$)	Fiore et al. [98], ($n = 128$)	Riveiro et al. [99], ($n = 32$)

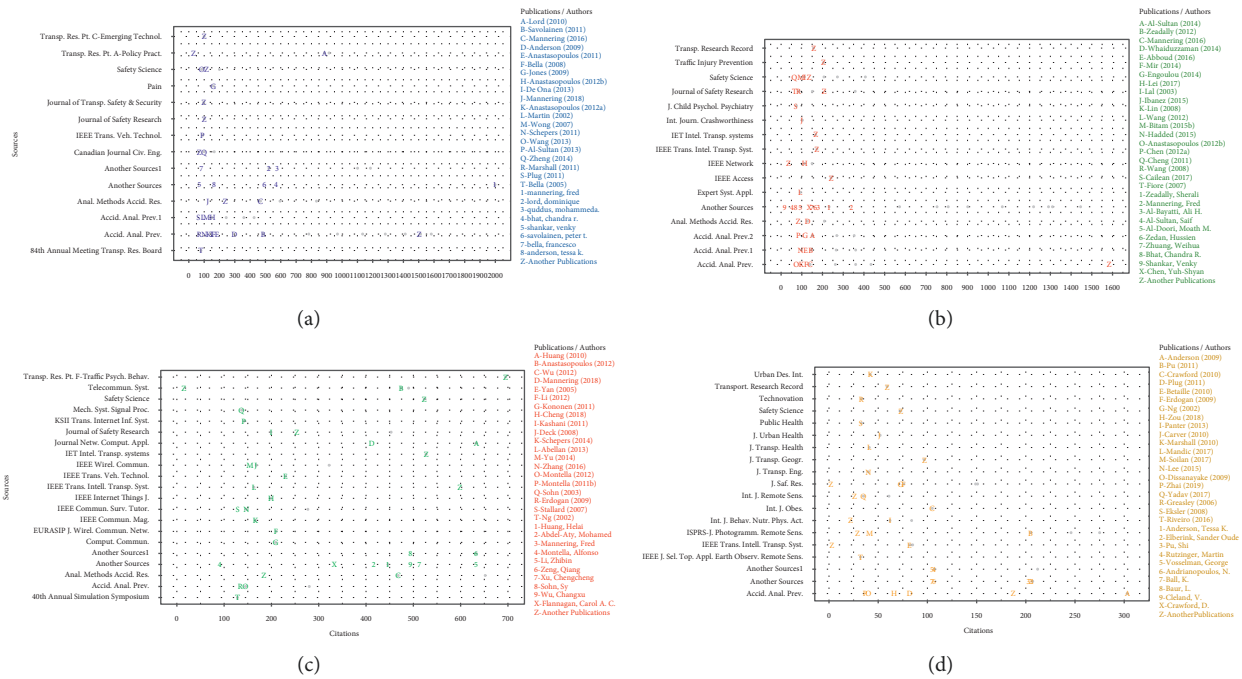

Figure 2: Most cited papers, authors, and journals for the (a) RTA + HA + SM, (b) RTA + HA + ML, (c) RTA + HA + SC, and (d) RTA + HA + GIS clusters.

Similarly, the most cited authors are *Sherali Zeadally* ($n = 921$, 14,15%), *Fred Mannering* ($n = 885$, 13,59%), and *Ali H. Al-Bayatti* ($n = 736$, 11,31%). The most cited journals are *Accident Analysis and Prevention* with 114 documents and 3083 (33,51%) citations, *Journal of Network and Computer Applications* with 2 documents and 1045 (11,35%) citations, and *IEEE Transactions on Vehicular Technology* with 28 documents and 970 (10,54%) citations.

In the RTA + HA + GIS cluster, the most cited papers are *Kernel density estimation and K-means clustering to profile road accident hotspots* ($n = 303$, 20,47%) [35], *Recognizing basic structures from mobile laser scanning data for road inventory studies* ($n = 205$, 13,85%) [39], and *The longitudinal influence of home and neighbourhood environments on children's body mass index and physical activity over 5 years: the CLAN study* ($n = 105$, 13,42%) [42]. As for the most cited authors, these are *Tesa K. Anderson* ($n = 303$, 18,38%), *Sander Oude Alberink* ($n = 205$, 14,43%), and *Shi Pu*($n = 205$, 14,43%). In addition, the most cited journals are *Accident Analysis and Prevention* with 22 documents and 715 (41,93%) citations, *ISPRS Journal of Photogrammetry and Remote Sensing* with 3 documents and 275 (16,13%) citations, and *Journal of Safety Research* with 4 documents and 151 (8,85%).

Overall, *Accident Analysis and Prevention* is the most cited journal in the four clusters, the *Journal of Safety Research and Safety Science* appears in the top 10 journals among all clusters, and *Analytic Methods in Accident Research* appears in the top 10 of the clusters RTA + HA + SA, RTA + HA + ML, and RTA + HA + SC as shown in Figure 2.

3.3. Methods of RTA Based on the Abstracts. Figure 3 shows word clouds based on the methods, mentioned in the abstracts, used to analyze the RTAs. In the RTA + HA + SA cluster (Figure 3(a)), the negative binomial regression has been used consistently for several years. Currently, Poisson regression, Bayesian networks, and kernel density estimation are used to a similar extent. In addition, the issue of Unobserved Heterogeneity is important number of studies within the RTA + HA + SA cluster. On the other hand, variables associated with human factors such as driving behavior and driving performance have been identified. According to our analyses, methods such as deep learning, convolutional neural networks, transfer learning, and computer vision correspond to the current trends in the RTA + HA + ML cluster (Figure 3(b)). On the other hand, the RTA + HA + SC cluster can be identified that the routing protocols were used before 2015, and sensors networks were frequently used between 2016 and 2018 (Figure 3(c)). Starting in 2019, 5G technologies, transport systems smartphones (ITSs), Internet of Things (IoT), and VANETS have been more frequently used (see Figure 3(c)). Finally, in the RTA + HA + GIS cluster, spatial analysis and kernel density estimation correspond to the methods with the highest usability for analyzing RATs (Figure 3(d)).

Figure 4 shows the 10 most used analytical methods for RTA analysis for each cluster. In the RTA + HA + SA cluster, the spatial-temporal models are shown as the main method, representing 20.67% of the methods, followed by the negative binomial models (16.82%) and machine learning methods (15.86%) (Figure 4(a)). As for the RTA + HA + ML cluster, neural network models (26.07%), general ML models (21.55%), and data mining techniques (11.42%) are the most frequently used techniques (Figure 4(b)). Regarding methods used to analyze RTAs in the RTA + HA + SC cluster (Figure 4(c)), we found that vehicular networks (48.05%),

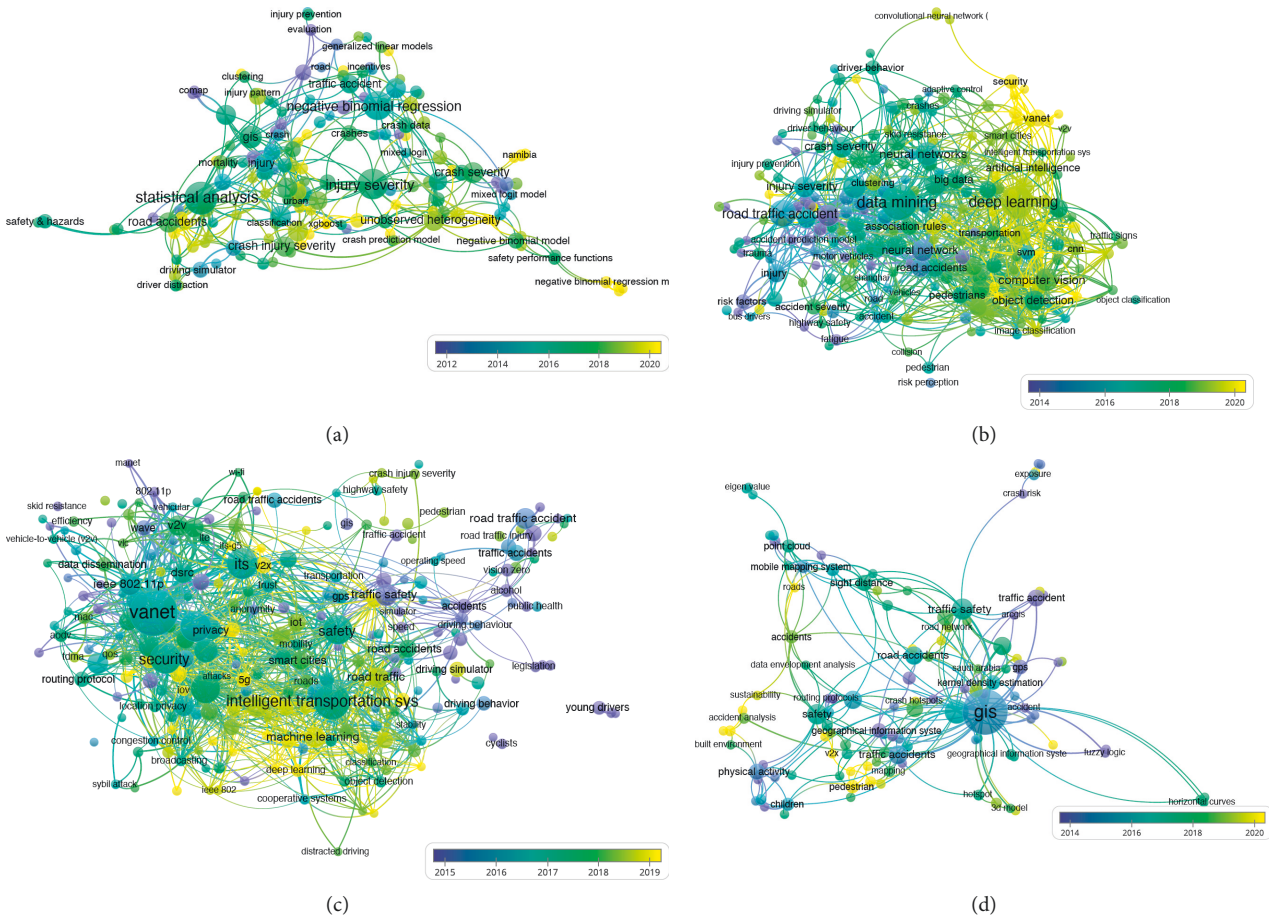

FIGURE 3: Wordclouds of the main analytical methods used for analyzing road traffic accidents in the (a) RTA + HA + SM, (b) RTA + HA + ML, (c) RTA + HA + SC, and (d) RTA + HA + GIS clusters.

intelligent transportation systems (20.92%), and Internet of Things (7%) are the most frequently used. Finally, in the RTA + HA + GIS cluster, spatial analysis (17.59%) is the method used more frequently, followed by kernel density estimation (13.88%) and hot spot analysis (13.88%) (Figure 4(d)).

Based on the information from the abstracts, three major topics were derived related to the strategies utilized for the analysis of RTAs (Figure 5). These topics, broadly speaking, include methods used to analyze RTAs, variables included to study RTAs, and indicators associated with road safety such as crash frequency, crash injury severity, fatalities, and mortality. In the RTA + HA + SA cluster, the first topic is defined by the identification and location of accidents using GIS and kernel density estimation methods; the second topic is mainly composed of variables associated with the environment, road geometry, alcohol use, age, severity (i.e., fatalities, mortality, injuries, etc.), and frequency, in addition to classic methods such as Poisson and negative binomial regression models; and the third topic includes methods such as multinomial logit models and logit models as well as unobserved heterogeneity, single-vehicle crashes, and SVM (Figure 5(a)). Similarly, in the RTA + HA + ML cluster, the first topic contains motor-vehicle-crashes analysis using regression model and Poisson regression and variables such as geometric design; the second topic includes frequency and severity analysis supported by SVM and logistic regression; and the third topic includes variables associated with frequency, severity, injuries, and prevalence, as well as other variables such as weather, design of the road, speed, age and behavior of the driver, and performance of preventive measures (Figure 5(b)). On the other hand, the first topic in the RTA + HA + SC includes, in general, RTA severity (i.e., traffic fatalities and mortality); the second topic includes technological elements associated with ITS; and the third topic includes a general list of technological elements used to collect road traffic data (Figure 5(c)). Finally, in the RTA + HA + GIS cluster, we identified walking, physical activity, and travel as the first topic; the second topic is defined by the identification and location of accidents using the kernel density estimation method; and the third topic includes classical regression and classification methods for RTA analysis (Figure 5(d)).

3.4. Relationship between Methods for RTAs and Variables Used Based on Papers' Methodologies. We identified that in the RHA + HA + SA cluster, the papers with the highest number of relationships are Wang et al. [81] with 5 methods and 18 associated variables, Savolainen et al. [36] with 9

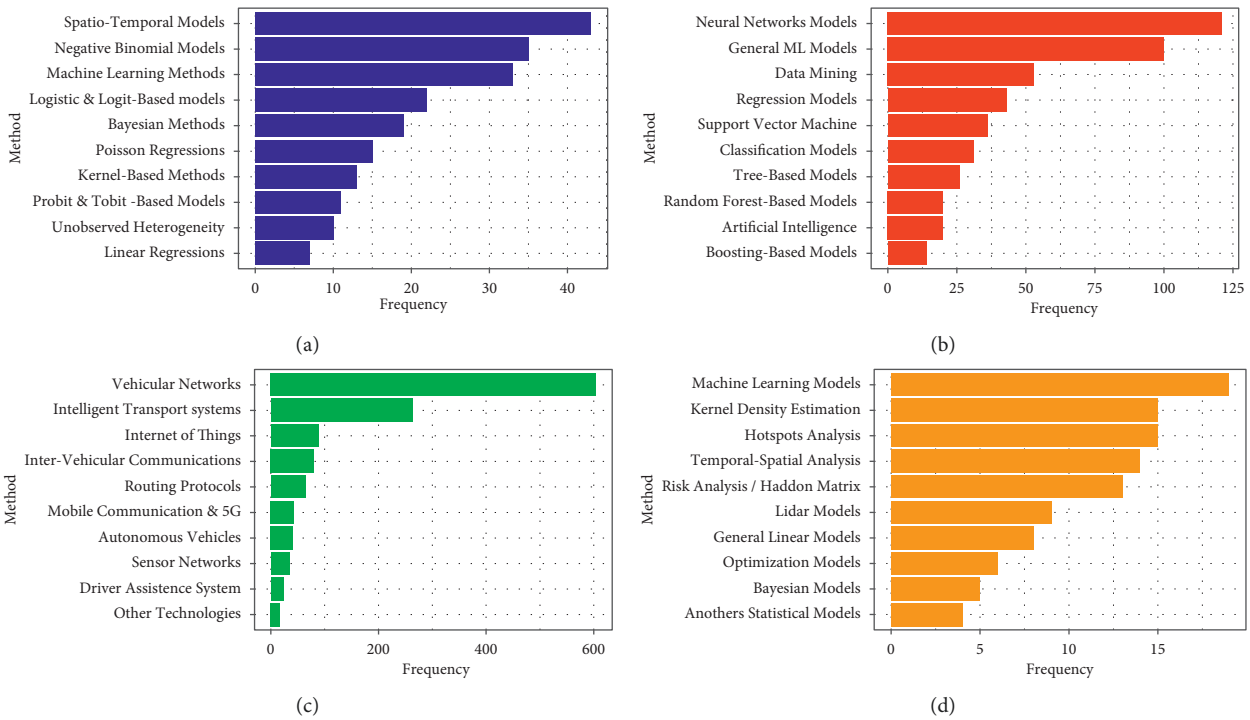

Figure 4: Top-10 methods for analyzing road traffic accidents and highway accidents (a) RTA + HA + SM, (b) RTA + HA + ML, (c) RTA + HA + SC, and (d) RTA + HA + GIS clusters.

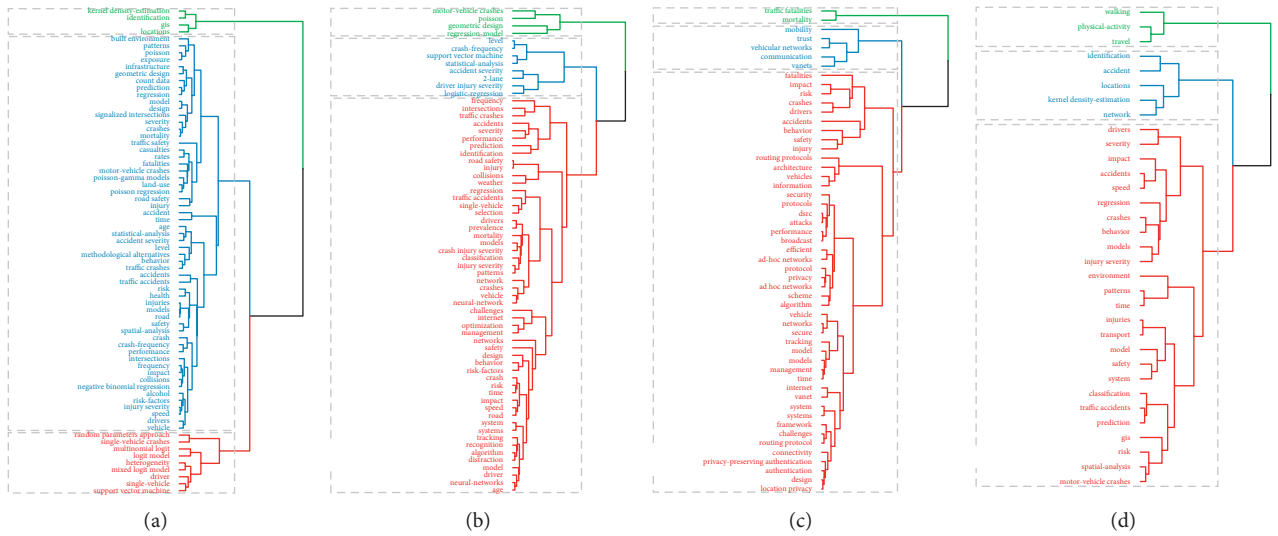

Figure 5: Dendrogram of main topics based on the analytical methods used for analyzing road traffic accidents in the (a) RTA + HA + SM, (b) RTA + HA + ML, (c) RTA + HA + SC, and (d) RTA + HA + GIS clusters.

methods and 14 associated variables and Lord & Mannering [33] with 9 methods and 10 associated variables (Figure 6(a)). According to our analysis, the most used models are regression models ($n = 12$ publications), spatial models ($n = 11$), binomial negative regression ($n = 10$), classification models ($n = 8$), and Poisson regression and temporal models ($n = 7$). The most used variables are "age" ($n = 20$), "year" ($n = 17$), "car" ($n = 14$), "severity" ($n = 13$), and "rain" ($n = 12$).

In the RHA + HA + ML cluster, the papers with the highest number of relationships are Mannering [43] with 13 methods and 13 associated variables, Montella [85] with one method and 14 associated variables, and Zhang et al. [78] with 2 methods and 11 associated variables (Figure 6(b)). The most used models are regression model ($n = 17$), classification model ($n = 8$), Bayesian model in ($n = 7$), and neural network and binomial negative regression ($n = 5$). The most used variables are "age" ($n = 20$),

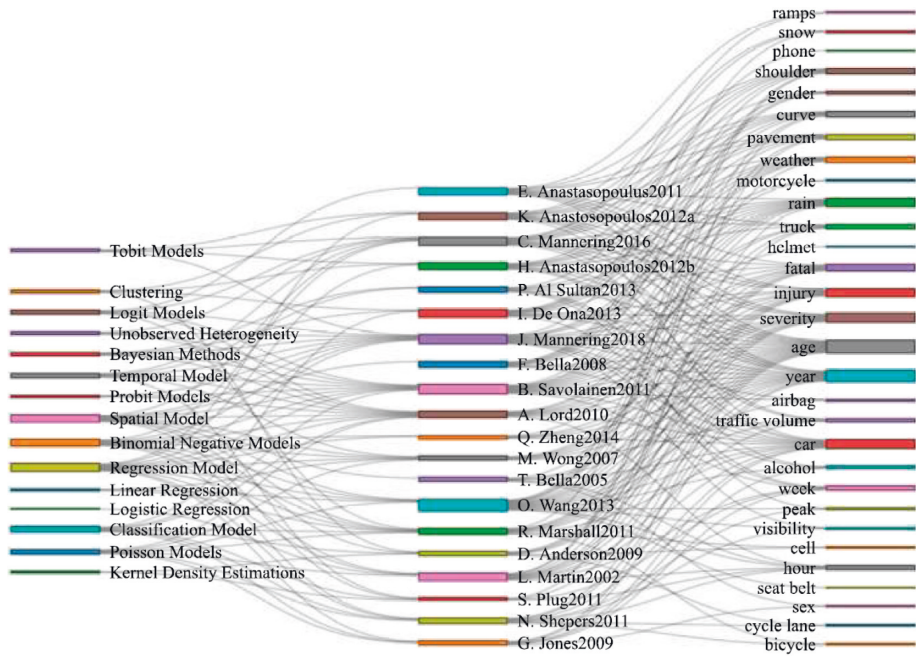

(a)

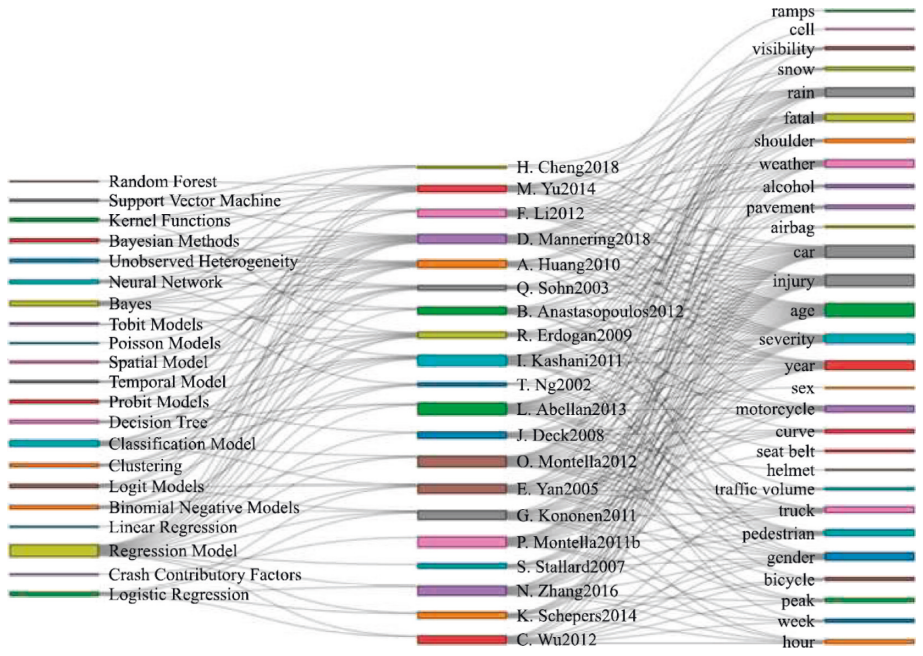

(b)

Figure 6: Continued.

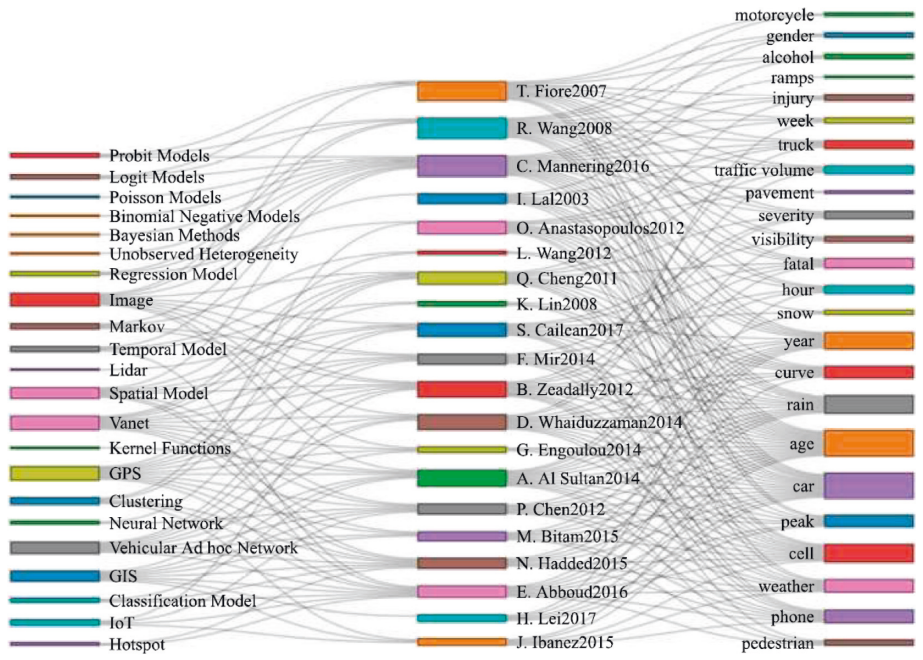

(c)

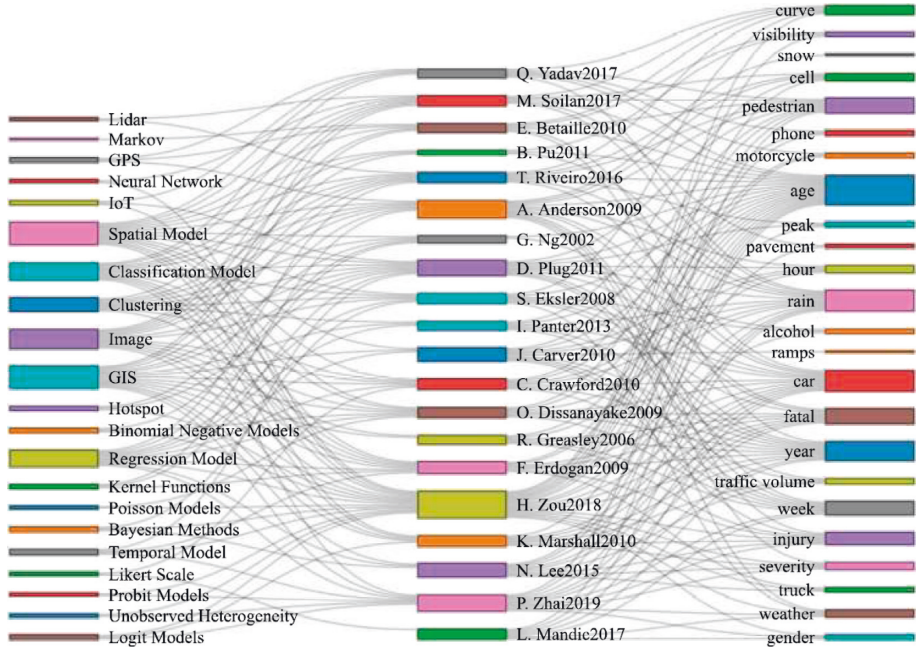

(d)

Figure 6: Graph Sankey–Ferreira, relationship between papers, methods, and variables (a) RTA + HA + SM, (b) RTA + HA + ML, (c) RTA + HA + SC, and (d) RTA + HA + GIS clusters.

"car" ($n = 18$), "injury" ($n = 16$), "year" ($n = 13$), and "rain" ($n = 12$).

On the other hand, the publications with the highest number of relationships in the RHA + HA + SC cluster are Mannering et al. [41] with 10 methods and 16 associated variables, Wang & Abdel-Aty [92] with 4 methods and 16 associated variables, and Fiore et al. [98] with 3 methods and 15 associated variables (Figure 6(c)). In this cluster, the most used models are VANETS ($n = 11$), GPS ($n = 11$), spatial model ($n = 8$) and GIS ($n = 8$), while the most used variables are "age" ($n = 20$), "car" ($n = 19$), "rain" ($n = 14$), "cell" ($n = 14$), "year" ($n = 13$), and "weather" ($n = 10$).

As for the RHA + HA + GIS cluster, the papers with the highest number of relationships are Zou et al. [59] with 14 methods and 18 associated variables, Anderson [35] with 7 methods and 12 associated variables, and Plug et al. [45] with 9 methods and 10 associated variables (Figure 6(d)). Regarding models for RTA analysis, the most frequently used models in this cluster are GIS ($n = 15$), spatial models ($n = 15$), image processing ($n = 13$), classification models

($n = 12$), regression models ($n = 11$), and clustering ($n = 9$). On the other hand, the variables mostly used are "age" ($n = 20$), "car" ($n = 14$), "rain" ($n = 14$), "year" ($n = 13$), and "pedestrian" ($n = 10$).

Overall, regression, classification, and spatial models are within the top-5 methods most frequently used to analyze RTAs in three of the four clusters analyzed. In addition, "age" is the variable most frequently analyzed with a total of 80 publications, while "car," "year," and "rain" correspond to the most analyzed in the publications included in the four clusters.

3.5. Variables Influencing the Frequency and Severity of RTAs Based on Papers' Abstracts. Figure 7 depicts the variables influencing the frequency and severity of RATs. In the RHA + HA + SA cluster, "age," "sex," "van," "model" (vehicle type), and "snowy" (presence of snow) can be identified as the main variables that increase the frequency of road accidents (Figure 7(a)). Conversely, "effective strategy" and "measure," which refer to the implemented road safety measures, are mitigating factors of the frequency of RTAs, and "helmet" (the use of a helmet) is identified as a factor that mitigates the severity of road accidents (Figure 7(a)). In addition, the main variables increasing RTA frequency in the RHA + HA + ML cluster are "age," "drink" (consumption of alcohol while driving), "mobile phone" (use of the mobile phone while driving), "speed" (excess speed), and "visibility," while "effective strategy" and "policy," which refer to the implemented road safety measures identified as mitigating factors (Figure 7(b)). Regarding severity, "helmet" (i.e., the use of a helmet) and "prevention strategy" are identified as factors that mitigate the RTA severity, while "age group" and "speed limit" (i.e., violation of the limits of speed) increase it (Figure 7(b)).

We found that "year," "vehicle" (type of vehicle), "mobility," "cannabis use" (use of cannabis while driving), and "angle" (crash angle) are the main variables increasing RTA frequency in the RHA + HA + SC cluster, while the mitigating factors of RTA frequency are "traffic safety" and "safety information" (Figure 7(c)). Interestingly, no factors affecting RTA severity were identified. On the other hand, we identified that "age," "car" (type of vehicle), "peak," and "noise" are the main variables increasing RTA frequency, while "strategy" and "policy" were identified as mitigating factors in the RHA + HA + GIS cluster (Figure 7(d)). Regarding RTA severity, "speed traffic" and "speed road" were identified as factors increasing it.

Overall, our analyses indicate that (1) variables such as "age" and those associated with the type of vehicle (i.e., "model," "car," "vehicle," or "van") are represented in three of the four clusters, and (2) variables that mitigate the frequency and severity of RTAs are related with the implementation of safety measures.

4. Discussion

The first goal of this systematic literature review (SLR) was to identify the most cited research papers, journals, authors, and methods that contribute to the state of the art of RTAs based on statistical analysis, machine learning (ML), technological elements of smart cities, and geographic information systems (GIS). As shown in Figure 1, an exponential growth can be observed from 2010 onwards, mainly in the RTA + HA + SC and RTA + HA + ML clusters. In the first cluster, this behavior may be due to the contribution of the Industry 4.0 revolution with technologies such as Internet of Things (IoT), intelligent transportation systems (ITSs), and wireless sensor networks (WSNs) [4] (Figure 4(c)). The exponential growth in the second cluster may be related to the appearance of processors capable of executing computational models with large databases [101]. The performance of the RTA + HA + SA and RTA + HA + GIS clusters is similar because the publications applying statistical models tend to rely on GIS to clearly and concisely show the results as previously discussed by [5]. Some publications using this strategy include Refs. [35, 39, 42], among others.

Zou & Vu [102] proposed four clusters to identify the main publications in road safety via scientometric analysis: *Cluster 1*: effects of driving psychology and behavior on road safety; *Cluster 2*: causation, frequency, and injury severity analysis of road crashes; *Cluster 3*: epidemiology, assessment, and prevention of road traffic injury; and *Cluster 4*: effects of driver risk factors on driver performance and road safety. Following this approach, in this SLR, we proposed the same number of clusters to analyze the frequency and severity of RTAs: *Cluster 1*: statistical analysis (RTA + HA + SA; $n = 399$, 10.26%), *Cluster 2*: machine learning (RTA + HA + ML; $n = 858$, 22.06%), *Cluster 3*: technological elements of smart cities (RTA + HA + SC; $n = 2327$, 59.85%), and *Cluster 4*: Geographic Information Systems (RTA + HA + GIS; $n = 304$, 7.81%). Figure 2 depicts the 20 most cited publications analyzing RTAs per cluster, which is in line with the proposal by Zou et al. [103] when analyzing the top 50 most cited publications in the journal *Accident Analysis and* Prevention. In this SLR, we identified that the most cited publications are the first three of the RHA + HA + SA cluster (i.e., Mannering et al. [104] with 885 citations, Savolainen et al. [36] with 487 citations and Mannering et al. [19] with 468 citations); and the first three of the RHA + HA + SC cluster (i.e., Al-Sultan et al. [34] with 633 citations, Zeadally et al. [38] with 475, Mannering et al. [41] with 468 citations, and Whaiduzzaman et a [44] with 412 citations (Figure 2). These publications have in common that they correspond to literature reviews, highlighting the importance of these type of publications for scientific production since they serve as a reference for exploring gaps in the literature and propose new research venues focused on expanding the frontier of knowledge. We strongly believe that these results constitute a valuable resource for future studies related to RTAs.

The most cited author is Fred Mannering, who presents four publications in the Journal Analytic Methods in Accident Research: *Unobserved heterogeneity and the statistical analysis of highway accident data* [41] with 523 citations and *Temporal instability and the analysis of highway accident data* [105] with 155 citations, in addition to *Big data, traditional data and the tradeoffs between prediction and*

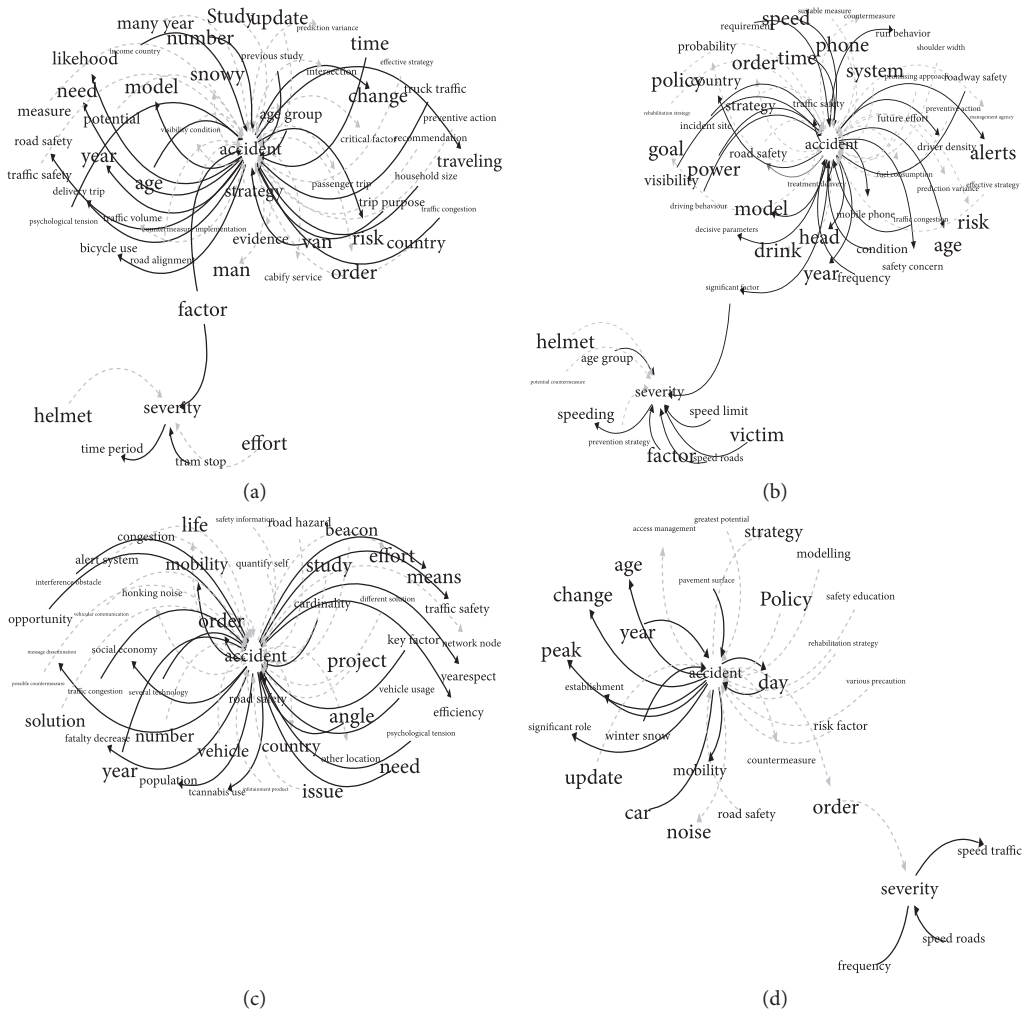

Figure 7: Variables related to the frequency and severity of road accidents for the (a) RTA + HA + SM, (b) RTA + HA + ML, (c) RTA + HA + SC, and (d) RTA + HA + GIS clusters. Here, solid dark arcs represent variables that contribute to the frequency and/or severity of road accidents, while gray arcs represent the variables that mitigate their frequency and/or severity.

causality in highway-safety analysis ($n = 26$) [104]. This article is not among the top 20 publications in any of the clusters but is part of this SLR and *Analytic methods in accident research: Methodological frontier and future directions* ($n = 722$) [106]. This last paper was not included in any of the clusters generated by Web of Science. These publications correspond to literature reviews that address advantages and disadvantages of the methods and variables used to model RTAs, as well as the problems and difficulties when applying specific methods. In addition, these publications highlight the importance of taking into account unobserved heterogeneity when predicting RTAs.

Other similar SLRs show the 50 most cited papers in the journal *Accident Analysis and Prevention* [103] and identified research papers with the greatest influence in the field of RTAs. The authors hypothesized that the oldest papers accumulate the greatest amount of citations, emphasizing that research papers from the 1990s and the first decade of 2010 are the most important [103]. In the present SLR, we contemplate other journals within this line of research and found the most cited papers are from 2010 onwards.

VOSViewer® has previously been used to identify clusters in which causality and accident frequency via co-occurrence of keywords [59], and to illustrate the methods, technological tools, and variables correlated with the frequency and severity of RTAs [103]. Here, we were able to distinguish that generalized linear models, mainly negative binomial regression and Poisson regression, have been widely used between the years 2012 and 2020 (Figure 3(a)). However, methods such as spatial analysis and the analysis of unobserved heterogeneity are of particular importance today (Figure 5(d)). Unobserved heterogeneity is understood as the error made by not including in the analysis of RTAs variables that are correlated with observable variables. In many cases, these "unobserved" variables are unknown by the analyst [41]. Although unobserved heterogeneity is not a method, it is a problem that must be addressed to improve the quality of the road accident prediction models.

In Figure 3(b), the most recently implemented methods in the RHA + HA + ML cluster are artificial intelligence, deep learning, CNN, transfer learning, and computer vision. We believe that these findings may be explained by the

development of GPUs [107] and next-generation processors. Similarly, in the RHA + HA + SC cluster, 5G, ITS-G5, V2X, deep learning technologies (Figure 3(c)) are emerging as suitable alternatives for collecting RTA data due to the development of technologies associated with the fourth industrial revolution.

In terms of variables considered when predicting frequency and severity of RTAs, we identified four main sources: variables related to human factors, variables related to climatological and road factors, variables defining vehicle-specific characteristics, and variables associated with accident characteristics (Figure 7). In Silva et al. (Silva, Andrade, & Ferreira), these four groups of variables were also identified. However, in the present SLR, we provide a key visualization that allows us to easily identify which variable was analyzed in each publication. Although this same group of variables was utilized by Mannering et al. [19] to textually describe the reason why each variable was part of the corresponding group and how it contributes to the occurrence of RTAs. We strongly believe that a graphical representation such as Figure 7 is useful for this type of analysis and facilitates a quick understanding of this important topic.

We identified that variables such as age or age group, sex, type of vehicle, and year contribute the most to the occurrence of RTAs and correspond to those frequently analyzed among the 80 papers highly cited papers for all cluster (Figures 2 and 6). In contrast, variables associated with human factors (i.e., the use of a helmet and driving under the influence of alcohol) and traffic congestion and visibility, which have been identified as one of the factors associated with the frequency and severity of RTAs (Figure 7), are also the less frequently analyzed variable in all clusters (Figure 6). The use of helmets as a mitigating factor in the severity of RTAs involving motorcyclists is observed in Savolainen et al. [36], while driving under the influence of alcohol is analyzed as a cause of RTAs in Mannering et al. [105]. On the other hand, the analysis of the use of a mobile phone and its incidence on the frequency and severity of RTAs is even rarer; it has been proven that manipulating the cell phone while driving causes serious RTAs [108]. Figure 6 summarizes the methods and variables most frequently used to analyze RTAs across all research papers identified in this SLR. In all clusters, the use of a mobile phone has not been analyzed as a cause of RTAs but as a tool for communication, that is, to create VANETS as evidenced in 14 out of the 20 research papers comprising the RTA + HA + SC cluster (Figure 6(a)). Another variable that reduces the severity of RTAs is the use of seat belts by drivers and passengers of automobiles [108]. Unfortunately, this variable is only analyzed in 3 of the 80 main studies (Table 1 and Figure 2).

Another important aspects of this SLR is the use of quantitative tools for analyzing research papers covering the analytical tools used to assess RTAs and the development of specific visualizations. In particular, Figure 2 shows the top 80 highly cited publications and Figure 6 connects them with the different analytical methods and variables for predicting the frequency and severity of RTAs. This visualization was developed following Silva et al. [109]. Of note, this connectivity plot allows to easily identify how research publication makes use of different methods and variables and, to what extent, these methods contribute to the analysis of RTAs. Motella [85] identified several contributing factors to the occurrence of RTAs. However, a graphical representation, such as Figure 7, allows us to (1) illustrate and determine potential causal relationships between different factors and the frequency and severity of RTAs, and (2) facilitates a more user-friendly presentation for the reader. This latter aspect makes easy to understand complex information, especially when large volumes of data are available.

In light of the results of this SLR, we suggest the following topics for future research related to the analysis of RTAs, which can be framed in four different areas: (1) data sources and organization; (2) statistical- and ML-based methods to be used; (3) variables to be analyzed; and (4) visualization tools for easily and intuitively communicate the results.

(1) Database sources and organization. In this SLR, the Web of Science database was used as the publication database. For future literature reviews, other bibliographic databases (i.e., SCOPUS and Dimensions) and resources should be included and explored.

(2) Data analytic methods. Considering the trends identified in this SLR, future studies would greatly benefit of comparing the feasibility and predictive power and different methods for RTA analysis such as spatiotemporal vs. ML-based methods (i.e., recurrent neural network model and/or an assembly method). In this regard, it would be crucial to ensure that ML-based methods are capable of addressing the unobserved heterogeneity.

(3) Variables to be analyzed. In this SLR, human factors that cause RTA accidents (i.e., the use of a cell phone while driving and driving under the influence of alcohol) as well as other mitigating factors such as the use of a helmet (for motorcyclists) and seat belt (for drivers and car occupants) were identified. Future studies assessing RTAs should properly analyze, using different statistical and ML-based methods, the influence of these and other risk and mitigating factors on RTAs in order to establish a baseline comparison and provide more accurate results.

(4) Data visualization tools. Data visualization makes possible to understand information more effectively than representations based on numbers or text, since the human mind is more easily able to process graphic images than tables with numerical or textual information [110]. Currently, tools for analyzing, presenting, and transforming bibliometric data from metadata (i.e., title, journal, authors, date of publication, keywords, abstract, references, and country of origin) are available. Some of these tools include, but are not limited to, biblioshiny ([https://bibliometrix.org/Biblioshiny.html]), VOSviewer®, CiteSpace© [111], CitNetExplorer [112], and the R package

causalizeR [14]. These tools, correctly integrated, will allow the extraction of information from bibliometric data. Although here we have shown the usefulness of these tools to visualize this type of data, further lines of research include the possibility of expanding these tools or developing new data visualization approaches for analyzing RTA-related publications.

5. Conclusions

Literature reviews are useful to support other investigations in the production of new scientific knowledge. Here, we use bibliometric analyses to identify the main papers, journals, and authors significantly contributing to the scientific production in RTA analysis using statistical and ML-based methods as well as technological elements of smart cities. Interestingly, most cited publications identified in this study correspond to literature reviews. The position adopted in this work is that bibliometric analyses can be used to complement research in all areas of knowledge in which there are scientific publications in known databases. It would be ideal that research topics suggested herein are materialized in future studies.

In the present SLR related to the analysis of RTAs, we found that the growth of scientific production has been evidenced in the last decade. This result may be due, in part, to the fact that new generations of computers and data analytical methods have emerged or have been implemented to allow the analysis of large databases faster, more securely, and with high accuracy thanks to the adoption and development of technological elements of smart cities to collect data produced on the world's roads in real time.

Unobserved heterogeneity is not a statistical analysis method but a problem that arises when applying other statistical methods to analyze RTAs. Thus, it is important to develop and/or use models/methods that are robust and have good performance for predicting RTAs under the potential presence of unobserved heterogeneity.

Bibliometric tools such as VOSviewer® and the implementation of several scientometric methods in the Bibliometrix and causalizeR packages of R constitute powerful and easy-to-use tools to analyze large volumes of publications. Cautiously using these tools in a complementary way gives researchers the possibility, in a short amount of time, of scrutinizing patterns and relationships that would be almost impossible to perform manually.

Human factors are one of the main causes of RTAs. However, in this SLR, we showed that, in the most cited publications, these factors have not been sufficiently analyzed. It is important to highlight that the use of helmets in the case of motorcycle users and the use of seat belts for car users are factors that mitigate the severity of road accidents, as well as the use of cell phones while driving and driving under the influence of alcohol are factors that increase the frequency of RTAs. Therefore, it is worthwhile for future research to include human factors as predictor variables in their models, since it is possible that they may be able to increase the performance of said models. Finally, data visualization tools allow the presentation of research results with high informative content in a coherent and clear manner, allowing the reader of these publications an easy understanding of said content. Hence, it is advisable to use them whenever possible.

Data Availability

The data retrieved from Web of Science and used to support the findings reported in this article are available from the corresponding author under reasonable request.

Disclosure

The sponsor of the study had no role in study design, data collection, data analysis, data interpretation, or writing of the manuscript. CFMV is a doctoral student at the Universidad del Norte, Barranquilla, Colombia. Some of this work is to be presented in partial fulfilment of the requirements for the PhD degree.

Conflicts of Interest

None of the authors of this article has a financial or personal relationship with other people or organizations that could inappropriately influence or bias the content of the article.

Authors' Contributions

JIV and GAGL conceived the study; JIV helped with the methodology; JIV and GAGL validated the study; CMFV did the formal analysis; CMFV investigated the study; CMFV, JIV, and GAGL helped with the resources; CMFV and JIV curated the data; CMFV prepared the original draft of the manuscript; CMFV, JIV, and GAGL reviewed and edited the manuscript; CMFV and JIV visualization; JIV and GAGL supervised the study; GAGL performed the project administration; and CMFV and GAGL helped with the funding acquisition. Jorge I. Velez and Guisselle A. Garcia-Llinas contributed equally to this work.

Acknowledgments

CMFV was supported by COLCIENCIAS, project *"Design of a framework for Integral Road Traffic Accident Management in Smart Cities,"* project # 785 of 2017, contract 84-091-894.

References

[1] Who, *OMS | 10 datos sobre la seguridad vial en el mundo*, WHO, 2017.

[2] "Ops/OMS., "OPS/OMS" | Nuevo informe de la OMS destaca que los progresos han sido insuficientes en abordar la falta de seguridad en las vías de tránsito del mundo," 2019, https://www.paho.org.

[3] "ONSV, "Observatorio Nacional de Seguridad Vial," 2019, https://ansv.gov.co/observatorio/.

[4] L. Joyanes, *Industria 4.0 - La Cuarta Revolución Industrial*, Bogotá, Primera, 2017.

[5] S. Erdogan, "Explorative spatial analysis of traffic accident statistics and road mortality among the provinces of Turkey," *Journal of Safety Research*, vol. 40, no. 5, pp. 341–351, 2009.

[6] S. Djahel, R. Doolan, G.-M. Muntean, and J. Murphy, "A communications-oriented perspective on traffic management systems for smart cities: challenges and innovative approaches," *IEEE Commun. Surv. Tutorials*, vol. 17, no. 1, pp. 125–151, 2015.

[7] J. Tang, J. Liang, C. Han, Z. Li, and H. Huang, "Crash injury severity analysis using a two-layer Stacking framework," *Accident Analysis & Prevention*, vol. 122, pp. 226–238, 2019.

[8] H. He and Y. Fan, "A novel hybrid ensemble model based on tree-based method and deep learning method for default prediction," *Expert Systems with Applications*, vol. 176, Article ID 114899, 2021.

[9] A. Gregoriades and K. C. Mouskos, "Black spots identification through a Bayesian Networks quantification of accident risk index," *Transp. Res. PART C-EMERGING Technol.*vol. 28, no. SI, pp. 28–43, 2013.

[10] X. Li, D. Lord, Y. Zhang, and Y. Me, "Predicting motor vehicle crashes using Support Vector Machine models," *Accident Analysis & Prevention*, vol. 40, no. 4, pp. 1611–1618, 2008.

[11] N. J. van Eck and L. Waltman, "Software survey: VOSviewer, a computer program for bibliometric mapping," *Scientometrics*, vol. 84, no. 2, 2010.

[12] J. Antoch, "Environment for statistical computing," *Comput. Sci. Rev.*vol. 2, no. 2, pp. 113–122, 2008.

[13] R. Rodríguez-Soler, J. Uribe-Toril, and J. De Pablo Valenciano, "Worldwide trends in the scientific production on rural depopulation, a bibliometric analysis using bibliometrix R-tool," *Land Use Policy*, vol. 97, Article ID 104787, 2020.

[14] F. J. Ancin-Murguzur and V. H. Hausner, "CausalizeR: a text mining algorithm to identify causal relationships in scientific literature," *PeerJ*, vol. 9, 2021.

[15] L. Xie, Z. Chen, H. Wang, C. Zheng, and J. Jiang, "Bibliometric and visualized analysis of scientific publications on atlantoaxial spine surgery based on Web of science and VOSviewer," *World Neurosurg*, vol. 137, pp. 435–442, 2020.

[16] R. Core Team, *A Language and Environment for Statistical Computing*, R Foundation for Statistical Computing, Vienna, Austria, 2021.

[17] B. Hernandez Sanchez, *Software VOSviewer Bibliométria - Investiga Y Educa*, Aprendizaje Basado en Proyectos, 2018.

[18] F. D. B. de Sousa, "Management of plastic waste: a bibliometric mapping and analysis," *Waste Management & Research*, vol. 39, no. 5, pp. 664–678, 2021.

[19] F. L. Mannering, V. Shankar, and C. R. Bhat, "Unobserved heterogeneity and the statistical analysis of highway accident data," *Anal. Methods Accid. Res.*vol. 11, pp. 1–16, 2016.

[20] M. T. Lukusa and F. K. H. Phoa, "A Horvitz-type estimation on incomplete traffic accident data analyzed via a zero-inflated Poisson model," *Accident Analysis & Prevention*, vol. 134, p. 2020.

[21] Z. Ma, H. Zhang, S. I.-J. Chien, J. Wang, and C. Dong, "Predicting expressway crash frequency using a random effect negative binomial model: a case study in China," *Accident Analysis & Prevention*, vol. 98, pp. 214–222, 2017.

[22] Z. Xie and J. Yan, "Detecting traffic accident clusters with network kernel density estimation and local spatial statistics: an integrated approach," *Journal of Transport Geography*, vol. 31, pp. 64–71, 2013.

[23] J. Zhang, Z. Li, Z. Pu, and C. Xu, "Comparing prediction performance for crash injury severity among various machine learning and statistical methods," *IEEE Access*, vol. 6, pp. 60079–60087, 2018.

[24] S. Erdogan, V. Ilci, O. M. Soysal, and A. Korkmaz, "A model suggestion for the determination of the traffic accident hotspots on the Turkish highway road network: a pilot study," *Bol. CIENCIAS Geod.*vol. 21, no. 1, pp. 169–188, 2015.

[25] I. Bak, K. Cheba, and B. Szczecinska, "The statistical analysis of road traffic in cities of Poland," *3RD INTERNATIONAL CONFERENCE GREEN CITIES - GREEN LOGISTICS FOR GREENER CITIES*, vol. 39, pp. 14–23, 2019.

[26] K. Reeves, J. S. Chandan, and S. Bandyopadhyay, "Using statistical modelling to analyze risk factors for severe and fatal road traffic accidents," *International Journal of Injury Control and Safety Promotion*, vol. 26, no. 4, pp. 364–371, Oct 2019.

[27] J. de Ona, G. Lopez, R. Mujalli, and F. J. Calvo, "Analysis of traffic accidents on rural highways using latent class clustering and bayesian networks," *Accident Analysis & Prevention*, vol. 51, pp. 1–10, 2013.

[28] S. Mandic, "Adolescents' perceptions of cycling versus walking to school: understanding the New Zealand context," *Journal of Transport & Health*, vol. 4, pp. 294–304, 2017.

[29] D. Singh and C. K. Mohan, "Deep spatio-temporal representation for detection of road accidents using stacked autoencoder," *IEEE Transactions on Intelligent Transportation Systems*, vol. 20, no. 3, pp. 879–887, 2019.

[30] M. Yadav, P. Khan, A. K. Singh, and B. Lohani, "Generating gis database of street trees using mobile lidar data," *ISPRS TC V MID-TERM SYMPOSIUM GEOSPATIAL TECHNOLOGY - PIXEL TO PEOPLE*, vol. 4, no. 5, pp. 233–237, 2018.

[31] H. Huang and M. Abdel-Aty, "Multilevel data and Bayesian analysis in traffic safety," *Accident Analysis & Prevention*, vol. 42, no. 6, pp. 1556–1565, Nov, 2010.

[32] M. R. Reddy, K. G. Srinivasa, and B. E. Reddy, "Smart vehicular system based on the internet of things," *Journal of Organizational and End User Computing*, vol. 30, no. 3, pp. 45–62, 2018.

[33] D. Lord and F. Mannering, "The statistical analysis of crash-frequency data: a review and assessment of methodological alternatives," *Transp. Res. PART A-POLICY Pract.*vol. 44, no. 5, pp. 291–305, 2010.

[34] S. Al-Sultan, M. M. Al-Doori, A. H. Al-Bayatti, and H. Zedan, "A comprehensive survey on vehicular Ad Hoc network," *Journal of Network and Computer Applications*, vol. 37, pp. 380–392, 2014.

[35] T. K. Anderson, "Kernel density estimation and K-means clustering to profile road accident hotspots," *Accident Analysis & Prevention*, vol. 41, no. 3, pp. 359–364, 2009.

[36] P. T. Savolainen, F. Mannering, D. Lord, and M. A. Quddus, "The statistical analysis of highway crash-injury severities: a review and assessment of methodological alternatives," *Accident Analysis & Prevention*, vol. 43, no. 5, pp. 1666–1676, 2011.

[37] P. C. Anastasopoulos, F. Mannering, V. N. Shankar, and J. E. Haddock, "A study of factors affecting highway accident rates using the random-parameters tobit model," *Accident Analysis & Prevention*, vol. 45, pp. 628–633, 2012.

[38] S. Zeadally, R. Hunt, Y.-S. Chen, A. Irwin, and A. Hassan, "Vehicular ad hoc networks (VANETS): status, results, and challenges," *Telecommunication Systems*, vol. 50, no. 4, pp. 217–241, 2012.

[39] S. Pu, M. Rutzinger, G. Vosselman, and S. O. Elberink, "Recognizing basic structures from mobile laser scanning data for road inventory studies," *ISPRS Journal of*

Photogrammetry and Remote Sensing, vol. 66, no. 6, pp. S28–S39, 2011.

[40] C. Wu, L. Yao, and K. Zhang, "The red-light running behavior of electric bike riders and cyclists at urban intersections in China: an observational study," *Accident Analysis & Prevention*, vol. 49, pp. 186–192, 2012.

[41] F. Mannering, V. Shankar, and C. R. Bhat, "Unobserved heterogeneity and the statistical analysis of highway accident data," *Anal. METHODS Accid. Res.*vol. 11, pp. 1–16, 2016.

[42] D. Crawford, "The longitudinal influence of home and neighbourhood environments on children's body mass index and physical activity over 5 years: the CLAN study," *International Journal of Obesity*, vol. 34, no. 7, pp. 1177–1187, 2010.

[43] F. Mannering, "Temporal instability and the analysis of highway accident data," *Anal. METHODS Accid. Res.*vol. 17, pp. 1–13, 2018.

[44] M. Whaiduzzaman, M. Sookhak, A. Gani, and R. Buyya, "A survey on vehicular cloud computing," *Journal of Network and Computer Applications*, vol. 40, pp. 325–344, 2014.

[45] C. Plug, J. Cecilia, and C. Caulfield, "Spatial and temporal visualisation techniques for crash analysis," *Accident Analysis & Prevention*, vol. 43, no. 6, pp. 1937–1946, 2011.

[46] P. C. Anastasopoulos and F. L. Mannering, "An empirical assessment of fixed and random parameter logit models using crash- and non-crash-specific injury data," *Accident Analysis & Prevention*, vol. 43, no. 3, pp. 1140–1147, 2011.

[47] X. D. Yan, E. Radwan, and M. Abdel-Aty, "Characteristics of rear-end accidents at signalized intersections using multiple logistic regression model," *Accident Analysis & Prevention*, vol. 37, no. 6, pp. 983–995, Nov 2005.

[48] K. Abboud, H. A. Omar, and W. Zhuang, "Interworking of dsrc and cellular network technologies for V2X communications: a survey," *IEEE Transactions on Vehicular Technology*, vol. 65, no. 12, pp. 9457–9470, 2016.

[49] D. Betaille and R. Toledo-Moreo, "Creating enhanced maps for lane-level vehicle navigation," *IEEE Transactions on Intelligent Transportation Systems*, vol. 11, no. 4, pp. 786–798, 2010.

[50] F. Bella, "Driving simulator for speed research on two-lane rural roads," *Accident Analysis & Prevention*, vol. 40, no. 3, pp. 1078–1087, 2008.

[51] Z. Li, P. Liu, W. Wang, and C. Xu, "Using support vector machine models for crash injury severity analysis," *Accident Analysis & Prevention*, vol. 45, pp. 478–486, 2012.

[52] Z. Hameed Mir and F. Filali, "LTE and IEEE 802.11p for vehicular networking: a performance evaluation," *EURASIP Journal on Wireless Communications and Networking*, vol. 2014, no. 1, p. 1, 2014.

[53] G. T. Jones, C. Power, and G. J. Macfarlane, "Adverse events in childhood and chronic widespread pain in adult life: results from the 1958 British Birth Cohort Study," *Pain*, vol. 143, no. 1–2, pp. 92–96, 2009.

[54] D. W. Kononen, C. A. C. Flannagan, and S. C. Wang, "Identification and validation of a logistic regression model for predicting serious injuries associated with motor vehicle crashes," *Accident Analysis & Prevention*, vol. 43, no. 1, pp. 112–122, 2011.

[55] R. G. Engoulou, M. Bellaiche, S. Pierre, and A. Quintero, "VANET security surveys," *Computer Communications*, vol. 44, pp. 1–13, 2014.

[56] K. S. Ng, W. T. Hung, and W. G. Wong, "An algorithm for assessing the risk of traffic accident," *Journal of Safety Research*, vol. 33, no. 3, pp. 387–410, 2002.

[57] N. Cheng, "Big data driven vehicular networks," *IEEE Netw*, vol. 32, no. 6, pp. 160–167, 2018.

[58] A. Lei, H. Cruickshank, Y. Cao, P. Asuquo, C. P. A. Ogah, and Z. Sun, "Blockchain-based dynamic key management for heterogeneous intelligent transportation systems," *IEEE Internet of Things Journal*, vol. 4, no. 6, pp. 1832–1843, 2017.

[59] X. Zou, W. L. Yue, and H. Le Vu, "Visualization and analysis of mapping knowledge domain of road safety studies," *Accident Analysis & Prevention*, vol. 118, pp. 131–145, 2018.

[60] A. T. Kashani and A. S. Mohaymany, "Analysis of the traffic injury severity on two-lane, two-way rural roads based on classification tree models," *Safety Science*, vol. 49, no. 10, pp. 1314–1320, 2011.

[61] S. K. L. Lal, A. Craig, P. Boord, L. Kirkup, and H. Nguyen, "Development of an algorithm for an EEG-based driver fatigue countermeasure," *Journal of Safety Research*, vol. 34, no. 3, pp. 321–328, 2003.

[62] J. Panter, K. Corder, S. J. Griffin, A. P. Jones, and E. M. F. van Sluijs, "Individual, socio-cultural and environmental predictors of uptake and maintenance of active commuting in children: longitudinal results from the SPEEDY study," *International Journal of Behavioral Nutrition and Physical Activity*, vol. 10, 2013.

[63] C. Deck and R. Willinger, "Improved head injury criteria based on head FE model," *International Journal of Crashworthiness*, vol. 13, no. 6, pp. 667–678, 2008.

[64] J. A. G. Ibanez, S. Zeadally, and J. Contreras-Castillo, "Integration challenges of intelligent transportation systems with connected vehicle, cloud computing, and internet of things technologies," *IEEE Wireless Communications*, vol. 22, no. 6, pp. 122–128, 2015.

[65] A. Carver, A. Timperio, K. Hesketh, and D. Crawford, "Are safety-related features of the road environment associated with smaller declines in physical activity among youth?" *J. URBAN Heal. NEW YORK Acad. Med.*vol. 87, no. 1, pp. 29–43, 2010.

[66] P. C. Anastasopoulos, V. N. Shankar, J. E. Haddock, and F. Mannering, "A multivariate tobit analysis of highway accident-injury-severity rates," *Accident Analysis & Prevention*, vol. 45, pp. 110–119, 2012.

[67] J. P. Schepers, E. Fishman, P. Den Hertog, K. K. Wolt, and A. L. Schwab, "The safety of electrically assisted bicycles compared to classic bicycles," *Accident Analysis & Prevention*, vol. 73, pp. 174–180, 2014.

[68] X. Lin, R. Lu, C. Zhang, H. Zhu, P.-H. Ho, and X. Sherman, "Security in vehicular ad hoc networks," *IEEE Communications Magazine*, vol. 46, no. 4, pp. 88–95, 2008.

[69] W. E. Marshall and N. W. Garrick, "Street network types and road safety: a study of 24 California cities," *Urban Design International*, vol. 15, no. 3, pp. 133–147, 2010.

[70] J. L. Martin, "Relationship between crash rate and hourly traffic flow on interurban motorways," *Accident Analysis & Prevention*, vol. 34, no. 5, pp. 619–629, 2002.

[71] J. Abellan, G. Lopez, and J. de Ona, "Analysis of traffic accident severity using decision rules via decision trees," *Expert Systems with Applications*, vol. 40, no. 15, pp. 6047–6054, 2013.

[72] Q. Wang, S. Leng, H. Fu, and Y. Zhang, "An IEEE 802.11p-based multichannel MAC scheme with channel coordination for vehicular ad hoc networks," *IEEE Transactions on Intelligent Transportation Systems*, vol. 13, no. 2, pp. 449–458, 2012.

[73] S. C. Wong, N. N. Sze, and Y. C. Li, "Contributory factors to traffic crashes at signalized intersections in Hong Kong,"

Accident Analysis & Prevention, vol. 39, no. 6, pp. 1107–1113, 2007.

[74] R. Yu and M. Abdel-Aty, "Analyzing crash injury severity for a mountainous freeway incorporating real-time traffic and weather data," *Safety Science*, vol. 63, pp. 50–56, 2014.

[75] S. Bitam, A. Mellouk, and S. Zeadally, "VANET-CLOUD: a generic cloud computing model for vehicular ad HOC networks," *IEEE Wireless Communications*, vol. 22, no. 1, pp. 96–102, 2015.

[76] M. Soilan, B. Riveiro, J. Martinez-Sanchez, and P. Arias, "Segmentation and classification of road markings using MLS data," *ISPRS Journal of Photogrammetry and Remote Sensing*, vol. 123, pp. 94–103, 2017.

[77] J. P. Schepers, P. A. Kroeze, W. Sweers, and J. C. Wust, "Road factors and bicycle-motor vehicle crashes at unsignalized priority intersections," *Accident Analysis & Prevention*, vol. 43, no. 3, pp. 853–861, May 2011.

[78] G. Zhang, K. K. W. Yau, X. Zhang, and Y. Li, "Traffic accidents involving fatigue driving and their extent of casualties," *Accident Analysis & Prevention*, vol. 87, pp. 34–42, 2016.

[79] M. Hadded, P. Muhlethaler, A. Laouiti, R. Zagrouba, and L. A. Saidane, "TDMA-based mac Protocols for vehicular ad hoc networks: a survey, qualitative analysis, and open research issues," *IEEE Commun. Surv. TUTORIALS*, vol. 17, no. 4, pp. 2461–2492, 2015.

[80] J. Lee, B. Nam, and M. Abdel-Aty, "Effects of pavement surface conditions on traffic crash severity," *Journal of Transportation Engineering*, vol. 141, no. 10, 2015.

[81] C. Wang, M. A. Quddus, and S. G. Ison, "The effect of traffic and road characteristics on road safety: a review and future research direction," *Safety Science*, vol. 57, pp. 264–275, 2013.

[82] A. Montella, M. Aria, A. D'Ambrosio, and F. Mauriello, "Analysis of powered two-wheeler crashes in Italy by classification trees and rules discovery," *Accident Analysis & Prevention*, vol. 49, pp. 58–72, 2012.

[83] D. Dissanayake, J. Aryaija, and D. M. P. Wedagama, "Modelling the effects of land use and temporal factors on child pedestrian casualties," *Accident Analysis & Prevention*, vol. 41, no. 5, pp. 1016–1024, 2009.

[84] S. Al-Sultan, A. H. Al-Bayatti, and H. Zedan, "Context-aware driver behavior detection system in intelligent transportation systems," *IEEE Transactions on Vehicular Technology*, vol. 62, no. 9, pp. 4264–4275, 2013.

[85] A. Montella, "Identifying crash contributory factors at urban roundabouts and using association rules to explore their relationships to different crash types," *Accident Analysis & Prevention*, vol. 43, no. 4, pp. 1451–1463, 2011.

[86] M. Chen, J. Wan, and F. Li, "Machine-to-Machine communications: architectures, standards and Applications," *KSII Trans. INTERNET Inf. Syst.* vol. 6, no. 2, pp. 480–497, 2012.

[87] X. Zhai, H. Huang, N. N. Sze, Z. Song, and K. K. Hon, "Diagnostic analysis of the effects of weather condition on pedestrian crash severity," *Accident Analysis & Prevention*, vol. 122, pp. 318–324, 2019.

[88] L. Zheng, K. Ismail, and X. Meng, "Traffic conflict techniques for road safety analysis: open questions and some insights," *Canadian Journal of Civil Engineering*, vol. 41, no. 7, pp. 633–641, 2014.

[89] S. Y. Sohn and S. H. Lee, "Data fusion, ensemble and clustering to improve the classification accuracy for the severity of road traffic accidents in Korea," *Safety Science*, vol. 41, no. 1, pp. 1–14, 2003.

[90] H. T. Cheng, H. Shan, and W. Zhuang, "Infotainment and road safety service support in vehicular networking: from a communication perspective," *Mechanical Systems and Signal Processing*, vol. 25, no. 6, pp. 2020–2038, 2011.

[91] M. Yadav, A. K. Singh, and B. Lohani, "Extraction of road surface from mobile LiDAR data of complex road environment," *International Journal of Remote Sensing*, vol. 38, no. 16, pp. 4655–4682, 2017.

[92] X. Wang and M. Abdel-Aty, "Analysis of left-turn crash injury severity by conflicting pattern using partial proportional odds models," *Accident Analysis & Prevention*, vol. 40, no. 5, pp. 1674–1682, 2008.

[93] A. Greasley, "Using process mapping and business process simulation to support a process-based approach to change in a public sector organisation," *Technovation*, vol. 26, no. 1, pp. 95–103, 2006.

[94] P. Stallard and E. Smith, "Appraisals and cognitive coping styles associated with chronic post-traumatic symptoms in child road traffic accident survivors," *J. CHILD Psychol. PSYCHIATRY*, vol. 48, no. 2, pp. 194–201, 2007.

[95] A. M. Cailean and M. Dimian, "Current challenges for visible light communications usage in vehicle Applications: a survey," *IEEE Commun. Surv. Tutorials*, vol. 19, no. 4, pp. 2681–2703, 2017.

[96] V. Eksler, S. Lassarre, and I. Thomas, "Regional analysis of road mortality in Europe," *Public Health*, vol. 122, no. 9, pp. 826–837, 2008.

[97] F. Bella, "Validation of a driving simulator for work zone design," *HUMAN PERFORMANCE; SIMULATION AND VISUALIZATION*, no. 1937, pp. 136–144, 2005.

[98] M. Fiore, J. Harri, F. Filali, and C. Bonnet, "Vehicular mobility simulation for VANETs," *40TH ANNUAL SIMULATION SYMPOSIUM, Proceedings*, p. 301+, 2007.

[99] B. Riveiro, L. Diaz-Vilarino, B. Conde-Carnero, M. Soilan, and P. Arias, "Automatic segmentation and shape-based classification of retro-reflective traffic signs from mobile LiDAR data," *Ieee Journal of Selected Topics in Applied Earth Observations and Remote Sensing*, vol. 9, no. 1, pp. 295–303, 2016.

[100] H. Huang, Q. Zeng, X. Pei, S. C. Wong, and P. Xu, "Predicting crash frequency using an optimised radial basis function neural network model," *Transp. A-TRANSPORT Sci.* vol. 12, no. 4, pp. 330–345, 2016.

[101] "Intel"línea de. Tiempo de Procesadores," 2020, https://www.timetoast.com/timelines/linea-de-tiempo-de-procesadores.

[102] X. Zou and H. L. Vu, "Mapping the knowledge domain of road safety studies: a scientometric analysis," *Accident Analysis & Prevention*, vol. 132, 2019.

[103] X. Zou, H. L. Vu, and H. Huang, "Fifty years of accident analysis & prevention: a bibliometric and scientometric overview," *Accident Analysis & Prevention*, vol. 144, 2020.

[104] F. Mannering, C. R. Bhat, V. Shankar, and M. Abdel-Aty, "Big data, traditional data and the tradeoffs between prediction and causality in highway-safety analysis," *Anal. METHODS Accid. Res.* vol. 25, 2020.

[105] F. Mannering, "Temporal instability and the analysis of highway accident data," *Anal. Methods Accid. Res.* vol. 17, pp. 1–13, 2018.

[106] F. L. Mannering and C. R. Bhat, "Analytic methods in accident research: methodological Frontier and future directions," *Anal. Methods Accid. Res.* vol. 1, pp. 1–22, 2014.

[107] Nvidia, "Los inicios de Nvidia, el rey de las tarjetas gráficas," 2020.

[108] "Ops OMS., "OPS/OMS | Nuevo informe de la OMS destaca que los progresos han sido insuficientes en abordar la falta de seguridad en las vías de tránsito del mundo," 2019.
[109] P. B. Silva, M. Andrade, and S. Ferreira, "Machine learning applied to road safety modeling: a systematic literature review," *J. Traffic Transp. Eng. (English) Ed.* vol. 7, no. 6, pp. 775–790, 2020.
[110] M. S. Zakaria, "Data visualization as a research support service in academic libraries: an investigation of world-class universities," *The Journal of Academic Librarianship*, vol. 47, no. 5, Article ID 102397, 2021.
[111] T. Pang and J. Shen, "Visualizing the landscape and evolution of capacitive deionization by scientometric analysis," *Desalination*, vol. 527, Article ID 115562, 2022.
[112] N. J. van Eck and L. Waltman, "CitNetExplorer: a new software tool for analyzing and visualizing citation networks," *J. Informetr.* vol. 8, no. 4, pp. 802–823, 2014.

Hindawi
Journal of Advanced Transportation
Volume 2022, Article ID 8364988, 15 pages
https://doi.org/10.1155/2022/8364988

Research Article

Research on Parking Service Optimization Based on Permit Reservation and Allocation

Duo Xu and Huijun Sun

Key Laboratory of Transport Industry of Big Data Application Technologies for Comprehensive Transport, Beijing Jiaotong University, Beijing 100044, China

Correspondence should be addressed to Duo Xu; 516472407@qq.com

Received 2 February 2022; Revised 28 March 2022; Accepted 4 April 2022; Published 9 June 2022

Academic Editor: Elżbieta Macioszek

Copyright © 2022 Duo Xu and Huijun Sun. This is an open access article distributed under the Creative Commons Attribution License, which permits unrestricted use, distribution, and reproduction in any medium, provided the original work is properly cited.

Parking facilities in central urban areas have limited supply, high utilization, and turnover rate, leading to the high parking cost. To draw the issues of parking uncertainty, high search time, and underutilization of parking lots, this study shows the application of permits in parking management. It first analyzes the characteristics and costs of "arrival priority" and "reservation priority" modes, and then, it proposes the parking permit reservation and allocation mode based on "service order optimization" and designs an "ant colony-genetic" algorithm to solve the optimal service order. The numerical example shows that the measures of quantity control and matching optimization are effective in parking management. The parking reservation mode of "service order optimization" has advantages in parking lot utilization rate, service demand quantity, and total parking cost.

1. Introduction

Parking has an important influence on the choice of vehicle travel mode and road traffic order. As the number of vehicles in cities continues to grow, parking problem becomes increasingly prominent. Although each vehicle travels only 1 hour a day on average, finding a parking space takes a lot of time and cost [1]. Studies by Axhausen et al. show that the time spent by vehicles searching for parking spaces accounts for about 30% to 50% of the total travel time [2, 3]; Vuchic reveals that the cost of vehicle parking accounts for about 70% cost of a single trip [4]. Many scholars have studied the parking search time by way of empirical research, which is generally between 3 minutes and 15 minutes (see references [5–10] for details).

As pointed out by Inci, parking problems are "invisible" [11]. On the one hand, cruise vehicles searching for parking spaces are mixed with normal traffic flow and are difficult to identify. Some studies have tried to estimate this ratio, but have not reached a consistent conclusion [12–14]. On the other hand, some travelers adjust the departure time [15] and parking location [16] to avoid parking difficulties. Instead, the parking lot utilization rate is low, making managers underestimate the severity of the parking problem.

The parking problem is mainly caused by the contradiction between supply and demand, so traffic demand management has been regarded as an effective measure to alleviate this problem. Parking charging (including static charging and dynamic charging) is the earliest management method applied in the parking field and receives much attention from scholars. We can refer to the research overview of Inci et al. [17, 18]. Generally speaking, charging has the advantages of effectively adjusting demand and internalizing some external costs into manager's income. The disadvantages of charging are as follows: firstly, the adjustment accuracy is low and there is hysteresis, which makes managers retain some parking spaces to cope with fluctuations in demand and then achieve maximal system efficiency. For example, the SFpark project in San Francisco sets charging on the premise of keeping 15% of the parking spaces vacant [19]. Gu et al. believed that the optimal fee should make parking facility usage rate reach 85%–95% [20]. In addition, the charge itself does not contain information. Even if the parking supply can (exactly) meet the demand, travelers arriving later still need to spend certain time searching for vacant parking spaces. When there are few parking spaces, the search cost will increase rapidly [21–23].

With the development of the Internet and communication technologies, managers have strengthened their control over parking behavior, and a parking management mode based on quantity control has appeared. Montgomery pioneered the application of quantitative control concepts (Crocker and Dales) for managing environmental pollution externalities into parking management as an alternative to price control [24–26]. Yang and Wang first proposed a tradable parking credit management model in which managers issue parking permits to travelers, and travelers can trade and use parking permits in light of actual needs [15]. Subsequently, many scholars have done research on permit management issues in parking [27–34]. The advantage of the parking permit mode is that it can split the direct connection between charging and demand into two independent parts, with price corresponding to application, and supply corresponding to allocation. The disparity between the application and the allocated amount only appears in the scheduled allocation stage of the permit. Therefore, no actual cost is incurred during travel. At the same time, the permit can contain parking space information, thus greatly reducing the parking search time for late arrivals.

In addition, some scholars have studied the short-term parking space reservation allocation strategy for special situations (e.g., unpunctuality or uncertainty in travelers' arrival/departure time, and time-limited opening spaces for shared parking) [35–39], trading mechanisms [40, 41], and optimization algorithms [42–49]. Through simulated experiments and empirical experiments, it is found that parking reservation and allocation can significantly reduce drivers' search costs and emissions.

Based on the existing research, this paper studies the problem of high parking costs caused by the contradiction between supply and demand and proposes an improved parking permit management mode to overcome the shortcomings of traditional charging mode and permit reservation mode in terms of parking uncertainty (go back and forth between parking lots), long search time, and underutilization of parking lots. It also looks forward to the application of the model in the management of shared parking resources (integrating and utilizing different types of park supplies).

The remainder of this paper is organized as follows. The next section establishes assumptions and defines the symbols used. Section 3 analyzes and compares the parking costs of the two modes of "arrival priority" and "reservation priority," and finds the factors that restrict service capacity. Section 4 proposes the parking permit mode of "service order optimization" and designs the "ant colony-genetic" algorithm for solving the optimal service order. Section 5 analyzes the effects of various parking management modes through numerical examples. Section 6 provides conclusions and recommendations for future studies.

2. Assumptions

This study takes the parking behavior of a certain (non-unique) business district (CBD) in the city as the research object and establishes the following hypotheses based on the actual vehicle travel and parking in the city .

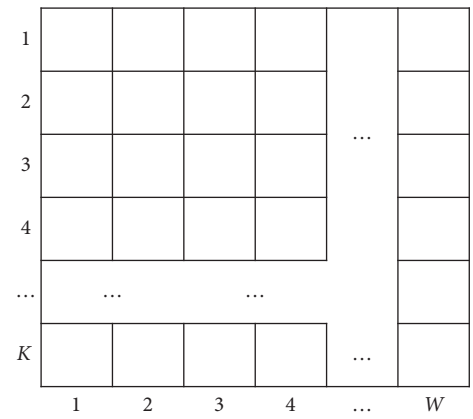

Figure 1: Schematic diagram of the available period of lot 1.

A1. Road network and parking lot. In the linear road network model, the departure point of travelers is at one end of the road, and the business district is at the other end of the road. There are two types of parking lots around the commercial area, parking lot 1 with limited capacity at the destination, and parking lot 2 with no capacity limitation within walking distance acceptable to travelers around the destination. The parking lot opening time includes a limited number of time panes (defined as a unit time, such as 15 minutes). Figure 1 depicts K parking lot, W panes in parking lot 1:

Parking lot 1 at the destination in A1 is the main research object of this paper, its supply is limited; parking lot 2 around the destination is the second best choice when travelers cannot choose parking lot 1, which can be regarded as a generalized parking lot that may actually consist of multiple parking lots. For the establishment of parking lot 2, on the one hand, it reflects the satisfiability of parking needs; that is, travelers can generally complete parking by choosing a parking lot that is far away; on the other hand, when there is no vacant parking space in parking lot 1, travelers will go to and from two parking lots, which reflects travelers' search process.

A2. Parking management mode. This paper sets three parking lot management modes: "arrival priority," "reservation priority," and "service order optimization" modes. Where the "arrival priority" mode corresponds to general charging, the "reservation priority" and "service order optimization" modes correspond to the scheduled allocation of parking permits.

The "arrival priority" mode represents the current charging management mode adopted by the city, and this paper sets it as the control group 1. The "reservation priority" mode is set as the control group 2 in this paper, and neither of the two control groups is set with specific optimization goals. The "service order optimization" mode is the experimental group of this paper, and the manager's goal is to minimize the total cost of travelers.

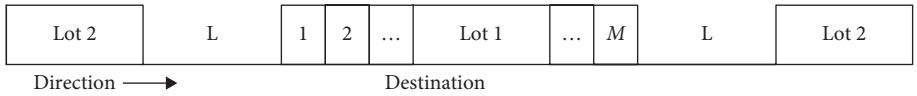

Figure 2: The parking process of travelers in mode n.

Table 1: Nomenclature.

Notation	Interpretation
W	Number of time panes opened in the parking lot every day
x_M	Distance between parking lot 1 and parking lot 2
t^i	Expected arrival time (pane) of traveler i
l^i	Parking duration (panes) of traveler i
z^i	Parking reservation time of traveler i
$N_d(h,i)$	Arrival number at parking lot 1 between the arrival time interval of traveler h and i
$n(i)$	Occupied spaces number in parking lot 1 when traveler i arrives
$u(i)$	Reserved panes number in parking lot 1 when traveler i reserves
j	Modes, including "arrival priority," "reservation priority," and "service order optimization" and modes, including "arrival priority"-n, "reservation priority"-r, and "service order optimization"-r^*
K	The total number of parking spaces in the parking lot 1 ($k = 1, 2, ..., K$ indicates the number of parking spaces)
$\text{prob}_j^k(i)$	In mode j, the probability of a traveler i parking at the position k of parking lot 1
$\text{prob}_j(i)$	In mode j, the probability that any pane of parking lot 1 is occupied after the traveler i completes the parking reservation
$\chi(i)$	0-1 variable, in mode r, whether the traveler i successfully finds parking space in the parking lot 1
$\chi_{k,w}(i)$	0-1 variable, in mode r^*, whether the traveler i gets the parking position k at pane w in the parking lot 1
α	The value of time
λ	Unit search time without information guidance
ε	$0 < \varepsilon < 1$, the search time reduction factor under information guidance
v_c	Car velocity
v_w	Walking velocity
$C_j^t(i)$	In mode j, the travel cost of traveler i
$C_j^s(i)$	In mode j, the search cost of traveler i
TC_j	The total system cost of the mode j

A3. Travelers and itinerary. There are differences in parking demand, which are represented by two variables, different arrival time and parking duration. Travelers prefer the nearest parking lot 1. Without guidance information, travelers will search for parking spaces in parking lot 1 one by one. If parking cannot be completed, they will go back and forth to parking lot 2, as shown in Figure 2. With the presence of guidance information (parking permit), the traveler decides whether to go to the parking lot 1 according to whether the parking space in the parking lot 1 is successfully reserved.

Travelers have no specific experiences regarding parking lots and other people's travel plans. Therefore, without exact information guidance, travelers can only park according to the principle of minimum perceived cost, which is a blind behavior. It should be noted that even if the usage of parking lot 1 is posted on the surrounding roads in the form of variable information boards, etc., when travelers drive from parking lot 2 (or a location closer to the departure point) to parking lot 1, parking status of parking lot 1 may still change (travelers who are closer to the destination than the target traveler fills up the parking space, or some vehicles leave when travels drive to the parking lot 1), so the above guidance information still cannot be defined as "exact information."

A4. Parking cost. According to the traveler's itinerary, two types of costs are set. One is the travel cost, including the cost of vehicle driving before reaching the parking lot and the cost of walking to the destination after parking. The other is the search cost, which appears in the process of searching for a parking space in the parking lot.

All travelers experience the driving process from the departure point to the parking lot 2. For simplicity, the overlapping cost in this part is ignored. There are three types of travel costs based on whether the traveler directly parks in parking lot 1 or 2 and goes to and from parking lot 1 and 2. Parking lot 2 is a generalized parking lot, which may include multiple parking lots and multiple parking entrances. Travelers can easily find parking spaces. Therefore, it is assumed that the parking search cost only exists in parking lot 1. In addition, parking fees are internal costs (transferred from travelers to managers), so this paper will not consider them separately.

The symbols and parameters are defined in Table 1.

3. Parking Cost in "Arrival Priority" and "Reservation Priority" Modes

According to A3 and A4, the travel cost $C_j^t(i)$ of the traveler i in the mode j is as follows:

$$C_j^t(i) = \begin{cases} \dfrac{\alpha x_M}{v_c} & i \in \text{lot1}, j \in \{n, r, r^*\}, \\ \dfrac{\alpha x_M}{v_w} & i \in \text{lot2}, j \in \{r, r^*\}, \\ \alpha x_M \left(\dfrac{1}{v_w} + \dfrac{2}{v_c}\right) & i \in \text{lot1} - \text{lot2}, j = n, \end{cases} \tag{1}$$

where the mode n corresponds to situation one and situation three; that is, the traveler completes the parking in the parking lot 1 or turns back to the parking lot 2 after arriving at the parking lot 1. The permit modes r and r^* correspond to the first two situations; that is, the traveler successfully or unsuccessfully reserves the permit for parking lot 1.

Similarly, the traveler i's search cost $C_j^s(i)$ in the mode j is as follows:

$$C_j^s(i) = \begin{cases} \alpha k\lambda & i \in \text{lot1}, j = n, \\ \alpha K\lambda & i \in \text{lot1} - \text{lot2}, j = n, \\ \alpha\varepsilon k\lambda & i \in \text{lot1}, j \in \{r, r^*\}, \\ 0 & i \in \text{lot2}, j \in \{r, r^*\}. \end{cases} \tag{2}$$

Without information guidance, when traveler i searches until the k th parking space in parking lot 1 ($1 \le k \le K$), the time it takes is $k\lambda$; if the traveler returns from parking lot 1 to parking lot 2, then he will search the entire parking lot 1, and the search time is $K\lambda$. When parking space information is acquired, the search time is reduced by ε times.

From equations (1) and (2), the total traveler cost in the mode j is as follows:

$$TC_j = \sum_N \left[C_j^t(i) + C_j^s(i)\right]. \tag{3}$$

3.1. Parking Cost in "Arrival Priority" Mode. In mode n, travelers arrive at the parking lot in the order of travel plans. According to the definition, $n(i)$ is the number of parking spaces occupied when traveler i arrives at parking lot 1 (including those who have not parked but arrive before the traveler i), and $N_d(i-1, i)$ is the number of vehicles leaving the parking lot within the arrival time interval of two adjacent travelers. When $n(i) < K$, travelers can complete parking in parking lot 1. $n(i)$ can be expressed as follows:

$$n(i) = \begin{cases} \min\{K, n(i-1) + 1\} - N_d(i-1, i) & i > 1, \\ 0 & i = 1. \end{cases} \tag{4}$$

Equation (4) has two meanings. One is that when the earliest traveler arrives at the parking lot, the number of parking spaces used in the parking lot is 0; the other is that when the i th traveler arrives at the parking lot 1, the number of parking spaces used is the number of parking spaces used by the $i-1$ traveler minus the number of vehicles leaving the parking lot within the arrival time interval of the $i-1$ and i th traveler. Where the maximum number of parking spaces used does not exceed K, the number of leaving vehicles does not exceed the number of vehicles already in the parking lot, $N_d(i-1, i) \le n(i-1)$.

In case of large utilization rate and turnover rate of parking space in the parking lot 1, the parking spaces that have been used can be regarded as randomly distributed in the parking lot. Assume that used parking spaces have equal probability distribution in the parking lot, then for traveler i, the probability that any parking space is used can be expressed as follows:

$$\text{prob}_n(i) = \frac{n(i)}{K}. \tag{5}$$

When we search in order, the probabilities $\text{prob}_n^1(i)$ and $\text{prob}_n^k(i)$ of parking at the 1st position and the k th parking space are, respectively, as follows:

$$\text{prob}_n^1(i) = 1 - \text{prob}_n(i) = \frac{1 - n(i)}{K}, \tag{6}$$

$$\text{prob}_n^k(i) = \left[\frac{1 - n(i)}{K}\right]\left[\frac{n(i)}{K}\right]^{k-1}. \tag{7}$$

When the number of parking spaces used is $n(i)$ ($n(i) < K$), the traveler can definitely find a parking space from the first to $n(i) + 1$ parking space (the worst case is that the previous $n(i)$ parking space is occupied). The expected value $\text{E}[C_n^s(i)]$ of search cost $C_n^s(i)$ can be expressed as follows:

$$\text{E}\left[C_n^s(i)\right] = \begin{cases} \displaystyle\sum_{k=1}^{n(i)} k\lambda \cdot \text{prob}_n^k(i) n(i) < K, K\lambda n(i) = K. \end{cases} \tag{8}$$

When K value is large, equation (8) is approximately equal to

$$\text{E}\left[C_n^s(i)\right] = \begin{cases} \dfrac{K\lambda}{K - n(i)} & n(i) < K \\ K\lambda & n(i) = K \end{cases}. \tag{9}$$

According to equation (1), the travel cost $C_n^t(i)$ of traveler i in the mode n is as follows:

$$C_n^t(i) = \begin{cases} \dfrac{\alpha x_M}{v_c} & i \in \text{lot 1}, \\ \alpha x_M \left(\dfrac{1}{v_w} + \dfrac{2}{v_c}\right) & i \in \text{lot 1} - \text{lot 2}. \end{cases} \tag{10}$$

According to equations (9) and (10), the expected parking cost of travelers in the mode n is as follows:

$$\text{E}\left[C_n(i)\right] = \begin{cases} \dfrac{K\lambda}{K - n(i)} + \dfrac{\alpha x_M}{v_c}, & i \in \text{lot 1}, \\ K\lambda + \alpha x_M \left(\dfrac{1}{v_w} + \dfrac{2}{v_c}\right), & i \in \text{lot 1} - \text{lot 2}. \end{cases} \tag{11}$$

With the increase in parking demand, the utilization rate of parking space in the parking lot 1 will gradually increase. The parking cost curve can be plotted as shown in Figure 3.

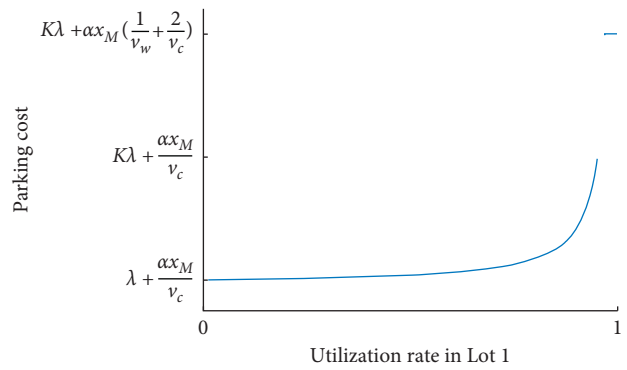

Figure 3: Parking cost of parking lot 1 in varying utilization rate.

Figure 3 shows that with the increasing utilization rate of parking space in the parking lot 1, the search cost and parking cost of travelers also gradually increase; when the parking lot is close to full use state, the search cost and parking cost increase significantly. When parking lot 1 has no vacant parking space available, travelers return to parking lot 2, and the travel cost jumps, leading to a jump in parking costs.

Since the parking demand is irregular, the system cannot reach an equilibrium state, and the leap-like changes in parking cost reflect the phenomenon in which vehicles cruise between parking lots in reality.

The total system cost is the sum of the parking costs of all travelers, namely,

$$TC_n = \sum_N \mathrm{E}[C_n(i)]. \tag{12}$$

The expected parking cost of traveler i depends on the value $n(i)$, so the equation (12) can be expressed as follows:

$$TC_n = \sum_N \mathrm{freq}[n(i)] \cdot C_n(i), \tag{13}$$

where $\mathrm{freq}[n(i)]$ represents the frequency of $n(i)$ occurrence and satisfies $\sum_N \mathrm{freq}[n(i)] = N$.

The parking space is used multiple times in a day. When the parking lot 1 is in a state of high utilization for a long time (e.g., the parking space utilization rate is between 0.9 and 1.0) and it is at a high turnover speed, the total parking cost in "arrival priority" mode will always be high. This situation corresponds to the fact that the parking lot has a large number of cruising vehicles inside and around it due to the prominent contradiction between supply and demand.

3.2. Parking Cost in "Reservation Priority" Mode. To deal with the problem of increased parking costs caused by high parking rates and high turnover rates, methods of increasing charges and reducing parking rates are proposed. For example, the SFpark project maintains the parking lot vacancy rate at about 15%. This method is equivalent to striving for lower system costs at the cost of partial parking resources.

The parking permit mode can well solve this problem. In the permit reservation mode r, the manager allocates parking permits containing time and location information according to demand, thereby solving the problem of parking uncertainty. If travelers successfully reserve a parking space in the parking lot 1, they will know exactly where the parking space is, so they can drive directly to the target parking space, without having to search the parking lot at a slower speed one by one; if they fail to reserve parking lot 1, they will go directly to the parking lot 2, without need to go to and from parking lot 1 and parking lot 2.

In mode r, the order of parking service demand is the predetermined order z^i. According to the travel plan, travelers make reservations in parking lot 1 in the order from 1st to Kth parking space. If there is no vacant parking space, then choose parking lot 2.

According to assumption A1, K parking spaces in parking lot 1 have a total of KW time-space units available for reservation at time period W. When traveler i makes reservations for parking lot 1, if $u(i)$ time-space unit is occupied, $u(i)$ can be expressed as follows:

$$u(i) = \sum_{\{q|z^q<z^i\}} \chi(q) l^q, \quad i, q \in N, \tag{14}$$

where χ_q indicates whether the q th vehicle has completed the reservation in the parking lot 1, and $\{q|z^q < z^i\}$ indicates the collection of travelers who reserve parking lot earlier than i.

Assume that the parking demand is equally probabilistic within the range of time and space, the probability that each time and space unit of the parking lot is used can be expressed as follows:

$$\mathrm{prob}_r(i) = \frac{u(i)}{KW}. \tag{15}$$

For traveler i, he can park only when a parking space is vacant in consecutive l^i periods of time. Based on this, the probability $\mathrm{prob}_r^1(i)$ and $\mathrm{prob}_r^k(i)$ that he finds parking at the first position and the k th position can be calculated, respectively, as follows:

$$\begin{aligned} \mathrm{prob}_r^1(i) &= \prod_{w=0}^{l^i-1}\left[1 - \frac{W \cdot \mathrm{prob}_r(i)}{W - w}\right], \\ \mathrm{prob}_r^k(i) &= \mathrm{prob}_r^1(i) \cdot \left[1 - \mathrm{prob}_r^1(i)\right]^{k-1}. \end{aligned} \tag{16}$$

Then, the probability that the traveler i can complete the parking and the expected search cost are as follows:

$$\sum_K \mathrm{prob}_r^k(i) = 1 - \left[1 - \mathrm{prob}_r^1(i)\right]^K, \tag{17}$$

$$\mathrm{E}[C_r^s(i)] = \sum_{k=1}^{K} \varepsilon k\lambda \cdot \mathrm{prob}_r^1(i) \cdot \left[1 - \mathrm{prob}_r^1(i)\right]^{k-1}. \tag{18}$$

When the K value is large, the equation (18) approximately equals to

$$\mathrm{E}[C_r^s(i)] = \frac{\varepsilon\lambda}{\mathrm{prob}_r^1(i)}, \tag{19}$$

According to equation (1), the travel cost $C_r^t(i)$ of traveler i in the mode r can be expressed as follows:

$$C_r^t(i) = \begin{cases} \dfrac{\alpha x_M}{v_c} & i \in \text{lot 1}, \\ \dfrac{\alpha x_M}{v_w} & i \in \text{lot 2}. \end{cases} \tag{20}$$

According to equations (19) and (20), the expected value of parking cost in the mode r can be expressed as follows:

$$\begin{aligned} \mathrm{E}\left[(C_r(i)\right] = &\left[\sum_K \mathrm{prob}_r^k(i)\right] \cdot \left\{\mathrm{E}\left[C_r^s(i)\right] + \frac{\alpha x_M}{v_c}\right\} \\ &+ \left[1 - \sum_K \mathrm{prob}_r^k(i)\right] \cdot \frac{\alpha x_M}{v_w}. \end{aligned} \tag{21}$$

The first term in equation (21) represents the traveler's expected parking cost in parking lot 1, and the second term represents the traveler's parking cost in parking lot 2.

The total cost of the mode r system is the sum of the parking costs of all travelers

$$TC_r = \sum_N \mathrm{E}\left[(C_r(i)\right]. \tag{22}$$

3.3. Comparison between "Arrival Priority" and "Reservation Priority" Modes. Sections 3.1 and 3.2 analyze the parking lot utilization rate under the two parking service modes of "arrival priority" and "reservation priority," the probability that travelers can complete parking in parking lot 1, and the cost of parking for travelers. This section compares the performance of the two modes around the above factors.

3.3.1. Parking Service Rate of Parking Lot 1. According to equations (5) and (15), the probability that a single time pane of a parking space in parking lot 1 is vacant determines the expected value of the probability that a traveler stops there. Equations (5) and (15) are based on equations (4) and (14), respectively. In the mode n and mode r, the order of parking service demand is different, and the characteristics of the needs of the traveler group are different, so it is hard to compare parking probability of a specific traveler. Without loss of generality, suppose that the two modes have served i demand, and the demand is evenly distributed in the time dimension. The service capacity of the two modes can be judged by the probability of being served when the $i+1$ demand arrives.

If the previous i demand occupies a total of $\sum_i l^q$ $(q \in i)$ panes in parking lot 1, then the average probability $\mathrm{prob}_j(i)$ $(\mathrm{prob}_n(i) = \mathrm{prob}_r(i))$ that each pane is occupied is as follows:

$$\mathrm{prob}_j(i) = \frac{\sum_i l^q}{KW}. \tag{23}$$

For the mode n, the probability that the $i+1$ th traveler can complete parking in the first parking space of parking lot 1 is as follows:

$$\mathrm{prob}_n^1(i+1) = 1 - \mathrm{prob}_n(i). \tag{24}$$

Based on this, the probability of completing parking in parking lot 1 can be calculated as follows:

$$\sum_K \mathrm{prob}_n^k(i+1) = 1 - \left[\mathrm{prob}_n(i)\right]^K. \tag{25}$$

For the mode r, the traveler's reservation is affected by two factors: whether the current parking space is vacant and whether there is no reservation during the future parking time. Then, the probability that the traveler completes the reservation in the first parking space of parking lot 1 is as follows:

$$\mathrm{prob}_r^1(i+1) = \prod_{w=0}^{l^i-1}\left[1 - \frac{W \cdot \mathrm{prob}_r(i)}{W - w}\right]. \tag{26}$$

Based on this, the probability of completing the parking reservation in parking lot 1 can be calculated as follows:

$$\sum_K \mathrm{prob}_r^k(i+1) = 1 - \left\{1 - \prod_{w=0}^{l^i-1}\left[1 - \frac{W \cdot \mathrm{prob}_r(i)}{W - w}\right]\right\}^K. \tag{27}$$

Observe the right side of equations (25) and (27). From $\mathrm{prob}_n(i) = \mathrm{prob}_r(i)$, it can be easily proved that

$$\prod_{w=0}^{l^i-1}\left[1 - \frac{W \cdot \mathrm{prob}_r(i)}{W - w}\right] \le 1 - \mathrm{prob}_n(i). \tag{28}$$

When $l^i = 1$, that is, when the parking duration of all travelers is 1, the equal sign of equation (27) holds. When the probability that each pane of parking lot 1 is occupied is $\mathrm{prob}_r(i) \longrightarrow 0$, the difference between the left and right sides of the Eq. is small, and vice versa.

The above conclusions are easy to understand. The parking space of parking lot 1 in mode n is only affected by whether they are vacant at the current time; in the mode r, travelers who actually depart late may also reserve parking permits early. Therefore, travelers need make sure that a certain parking space is available in time period $[t^i, t^i + l^i - 1]$ to make successful reservation. When the parking lot is used to a certain extent, the probability of continuous vacancy is lower compared to the previous case.

Let us take a simple example to illustrate the problem. Suppose the number of parking spaces in parking lot 1 is $K = 2$, the opening hours $W = 5$, the number of travelers $N = 4$, and the travel plan $t^i = i$ and $l^i = 2$.

As shown in Figure 4, if travelers arrive in chronological order, the number of demand that the parking lot can serve is 4. According to the reservation mode, there is a certain possibility (such as sequence 1243, 1423, 1432, 4123, 4132, and 4312) that only 3 service needs can be met.

3.3.2. Parking Cost. The cost of parking for travelers includes search cost and travel cost. The search cost of the two modes can be calculated by equations (8) and (18), respectively.

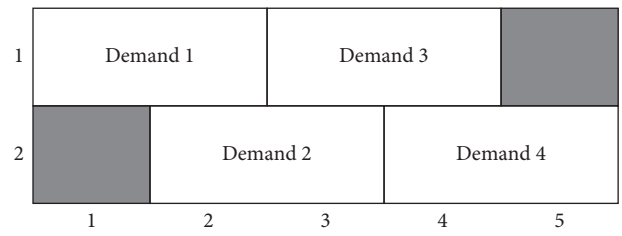

Figure 4: The impact of service order on the use of lot 1.

It is easy to prove that when some travelers choose parking lot 2, the search cost of this part of travelers in the mode r is 0, and the search cost in the mode n is $K\lambda$, so the mode r is more efficient.

When all travelers can be served by parking lot 1, the expected search cost of the i th traveler in the two modes is as follows:

$$\mathrm{E}\left[C_j^s(i)\right] = \begin{cases} \sum_{k=1}^{K} k\lambda \cdot \mathrm{prob}_j^1(i) \cdot \left[1 - \mathrm{prob}_j^1(i)\right]^{k-1} & j = n, \\ \sum_{k=1}^{K} \varepsilon k\lambda \cdot \mathrm{prob}_j^1(i) \cdot \left[1 - \mathrm{prob}_j^1(i)\right]^{k-1} & j = r. \end{cases} \tag{29}$$

According to equations (24) and (26), there is $\mathrm{prob}_r^1(i) \le \mathrm{prob}_n^1(i)$. Equation (29) shows that if we ignore that parking space information improves the search efficiency of travelers in the mode r (i.e., $\varepsilon < 1$), mode r has lower efficiency than mode n.

Considering the two situations comprehensively, it can be inferred that when the utilization rate and turnover rate of parking lot 1 are low (most travelers can complete parking in lot 1), the mode n may be more effective; when the utilization rate and turnover rate of parking lot 1 are high (some travelers need to complete parking in lot 2), the efficiency of mode r is higher.

In the same way, for the travel cost, the expected travel cost of the i th traveler in the two modes is as follows:

$$\mathrm{E}\left[C_j^t(i)\right] = \begin{cases} \mathrm{P} \cdot \dfrac{\alpha x_M}{v_c} + [1 - \mathrm{P}] \cdot \left(\dfrac{2\alpha x_M}{v_c} + \dfrac{\alpha x_M}{v_w}\right) & j = n, \\ \mathrm{P} \cdot \dfrac{\alpha x_M}{v_c} + [1 - \mathrm{P}] \cdot \dfrac{\alpha x_M}{v_w} & j = r, \end{cases} \tag{30}$$

where $P = \sum_K \mathrm{prob}_j^k(i)$.

According to equations (25) and (27), in equation (30), $\sum_K \mathrm{prob}_r^k(i) \le \sum_K \mathrm{prob}_n^k(i)$, it means that the traveler has higher probability of parking in parking lot 1 in the mode n, but if he parks in parking lot 2, the travel cost will be higher compared to mode r. Based on this, it can be inferred that when parking space in parking lot 1 can meet all needs, the two modes have the same travel cost; as the demand further increases, it is possible that all travelers park in parking lot 1 in the charging mode, but in the parking permit mode, some travelers need to choose parking lot 2, and the charging mode is more efficient at this time. When there is large demand and both modes have many travelers who choose parking lot 2, the parking permit mode is more efficient.

In summary, when the parking lot faces a large supply and demand contradiction, the "reservation priority"-based parking permit mode is more efficient, and when the parking lot supply is relatively sufficient, the "arrival priority"-based parking charging mode is more efficient. This is because during the parking permit reservation process, travelers still need to ensure that the parking spaces remain vacant for a period of time. This factor affects the service capacity of the parking lot.

4. Optimal Allocation of Parking Space Permits

The parking demand of travelers is aggregated to the total demand of the parking lot. In the case that the total demand for parking is determined, the management's different service orders (such as in the order of arrival or in the order of reservation) will result in completely different parking lot use forms and parking costs. Through the previous analysis, it can be seen that the service order will greatly affect the system efficiency. If the service order of parking permits can be optimized, the advantages of the two modes can be taken into account. In view of this, this section studies the parking permit allocation mode to improve the service order. In this mode, the manager first collects parking demand in a predetermined form and decides the allocation way of parking permits according to the optimal goal of the system.

4.1. Optimal Allocation Model for Parking Permits. In the parking permit mode r^* that optimizes the order of services, managers need to formulate strategies based on the needs of travelers and the supply of parking lots. Parking permit allocation strategy $\chi_{k,w}(i)$ meets

$$\sum_N \chi_{k,w}(i) \le 1, \quad k \in K; w \in W, \tag{31}$$

$$\sum_K \sum_W \chi_{k,w}(i) \le 1, \quad k \in K; w \in W, \tag{32}$$

$$\chi_{k,w}(i) \cdot \left(W - w - l^i\right) \ge 0, \quad k \in K; w \in W, \tag{33}$$

$$\chi_{k,w}(i) \cdot \sum_{\delta=1}^{l^i} \chi_{k,w+\delta}(q) = 0, \quad i \ne q; k \in K; w \in W. \tag{34}$$

Equation (31) indicates that any parking space is allocated at most once in a period of time, equation (32) indicates that any travel demand is allocated with at most one parking permit, and equation (33) indicates that the traveler's parking time needs to be in the opening hours of the parking lot. Equation (34) means that during the traveler's parking period, the parking space cannot be allocated to other travelers.

The conservation condition for the allocation of parking permits is as follows:

$$\chi(i) = \sum_{k=1}^{K} \sum_{w=1}^{W} \chi_{k,w}(i). \tag{35}$$

For all $i \in N$, $k \in K$, and $w \in W$, the costs of travelers in the mode r^* can be expressed as follows:

$$C_{r^*}^{s}(i) = \varepsilon\lambda \sum_{k=1}^{K} \sum_{w=1}^{W} k \cdot \chi_{k,w}(i), \tag{36}$$

$$C_{r^*}^{t}(i) = \frac{\alpha x_M}{v_c} \cdot \chi(i) + \frac{\alpha x_M}{v_w} \cdot [1 - \chi(i)]. \tag{37}$$

Equation (36) indicates that if the traveler parks in the parking lot 1, the search cost depends on the location of the parking space; otherwise, no search cost will be incurred. Equation (37) indicates that the travel cost of a traveler who parks in parking lot 1 is the travel cost over the distance x_M. Otherwise, it is the walking cost.

The total cost of parking for travelers can be the sum of search and travel costs:

$$TC_{r^*} = \sum_{i=1}^{N} C_{r^*}(i). \tag{38}$$

The goal of the system is to minimize the total parking cost TC_{r^*}. Since whether the traveler allocates a permit for parking lot 1 is determined by $\chi_{k,w}(i)$, according to equation (38), the objective function of the system is as follows:

$$\min TC_{r^*} = \sum_{i=1}^{N} C_{r^*}\left[\chi_{k,w}^{-1}(i)\right]. \tag{39}$$

The constraint conditions are shown in equation (31)–(34).

4.2. Optimization Allocation Algorithm Based on "Genetic-Ant Colony". According to the conclusion of Section 3, the higher the utilization rate of the parking lot, the more difficult it is to meet the parking demand of current travelers, and the greater the possibility that $\chi_{k,w}(i)$ is 0. That is, whether the parking demand is met is affected by the order. The compactness of the manager's service toward demand determines the utilization rate of parking lot 1, as well as the total cost of parking. The problem described in equation (39) can be transformed into solving the problem of a set of optimal service order SEQ^*.

The sorting combination of N travel demand is limited, so there is a minimum system cost. The optimization of the service order is similar to the traveling salesman problem (TSP). Considering that ant colony algorithm and genetic algorithm have better performance in local and global search, respectively, this paper uses the algorithm combining ant colony and genetics to find the optimal allocation order.

In the ant colony algorithm, we suppose that the service order corresponds to the path of ant colony, a single demand corresponds to a node on the path, and the total cost of parking based on different sorting of demands is the path cost of the ant colony. The ants of the current generation generate a set of path information after traversal to obtain the optimal path set of the current generation and update the pheromone concentration of the node transfer based on this. The genetic algorithm is nested in the ant colony algorithm, thus preventing the ant colony algorithm from falling into the local optimum. The path information corresponds to the gene sequence, and the nodes on the path correspond to single genes. Each time the ant colony algorithm forms a set of path information, the path information is mutated and optimized, and the optimal path is retained. The algorithm flow can be expressed as follows:

Step 1 is initialization. Set the number and initial position of the ant colony, pheromone and related update parameters, genetic variation parameters, the maximum number of iterations, etc.

Step 2: generate ant colony traversal path (demand distribution order). The ant determines the initial position and transfer direction according to the pheromone, and continuously searches for the unreached position to traverse all the demands.

Step 3: determine both parents of the ant colony (calculate the cost of the distribution plan). According to the cost of each ant (allocation plan), determine the current optimal plan as parent I, and all plans in this generation as parent II.

Step 4: ant colony cross-mutation and optimization (find the optimal allocation plan). The genes of both parents cross and mutate. Part of the gene sequence of parent I ants is extracted and combined with each ant gene of parent II, and the offspring ant colony equivalent to the parent II in number is generated by mutation. The ant colonies of the parent-child generations are optimized to update the pheromone.

Step 5: repeat steps 1 to 4 until the maximum number of iterations is reached.

The search behavior of ants is based on pheromone, and the pheromone update Eq. adopts the ant cycle model. Suppose the number of ants is M, and denote the pheromone matrix with $\tau(N \times N)$. $\tau(i,q)$ represents the pheromone concentration for arranging the travel demand q after the travel demand i is arranged, then

$$\tau(i,q)^{t+1} = (1-\rho)\tau(i,q)^{t} + \Delta\tau(i,q), \quad i \neq q, \tag{40}$$

$$\Delta\tau(i,q) = \sum_{K} \Delta\tau(i,q)^{k}, \tag{41}$$

$$\Delta\tau(i,q)^{k} = \frac{Q}{l(m)}. \tag{42}$$

In equations (40)–(42), t is the number of stages, ρ is the evaporation rate of pheromone, Q is the fixed parameter of pheromone update, and $l(m)$ is the total cost of each parking demand after the m th ant traverses.

The choice of the m th ant's search behavior at each step is determined by the transition probability p_{ij}^{k}.

$$p_{iq}^{m} = \begin{cases} \dfrac{[\tau(i,q)]^{\gamma}}{\sum_{S}[\tau(i,s)]^{\gamma}, S \subset \text{allowed}_m}, 0\text{else}. \end{cases} \quad (43)$$

In equation (43), allowed_m is the set of locations currently searchable by the ant m, and γ is the parameter. Since the distance between adjacent points is the same, the influence of ant visibility in the traditional model is ignored.

After the ant colony completes the node traversal, it reproduces and optimizes once. Suppose the optimal solution G^t until the stage t is the parent side; the solution F_M^t (M in number) searched by the ant colony in stage t is the other parent. The genes of both parents can be expressed as follows:

Parent I:

$$G^t = \left\{g_1^t, g_2^t, \ldots g_i^t, \ldots, g_N^t\right\}, \quad i \in N. \quad (44)$$

Parent II:

$$F_M^t = \begin{Bmatrix} f_{11}^t & f_{12}^t \cdots f_{1i}^t \cdots f_{1N}^t \\ f_{21}^t & f_{22}^t \cdots f_{2i}^t \cdots f_{2N}^t \\ \cdots & \cdots \cdots \cdots \cdots \cdots \\ f_{m1}^t & f_{m2}^t \cdots f_{mi}^t \cdots f_{1N}^t \\ \cdots & \cdots \cdots \cdots \cdots \cdots \\ f_{M1}^t & f_{M2}^t \cdots f_{Mi}^t \cdots f_{MN}^t \end{Bmatrix}, \quad m \in M; i \in N. \quad (45)$$

Both parental generations produce M offspring O_M^t through the following cross-mutation process. The crossover part is randomly generated from the parental generation G^t. M arrays $[X, Y]$ are randomly generated as the starting point and ending point of the crossover, which are expressed as follows:

$$\begin{aligned} X &= \{x(1), x(2), \ldots, x(M)\}, \\ Y &= \{y(1), y(2), \ldots, y(M)\}, \\ \forall x(m) &\le N, \quad \forall y(m) \le N, \\ \forall x(m) &\le y(m), \quad m \in M. \end{aligned} \quad (46)$$

The gene sequence in the parental generation G^t of the m cross-selection in stage t can be expressed as $\left\{g_{x(m)}^t, g_{x(m)+1}^t, \ldots, g_{y(m)}^t\right\}$.

The gene sequence selected by the parent G^t is combined with the parent F_M^t. Find and delete the same elements as sequence $G_m^t = \left\{g_{x(m)}^t, g_{x(m)+1}^t, \ldots, g_{y(m)}^t\right\}$ in the sequence $F_m^t = \{f_{m1}^t, f_{m2}^t, \ldots, f_{mN}^t\}$, and the relative positions of the remaining elements remain unchanged. Insert the sequence G_m^t into the $x(m)$ position of the original F_m^t to form the original offspring. Figure 5 shows the gene sequences of both parents.

Assume that the gene sequence of the parental generation G contains only two adjacent elements $g_{x(m)}^t$ and $g_{y(m)}^t$, which are, respectively, equal to the element f_{m2}^t and f_{mN-2}^t in the parental generation F. After crossover, the gene sequence composition of the offspring O is shown in Figure 6. The genes of the offspring O are composed of genes G and F. Where the relative positions of other elements in F do not change, the gene sequence in G is inserted into position $x(m)$ to $y(m)$.

The offspring will mutate with a lower probability η. Let the mutation behavior be the inversion of the access point of the gene sequence; that is, the gene sequence $\Gamma_m^t = \left\{g_{y(m)}^t, g_{y(m)-1}^t, \ldots, g_{x(m)}^t\right\}$ inserted at the $x(m)$ position. The original offspring forms the final offspring after the mutation process. Figure 7 shows the gene sequence after mutation (if any) in the offspring of Figure 6. Compared with the original offspring, the order of genes at positions $x(m)$ and $y(m)$ is reversed.

4.2.1. Optimization. After the genetic algorithm cross-mutation in stage t, the parent F and the offspring O have a total of $2M$ solutions. In order to update the pheromone efficiently, the ant colony conducts internal optimization, selects the first M solutions according to the pros and cons of the solution, and updates the pheromone according to the cost. Compare the optimal solution at this stage with that before the stage t and select the best to generate a new parent G^{t+1}.

5. Numerical Examples

To compare the effects of the three parking management modes of "arrival priority," "reservation priority," and "service order optimization," this section designs a numerical example to simulate the performance of three modes in parking costs, parking lot utilization rate, and the number of vehicles in parking lot 1 under different parking supply-demand level.

The opening time of the parking lot includes the number of time panes $W = 12$. Travel demand $N = 50$, and traveler's arrival time and parking duration are shown in Table 2. The number of parking spaces takes $K = 1 \sim 25$ separately. Considering the possibility of multiple people in one vehicle, we suppose the walking cost is 90 per vehicle and the vehicle travel cost is 10 per vehicle ($\alpha = 1/9$). In the parking lot, the search cost of a unit parking space without a parking target is $\lambda = 0.5$, and the search cost of unit parking space with a parking target is 0.2 ($\varepsilon = 0.4$).

The parameters of the ant colony and genetic combination algorithm are set as follows: the number of ants $M = 20$, the maximum number of iterations $NC = 1000$, the importance of pheromone $\gamma = 3$, the pheromone evaporation factor $\rho = 0.2$, the pheromone update parameter $Q = 150$, and the mutation rate of the offspring ants $\eta = 0.01$.

In Table 2, travel demand is sorted in a reserved order, which is applicable to modes r and r^*. In the mode n, the arrival sequence of travelers is determined according to the sequence of the expected arrival time, as shown in Table 3. The parking demand contained in Tables 2 and 3 is equal, but the sorting order is different.

Parent I:	g_1^t	g_2^t	g_3^t	⋯	$g_{x(m)-1}^t$	$g_{x(m)}^t$	$g_{y(m)}^t$	$g_{x(m)+1}^t$	⋯	g_{N-2}^t	g_{N-1}^t	g_N^t
Parent II:	f_{m1}^t	f_{m2}^t	f_{m3}^t	⋯	$f_{mx(m)-1}^t$	$f_{mx(m)}^t$	$f_{my(m)}^t$	$f_{my(m)+1}^t$	⋯	f_{mN-2}^t	f_{mN-1}^t	f_{mN}^t

Figure 5: The gene sequence of both parents in the ant colony algorithm.

Offspring:	o_{m1}^t	o_{m2}^t	o_{m3}^t	⋯	$o_{mx(m)-1}^t$	$o_{mx(m)}^t$	$o_{my(m)}^t$	$o_{my(m)+1}^t$	⋯	o_{mN-2}^t	o_{mN-1}^t	o_{mN}^t
	f_{m1}^t	f_{m3}^t	f_{m4}^t	⋯	$f_{mx(m)}^t$	$g_{x(m)}^t$	$g_{y(m)}^t$	$f_{my(m)}^t$	⋯	f_{mN-3}^t	f_{mN-1}^t	f_{mN}^t

Figure 6: The offspring gene sequence in the ant colony algorithm.

Offspring:	o_{m1}^t	o_{m2}^t	o_{m3}^t	⋯	$o_{mx(m)-1}^t$	$o_{mx(m)}^t$	$o_{my(m)}^t$	$o_{my(m)+1}^t$	⋯	o_{mN-2}^t	o_{mN-1}^t	o_{mN}^t
	f_{m1}^t	f_{m3}^t	f_{m4}^t	⋯	$f_{mx(m)}^t$	$g_{y(m)}^t$	$g_{x(m)}^t$	$f_{my(m)}^t$	⋯	f_{mN-3}^t	f_{mN-1}^t	f_{mN}^t

Figure 7: The offspring gene sequence containing the variant gene.

Table 2: Travelers' parking demand under the "reservation priority" mode.

Arrival order	Arrival time	Duration	Arrival order	Arrival time	Duration	Arrival order	Arrival time	Duration
1	3	5	**18**	3	4	**35**	3	4
2	9	3	**19**	3	3	**36**	8	1
3	8	3	**20**	2	3	**37**	3	3
4	11	2	**21**	6	2	**38**	9	1
5	2	2	**22**	9	3	**39**	4	4
6	9	3	**23**	3	5	**40**	2	2
7	3	3	**24**	10	3	**41**	2	2
8	1	5	**25**	9	3	**42**	4	2
9	2	4	**26**	10	3	**43**	9	3
10	6	3	**27**	4	4	**44**	3	2
11	3	2	**28**	4	3	**45**	9	2
12	12	1	**29**	4	4	**46**	8	4
13	1	2	**30**	3	3	**47**	1	3
14	7	4	**31**	3	4	**48**	3	4
15	3	3	**32**	5	4	**49**	10	1
16	10	3	**33**	8	3	**50**	6	3
17	3	3	**34**	3	2			

Table 3: Parking demand of travelers under the "arrival priority" mode.

Arrival order	Arrival time	Duration	Arrival order	Arrival time	Duration	Arrival order	Arrival time	Duration
1	1	5	**18**	3	3	**35**	6	3
2	1	2	**19**	3	5	**36**	7	4
3	1	3	**20**	3	3	**37**	8	3
4	2	2	**21**	3	4	**38**	8	3
5	2	4	**22**	3	3	**39**	8	1
6	2	3	**23**	9	1	**40**	8	4
7	2	2	**24**	9	3	**41**	9	3
8	2	2	**25**	9	2	**42**	9	3
9	3	2	**26**	3	4	**43**	9	3
10	3	4	**27**	4	4	**44**	9	3
11	3	2	**28**	4	3	**45**	10	3
12	3	5	**29**	4	4	**46**	10	3
13	3	3	**30**	4	4	**47**	10	3
14	3	2	**31**	4	2	**48**	10	1
15	3	3	**32**	5	4	**49**	11	2
16	3	3	**33**	6	3	**50**	12	1
17	3	4	**34**	6	2			

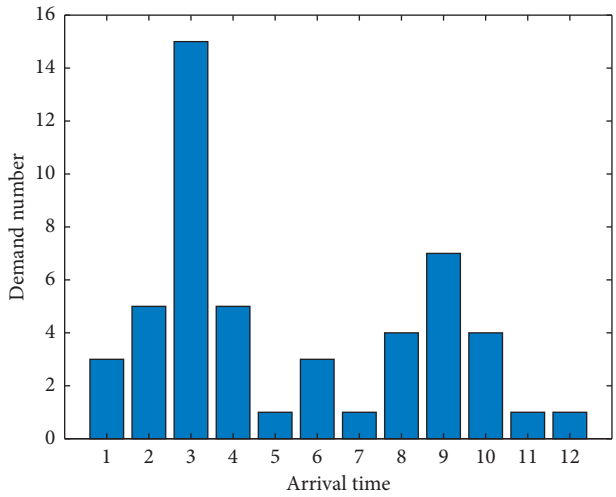

Figure 8: Parking demand distribution.

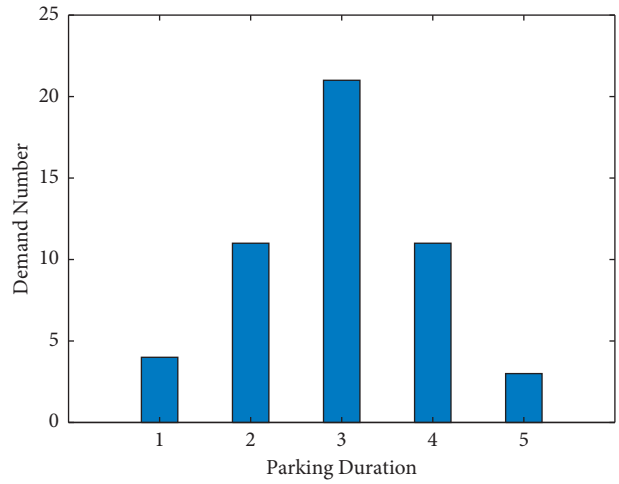

Figure 9: Parking duration distribution.

Figures 8 and 9, respectively, show the number of travel demands under different arrival time and different parking durations. Suppose that there are two peaks in parking demand, in time period 3 and time period 9, respectively, while the demand in the remaining period is small; in terms of parking duration, parking demands with medium duration are the most, and demand for longer or shorter travel decreases in turn.

According to the previous assumptions on parking behavior and cost, under different K values (representing different supply-demand level), the number of vehicles parked in the parking lot 1 and the utilization rate of the parking lot in the three modes, namely, the number of parked vehicles $*$ parking duration/(number of parking spaces $*$ parking lot opening hours) are shown in Figures 10 and 11.

By observing Figures 10 and 11, we draw the following conclusions:

(1) The order of service determines the number of parked vehicles in the parking lot and the parking lot utilization rate. In this example, the minimum number of parking spaces required for all travelers to complete parking in parking lot 1 is 23. When the number of parking spaces is less than 23, in comparison with mode n and mode r, the parking lot utilization rate and the parking number in mode n are higher than mode r in most cases. This phenomenon is consistent with the discussion in Section 3. The mode n has better parking service order than the mode r in overall. When the number of parking spaces exceeds 23, there is no difference between the two modes, and 50 travelers can complete parking in parking lot 1.

(2) Mode r^* is superior to the mode n and mode r in the two indicators of parking number and the utilization rate of parking lot 1. Since the mode r^* optimizes the service order, more parking needs can be met under the same number of parking spaces. When the parking lot contains only 1 parking space, the parking lot utilization rate in all the three modes is 1, but the mode r^* can meet 6 demands, while the modes n and r can only meet 4 and 5 demands, respectively. When the number of parking spaces is between 1 and 23, the two indicators of the mode r^* are also higher in varying degrees.

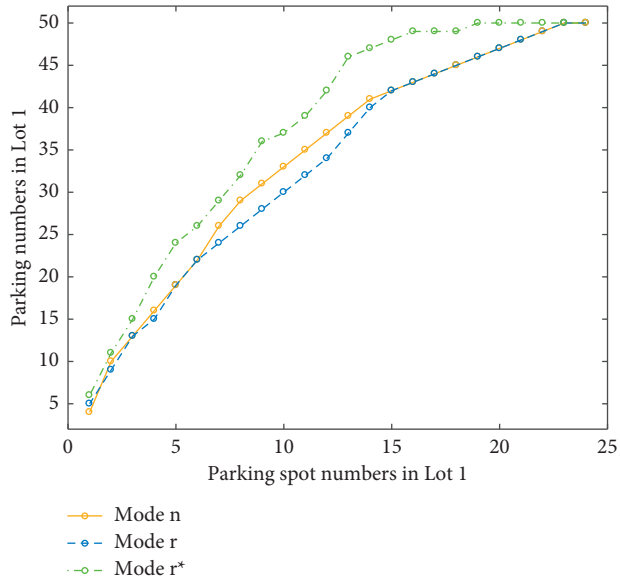

Figure 10: Parking number in lot 1 of the three modes.

Figure 12 reflects the per capita parking cost under the three modes.

According to the change trend of the graph, the parking lot availability can be divided into 4 stages based on the supply status, which are low (less than 4 parking spaces), relatively low (5 to 13 parking spaces), relatively high (14–21 parking spaces), and high (more than 22 parking spaces). By observing Figure 12, the following conclusions can be drawn:

(1) In different parking space numbers, the per capita cost of the parking reservation management mode

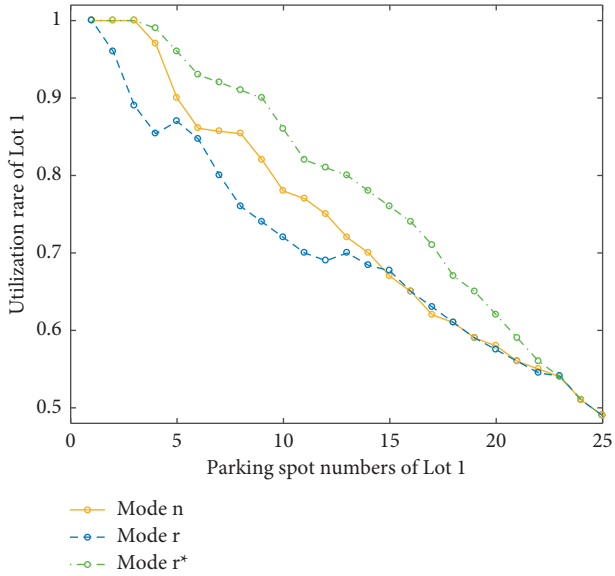

Figure 11: Utilization rate of lot 1 of the three modes.

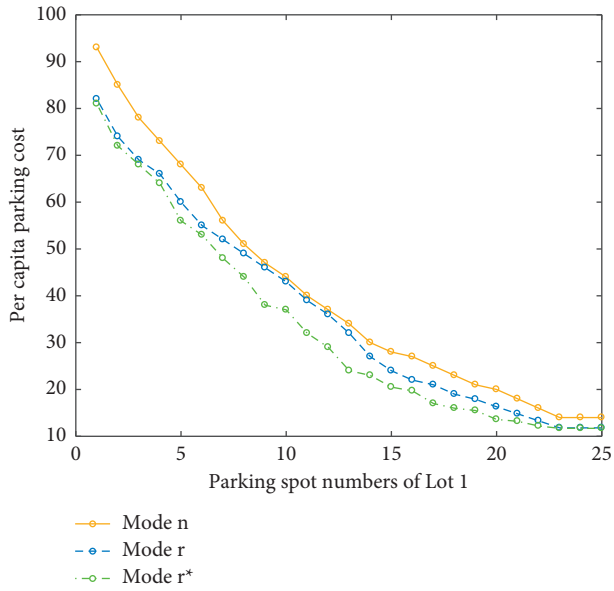

Figure 12: Per capita parking cost of travelers in the three modes.

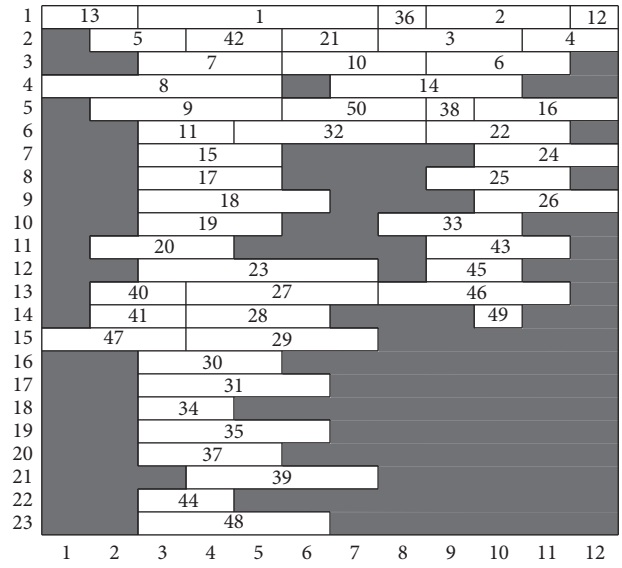

Figure 13: Usage of parking lot 1 in mode r.

(r, r^*) is lower than the per capita cost of the "arrival priority" mode (n) to varying degrees. It reflects that the parking reservation mode has a good effect in lowering search cost and parking uncertainty.

(2) As the number of parking spaces increases from small to large, more travelers can park their vehicles in parking lot 1. The uncertainty of travelers moving between two parking lots in parking is reduced, and the search cost has weakened impact on the total cost, which is reflected in the continuous reduction of the per capita cost difference in the graph between the "arrival priority" mode and the "reservation priority" mode.

(3) As the number of parking spaces increases, the impact of the cost affected by the order of demand on the total cost shows a trend of "strengthening first, then weakening." When the number of parking spaces is "small," the parking lot is saturated in any order of demand, and the difference in the order of demand creates little effect on parking costs. For its reflection, although the order of demand is different between mode r^* and mode r, the difference from per capita cost in mode n is relatively fixed. When the number of parking spaces changes to "relatively small," the order of demand gradually affects the cost (in this example, mode n has superior parking order than the mode r, so the difference in per capita cost between the two tends to shrink at this stage. In practice, this situation is much likely to occur). When the number of parking spaces increases to "relatively high" and most needs can be met in the parking lot, the influence of the order of demand shows a weakening trend, and there is savings in search cost under the parking permit management mode. Finally, when the number of parking spaces increases to "high," the cost difference between three modes returns to a relatively fixed state; that is, the search cost of the two permit modes in the parking lot 1 is reduced.

(4) When the number of parking spaces is "large," further increase in the number of parking spaces will no longer reduce the total cost. It can be seen from the graph that after the number of parking spaces exceeds 23, the total cost will no longer decrease.

(5) There is little difference between the mode r^* and the mode r when the number of parking spaces is "small" and "high," and the difference is obvious when the number of parking spaces is "relatively small" and "relatively high," indicating that the two parking permit modes have similar advantages in reducing search costs, and the mode r^* has a more obvious advantage in reducing the travel cost generated by the service order.

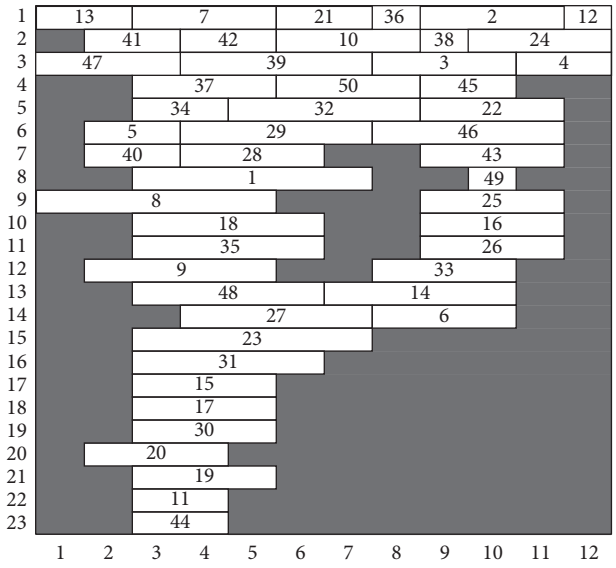

Figure 14: Usage of parking lot in mode r^*.

Figures 13 and 14 reflect the usage status of the parking lot within a day (the number of time interval is 12) under the management modes r and r^* when the number of parking spaces is sufficient (the number of parking spaces is 23).

When the number of parking spaces is 23, all travelers in mode r and mode r^* will complete their parking in parking lot 1. The total travel cost of the mode r is 590.2, and the total parking cost of the mode r^* is 584.2, indicating that the mode r^* is still superior to mode r if the parking demand can be fully guaranteed. It can be seen from the figure that the parking space with a smaller number in Figure 14 (indicating that the search cost in parking lot 1 is smaller) meets more parking needs in a day than the parking space with a smaller number in Figure 13. This conclusion shows that mode r^* can achieve the goal of reducing parking costs by increasing the utilization rate and turnover rate of convenient parking spaces in the parking lot.

6. Conclusions and Prospects

Insufficient parking supply in central urban areas makes travelers spend more time searching for parking spaces or face the risk of being unable to park in the target parking lot. The existing research mostly considered the universal parking permit and reservation mode. The former has deficiencies in the internal search cost and the utilization rate of the parking lot, while the latter has deficiencies in the parking service number. Focusing on the above factors, this paper analyzes parking cruising in (search cost) and between (additional travel cost) of the parking lots, and proposes an improved permit mode to further optimize the parking service.

This paper defines three parking management modes. The first is "arrival priority" mode, and the parking lot at the destination provides service according to the traveler's arrival time. If the parking lot is fully occupied when the traveler arrives at the destination, then he returns to a farther parking lot (parking lot 2). The second is "reservation priority" mode, and travelers reserve parking permits in advance and complete parking at designated parking spaces. If one fails to obtain parking permit through application, they choose other parking lots. The third is "service order optimization" service mode. Managers selectively allocate parking permits by combining parking needs under the goal of system optimization. After theoretical derivation and analysis of calculation examples, the following conclusions are drawn:

(1) The advantage of the "arrival priority" mode is that the system service order is closer to the optimal service order without the intervention of the manager; the disadvantage is that the traveler cannot access the information about other travelers' plan and parking lot usage information, thus unable to improve parking efficiency by adjusting his behavior. Travelers may take a long time to search or fail to find a vacant parking space in the target parking lot.

(2) The advantage of the "reservation priority" mode is that travelers can identify parking spaces in advance, search fast, and avoid round-trips between parking lots. The disadvantage is that the system's service order is inferior, which affects the service capacity of the parking lot. In some cases, travelers may experience a higher total cost compared to the "arrival priority" mode.

(3) Solving the service order problem of the permit mode is the key to further reducing the system cost. This problem is equivalent to the optimal allocation of permits. This paper applies the combination of ant colony and genetic algorithms with strong local and global optimization capabilities to find a satisfactory solution to the optimal service order, and verifies that the parking permit mode of "service order optimization" has better results in terms of the number of served parking demand, parking lot utilization rate at the destination, and per capita parking cost of travelers.

With the development of information technology, the permit mode can be applied to parking management more conveniently and economically. On the one hand, it will effectively improve the utilization efficiency of existing parking resources because of its advantages in precisely matching supply and demand and providing guidance information for parking lots. On the other hand, the permits mode optimizes the service order of demands and sets different priorities for requirements. It can be applied to the shared management of private parking spaces (prioritizing the parking needs of space owners), thus integrating more types of parking supply. Future research can continue to focus on the dynamics of parking management, evaluate real-time parking demand based on historical data, and set service priorities to achieve optimal matching between parking supply and demand.

Data Availability

The data used to support the findings of this study are included within the article.

Conflicts of Interest

The authors declare that they have no conflicts of interest or personal relationships that could have appeared to influence the work reported in this paper.

Acknowledgments

This work was supported by the National Natural Science Foundation of China (91846202, 71890972/71890970, and 72171020) and the 111 Project (B20071).

References

[1] T. Litman, *Parking Management Comprehensive Implementation Guide*, Victoria Transport Policy Institute, Victoria, BC, Canada, 2011.

[2] K. Axhausen, J. Polak, M. Boltze, and J. Puzicha, "Effectiveness of the parking guidance information system in frankfurt am main," *Traffic Energy & Control*, vol. 35, no. 5, pp. 304–309, 1994.

[3] R. Arnott and J. Rowse, "Modeling parking," *Journal of Urban Economics*, vol. 45, no. 1, pp. 97–124, 1999.

[4] V. R. Vuchic, *Transportation for Livable Cities*, Routledge, New York, NY, USA, 1999.

[5] D. C. Shoup, "Cruising for parking," *Transport Policy*, vol. 13, no. 6, pp. 479–486, 2006.

[6] J. N. van Ommeren, D. Wentink, and P. Rietveld, "Empirical evidence on cruising for parking," *Transportation Research Part A: Policy and Practice*, vol. 46, no. 1, pp. 123–130, 2012.

[7] J. B. Lee, D. Agdas, and D. Baker, "Cruising for parking: new empirical evidence and influential factors on cruising time," *Journal of Transport and Land Use*, vol. 10, no. 1, pp. 931–943, 2017.

[8] E. Inci, J. V. Ommeren, and M. Kobus, "The external cruising costs of parking," *Journal of Economic Geography*, vol. 17, no. 6, pp. 1301–1323, 2017.

[9] F. Alemi, C. Rodier, and C. Drake, "Cruising and on-street parking pricing: a difference-in-difference analysis of measured parking search time and distance in San Francisco," *Transportation Research Part A: Policy and Practice*, vol. 111, pp. 187–198, 2018.

[10] B. Assemi, D. Baker, and A. Paz, "Searching for on-street parking: an empirical investigation of the factors influencing cruise time," *Transport Policy*, vol. 97, pp. 186–196, 2020.

[11] E. Inci and R. Lindsey, "Garage and curbside parking competition with search congestion," *Regional Science and Urban Economics*, vol. 54, pp. 49–59, 2015.

[12] R. Weinberger, A. Millard-Ball, and R. C. Hampshire, *Parking Search Caused Congestion: Where's All the Fuss*, Paper Presented at Transportation Research Board Annual Meeting, 2017.

[13] R. C. Hampshire and D. Shoup, "What share of traffic is cruising for parking?" *Journal of Transport Economics and Policy*, vol. 52, no. 3, pp. 184–201, 2018.

[14] Transportation Alternatives, *No Vacancy. Park Slope's Parking Problem and How to Fix it*, New York, NY, USA, 2007.

[15] H. Yang and X. L. Wang, "Managing network mobility with tradable credits," *Transportation Research Part B: Methodological*, vol. 45, no. 3, pp. 580–594, 2011.

[16] A. Millard-Ball, R. C. Hampshire, and R. Weinberger, "Parking behaviour: the curious lack of cruising for parking in San Francisco," *Land Use Policy*, vol. 91, Article ID 103918, 2020.

[17] E. Inci, "A review of the economics of parking," *Economics of Transportation*, vol. 4, no. 1-2, pp. 50–63, 2015.

[18] S. Lehner and S. Peer, "The price elasticity of parking: a meta-analysis," *Transportation Research Part A: Policy and Practice*, vol. 121, pp. 177–191, 2019.

[19] Sfmta, "San Francisco parking census fact sheet," San Francisco, CL, USA, 2014.

[20] Z. Y. Gu, A. Najmi, M. Saberi, W. Liu, and T. H. Rashidi, "Macroscopic parking dynamics modeling and optimal real-time pricing considering cruising-for-parking," *Transportation Research Part C: Emerging Technologies*, vol. 118, Article ID 102714, 2020.

[21] S. P. Anderson and A. de Palma, "The economics of pricing parking," *Journal of Urban Economics*, vol. 55, no. 1, pp. 1–20, 2004.

[22] Z. C. Li, W. H. K. Lam, S. C. Wong, D. L. Zhu, D. L. Zhu, and H. J. Huang, "Modeling park-and-ride services in a multimodal transport network with elastic demand," *Transportation Research Record*, vol. 1994, no. 1, pp. 101–109, 2007.

[23] Z. S. Qian and R. Rajagopal, "Optimal dynamic parking pricing for morning commute considering expected cruising time," *Transportation Research Part C: Emerging Technologies*, vol. 48, pp. 468–490, 2014.

[24] W. D. Montgomery, "Markets in licenses and efficient pollution control programs," *Journal of Economic Theory*, vol. 5, no. 3, pp. 395–418, 1972.

[25] T. D. Crocker, "The structure of atmospheric pollution control system," *The Economic of Air Pollution*, vol. 61, pp. 81–84, 1966.

[26] J. H. Dales, *Pollution, Property, and Prices: An Essay in Policy-Making and Economics*, University of Toronto Press, Toronto, Canada, 1968.

[27] X. N. Zhang, H. Yang, and H. J. Huang, "Improving travel efficiency by parking permits distribution and trading," *Transportation Research Part B: Methodological*, vol. 45, no. 7, pp. 1018–1034, 2011.

[28] H. Yang, W. Liu, X. L. Wang, and X. N. Zhang, "On the morning commute problem with bottleneck congestion and parking space constraints," *Transportation Research Part B: Methodological*, vol. 58, pp. 106–118, 2013.

[29] W. Liu, H. Yang, Y. Yin, and F. Zhang, "A novel permit scheme for managing parking competition and bottleneck congestion," *Transportation Research Part C: Emerging Technologies*, vol. 44, pp. 265–281, 2014.

[30] T. Akamatsu and K. Wada, "Tradable network permits: a new scheme for the most efficient use of network capacity," *Transportation Research Part C: Emerging Technologies*, vol. 79, pp. 178–195, 2017.

[31] M. Xu and S. Grant-Muller, "Tradable credits scheme on urban travel demand: a linear expenditure system Approach and simulation in beijing," *Transportation Research Procedia*, vol. 25, pp. 2934–2948, 2017.

[32] J. Wang, X. N. Zhang, and H. M. Zhang, "Parking permits management and optimal parking supply considering traffic emission cost," *Transportation Research Part D: Transport and Environment*, vol. 60, pp. 92–103, 2018.

[33] J. Wang, X. N. Zhang, H. Wang, and M. Zhang, "Optimal parking supply in bi-modal transportation network considering transit scale economies," *Transportation Research Part E: Logistics and Transportation Review*, vol. 130, pp. 207–229, 2019.

[34] J. Wang, H. Wang, and X. N. Zhang, "A hybrid management scheme with parking pricing and parking permit for a many-to-one park and ride network," *Transportation Research Part C: Emerging Technologies*, vol. 112, pp. 153–179, 2020.

[35] Z. Y. Mei, C. Feng, W. C. Ding, L. H. Zhang, and D. H. Wang, "Better lucky than rich? Comparative analysis of parking reservation and parking charge," *Transport Policy*, vol. 75, pp. 47–56, 2019.

[36] X. Wang and X. Wang, "Flexible parking reservation system and pricing: a continuum approximation approach," *Transportation Research Part B: Methodological*, vol. 128, pp. 408–434, 2019.

[37] S. Shao, S. X. Xu, H. Yang, and G. Q. Huang, "Parking reservation disturbances," *Transportation Research Part B: Methodological*, vol. 135, pp. 83–97, 2020.

[38] F. Zhang, W. Liu, X. Wang, and H. Yang, "Parking sharing problem with spatially distributed parking supplies," *Transportation Research Part C: Emerging Technologies*, vol. 117, Article ID 102676, 2020.

[39] S. Wang, Z. Li, and N. Xie, "A reservation and allocation model for shared-parking addressing the uncertainty in drivers' arrival/departure time," *Transportation Research Part C: Emerging Technologies*, vol. 135, Article ID 103484, 2022.

[40] H. H. Xiao, M. Xu, and Z. Y. Gao, "Shared parking problem: a novel truthful double auction mechanism approach," *Transportation Research Part B: Methodological*, vol. 109, pp. 40–69, 2018.

[41] H. H. Xiao, M. Xu, and H. Yang, "Pricing strategies for shared parking management with double auction approach: differential price vs. uniform price," *Transportation Research Part E: Logistics and Transportation Review*, vol. 136, Article ID 101899, 2020.

[42] G. Y. Li, Y. X. Li, H. Y. Chen, and W. Deng, "Fractional-order controller for course-keeping of underactuated surface vessels based on frequency domain specification and improved particle swarm optimization algorithm," *Applied Sciences*, vol. 12, no. 6, 2022.

[43] W. Deng, Z. X. Li, X. Y. Li, H. Y. Chen, and H. M. Zhao, "Compound fault diagnosis using optimized MCKD and sparse representation for rolling bearings," *IEEE Transactions on Instrumentation and Measurement*, vol. 71, pp. 1–9, 2022.

[44] X. J. Ran, X. B. Zhou, M. Lei, W. Tepsan, and W. Deng, "A novel K-means clustering algorithm with a noise algorithm for capturing urban hotspots," *Applied Sciences*, vol. 11, no. 23, Article ID 11202, 2021.

[45] W. Deng, X. X. Zhang, Y. Q. Zhou et al., "An enhanced fast non-dominated solution sorting genetic algorithm for multi-objective problems," *Information Sciences*, vol. 585, pp. 441–453, 2022.

[46] H. Cui, Y. Guan, and H. Chen, "Rolling element fault diagnosis based on VMD and sensitivity MCKD," *IEEE Access*, vol. 9, Article ID 120297, 2021.

[47] Y. Yang, Z. Yuan, J. Chen, and M. Guo, "Assessment of osculating value method based on entropy weight to transportation energy conservation and emission reduction," *Environmental Engineering and Management Journal*, vol. 16, no. 10, pp. 2413–2423, 2017.

[48] Y. S. Ci, H. L. Wu, Y. C. Sun, and L. Wu, "A prediction model with wavelet neural network optimized by the chicken swarm optimization for on-ramps metering of the urban expressway," *Journal of Intelligent Transportation Systems*, vol. 26, no. 3, pp. 356–365, 2022.

[49] Y. Yang, K. He, Y. P. Wang, Z. Z. Yuan, Y. H. Yin, and M. Z. Guo, "Identification of dynamic traffic crash risk for cross-area freeways based on statistical and machine learning methods," *Physica A: Statistical Mechanics and Its Applications*, vol. 595, no. 1, Article ID 127083, 2022.

Hindawi
Journal of Advanced Transportation
Volume 2022, Article ID 7568836, 14 pages
https://doi.org/10.1155/2022/7568836

Research Article

The Effect of Key Indicators on the Operation Costs for Public Toll Roads

Bin Shang,[1] **Huibing Li**,[2] **and Hanchuan Pan**[3,4]

[1]*Shanghai Jian Qiao University, 1111 Hucheng Ring Road, Shanghai 201306, China*
[2]*School of Transport and Communications, Shanghai Maritime University, 1550 Haigang Ave., Shanghai 201306, China*
[3]*School of Urban Rail Transportation, Shanghai University of Engineering Science, 333 Longteng Road, Shanghai 201620, China*
[4]*School of Economics and Management, Tongji University, Shanghai 200092, China*

Correspondence should be addressed to Hanchuan Pan; panhanchuan@sues.edu.cn

Received 2 March 2022; Accepted 16 April 2022; Published 16 May 2022

Academic Editor: Elżbieta Macioszek

Copyright © 2022 Bin Shang et al. This is an open access article distributed under the Creative Commons Attribution License, which permits unrestricted use, distribution, and reproduction in any medium, provided the original work is properly cited.

At the end of the build-operate-transfer road concession period, an optimal model for the operation of public toll roads is created based on user heterogeneity regarding the values of time for different road users. The impact of user heterogeneity on operation costs for government and private firms is subsequently analyzed on the following critical variables: user values of time, road volume/capacity ratio, and road capacity. Concerning the values of time for different road users, the mean residual and failure functions are established to describe three optimization hypotheses: maximization of social welfare with operation by the government, two extreme cases with operation by a private firm, and a Pareto-optimal solution with operation by a private firm. It is concluded that the mean residual values of the time function are a linear function of the user values of time under a Pareto-optimal operation by the government. It is also determined that private profit is related to the demand-related operational cost of the government and private firm under a Pareto-optimal operation by a private firm. These conclusions suggest relevant recommendations for the government on policymaking for the operation of public toll roads.

1. Introduction

Many roads, especially highways, have been built according to the build-operate-transfer (BOT) model in the past forty years since it was established and applied in Turkey. Roads built based on the BOT model can be operated by a private firm for a specific time, usually lasting 30–50 years, depending on the contract. In some cases, the BOT concession period can be as long as 99 years, such as Highway 407 in Toronto, Canada [1].

At present, an increasing number of BOT roads are being transferred to the government with the expiration of the BOT contracts. After this transfer, the BOT road is normally expected to become public, which allows the drivers to use it for free, as described in Figure 1. The government then takes responsibility for operating the road using government funds. De Palma et al. [2] assumed that the required standard could not be maintained for the service provided to road users after the BOT concession period. However, as an essential means of transportation between cities, it is critical to ensure the necessary availability of the road to users after it has been transferred to the government.

Although the operation cost (OC), including but not limited to the maintenance cost, is not comparable to the initial construction cost of the road, it is still considered a considerable amount of government expenditure. The solution is to collect a toll for road use to compensate for the OC. This type of road is called a public toll road (PTR) [3], as shown in Figure 2. These roads are being charged for transportation use in China [4]. The Chinese government can whether operate the PTR road on its own by collecting certain amount of toll from the users or entrust a private firm with the same responsibility, which differs from the case of the BOT model.

Sufficient studies have focused on the construction and operation of BOT roads with heterogeneous users [1, 5–11]; however, few researchers have focused on the operation of PTR

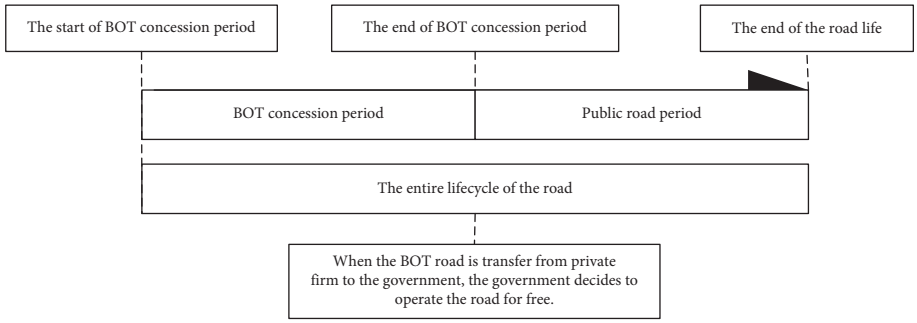

Figure 1: A BOT road becomes a public road.

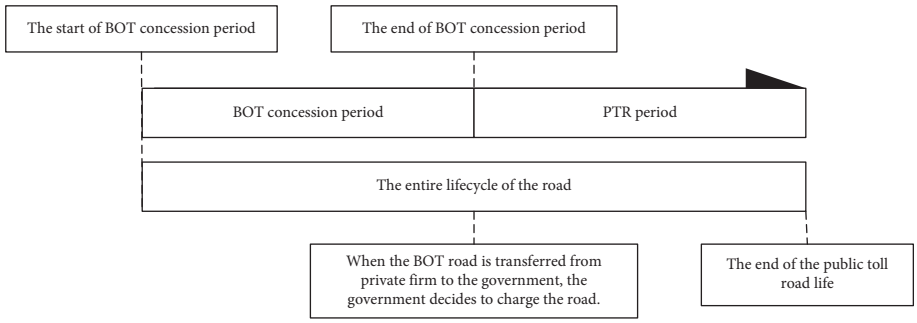

Figure 2: A BOT road becomes a public toll road (PTR).

with heterogeneous users. To the best of our knowledge, the function of OC during PTR has not been sufficiently studied.

In contrast to existing research, we explicitly examine the influence of heterogeneous users on the OC of PTR after the expiration of the BOT concession period by considering the benefits for government and private firms. Two options are available if the government continues to charge a toll for the road during the PTR period. The government can either operate the road independently or choose a private firm to operate it. Thus, the government must make decisions. In our model, by considering the OC in the objective function and introducing an additional constraint on OC, we are in a position to determine not only the effect of the value of time (VOT) on the OC of PTR but also the length of the PTR period as well as the level of toll to be charged from the users.

To analyze the impact of PTR on OC, we introduce a mean residual VOT function and a failure rate to characterize user heterogeneity. In addition, we examine the properties of OC with three basic variables: the length of the PTR period, the road capacity, and the price of the toll to maximize the social welfare of PTR with government operation. We further investigate two extreme cases of PTR with private firm operations and achieve the Pareto-optimality for PTR. Based on the studies mentioned above, this paper can provide insight, defining government policy on transportation.

The rest of the paper is organized as follows: Section 2 reviews the literature. Section 3 introduces the relevant definitions and assumptions. Section 4 presents the properties of OC by analyzing the operation by the government, two extreme cases with operation by a private firm, and Pareto-efficient PTR. Finally, Section 5 concludes the paper.

2. Literature Review

Most existing literature on BOT road studies focuses on capacity determination, toll charges, length of the concession period, private profit, and social welfare related to BOT roads. The analysis of social welfare can be traced back to Pigou [12]. Beckmann et al. [13] analyzed the social welfare of transportation (system with an economic model) and created a classic traffic (or transportation) model known as the Beckmann transformation, which had a significant impact on subsequent research. Subsequently, Walters [14] and Vickrey [15, 18] developed additional transportation models. A notable achievement of BOT studies is the self-financing theorem, deduced under the first-best condition on a one-way road with homogeneous users. The toll charge given by the self-financing theorem, which states that the total revenue of the toll road collected from users only covers its investment under certain conditions, is equal to the difference between the social and private marginal costs.

Further research was conducted on a general transportation network in both congestion pricing and the relationship between road investment and toll revenue [17, 18]. Niu and Zhang [19] examined the price, road capacity, and concession period decisions of Pareto-efficient BOT contracts under uncertain demand. Shi et al. [20] examined the optimal choice of BOT road capacity, toll, and subsidy underpaid minimum traffic guidance. Feng et al. [21] conducted studies on contracts renegotiated with a loss-averse private firm on the BOT road [21]. Based on whether the two periods, including construction period and private operation period, are defined together or not, Zhang et al. [25] made an analysis on the effects of concession period structures on contracts of BOT road.

Private profit and social welfare are the two main objective functions of the traditional transportation economic model. To consider these two objectives simultaneously, Daganzo [26], viewing variable tolls as a hybrid between pricing and rationing, designed a Pareto-improving model with the distribution of losses and gains of all road users via modifying the traditional social welfare approach. Guo and Yang [10] conducted a preliminary study of the concession period and examined unconstrained, profit-constrained, and social welfare-maximizing BOT contracts via three essential variables: road capacity, toll charge, and concession period with homogeneous users. Tan et al. [24] generalized the Pareto-optimal results from Guo and Yang [10]. They further examined the Pareto-optimal contract of the BOT by maximizing private profit and social welfare simultaneously with the assumption that both government and private firms are fully informed of the travel demand and toll charge. They also examined the impact of several regulatory regimes on the behavior of private firms. In reality, the road user value over time is heterogeneous.

Therefore, user heterogeneity exists in road pricing. Mohring [25] generalized self-financing theorems for both homogeneous and heterogeneous users of their unique value of time. Using the basic bottleneck model, Arnott and de Palma [5] examined the effect of congestion tolls on social welfare using the inelastic demand of heterogeneous users. Two cases were conducted: one when the toll revenue is refunded to all road users as an equal lump-sum payment. Mayet and Hansen [6] analyzed second-best congestion pricing based on the continuously distributed VOT of road users. They designed different toll charge cases depending on what social welfare is measured and whether toll revenue is part of the benefit. Yang et al. [7] investigated how heterogeneous users affect the social welfare and profit generated from a toll road in a general transportation network. Verhoef and Small [8] explored the properties of various public and private toll charges in a congested road network with heterogeneous users under elastic demand. They found that the toll of revenue maximization is more inefficient than the pricing of welfare maximization. User heterogeneity can mitigate these differences. The model of public-private partnership built the road to gain broad support for road pricing. Rouhani et al. [26] introduced a new approach that stimulates public support for road pricing, followed by an in-depth analysis of social welfare for road pricing. Wang and Wang et al. [27] developed a Stackelberg game model to optimize the governments subsidies' effectiveness for the public-private partnerships performance mode.

To examine the effects of new roads, Xiao and Yang [9] analyzed the likely bias in a monopoly environment away from the social optimum under the more realistic assumption that each trip maker has a unique value of time. Using cumulative distribution, they also investigated the road capacity, toll set, and efficiency loss by a monopolist under different regulatory mechanisms. With the fixed demand of heterogeneous users, Guo and Yang [10] built a biobjective optimization model based on travel time and travel cost. Using the failure rate and mean residual function, Tan and Yang [1] examined the impact of heterogeneous users on toll road franchising by analyzing the properties of Pareto-optimal BOT contracts and regulation mechanisms. They used a new solution with VOT and volume/capacity ratio substituting demand and capacity to gain further insight. Under the condition of a continuous distribution of the value of time (VOT), Nie and Liu [11] examined the impact of VOT on a pricing-refunding scheme that is both Pareto-improving and self-financing in a static congestion pricing model with two modes.

3. The Model

In this section, we first introduce relevant definitions for further analysis. In the following sections, we define the decision variables of the government and private firms by subscripts g and s, respectively. If the variable does not have subscripts g and s in the paper, it will be given subscripts g and s when used in the analysis.

It is assumed that there are two roads between origin A and destination B in the general network. One is the toll-free road, and the other is the PTR connecting two nodes (A and B) directly. PTR is the BOT road transferred from a private firm to the government. The PTR is assumed to hold the original BOT traffic property, which can shorten the travel time. Owing to its large OC, the government tends to charge for use of the PTR. Based on these two options, the government operates the road independently or determines a private firm to operate it. Section 1 defines the road life after the BOT concession period as the PTR period. Tan and Yang [1] proved that private firms intend to operate the BOT road for their entire road life. The results of this study are also applicable to our paper; namely, by obtaining the PTR franchising for the OC concession period, the private firm is willing to operate the PTR during the entire PTR period; thus, the OC concession period equals the PTR period. Meanwhile, if the government decides to operate the PTR independently, it will also operate it during the entire PTR period. The relationship between OC concession and PTR periods is shown in Figure 3. Based on the above analysis, the variable T does not need to be analyzed in our study.

For the toll-free road, it is assumed that there is no congestion, the travel time t_e is fixed, and the existing capacity is y_1. The travel time of PTR follows a continuously differentiable function $t(q, y)$ where $y > y_1$ and $q \geq 0$ are the capacity and travel demand (traffic flow) of the PTR, respectively. Without loss of generality, the function $t(q, y)$ is of the following properties $\partial t/\partial q > 0, \partial^2 t/\partial^2 q > 0$ for any $y > y_1$ and $\partial t/\partial y < 0$ for any $q \geq 0$. It is also assumed that $t_e > t_0$, where t_0 is the travel time for the toll-free road with free flow and the travel time of PTR $t(q, y)$ is shorter than t_e all the time so that the PTR will be able to attract those travelers whose saved VOT is either equal to or exceeds the amount of the toll p which they pay.

Assuming the number of total users, Q, including the PTR and the toll-free road users, is fixed, the VOT of Q follows a continuously differentiable cumulative distribution $F(\beta)$, and $f(\beta)$ is the corresponding probability

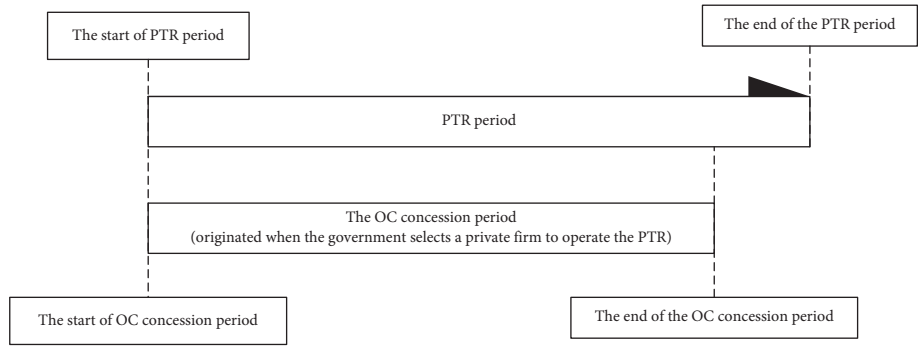

Figure 3: The relationship between OC concession period and PTR period.

density function that supports $\Theta = (\beta_0, \beta^0) \subset (0, +\infty)$. In this study, we further examine the case of the separating equilibrium [8].

In reality, the VOT varies with different PTR users. We assume that the distribution of all road users' VOT can be expressed by a continuously decreasing function $\beta(x)$. Here, $\beta(x)$ represents the VOT of the x^{th} user. Let $F(\beta)$ be the cumulative distribution function of VOT by $\beta(x) = F^{-1}(1 - x/Q)$ [6, 9].

β_c is defined as the VOT of the marginal user using PTR. It is assumed that users of PTR with a VOT higher than or equal to β_c decide to choose PTR for their travel, and the other users whose VOT is less than β_c decide to select the toll-free road. Users will choose a toll-free road if the saved VOT is less than the toll charge. Hereafter, we use β to substitute the cutoff value β_c.

Using the notation VOT and $F(\beta)$, we determine the relationship between the travel demand q of PTR and the cutoff VOT β as follows:

$$q = Q \cdot [1 - F(\beta)] = Q \cdot \overline{F}(\beta), \tag{1}$$

where $\overline{F}(\beta)$ is the probability of road users using PTR. With (1), demand q has a one-to-one correspondence with the cutoff VOT β. The users of PTR with more VOT tend to pay the toll to save time and generate more profit. It is assumed that the toll amount is a function of demand q and road capacity y:

$$p = \beta \cdot [t_e - t(q, y)]. \tag{2}$$

With (1) and (2), we can determine variables p and y by variables β and capacity y. Hereafter, we use β and y as independent variables substituting toll p and capacity y, respectively. In the following section of the paper, the toll p is assigned a subscript s when the private firm operation is analyzed and a subscript g when the government operation is analyzed.

To examine the case with a tractable analytical framework, two essential concepts—the mean residual VOT function and failure rate function—are proposed for reliability. If q users with a cutoff VOT β choose PTR, the probability of the following user not choosing the road is defined as the failure rate. Mathematically,

$$h_\beta \equiv \frac{f(\beta)}{\overline{F}(\beta)}. \tag{3}$$

If we assume that users choosing PTR have a VOT higher than the cutoff VOT β, the mean residual VOT will equal the result of the average excess VOT for the users subtracting the cutoff VOT β; namely,

$$l(\beta) = [v | v \geq \beta] - \beta, \tag{4}$$

where $E[\cdot]$ denotes the expectation value. It is well known that among the distribution functions $F(\beta)$, mean residual VOT function $l(\beta)$, or failure rate function $h(\beta)$, any one can be determined by the other two functions [28]. Bryson and Siddiqui [29] established the relationship between the mean residual VOT and failure rate as follows:

$$h(\beta) \cdot l(\beta) = l'(\beta) + 1. \tag{5}$$

With the mean residual VOT function and survival probability, the toll revenue per unit time $R(\beta, y)$ can be calculated as follows:

$$R(\beta, y) = q \cdot p = Q \cdot \overline{F}(\beta) \cdot p = Q \cdot \overline{F}(\beta) \cdot \beta \cdot [t_e - t(q, y)]. \tag{6}$$

In the second paragraph of this section, we point out that the PTR period T is not considered in this study. Thus, the total social surplus $S(\beta, y)$ is generated by the saved time, the value of which is measured in monetary terms. Hence, based on (4),

$$\begin{aligned} S(\beta, y) &= Q \cdot \overline{F}(\beta) \cdot [t_e - t(q, y)] \cdot E\left(\frac{v}{v} \geq \beta\right) - R(\beta, y) \\ &= Q \cdot \overline{F}(\beta) \cdot [t_e - t(q, y)] \cdot [l(\beta) + \beta] - R(\beta, y). \end{aligned} \tag{7}$$

In line with Shi et al. [30], we assume that the OC cost is composed of two parts: demand-related OC and capacity-related OC. Demand-related OC is related to road traffic demand, and capacity-related OC is related to road capacity. Let $m_s q, m_g q, I(y)$ be the perfect information for private firms and the government. m_s, m_g are the demand-related OC of private firms and government per unit travel time, respectively. Let $M_s(q)$ and $M_g(q)$ be private and

governmental OC during the PTR period, respectively. Note that $I(y)$ is a function of PTR capacity, so we substitute "capacity-related OC" with "the sum of maintenance and construction costs" when using $I(y)$ in the following section for convenience.

There would be three objective functions with heterogeneous users with the above notations: private profit objective function, social welfare objective functions with government operations, and social welfare objective function with private firm operations. To obtain satisfactory results, we can choose a combination of (β, y) to maximize the above objective functions or optimize private profit and social welfare simultaneously (Pareto-optimal). These functions are expressed as follows:

Supposing that the government tends to earn a profit, the profit equals the result of the total revenue from which the sum of demand-related OC and capacity-related OC during the PTR period is subtracted:

$$P_g(\beta, y) = R(\beta, y) - M_g(q) - I(y). \tag{8}$$

The private profit equals the total revenue from which the sum of demand-related OC and capacity-related OC during the PTR period is subtracted:

$$P_s(\beta, y) = R(\beta, y) - M_s(q) - I(y). \tag{9}$$

The total social welfare of PTR with government operation, $W_g(\beta, y)$, equals the sum of the total consumer surplus and the government profit during the PTR period:

$$W_g(\beta, y) = S(\beta, y) + P_g(\beta, y) = Q \cdot \overline{F}(\beta) \cdot [t_e - t(q, y)] \cdot [l(\beta) + \beta] - M_g(q) - I(y). \tag{10}$$

The total social welfare of PTR with private firm operation, $W_s(\beta, y)$, equals the sum of the total consumer surplus and the private firm profit during the PTR period:

$$W_s(\beta, y) = S(\beta, y) + P_s(\beta, y) = Q \cdot \overline{F}(\beta) \cdot [t_e - t(q, y)] \cdot [l(\beta) + \beta] - M_s(q) - I(y). \tag{11}$$

When a private firm operates the PTR, the Pareto-optimal OC objective function for heterogeneous users can be determined by capacity y and the cutoff VOT β to meet the requirements of the government and private firms simultaneously. We then formulate a biobjective programming function as follows:

$$\max_{(T,\beta,r)\in\Omega} \begin{pmatrix} W_s(\beta, y) \\ P_s(\beta, y) \end{pmatrix}, \tag{12}$$

where $\Omega = \{(\beta, r)\colon\ y > y_1, \beta \in \Omega\}$ and capacity y are higher than y_1, and y_1 is the road capacity when the road is transferred from a private firm. Private profit $P_s(\beta, y)$ and social welfare $W_s(\beta, y)$ are defined in (9) and (11), respectively. To gain further insight, we define the following Pareto-optimal OC contract.

Definition 1 (a Pareto-optimal OC contract). An OC combination $(\beta^*, y^*) \in \Omega$ is called a Pareto-optimal contract if there is no other triple combination $(\beta, y) \in \Omega$ such that $P(\beta, y) \geq P(\beta^*, y^*)$ and $W(\beta, y) \geq W(\beta^*, y^*)$ have at least one strict inequality.

With the Pareto concept and above Pareto-optimal contract definition, we know that the improvement of the profit of one participant would make the other worse off; namely, neither participant can improve their profit simultaneously. In the following sections, we examine the impact of heterogeneous users on social welfare with governmental operations and investigate two extreme cases with private firm operations, the Pareto-optimal contract, and various regulatory regimes.

Note that although the discounting rate has an important effect on the optimal contract for private profit and social welfare, it does not affect the above results because both social welfare and private profit are invariant with calendar time in this research (for more details, see [1, 10]).

4. Analysis of Optimal OC Contracts

In this section, we first examine the properties of governmental OC using (10) and then investigate how to maximize social welfare and private profit under the PTR period with the first-order conditions of the two extreme cases. We then examine the properties of Pareto-efficient contracts of the OC problem in (12). To analyze the problem reasonably, we introduce three common assumptions, which form the analytical basis for the following subsections.

Assumption 1. Term $q\beta(q)$ is the concave function of q; $\beta h(\beta)$ increases with β.

Assumption 2. The travel time function $t(q, y)$ is homogeneous of degree zero in flow q and road capacity y; that is, $t(\alpha q, \alpha y) = t(q, y)$ for any $\alpha > 0$.

We set $r = q/y$ as the volume-to-capacity ratio in the following subsections to analyze the OC problem thoroughly. Wang et al. [31] studied the fundamental properties of the volume-to-capacity ratio of BOT roads in general networks. To simplify the case for better understanding,

$t(q, y)$ can be written as $t(r)$, which is an increasing and strictly convex continuous function of v/c ratio r.

Assumption 3. The return to scale in demand-related OC of private firms and governments is constant; namely, $M_s(q) = m_s q$ and $M_g(q) = m_g q$; capacity-related OC is also a constant return to scale; namely $I(y) = ky$, where m_s, m_g represent the constant costs per demand-related unit, and k represents the constant cost per capacity-related unit.

Based on the assumptions mentioned above, equations (9)–(11) can be converted into

$$P(\beta, r) = Q \cdot \overline{F}(\beta) \cdot \left\{\beta \cdot \left[t_e - t(r)\right] - m_s - \frac{k}{r}\right\}, \tag{13}$$

$$W_g(\beta, r) = Q \cdot \overline{F}(\beta) \cdot \left\{\left[I(\beta) + \beta\right] \cdot \left[t_e - t(r)\right] - m_g - \frac{k}{r}\right\}, \tag{14}$$

$$W_s(\beta, r) = Q \cdot \overline{F}(\beta) \cdot \left\{\left[I(\beta) + \beta\right] \cdot \left[t_e - t(r)\right] - m_s - \frac{k}{r}\right\}. \tag{15}$$

Note that with the definition of $r = q/y$, it is clear that a feasible solution (β, r) of (13)–(15) correspond one-to-one to (β, y).

4.1. Toll and Capacity of the PTR with Governmental Operation. If m_g is less than m_s, the government tends to operate the road independently, and for the PTR period, social welfare is maximized with a determined combination of optimal price and capacity [3]. Equation (14) is the objective function in this case.

Let $(\widetilde{\beta}_g, \widetilde{r}_g)$ be the solution to maximize social welfare $W_g(\beta, r)$ when the government operates the PTR. With the incorporation of $(\widetilde{\beta}_g, \widetilde{r}_g)$ as the corresponding solution of $W_g(\beta, r)$, the demand $\widetilde{q}_g$ corresponds to the cutoff VOT $\widetilde{\beta}_g$ with (1). We then deduce the following first-order optimal condition with $(\widetilde{\beta}_g, \widetilde{r}_g)$,

$$\widetilde{\beta}_g = \frac{\widetilde{r}_g \cdot m_g + k}{\widetilde{r}_g \cdot \left[t_e - t\left(\widetilde{r}_g\right)\right]}, \tag{16}$$

$$I\left(\widetilde{\beta}_g\right) + \widetilde{\beta}_g = \frac{k}{\widetilde{r}_g^2 t'\left(\widetilde{r}_g\right)}, \tag{17}$$

where $\widetilde{r}_g$ denotes the social optimal v/c ratio (or service quality) when the government operates the road; namely $\widetilde{r}_g = \widetilde{q}_g/\widetilde{y}_g$.

With equations (2) and (16), the social optimal toll charge $\widetilde{p}_g$ when the government operates the road can be calculated as follows:

$$\widetilde{p}_g = \widetilde{\beta}_g \cdot \left[t_e - t\left(\widetilde{r}_g\right)\right] = m_g + \frac{k}{\widetilde{r}_g} = m_g + \frac{k \cdot \widetilde{y}_g}{\widetilde{q}_g}. \tag{18}$$

The government can operate the PTR with the toll charge in (18) to achieve optimal social welfare: (18) indicates that the social optimal toll charge is precisely equal to the sum of the OC per demand-related unit and the capacity-related OC for each trip. According to (18), the government does not profit from the PTR if the toll is charged. The total revenue generated from charging users' tolls equals the sum of demand-related OC and capacity-related OC, obeying the self-financing theory [32–34]. Under the first-order condition (17), the social optimal toll charge can also be expressed as

$$\widetilde{p}_g = m_g + \frac{k}{\widetilde{r}_g} = m_g + \left[I\left(\widetilde{\beta}_g\right) + \widetilde{\beta}_g\right] \cdot \widetilde{r}_g \cdot t'\left(\widetilde{r}_g\right) = m_g + E\left[x | x \geq \widetilde{\beta}_g\right] \cdot \widetilde{r}_g \cdot t'\left(\widetilde{r}_g\right), \tag{19}$$

where $E[x|x \geq \widetilde{\beta}_g]$ is the mathematical expectation of VOT when it is higher than $\widetilde{\beta}_g$, which is also referred to as the average VOT of the actual PTR users. Equations (18) and (19) follow the first-best road capacity and pricing rules. Namely, the social optimal toll charge equals the sum of the congestion externality and demand-related OC [34].

The government would like the revenue $R(\beta, r)$ collected from road users to cover the sum of demand-related OC $M_g(q)$ and capacity-related cost $I(y)$, so it is necessary to analyze maximized social welfare without operational profit. Therefore, the issue can be described as follows:

$$W_g(\beta, r) = Q \cdot \overline{F}(\beta) \cdot \left\{\left[I(\beta) + \beta\right] \cdot \left[t_e - t(r)\right] - m_g - \frac{k}{r}\right\}, \tag{20}$$

subject to

$$P_g(\beta, r) = Q \cdot \overline{F}(\beta) \cdot \left\{\beta \cdot \left[t_e - t(r)\right] - m_g - \frac{k}{r}\right\} = 0, \tag{21}$$

where the profit $P_g(\beta, r)$ made by the government is zero. Referring to the above optimization, we notice that the optimization approach suggested for the private firm when operating the BOT road is suitable for government operation during the PTR period as well. However, the sufficient conditions of this optimization issue are changed.

We assume that (β_g^*, y_g^*) is a zero-profit optimal solution to the maximization function (14) and that (β_g^*, y_g^*) denotes the corresponding zero-profit solution to (21). Using the Lagrange method, the constraint problem above can be transformed into the following Lagrange problem:

$$L_g(\beta, r, \eta) = W_g(\beta, r) + \eta_g P_g(\beta, r), \tag{22}$$

where $\eta_g \geq 0$ denotes the Lagrange multiplier. Therefore, we obtain the following first-order condition:

$$\frac{\partial L_g}{\partial \beta}|_{\beta_g^*, r_g^*} = Q \cdot \overline{F}(\beta_g^*)\left[-h(\beta_g^*)\left(\left(l(\beta_g^*)+\beta_g^*\right)\left(t_e - t(r_g^*)\right) - m_g - \frac{k}{r_g^*}\right) + \left(l\prime(\beta_g^*)+1\right)\left(t_e - t(r_g^*)\right)\right] + \eta_g \cdot Q\overline{F}(\beta_g^*)\left[-h(\beta_g^*)\left(\beta_g^*\left(t_e - t(r_g^*)\right) - m_g - \frac{k}{r_g^*}\right) + \left(t_e - t(r_g^*)\right)\right], \tag{23}$$

$$\frac{\partial L_g}{\partial r}|_{\beta_g^*, r_g^*} = Q \cdot \overline{F}(\beta_g^*)\left\{\left[l(\beta_g^*)+\beta_g^*\right]\left[-t'(r_g^*)\right] + \frac{k}{(r_g^*)^2}\right\} + \eta_g \cdot Q\overline{F}(\beta_g^*)\left\{\beta_g^*\left[-t'(r_g^*)\right] + \frac{k}{(r_g^*)^2}\right\} = 0, \tag{24}$$

$$\frac{\partial L_g}{\partial \eta_g}|_{\beta_g^*, r_g^*} = P_g(\beta_g^*, r_g^*) = Q \cdot \overline{F}(\beta_g^*) \cdot \left\{\beta_g^* \cdot \left[t_e - t(r_g^*)\right] - m_g - \frac{k}{r_g^*}\right\} = 0. \tag{25}$$

From equation (5), equations (24) and (25) can be rewritten as

$$\beta_g^* \cdot \left[1 - \frac{\eta_g}{1+\eta_g} \cdot \frac{1}{\beta_g^* h(\beta_g^*)}\right] = \frac{m_g \cdot r_g^* + k}{r_g^*\left[t_e - t(r_g^*)\right]}, \tag{26}$$

$$\beta_g^* + \frac{l(\beta_g^*)}{1+\eta_g} = \frac{k}{(r_g^*)^2 t'(r_g^*)}. \tag{27}$$

Eliminating Lagrange multiplier η_g from (26) and (27), we obtain

$$\frac{1}{h(\beta_g^*) \cdot l(\beta_g^*)} \cdot \frac{k}{r_g^* t'(r_g^*)} - \frac{m_g \cdot r_g^* + k}{t_e - t(r_g^*)} = r_g^* \beta_g^* \left[\frac{1}{\beta_g^* h(\beta_g^*)} + \frac{1}{h(\beta_g^*) \cdot l(\beta_g^*)} - 1\right], \tag{28}$$

which determines the relationship between the optimal v/c ratio r_g^* and the cutoff VOT β_g^* from the zero-profit solution (β_g^*, r_g^*). We regard r_g^* as a function of β_g^*, and the function $r_g^* = r_g^*(\beta_g^*)$ is continuous and differentiable. Applying the derivation rule of the implicit function, we can derive r_g^* with respect to β_g^*:

$$\left\{\frac{d}{dr}\left(\frac{k}{r_g^* t'(r_g^*)}\right) \cdot \frac{1}{h(\beta_g^*) l(\beta_g^*)} + \beta_g^* - \frac{d}{dr}\left(\frac{m_s \cdot r_g^* + k}{t_e - t(r_g^*)}\right) - \left[\frac{\beta_g^*}{h(\beta_g^*) l(\beta_g^*)} + \frac{1}{h(\beta_g^*)}\right]\right\} \frac{\mathrm{d}r}{\mathrm{d}\beta} = -r_g^* \cdot \frac{\eta_g}{1+\eta_g} \cdot \frac{l''(\beta_g^*)}{h^2(\beta_g^*) l(\beta_g^*)}. \tag{29}$$

With (26) and (27), we have

$$\frac{\mathrm{d}}{\mathrm{d}r}\left(\frac{k}{r_g^* t'(r_g^*)}\right) \cdot \frac{1}{h(\beta_g^*) l(\beta_g^*)} + \beta_g^* - \frac{\mathrm{d}}{\mathrm{d}r}\left(\frac{m_s \cdot r_g^* + k}{t_e - t(r_g^*)}\right) - \left[\frac{\beta_g^*}{h(\beta_g^*) l(\beta_g^*)} + \frac{1}{h(\beta_g^*)}\right] = 0. \tag{30}$$

Then, if $r_g^* \eta_g / [(1+\eta_g) \cdot h^2(\beta_g^*) m(\beta_g^*)] > 0$, we have $l''(\beta_g^*) = 0$. Based on the analysis above, we posit Proposition 1.

Proposition 1. *With Assumptions 1–3, for any optimal solution to social welfare maximization (14) under government operation, the mean residual VOT function $l(\beta)$ is a linear function of β that is unrelated to r_g and β_g.*

Proposition 1 shows that regardless of the relationship between r_g and β_g, $l(\beta)$ is always a linear function of β_g with the optimal solution.

4.2. Two Extreme Cases under Private Firm Operation. In this section, we analyze the case in which the road is operated by a private firm and two important extreme cases, either the optimization of social welfare (SO) or the optimization of the private profit made by a private firm (OP). Let $(\tilde{\beta}, \tilde{r})$ and $(\overline{\beta}, \overline{r})$ be the solutions to SO and OP, respectively, which maximize social welfare $W_s(\beta, r)$ and private profit $P_s(\beta, r)$. The demand $\tilde{q}$ corresponds to the $\tilde{\beta}$ in (1), and the demand $\overline{q}$ also corresponds to $\overline{\beta}$ with (1). Note that from the notation in Section 3 and Assumptions 1–3, the solutions to SO and MO, that is, $(\tilde{\beta}, \tilde{r})$ and $(\overline{\beta}, \overline{r})$, are globally unique extreme values of function W and profit function P. We derive the following first-order conditions: $(\tilde{\beta}, \tilde{r})$ and $(\overline{\beta}, \overline{r})$.

$$\tilde{\beta} = \frac{\tilde{r} \cdot m_s + k}{\tilde{r} \cdot [t_e - t(\tilde{r})]}, \tag{31}$$

$$l(\tilde{\beta}) + \tilde{\beta} = \frac{k}{\tilde{r}^2 t'(\tilde{r})}, \tag{32}$$

$$\overline{\beta} - \frac{1}{h(\overline{\beta})} = \frac{\overline{r} \cdot m_s + k}{\overline{r} \cdot [t_e - t(\overline{r})]}, \tag{33}$$

$$\overline{\beta} = \frac{\theta}{\overline{r}^2 t'(\overline{r})}. \tag{34}$$

Based on the first-order condition in (31), the toll charge of the PTR can be converted to

$$\begin{aligned} \tilde{p} &= \tilde{\beta} \cdot [t_e - t(\tilde{r})] \\ &= m_s + \frac{k}{\tilde{r}} \\ &= m_s + \frac{k \cdot \tilde{y}}{\tilde{q}}. \end{aligned} \tag{35}$$

Equation (35) implies that the toll charge of the SO is equal to the OC per demand-related unit and capacity-related OC for each trip. The private firm does not profit from its operation. The total revenue achieved is exactly equal to the sum of OC, which obeys the self-financing theory [33]. With the first-order condition in (32), the toll charge of the SO can be expressed as

$$\begin{aligned} \tilde{p} &= m_s + \frac{k}{\tilde{r}} \\ &= m_s + [l(\tilde{\beta}) + \tilde{\beta}] \cdot \tilde{r} \cdot t'(\tilde{r}) \\ &= m_s + E[x | x \geq \tilde{\beta}] \cdot \tilde{r} \cdot t'(\tilde{r}), \end{aligned} \tag{36}$$

where $E[x|x \geq \tilde{\beta}]$, the average VOT of the actual PTR users, is the mathematical expectation of VOT when it is greater than $\tilde{\beta}$. Equations (35) and (36), similar to those in Section 4.1, also obey the first-best road capacity and pricing rules.

With first-order conditions (33) and (34), the toll charge of MO can be formulated as

$$\overline{p} = m_s + \frac{k}{\overline{r}} + \frac{[t_e - t(\overline{r})]}{h(\overline{\beta})} = m_s + \overline{\beta} \overline{r} t'(\overline{r}) + \frac{[t_e - t(\overline{r})]}{h(\overline{\beta})}. \tag{37}$$

The toll charge of the MO comprises three parts. The first term on the left-hand side of (37) is the demand-related OC. The second term represents the congestion charge, which equals the marginal external cost.

Although there is a difference between the solutions of MO and SO, based on Assumptions 1–3, we can also deduce a close relationship between them.

Proposition 2. *Under Assumptions 1–3, $\tilde{y} \geq \overline{y} \geq y_1$, $\tilde{p} \leq \overline{p}$ and $\tilde{\beta} \leq \overline{\beta}$, $\tilde{q} \geq \overline{q}$.*

Proof. $\tilde{p} \leq \overline{p}$, $\tilde{\beta} \leq \overline{\beta}$, and $\tilde{q} \geq \overline{q}$ are demonstrated by Tan and Yang [1] and applied in our model.

We only provide the proofing of $\tilde{y} \geq \overline{y} \geq y_1$.

$$W(\tilde{\beta}, \tilde{r}) = k\tilde{y} \cdot \left[\frac{t_e - t(\tilde{r})}{\tilde{r} t'(\tilde{r})} - \frac{m_s}{k} \cdot \tilde{r} - 1 \right], \tag{38}$$

$$W(\overline{\beta}, \overline{r}) = k\overline{y} \cdot \left\{ \frac{t_e - t(\overline{r})}{\overline{r} t'(\overline{r})} \left[\frac{l(\overline{\beta})}{\overline{\beta}} + 1 \right] - \frac{m_s}{k} \cdot \overline{r} - 1 \right\}. \tag{39}$$

The term $[t_e - t(r)]/rt'(r)$ is a decreasing function of r for $r \leq \hat{r}$ and $l(\overline{\beta})/\overline{\beta} \geq 0$. Then,

$$\frac{t_e - t(\tilde{r})}{\tilde{r} t'(\tilde{r})} - \frac{m_s}{k} \cdot \tilde{r} - 1 \leq \frac{t_e - t(\overline{r})}{\overline{r} t'(\overline{r})} - \frac{m_s}{k} \cdot \overline{r} - 1 \leq \frac{t_e - t(\overline{r})}{\overline{r} t'(\overline{r})} \left[\frac{l(\overline{\beta})}{\overline{\beta}} + 1 \right] - \frac{m_s}{k} \cdot \overline{r} - 1. \tag{40}$$

This implies that the capacity $\tilde{y}$ of SO is higher than the capacity $\bar{y}$ of MO if $W(\tilde{\beta}, \tilde{r}) \geq W(\bar{\beta}, \bar{r})$. The government must maintain the existing road capacity not less than y_1, which is also required for private firms. This completes this proof.

Proposition 2 implies that private firms tend to determine a higher toll charge, lower road capacity, and not offer traffic services to unnecessarily more road users (users with a higher cutoff VOT β), which results in road users' demand for traffic being lower. □

4.3. Properties of Pareto-Efficient OC Contracts. According to (13) and (15), the Pareto-optimal problem can be defined as

$$\max_{(\beta,r)\in\Omega} \begin{pmatrix} W_s(\beta, r) \\ P(\beta, r) \end{pmatrix} = \begin{pmatrix} Q \cdot \overline{F}(\beta) \cdot \left\{ [l(\beta) + \beta] \cdot [t_e - t(r)] - m_s - \dfrac{k}{r} \right\} \\ \\ Q \cdot \overline{F}(\beta) \cdot \left\{ \beta \cdot [t_e - t(r)] - m_s - \dfrac{k}{r} \right\} \end{pmatrix}, \tag{41}$$

where $\Omega = \{(\beta, r): \beta \in \Omega, r > 0\}$. The relationship between the solution and (41), and the combination of the VOT and road capacity (β, y) is a one-to-one correspondence. With the definition of the Pareto-optimal OC contract in Section 3, we know that if a solution pair $(\beta, r) \in \tilde{\Omega}$, such as $P(\beta, r) \geq P(\beta^*, r^*)$ and $W(\beta, r) \geq W(\beta^*, r^*)$ with at least one strict inequality, is not found, a pair $(\beta^*, r^*) \in \tilde{\Omega}$ of OC function (41) can be called a Pareto-optimal solution.

Under Assumptions 1–3, we obtain the upper bound of the v/c ratio in the Pareto-optimal function in (41) using the same terms in $r \cdot [t_e - t(r)]$, as described by Tan and Yang [1] for a similar reason (see Appendix A for further details).

Proposition 3. *Under Assumptions 1–3, if (β^*, r^*) is a Pareto-optimal solution to (41), then $r^* \leq \hat{r}$, where*

$$\hat{r} = \arg\max_{r\geq 0} \{r \cdot [t_e - t(r)]\}. \tag{42}$$

From the optimal condition (42), we have

$$t_e - t(\hat{r}) = \hat{r} t'(\hat{r}). \tag{43}$$

The term $t_e - t(\hat{r})$ of (43) is the travel time saved if travelers choose to use the PTR. The term $\hat{r}t'(\hat{r})$ of (43), which can be written as $q \cdot \partial t(q, y)/\partial q$, is the congestion externality. Proposition 3 implies that none of the Pareto-optimal v/c ratios r can exceed a critical ratio $\hat{r}$, in which the saved travel time is precisely equal to its congestion externality per unit time.

Additionally, the same term $Q \cdot \overline{F}(\beta)$ of social welfare $W_s(\beta, r)$ and private profit $P_s(\beta, r)$ in (41) denotes the total number of cars using the PTR during its whole life. The term $\beta \cdot [t_e - t(r)]$ of private profit at $r = \hat{r}$ is the average profit made from every single trip of a car.

With (43), we have

$$\beta[t_e - t(\hat{r})] - \left(m_s + \frac{k}{r}\right) = \beta q \frac{\partial t(q, y)}{\partial q} - \left(m_s + \frac{ky}{q}\right), \tag{44}$$

where the last term $m_s + k \cdot y/q = (m_s q + ky)/q$ is the sum of the demand-related OC and capacity-related OC of the private firm for each car trip. The term $(l(\beta) + \beta) \cdot (t_e - t(r))$ in (41) at $r = \hat{r}$ is the average social surplus on each trip, which is equal to the sum of the average private firm surplus and the average consumer surplus. Then, the average social surplus on each trip can be written as

$$[l(\beta) + \beta][t_e - t(\hat{r})] - \left(m_s + \frac{k}{r}\right) = [l(\beta) + \beta] q \frac{\partial t(q, y)}{\partial q} - \left(m_s + \frac{k \cdot y}{q}\right). \tag{45}$$

Therefore, (45) and (44) imply that the average social surplus equals the difference between the cost-based congestion externality and the OC per trip. From the proof of Proposition 3 in Appendix A, we know that the private firm obtains a negative profit, while profit and social welfare strictly decrease with r and in the domain $(\hat{r}, +\infty)$ for any cutoff VOT β. Therefore, we restrict our research to the domain of $(\hat{r}, +\infty)$.

Under Assumptions 1–3, especially if $qB(q)$ is concave, the revenue function $R(q, y)$ is also concave, social welfare W is a strictly concave function of demand q and capacity y, and private profit P is a unimodal function of demand q for any given y and strictly concave function of y. We also assume that for the Pareto-optimal problem (41), the Pareto-optimal outcome corresponds one-to-one to the Pareto-optimal solution. We then apply the ε-constraint method [35] to solve (41). Miettinen [35] pointed out that one of the objective functions can be selected for optimization, and the other can be transformed into a constraint condition by setting a lower bound. Using this method, we transform Pareto-optimal problem (41) into the following problem:

$$\max_{(\beta,r)} W(\beta, r), \tag{46}$$

subject to

$$P_s(\beta, r) = Q \cdot \overline{F}(\beta) \cdot \left\{\beta \cdot [t_e - t(r)] - m_s - \frac{k}{r}\right\} \geq P^*, \tag{47}$$

$$Q \cdot \overline{F}(\beta) \cdot \left[p(\beta, r) - m_s - \frac{k}{r}\right] \leq Q \cdot \overline{F}(\beta) \cdot \left(m_g - m_s\right), \tag{48}$$

$$m_g \geq m_s, q \geq 0, y \geq y_1, \tag{49}$$

where $P^* \geq 0$ is the lower bound of the profit that the private firm can accept. Profit P^* is associated with the Pareto-efficient optimal solution (β^*, r^*). Constraint condition (47) means private profit will not be higher than the OC difference between government and private firms. If private profit exceeds the difference, the government decides to operate the road itself.

Condition (48) can be written as

$$Q\overline{F}(\beta) \cdot \left[p(\beta, r) - m_g - \frac{k}{r}\right] \leq 0. \tag{50}$$

Equation (50) implies that government profit is negative or equal to zero if the government operates the road itself. In this case, a private firm will be offered a contract to operate the road, while the government will avoid the loss. This constraint is identical to the condition in $m_g > m_s$. With the constraint condition of (50), our model differs from the traditional BOT model.

The above-transformed problem is generally solved using the Kuhn–Tucker method [32]. We set η_1 and η_2 as the Lagrange multipliers of the constraints in (47) and (48), respectively. To gain further insights into the impact of heterogeneous users on Pareto-efficient OC contracts with OC, we assume the Lagrange multipliers η_1 and η_2 as follows.

Assumption 4. The Lagrange multipliers $\eta_1 \geq \eta_2$.

The Lagrange multiplier is usually defined as a sensitivity coefficient (or shallow price) in economic explanation, and it eliminates marginal profit for some additional amount of resources. So, the condition $\eta_1 \geq \eta_2$ implies that the constraint of private profit (47) is more critical than the constraint of (48); namely, the private firm is more sensitive to its profit.

We obtain first-order conditions with Pareto-efficient optimal solution (β^*, r^*) using the Kuhn–Tucker method (see Appendix B for details).

$$\beta^*\left[1 - \frac{\eta_1 - \eta_2}{1 + \eta_1 - \eta_2} \cdot \frac{1}{\beta^* h(\beta^*)}\right] = \frac{1}{[t_e - t(r^*)]}\left[\left(\frac{m_s + k}{r^*}\right) - \frac{\eta_2\left(m_g - m_s\right)}{1 + \eta_1 - \eta_2}\right], \tag{51}$$

$$\beta^* + \frac{l(\beta^*)}{1 + \eta_1 - \eta_2} = \frac{k}{(r^*)^2 t'(r^*)}. \tag{52}$$

From the Kuhn–Tucker condition, the Lagrange multipliers are $\eta_1 \geq 0$ and $\eta_2 \geq 0$. From the previous section, we know that constraints (47) and (48) must be satisfied. If the Lagrange multipliers are $\eta_1 = 0$ or $\eta_2 = 0$, constraints (47) and (48) will become inactive, the Lagrange multipliers η_1 and η_2 will not be equal to zero, and then $\eta_1 > 0$ and $\eta_2 > 0$. If $\eta_1 > 0$ and $\eta_2 > 0$, from the first-order conditions (B.4) to (B.7), we obtain the following equations:

$$P(\beta, r) - P^*(\beta^*, r^*) = qp - m_s q - ky - P^*(\beta^*, r^*) = 0, \tag{53}$$

$$Q\overline{F}(\beta) \cdot p(\beta, r) - m_g q - ky = 0. \tag{54}$$

From (53) and (54), we have

$$P^* = \left(m_g - m_s\right)q. \tag{55}$$

Proposition 4. *Under Assumptions 1–3, for any Pareto-optimal solution to (41), the private profit is determined by the demand-related OC of the government and private firm.*

Proposition 4 shows that for any Pareto-optimal solution to (41), the lower bound of the private firm profit P^* is equal to $(m_g - m_s)q$. The Pareto-optimal private profit is a linear function of travel demand. Private profit equals the difference between the demand-related OC of the government and private firms during the PTR period.

5. Conclusions and Policy Implications

5.1. Conclusions. This study's results reveal that the OC exercises a vital function in PTR projects, while this part of the cost is usually neglected during the BOT concession period. We further examined the effect of different VOTs of heterogeneous users on OC for the PTR, characterized by the mean residual function and the failure rate function. We classified and analyzed the optimal solutions for both contracts concerning OC for government and private firms. We also studied Pareto-optimal solutions with private operations using biobjective programming. This study defined the optimal toll price under the maximization of social welfare with government operation. We proved that the mean residual function is a linear function of value-of-time of heterogeneous users under Pareto-optimum under the Pareto-optimum with government operation. In contrast, private profit equals the difference between OC of government and private firm under Pareto-optimum with private firm operation. We also compared the PTR

variables, including road capacity, toll for users, and traffic demand, in two extreme cases under private firm operation: the optimization of social welfare and the optimization of private profit. The private firm operates on the road during the entire PTR period. The lower-bound profit of the private firm on the Pareto-optimum is a linear function of demand.

5.2. Policy Implications. Based on the discussion of the above models, some policy implications can be drawn for PTR road operations. According to the regulations, road tolls are divided into debt repayment period tolls and maintenance period tolls. Road maintenance period tolls are distinguished from debt repayment period tolls because the latter do not consider construction funding. The first implication pertains to the management of a road when it becomes a PTR. In the operation and management of PTR, we assume that the government can choose to operate the road by itself or choose a private firm to continue the operation. At this time, the road tolls are the maintenance period tolls (i.e., the government does not need to consider construction funding), and the government's decision-making department mainly considers management efficiency and operational supervision, rather than the issue of construction funding, so the government will have more freedom to operate the road by itself or choose a private firm to operate it.

Second, if the government decides to operate the road independently, it can consider two goals: maximizing social welfare and self-financing. Governments generally charge road traffic to maximize social welfare. The discussion in this study provides a particular selectivity for the government to formulate relevant road toll policies. Owing to the different traffic flows of different PTR, which leads to obvious differences in the total tolls of each PTR in a certain period, the government can consider the operation of PTR from the perspective of the entire region by considering the maximization of social welfare and the tolling of PTR from a more extensive scope.

Third, it has been stated at the beginning of Section 5.2 that the government would have a greater say in choosing a private firm to continue operating the road, regardless of construction funding. The government has to consider two issues: selecting a private firm based on management efficiency [3] and supervision management. In Part 4, the Pareto model is used to analyze the process of contracting between government and private firms. The government can supervise and regulate the operation management of the private firm by formulating relevant clauses in the contract, including the price of tolls and flexible operation periods based on traffic volumes. For example, when traffic volumes increase to a certain level, the government recovers operation rights to maximize social welfare.

Fourth, according to the relationship between the heterogeneous traffic volumes and the toll prices in the model, the government can adopt differentiated toll policies based on traffic volumes and the vehicle types. For example, it may adopt different toll prices or adjust the toll prices of different vehicles during different periods.

This paper suggests practical applications that the government can consider during its decision-making process. These suggestions also can be referenced by researchers for future studies in the field of PTR operation. Our conclusions can be further applied to other construction projects to be developed in the BOT model.

The paper has some limitations. First, the charging mechanism of PTR is the focus in further research, such as how to adjust the charging mechanism in different PTR sections and different time. In addition, it is necessary to further study the operation of PTR network, such as the operation of PTR network under the maximum social welfare. We believe that further research into these issues will yield more results in the area of PTR.

Appendix

A. Proof of Proposition 3

We use the method of reduction to absurdity to prove Proposition 3; namely, if any feasible solution (β, r) with $r > \widehat{r}$ is not a Pareto-optimal solution to (41), Proposition 3 is true. From Section 4.2, we know that a social optimal solution $(\widetilde{\beta}, \widetilde{r})$ maximizes social welfare with zero profit $P(\widetilde{\beta}, \widetilde{r}) = 0$ under the government operation. Therefore, if a feasible solution (β, r) with $r > \widehat{r}$ gives rise to a negative profit, the social welfare optimal solution $(\widetilde{\beta}, \widetilde{r})$ is dominating compared to the pair (β, r) since the social welfare $W(\widetilde{\beta}, \widetilde{r}) \geq W(\beta, r)$ and the profit $P(\widetilde{\beta}, \widetilde{r}) > P(\beta, r)$. On the other hand, if a feasible solution (β, r) with $r > \widehat{r}$ gives rise to a nonnegative profit, we can also get nonnegative social welfare. We rewrite the social welfare and profit of (41) as follows.

$$W_s(\beta, r) = Q \cdot \overline{F}(\beta) \cdot \left\{ \frac{[m(\beta) + \beta] \cdot r \cdot [t_e - t(r)] - k}{r} - m_s \right\}, \tag{A.1}$$

$$P(\beta, r) = Q \cdot \overline{F}(\beta) \cdot \left\{ \frac{\beta \cdot r \cdot [t_e - t(r)] - k}{r} - m_s \right\}. \tag{A.2}$$

Under the condition that the single travel time function $t(r)$ is increasing and strictly convex of v/c ratio r, the same term $r \cdot [t_e - t(r)]$ of equations (A.1) and (A.2) is strictly decreasing function of r in the domain of $r > \widehat{r}$, where $\widehat{r}$ is defined in (44). Based on the above analysis, we know that social welfare $W_s(\beta, r)$ and profit $P(\beta, r)$ become strictly decreasing function of r and nonnegative in the domain of $(\widehat{r}, t + n\infty)$; namely, the value of $W_s(\beta, r)$ and $P(\beta, r)$ with $r = \widehat{r}$ dominates, compared to $W_s(\beta, r)$ and $P(\beta, r)$ with $r > \widehat{r}$. This completes this proof.

B. Proof of Properties of Pareto-Efficient Solution

It is assumed that (β^*, r^*) is any Pareto-optimal solution to the OC problem (12), and (β^*, r^*) is the Pareto-optimal solution to the OC problem (41). From the constrained

programming problem (46)–(49), the following Lagrange-like function can be defined as

$$L = W(\beta, r) + \eta_1 [P(\beta, r) - P^*(\beta^*, r^*)] + \eta_2 \left[-Q\overline{F}(\beta) \cdot p(\beta, r) + M_g 0(q) + I(y)\right], \tag{B.1}$$

where $\eta_1 \geq 0$ and $\eta_2 \geq 0$ are Lagrange multipliers associated with the constraints in (47) and (48), respectively. Using (3), the following first-order conditions of Kuhn–Tucker for the optimality of the above problem hold [32].

$$\begin{aligned}
\frac{\partial L}{\partial \beta}|_{(\beta^*, r^*)} &= Q \cdot \overline{F}(\beta^*) \left[-h(\beta^*) \left((m(\beta^*) + \beta^*)(t_e - t(r^*)) - m_s - \frac{k}{r^*} \right) + (m'(\beta^*) + 1)(t_e - t(r^*)) \right] \\
&\quad + \eta_1 \cdot Q \cdot \overline{F}(\beta^*) \left[-h(\beta^*) \left(\beta^* (t_e - t(r^*)) - m_s - \frac{k}{r^*} \right) + (t_e - t(r^*)) \right] \\
&\quad + \eta_2 \cdot Q \cdot \overline{F}(\beta^*) \left[-h(\beta^*) \left(-\beta^* (t_e - t(r^*)) + m_g + \frac{k}{r^*} \right) - (t_e - t(r^*)) \right] = 0,
\end{aligned} \tag{B.2}$$

$$\begin{aligned}
\frac{\partial L}{\partial r}|_{(\beta^*, r^*)} &= Q \cdot \overline{F}(\beta^*) \left\{ [m(\beta^*) + \beta^*][-t'(r^*)] + \frac{k}{(r^*)^2} \right\} \\
&\quad + \eta_1 \cdot Q \cdot \overline{F}(\beta^*) \left\{ \beta^* [-t'(r^*)] + \frac{k}{(r^*)^2} \right\} + \eta_2 \cdot Q \cdot \overline{F}(\beta^*) \left\{ \beta^* t'(r^*) - \frac{k}{(r^*)^2} \right\} = 0,
\end{aligned} \tag{B.3}$$

$$P(\beta^*, r^*) - P^* \geq 0, \tag{B.4}$$

$$M_g(q^*) + I(y) - Q\overline{F}(\beta^*) \cdot p(\beta^*, r^*) \geq 0, \tag{B.5}$$

$$\eta_1 \cdot \frac{\partial L}{\partial \eta_1} = \eta_1 [P(\beta, r) - P^*(\beta^*, r^*)] = 0, \tag{B.6}$$

$$\eta_2 \cdot \frac{\partial L}{\partial \eta_2} = \eta_2 \left[M_g(q) + I(y) - Q\overline{F}(\beta^*) \cdot p(\beta^*, r^*) \right] = 0, \tag{B.7}$$

$$\eta_1 \geq 0, \tag{B.8}$$

$$\eta_2 \geq 0. \tag{B.9}$$

With (5), the first-order conditions (B.2) and (B.3) can be written as (51) and (52). With (53) and (54), the above equation can be transformed into the following:

$$L = W(\beta, r) + \eta_1 [P(\beta, r) - P^*(\beta^*, r^*)] + \eta_2 \left[-Q\overline{F}(\beta^*) \cdot p(\beta^*, r^*) + M_g(q) + I(y)\right], \tag{B.10}$$

s.t. equations (53) and (54).

Further analysis is detailed in Section 4.3. This completes the proof.

Data Availability

All data, models, and codes that support the findings of this study are available from the authors upon reasonable request.

Conflicts of Interest

The authors declare that they have no conflicts of interest regarding the publication of this paper.

Acknowledgments

This work was supported by the School-Level Project of Shanghai Jian Qiao University (SJQ17011) and the China Postdoctoral Science Foundation (2021M692413).

References

[1] Z. Tan and H. Yang, "The impact of user heterogeneity on road franchising," *Transportation Research Part E: Logistics and Transportation Review*, vol. 48, no. 5, pp. 958–975, 2012.

[2] A. De Palma, M. Kilani, and R. Lindsey, "Maintenance, service quality and congestion pricing with competing roads," *Transportation Research Part B: Methodological*, vol. 41, no. 5, pp. 573–591, 2007.

[3] B. Shang, Q. Sun, H. Feng, and J. Chang, "Determining the operator for the public toll road," *Journal of Advanced Transportation*, vol. 2021, Article ID 6652278, 14 pages, 2021.

[4] Ministry of Transport of the People's Republic of China, "Toll Road Management Regulations (Revised Draft), Ministry of Transport of the People's Republic of China," Beijing, China, 2018, http://www.gov.cn/xinwen/2018-12/21/content_5350738. htm.

[5] R. Arnott and A. de Palma, "The welfare effects of congestion tolls with heterogeneous commuters," *Journal of Transport Economics and Policy*, vol. 28, no. 2, pp. 139–161, 1994.

[6] J. Mayet and M. Hansen, "Congestion pricing with continuously distributed values of time," *Journal of Transport Economics and Policy*, vol. 34, no. 3, pp. 359–370, 2000.

[7] H. Yang, W. H. Tang, W. Man Cheung, and Q. Meng, "Profitability and welfare gain of private toll roads in a network with heterogeneous users," *Transportation Research Part A: Policy and Practice*, vol. 36, no. 6, pp. 537–554, 2002.

[8] E. T. Verhoef and K. A. Small, "Product differentiation on roads: constrained congestion pricing with heterogeneous users," *Journal of Transport Economics and Policy*, vol. 38, no. 1, pp. 127–156, 2004.

[9] F. Xiao and H. Yang, "Efficiency loss of private road with continuously distributed value-of-time," *Transportmetrica*, vol. 4, no. 1, pp. 19–32, 2008.

[10] X. Guo and H. Yang, "User heterogeneity and bi-criteria system optimum," *Transportation Research Part B: Methodological*, vol. 43, no. 4, pp. 379–390, 2009.

[11] Y. Nie and Y. Liu, "Existence of self-financing and Pareto-improving congestion pricing: impact of value of time distribution," *Transportation Research Part A: Policy and Practice*, vol. 44, no. 1, pp. 39–51, 2010.

[12] A. C. Pigou, *The Economics of Welfare*, Macmillan and Company, London, UK, 1920.

[13] M. Beckmann, C. B. Mcguire, and C. B. Winsten, *Studies in the Economics of Transportation*, Yale University Press, New Haven, CT, USA, 1956.

[14] A. A. Walters, "The theory and measurement of private and social cost of highway congestion," *Econometrica*, vol. 29, no. 4, pp. 676–699, 1961.

[15] W. Vickrey, "Pricing in urban and suburban transport," *The American Economic Review*, vol. 53, no. 2, pp. 452–465, 1963.

[16] W. Vickrey, "Congestion theory and transport investment," *The American Economic Review*, vol. 59, no. 2, pp. 251–261, 1969.

[17] H. Yang and H. J. Huang, *Mathematical and Economic Theory of Road Pricing*, Elsevier, Oxford, UK, 2005.

[18] K. A. Small and E. T. Verhoef, *The Economic of Urban Transportation (Version 2)*Routledge, London, UK, 2007.

[19] B. Niu and J. Zhang, "Price, capacity and concession period decisions of Pareto-efficient BOT contracts with demand uncertainty," *Transportation Research Part E: Logistics and Transportation Review*, vol. 53, pp. 1–14, 2013.

[20] S. Shi, Q. An, and K. Chen, "Optimal choice of capacity, toll, and subsidy for build-operate-transfer roads with a paid minimum traffic guarantee," *Transportation Research Part A: Policy and Practice*, vol. 139, pp. 228–254, 2020.

[21] Z. Feng, Y. Zhang, S. Zhang, and J. Song, "Contracting and renegotiating with a loss-averse private firm in BOT road projects," *Transportation Research Part B: Methodological*, vol. 112, pp. 40–72, 2018.

[22] Y. Zhang, Z. Feng, and S. Zhang, "The effects of concession period structures on BOT road contracts," *Transportation Research Part A: Policy and Practice*, vol. 107, pp. 106–125, 2018.

[23] C. F. Daganzo, "A Pareto optimum congestion reduction scheme," *Transportation Research Part B: Methodological*, vol. 29, no. 2, pp. 139–154, 1995.

[24] Z. J. Tan, H. Yang, and X. L. Guo, "Properties of Pareto-efficient contracts and regulations for road franchising," *Transportation Research Part B: Methodological*, vol. 44, no. 4, pp. 415–433, 2010.

[25] H. Mohring, "The peak load problem with increasing returns and pricing constraints," *The American Economic Review*, vol. 60, no. 4, pp. 693–705, 1970.

[26] O. M. Rouhani, R. R. Geddes, H. O. Gao, and G. Bel, "Social welfare analysis of investment public-private partnership approaches for transportation projects," *Transportation Research Part A: Policy and Practice*, vol. 88, pp. 86–103, 2016.

[27] D. Wang, X. Wang, L. Wang, H. Liu, M. Sing, and B. Liu, "Optimisation of government subsidies in infrastructure public-private partnerships," *Journal of Engineering, Design and Technology*, 2021, In press.

[28] C. Lai and M. Xie, *Stochastic Ageing and Dependence for Reliability*, Springer, New York, USA, 2006.

[29] M. C. Bryson and M. M. Siddiqui, "Some criteria for aging," *Journal of the American Statistical Association*, vol. 64, no. 328, pp. 1472–1483, 1969.

[30] S. Shi, Y. Yin, and X. Guo, "Optimal choice of capacity, toll and government guarantee for build-operate-transfer roads under asymmetric cost information," *Transportation Research Part B: Methodological*, vol. 85, pp. 56–69, 2016.

[31] S. Wang, Q. Meng, and Z. Liu, "Fundamental properties of volume-capacity ratio of a private toll road in general networks," *Transportation Research Part B: Methodological*, vol. 47, pp. 77–86, 2013.

[32] H. Mohring and M. Harwitz, *Highway Benefits: An Analytical Framework*, Northwestern University Press, Evanston, IL, USA, 1962.
[33] G. Roth, *Roads In a Market Economy, Avebury Technical*, Ashgate Publishing Limited, Aldershot, Hants, UK, 1996.
[34] D. M. Newbery, "Cost recovery from optimally designed roads," *Economica*, vol. 56, no. 222, pp. 165–185, 1989.
[35] K. M. Mietteinen, *Nonlinear Multi-Objective Optimization*, Kluwer Academic Publishers, Norwell, MA, USA, 1999.
[36] D. A. Wismer and R. Chattergy, *Introduction to Nonlinear Optimization: A Problem Solving Approach*, North-holland Publishing Company, New York, USA, 1978.

Hindawi
Journal of Advanced Transportation
Volume 2022, Article ID 6338365, 14 pages
https://doi.org/10.1155/2022/6338365

Research Article

Heterogeneous Social Linked Data Integration and Sharing for Public Transportation

Wei Zhao,[1,2,3] **Bing Zhou**,[1,2] **and ChaoYang Zhang**[1]

[1]*School of Information Engineering, Zhengzhou University, Zhengzhou 450000, China*
[2]*Cooperative Innovation Center of Internet Healthcare, Zhengzhou University, Zhengzhou 450000, China*
[3]*School of Cyber Science and Engineering, Zhengzhou University, Zhengzhou 450002, China*

Correspondence should be addressed to Wei Zhao; iezhaowei@zzu.edu.cn

Received 25 January 2022; Accepted 12 April 2022; Published 11 May 2022

Academic Editor: Elżbieta Macioszek

Copyright © 2022 Wei Zhao et al. This is an open access article distributed under the Creative Commons Attribution License, which permits unrestricted use, distribution, and reproduction in any medium, provided the original work is properly cited.

Solid (social linked data) technology has made significant progress in social web applications developed, such as Facebook, Twitter, and Wikipedia. Solid is based on semantic web and RDF (Resource Description Framework) technologies. Solid platforms can provide decentralized authentication, data management, and developer support in the form of libraries and web applications. However, thus far, little research has been conducted on understanding the problems involved in sharing public transportation data through Solid technology. It is challenging to provide personalized and adaptable public transportation services for citizens because the public transportation data originate from different devices and are heterogeneous in nature. A novel approach is proposed in this study, in order to provide personalized sharing of public transportation data between different users through integrating and sharing these heterogeneous data. This approach not only integrates diverse data types into a uniform data type using the semantic web but also stores these data in a personal online data store and retrieves data through SPARQL on the Solid platform; these data are visualized on the web pages using Google Maps. To the best of our knowledge, we are the first to apply Solid in public transportation. Furthermore, we conduct performance tests of the new C2RMF (CSV to RDF Mapping File) algorithm and functional and non-functional tests to demonstrate the stability and effectiveness of the approach. Our results indicate the feasibility of the proposed approach in facilitating public transportation data integration and sharing through Solid and semantic web technologies.

1. Introduction

Data sharing for public transportation could address the complex city challenges and implement the efficient and effective management of city spaces, and it could be an effective way to reduce pollution, carbon emissions, global climate change, and even manage health risks in smart cities [1]. Data sharing can involve data such as bus routes, live bus arrival times, train routes, car parking availabilities, and live traffic routes. In addition, a range of data acquisition methods exists. Furthermore, there exist different system sources and data storage formats. This makes the data composition unstructured, which causes heterogeneity in the data composition. Furthermore, heterogeneous data make it difficult to share public transportation data [2–6].

To address these challenges, many studies have been made over the past years. Some researchers tried to integrate heterogeneous data by Web API [7, 8]. They built a virtual integration way in which a unified query interface is provided to a large number of heterogeneous data sources, but this method is limited to popular programming languages and cannot get over the challenges of evolving API that need to modify the existing client codebase [9].

To realize the unified management of heterogeneous data in data applications, one method is to use ETL tools to process heterogeneous data in a unified form. However, this method is costly, and changes in data and analysis requirements will cause the original ETL process to fail [10].

Other studies have shown that the semantic web is "a common framework that allows data to be shared and reused

across application, enterprise, and community boundaries [11]." Semantic web technology [12] promotes data integration from multiple heterogeneous data sources, enables the development of information-filtering systems, and supports knowledge discovery tasks. It helps to integrate diverse data and share these data through the semantic web. However, most of the content on the World Wide Web has not yet been marked up to comply with the semantic web specification. Therefore, how to automatically add tags that conform to the semantic web specification to the existing web content is one of the difficult problems facing the practical application of the semantic web.

To provide personalized sharing of public transportation data between different users through integrating and sharing these heterogeneous data, a new approach is proposed in this study. The proposed approach mainly has three key elements: a data processing method, a CSV to RDF (Resource Description Framework) Mapping File algorithm, and a system framework. Firstly, in order to integrate heterogeneous data, a data processing method is proposed. This data processing method includes the process of collecting, organizing, and normalizing data. Data processing is the basic element of data and data system management and involves the management process of the full life cycle of data. Based on the above point, the main focus is on unstructured data integration. C2RMF (CSV to RDF Mapping File) algorithm is designed, which mainly converts CSV files into RDF files and converts them into a unified data format for subsequent processing. Third, to share these integrated heterogeneous data, a system framework is proposed. This framework mainly performs unified data storage, query, and visualization of the unified transformed files. The main contributions of this study are summarized as follows:

(i) The proposed data processing method involves collecting, integrating, generating, and sharing the heterogeneous public transportation data.

(ii) Based on the proposed method, the newly developed C2RMF algorithm for integrating heterogeneous data is proposed.

(iii) A novel system framework for integrating and sharing these heterogeneous public transportation data is proposed.

The remainder of this paper is organized as follows. Section 2 describes related work. Section 3 describes the proposed methodology in detail. Section 4 describes the system framework. Section 5 describes the system implementation process. The next section describes the experimental environment, data, process and results, and analysis. The conclusions and recommendations are given in the final section [13].

2. Related Work

2.1. RDFS and OWL. Integration and sharing of heterogeneous public transportation data is an important problem in recent years. Previous research and related technologies had solved users' needs to a certain extent, but there are still some problems [7–12]. Recently, RDF (Resource Description Framework) has been widely used to expose, share, and connect pieces of data on the web. RDF is a W3C recommendation graph database model. RDF provides a model of nodes and relationships and is a more general model for the World Wide Web. RDF includes a range of statements, with each statement describing a resource. Every statement includes three parts: a subject, a predicate, and an object. The subject represents the resource; the predicate mainly represents a relationship between the subject and object and the property of that resource; the object represents the value of that property.

Although RDF provides the ability to create a graph of data, it is the RDF schema (RDFS) that supplies the building blocks for more complex vocabularies by enabling the definition of data types and structures within an RDF graph [14]. RDFS provides "all that is needed for interoperability of the vast amount of data on the web [15]." The RDFS can define a set of word sets that can be clearly described based on RDF resources and can be used to describe the subclass or superclass relation, subattribute or superattribute, domain and range of attributes, and instance constraints of the class. Another RDF data model named OWL (Web Ontology Language), which is a W3C recommendation, is a family of knowledge representation languages for authoring ontologies. It can describe more complex logical relationships between concepts. OWL extends RDFS and provides a more descriptive schema layer that can be used where the basic definitions afforded by RDFS are not expressive enough [16].

With the help of the data interconnection network constructed by RDFS and Web Ontology Language (OWL), they are combined with different heterogeneous datasets published on the web. However, they often lack a unified data operation mode for information storage and retrieval of unstructured data.

2.2. Social Linked Data. Solid is also proposed to provide important capabilities for web-based data-sharing systems for public transportation as Solid is based on semantic web and RDF technologies, and it provides a unified data operation mode. In Solid, every user can store their dataset in an online storage space called a personal online data store (pod). Pods can be deployed on personal servers or on public servers by other pod providers. Application data in Solid are stored in documents that are identified by a Uniform Resource Identifier (URI) [17].

Pod refers to a personal online data store that is used to store user data on a Solid platform. It is possible for a user to have more than one pod [18]. A user can select diverse pod providers because Solid applications can operate with any pod server without the limitation of service provider and location. Diverse pod providers can provide diverse degrees of security, availability, and reliability. Different pods can access their data resources and deliver content to each other [17].

In summary, Solid is a web decentralization technology, and a Solid platform can provide a relatively effective and safe means of executing web applications. However, Solid technology still mainly focuses on social media networks. Few studies have considered using Solid in the transportation field. To fill this gap, this study applied Solid technology to public transportation data sharing based on the semantic web, and a new alternative approach was proposed to integrate and share these heterogeneous data.

3. Methodology

The methodology used in this study, presented in Figure 1, analyzed the system functional and non-functional requirements by analyzing the capability and usability of diverse public transportation apps. Next, the system design is given, and the system is implemented based on the system requirements and data processing. Finally, recommendations were devised through experiments and analysis of results.

3.1. Requirement Analysis Based on Comparison of Capability and Usability of Public Transportation Apps. The system requirements were collected based on the capability of diverse public transportation apps compared with the usability of diverse public transportation apps. The public transportation apps in this study were categorized into four groups based on their capabilities and usability. The first group includes minicab apps, including Uber and Aqua cars. The second group includes train and coach apps including Trainline, Virgin Trains, and National Express and bus apps such as First Bus and UK Bus. The third group includes car parking apps such as JustPark and YourParkingSpace, and the last group includes Google and the system. The capabilities and usability of these apps are compared below (see Tables 1 and 2, respectively).

Defining attributes of usability, saving favorite routes, and recent searches and routes, as shown in Table 2, belong to an efficiency attribute because they are related to the accuracy and completeness with which users achieve goals. Sending the selected route to the phone, suggesting an appropriate route based on what the user needs, and sharing an appropriate route to car parking is part of a satisfaction attribute because they have a positive effect on the app usage. Help and FAQ functions make it easy to learn to use apps so that the user can rapidly start getting work done through the app, which is the learnability attribute. Social capabilities allow users to share experiences, including comments, pictures, and videos, and interact with other tourists. It is interesting for users to improve the use of a recommender during a visit to a particular place [19].

3.2. Functional and Non-Functional Requirements. User requirements can be divided into two types: functional and non-functional requirements [20]. Functional requirements can be elicited directly from a user through software feature requests [21]. The non-functional requirement can be defined as part of the attributes of the system [20]. The functional requirements of the new system are listed in Table 3 (functional requirement table), and the non-functional requirements of the new system are listed in Table 4 (non-functional requirement table).

4. System Design

4.1. Proposed Data Processing Method. The proposed data processing method has six key elements: data collected, data integrated and generated, data stored, data searched, and data shared. These elements collect data from different data resources and transfer a uniform RDF model and then save the pod server on the Solid platform, and finally share these data through a web application (see Figure 2).

First, data are collected; the public transportation data are collected from tracking devices and sensors that are located in the entire city and installed on cameras and mobile phones [22]. These public data are referred to as open data because they can be freely used and redistributed by someone either for or at marginal cost through existing web applications, for example, data.gov.uk [23]. During the data collection phase, diverse data sources will be collected through different data sources, such as the data of the Uber system [24], the data of the National Express system [25], and the data of car parking systems [26].

Second, we discuss data integrated and generated elements. There are diverse open data sources in public transportation, for example, National Express is XML; Uber and car parking datasets are structured data like CSV; and Trainline data are unstructured data, like TXT. Therefore, it is necessary to consider heterogeneous datasets and translate them into a uniform data type. An appropriate semantic model can supply an interoperable representation of data [27]. Therefore, semantic web technologies are suggested to address these requirements because they will supply the necessary capabilities for public transportation dataset unification of different open datasets. Each data source needed a diverse method to be extracted and changed into a uniform RDF data model because the RDF data model makes it easier to integrate system data than traditional data models, for example, relational data [28].

Third, data are stored; RDF is a graphics-based data model that can represent any data structure. RDFS can be defined within the RDF so that data structures and types can be adapted as the application demands. RDFS and OWL are programs that change diverse data types into a uniform RDF, adding a semantic mark-up that describes the meaning of each data item. Different data were unified in the RDF and stored in the pod server on the Solid platform, which is a new method because Solid technology was first used in the public transportation area. Solid technology allows users to have full control of their data, including access control and storage location.

Fourth is the data searched element: there are two possible methods for data searching on a Solid platform. One is the RESTful method in terms of the LDP [29]. Another is the SPARQL query method [18]. In a Solid platform, all pod servers must support the LDP, while some servers may optionally support SPARQL.

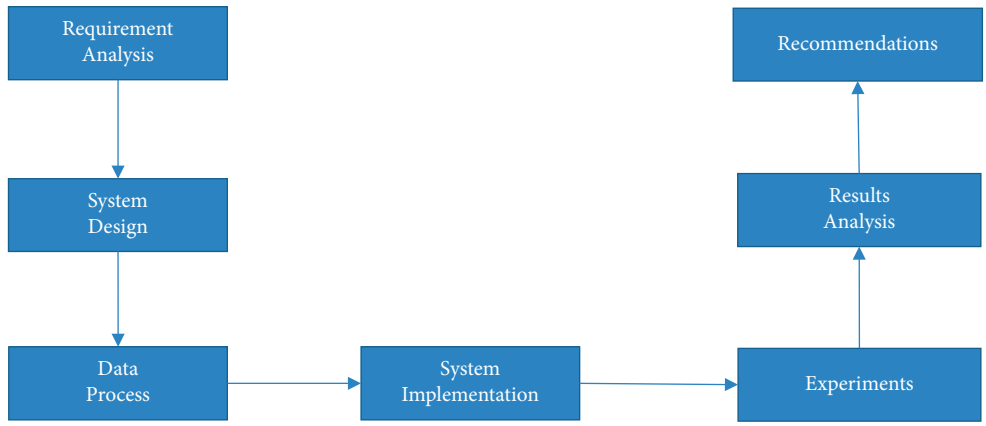

Figure 1: Research methodology.

Finally, we have the data shared element: based on the above steps, users will have access to these data based on their different authority levels, such as access to the entire dataset or only part of the dataset and access to modifying data and comments after data are shared on the website.

4.2. System Framework. Figure 2 describes a complete process in which data is collected, integrated, stored, and shared. Each functional capability is defined as a separate function, permitting separate programming and evolution, as shown in Figure 2, which derives from architectures in Slogger: a profiling and analysis system based on semantic web technologies [30]. Figure 3 shows the system framework for implementing a web-based data-sharing system, including transformers, semantic web query algorithms, and visualization technology. This new proposed system framework for implementing public transportation data sharing is mainly based on Solid.

5. System Implementation

5.1. C2RMF (CSV to RDF Mapping File) Algorithm. To change the CSV data of car parking into RDF for integrating heterogeneous data, the new C2RMF (CSV to RDF Mapping File) algorithm was developed. Converting CSV files to RDF files based on mapping files is currently the main way including the C2RMF algorithm. Some existing tools or ways are accomplished for CSV to RDF including our proposed algorithm. But these tools use different mapping techniques, and it is difficult to use and share these mapping engines. Furthermore, most of them lack the use of semantic web technology and W3C recommended standards [31].

C2RMF algorithm is fully in accordance with W3C recommendation [32], a Java-based method which converts CSV data into RDF. If no specific format is provided, the result is serialized as a TURTLE file by default. The algorithm can convert CSV files into RDF files and also can change some structured data of public transportation into RDF, adding a semantic mark-up that describes the meaning of each data item. The algorithm can convert each row of the input CSV data into a new instance of a uniform RDF class. Each value in the column of the source CSV is transformed into a new triple where each key represents a column position in the source, CSV stands for the subject, each property depending on the name of the column header stands for the predicate, and each value of the column stands for the object. The algorithm is also entirely customizable to meet specific user requirements in terms of the mapping file.

Define the RDF graph. Let M and N be a finite set of uniform resource identifiers and literals. A tuple $(s, p, o) \in M \times M \times (M \cup N)$ can be called an RDF triple. Each RDF triple $t = (s, p, o)$ indicates that resource s and resource o have a relationship p, where s, p, and o represent a subject, a predicate, and an object, respectively, and thus a finite set of triples is called an RDF graph. C2RMF algorithm is shown in Table 5.

Figure 4 shows the transfer process of the C2RMF algorithm and illustrates the corresponding relationship between the contents of the CSV and RDF files.

5.2. Semantic Web Query Process. To retrieve transportation route alternatives from the Solid server, semantic web queries were developed using SPARQL. SPARQL is the W3C standard for creating, querying, and updating linked databases. SPARQL is the standard query language for the RDF model. SPARQL has proven to be a powerful querying language. SPARQL queries in Solid are divided into two queries: local queries and link-following queries. The local query can access only predicates that are located on the local user's pod, whereas the link-following query can access predicates on many pods [17]. The query process retrieves transportation route alternatives in terms of routeId or tripId. The semantic web query considers the synonym heterogeneity for querying between two stations because the station names are diverse in the domain ontology with the same separate definitions.

Similar to SQL, SPARQL retrieves data from the query dataset through a Select statement to determine which result of the selected data will be returned. Additionally, SPARQL uses a Where clause to state criteria to discover a match in the query dataset. A SPARQL query comprises five parts: namespace prefix, result set, dataset, query triple pattern, and modifiers. Similar to SQL, Running a SPARQL query will return all the match data. In the SPARQL query example

Table 1: Capability of diverse public transportation apps (Y denotes yes, N denotes no, and P denotes partial).

	Search route based on leaving date and depart time	Search route based on starting position and destination	Display the diverse routes including different vehicles	Display the diverse routes including stopped stations	Display ticket and payment information based on searched route	Display schedule based on search route and vehicle	Book user schedule based on user needs	Display traffic accidents of the selected route	Display traffic jam of the selected route	Search car parking based on date and parking close to where user needs it	Create account and sign in
Uber	Y	Y	P	P	P	Y	Y	N	N	N	Y
Aqua cars	Y	Y	P	P	P	Y	Y	N	N	N	Y
National express	Y	Y	P	Y	Y	Y	Y	N	N	N	Y
First Bus	Y	Y	P	Y	Y	Y	Y	N	N	N	Y
UK Bus	Y	Y	P	Y	Y	Y	Y	N	N	N	Y
Trainline	Y	Y	Y	Y	Y	Y	Y	N	N	N	Y
Virgin Trains	Y	Y	P	Y	Y	Y	Y	N	N	N	Y
YourParkingSpace	N	N	N	N	N	N	N	N	N	Y	Y
JustPark	N	N	N	N	N	N	N	N	N	Y	Y
Google	Y	Y	Y	Y	Y	Y	Y	Y	Y	Y	Y
My system	Y	Y	Y	Y	Y	Y	Y	Y	Y	Y	Y

Table 2: Usability of diverse public transportation apps.

	Save favorite routes	Save recent searches and routes	Send the selected route to the phone	Suggest an appropriate route based on user needs	Suggest an appropriate route to go to car parking	Help and FAQ	Social aspects
Uber	Y	Y	N	Y	N	Y	N
Aqua cars	Y	Y	N	Y	N	Y	Y
National express	Y	Y	N	Y	N	Y	Y
First Bus	Y	Y	N	Y	N	Y	N
UK Bus	Y	Y	N	Y	N	Y	N
Trainline	Y	Y	N	Y	N	Y	N
Virgin Trains	Y	Y	N	Y	N	Y	Y
YourParkingSpace	N	N	N	N	Y	Y	Y
JustPark	N	N	N	N	Y	Y	Y
Google	Y	Y	Y	Y	Y	Y	N
My system	Y	Y	N	Y	Y	Y	Y

Table 3: Functional requirement.

No	Description	Proposer
1	Search route based on leaving date and depart time and starting position and destination	User
2	Display the diverse routes that include different vehicles and detailed stop stations	User
3	Display the traffic accident of searching routes	User
4	Display the traffic jam of searching routes	User
5	Suggest an appropriate route based on user needs	System
6	Search car parking based parking date and parking close to where user needs it through users' position	User
7	Create account and sign in, and find an appropriate route based on user needs and book it	User
8	Save favorite routes and recent searching routes	User
9	Help and FAQ	User
10	Social media including Twitter, Instagram, and Facebook	User
11	Suggest an appropriate route to go to car parking	System
12	The system can restrict different levels of users so only authorized users can do what they ought to do	System

Table 4: Non-functional requirement.

No	Definition	Description
1	Usability	System states that all menus and navigation are easy to use, system can be used by adult members of the public without training
2	Security	System data are stored safely and protected
3	Compatibility	Different browser compatibility and operating system compatibility
4	Performance	All pages on website system load in less than 5 s
5	Extensibility	System architecture can integrate other new public transportation data
6	Availability	System shall be available for use within 24 hours a day

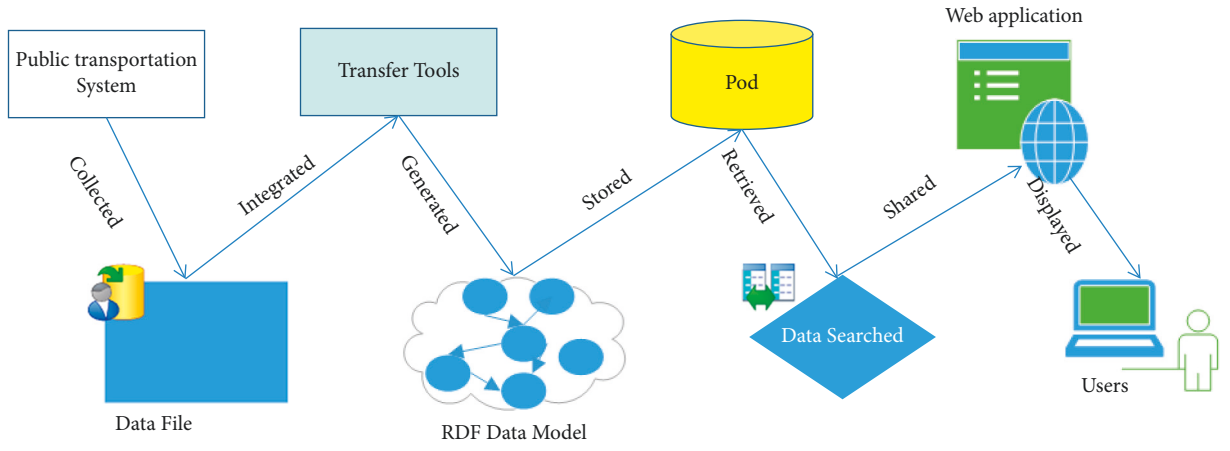

Figure 2: Data processing graph.

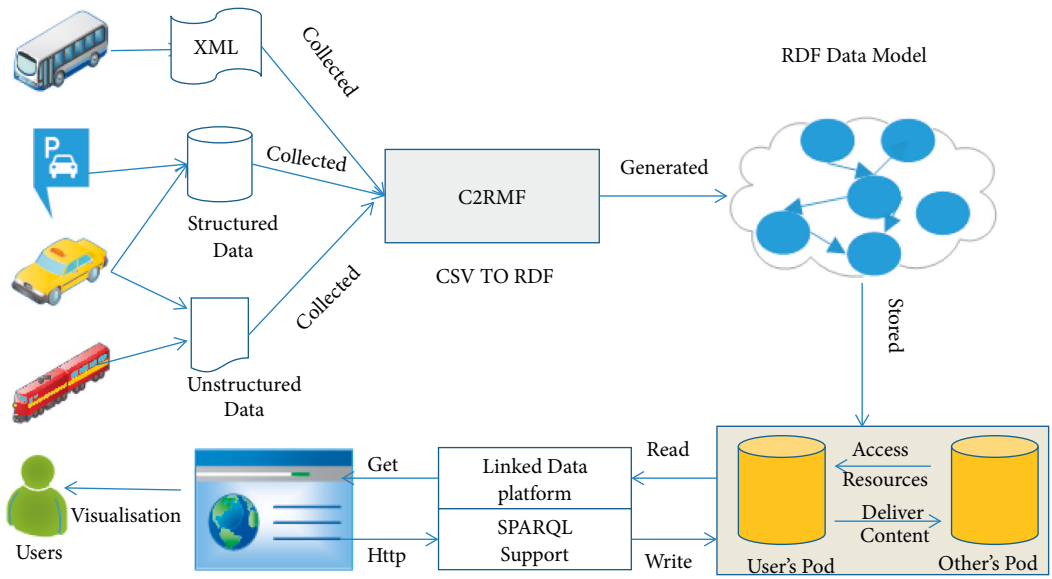

Figure 3: System framework.

Table 5: C2RMF algorithm.

C2RMF algorithm
Input: CSV files; mapping files.
Output: RDF file
(1): Read the CSV file to get the columnsize
(2): Read the CSV file to get the rowsize
(3): Get column. Property of the CSV file
(4): For $i = 1 \ldots$.Rowsize do
(5): For each Column [i]. Property do
(6): $s \longleftarrow i$
(7): $p \longleftarrow$ Get mapping. URI [i] of the mapping file
(8): $o \longleftarrow$ Columns [i]. value
(9): Generate RDF triple (s, p, o)
(10): End for
(11): **Return** RDF triple in the RDF datasets.

below, the SELECT clause specifies the result variable to be returned, and * means to return all result variables. The FROM clause defines the dataset to query. WHERE clause specifies query conditions. Finally, the query returns all these declared query variables in the final subset, in terms of the subjects, predicates, or objects they are defined to in the bus.ttl. "Order by? TripHeadsign" orders the subset in alphabetical order. The SPARQL query is shown in Figure 5.

5.3. Visualization. There are two key modules during the visualization component in the web-based data-sharing system visualization. Google Maps can establish a stable connection from the server to the client and provide downloading of extra map information for displaying map information on the client [33]. Additionally, the application programming interface (API) function, provided by Google, comprises a couple of classes, functions, and data structures that could be used by a developer through JavaScript or others [34]. In this system, the Google Map API is called to initialize the selected map area for display on the web page. SPARQL is used to retrieve relative route data through the pod server, and then CSS and JavaScript are used to show selected Uber and bus routes, displaying the message on the map based on retrieving data. Figure 6 shows the visualization framework for implementing a web-based data-sharing system.

6. Experiment

The experiment can be dived into two parts, the performance test of the C2RMF algorithm and system testing.

6.1. Conversion Performance Test. To verify the performance of the C2RMF algorithm, two ways of converting CSV to RDF data were tested in this testing process, one is the C2RMF algorithm, and the other is a transformer tool named stlab.csv2rdf-1. This csv2rdf is a typical Java-based and open-source tool, which depends on Apache Jena to convert CSV data into RDF [35]. There are other transfer tools that can achieve this purpose, such as Geometry RDF and Table 6. But Csv2rdf is chosen as it is very easy and intuitive to use, and well provide to achieve data transformation.

6.1.1. Testing Environment. The system hardware testing environment includes a Huawei Cloud Server configured with Kunpeng 920 2.6 GHz, 8vCPUs, and 32 GB of RAM. The system software testing environment comprises an Open Euler 20.03 64 bit operating system (server), JDK 1.8.0.

6.1.2. Testing Data. Four datasets from different sources were used for this test [36].

6.1.3. Testing Results. There are two steps in the conversion performance test process, one step is the comparison of the

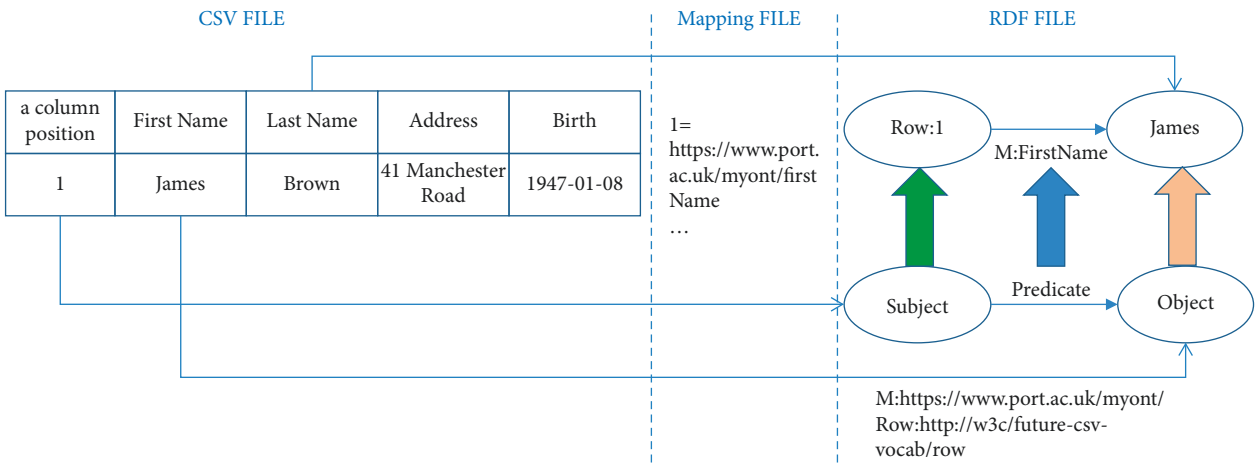

Figure 4: C2RMF algorithms.

```
@PREFIX custom_trip: <https://www.port.ac.uk/custom#>          (Namespace Prefix)
SELECT * ' +                                                   (Result Set)
FROM < https://localhost:8443/public/bus.ttl>                  (Data Set)
' WHERE ' + '{' +                                              (Query Triple Pattern)
  ' ?the Trip custom_trip:routeId ?routeId .'+
  ' ?the Trip custom_trip:tripId ?tripId .'+
  ' ?The Trip custom_trip:tripHeadsign ?tripHeadsign .}
ORDER by ?tripHeadsign '                                       ( Modifiers)
```

Figure 5: An example SPARQL query.

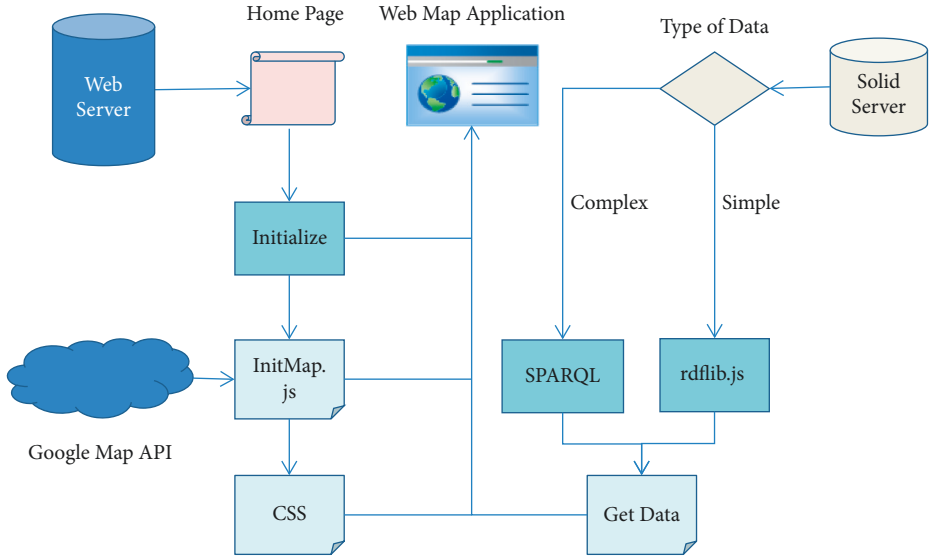

Figure 6: Visualization framework of implementing web-based data-sharing system.

execution time of the C2RMF algorithm and the csv2rdf based on these four datasets, and the four stages of experimental results are listed in Figure 7. The other refers to the two ways of CSV Transformers RDF based on Metro_Interstate_Traffic_dataset, and these experimental results are listed in Figure 8.

Table 6: The experimental datasets for conversion performance test.

Test datasets	Properties	Size (kb)
Bike-sharing-day-dataset	731 rows × 16 columns	56
Bike-sharing-hour-dataset	17379 rows × 17 columns	1130
Car-parking-dataset	35717 rows × 4 columns	1357
Metro_Interstate_Traffic_dataset	48204 rows × 9 columns	2768

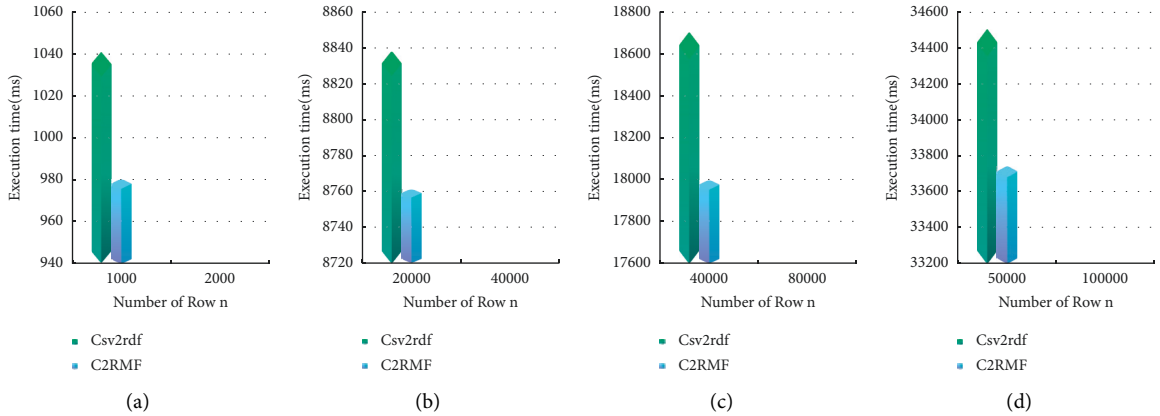

Figure 7: (a) Conversion execution time on the bike-sharing-day-dataset. (b) Conversion execution time on the bike-sharing-hour-dataset. (c) Conversion execution time on the car-parking-dataset. (d) Conversion execution time on the Metro_Interstate_Traffic_dataset.

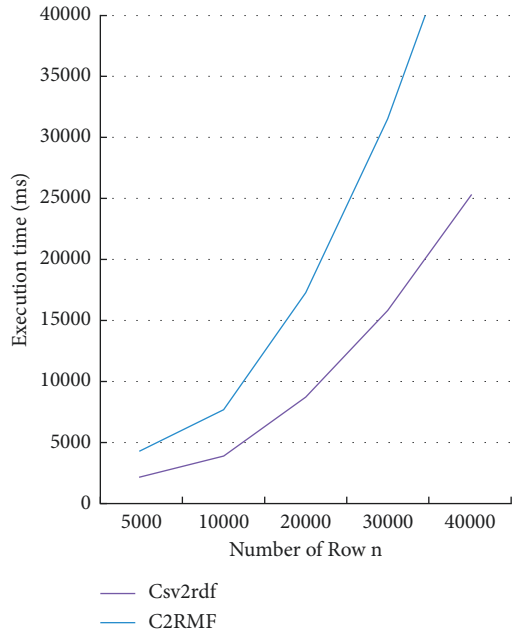

Figure 8: Comparison of the execution time by C2RMF algorithm and csv2rdf based on different number of rows.

6.2. System Testing. This part of system testing mainly includes functional testing and non-functional testing.

6.2.1. Testing Environment. The system hardware testing environment includes a desktop computer configured with an Intel (R) Core(TM) i7-4702MQ CPU 2.2 GHz and 8 GB of RAM. The system software testing environment comprises a Windows 10 Professional 64 byte operating system, a local Solid server version 5.1.6, SpringBoot version 2.1.6, an embedded Tomcat server, which is considered a local web server, and a transformer tool named CSV Transformers RDF algorithm.

6.2.2. Testing Data. During the test process, diverse CSV data were collected from different data sources using diverse addressing mechanisms [24–26].

6.2.3. Functional Testing and Results. Functional testing was used for an achieved program. The aim was to demonstrate that it supplies all of the behaviors required of it. The option of test cases is in terms of the user requirement of the software entity under test [37]. Functional testing is a form of black-box testing. Based on the above, functional testing was considered the main testing technology during the testing phase.

These figures show the functional testing results based on the testing data. Figure 9 shows the bus route list for sharing data on the Solid platform. Figure 10 shows a bus route on the Google Maps and retrieves data from the Solid platform. Figure 11 shows an Uber route on the Google Maps and retrieves data from the Solid platform. Figure 12 shows a car parking position on the Google Maps and retrieves data from the Solid platform.

Based on Table 7, the functional testing results of the new system are listed in Table 8.

6.2.4. Non-Functional Testing and Results. According to Table 4, the non-functional testing results are listed below:

Bus Routes

Chorlton, Southern Cemetery Bus Station
Piccadilly Gardens, Oldham Street
Middleton, Middleton Bus Station
Piccadilly Gardens, Lever Street
Alkrington, Lincoln Rd
Piccadilly Gardens, Piccadilly Gardens

Figure 9: The bus route list through Solid.

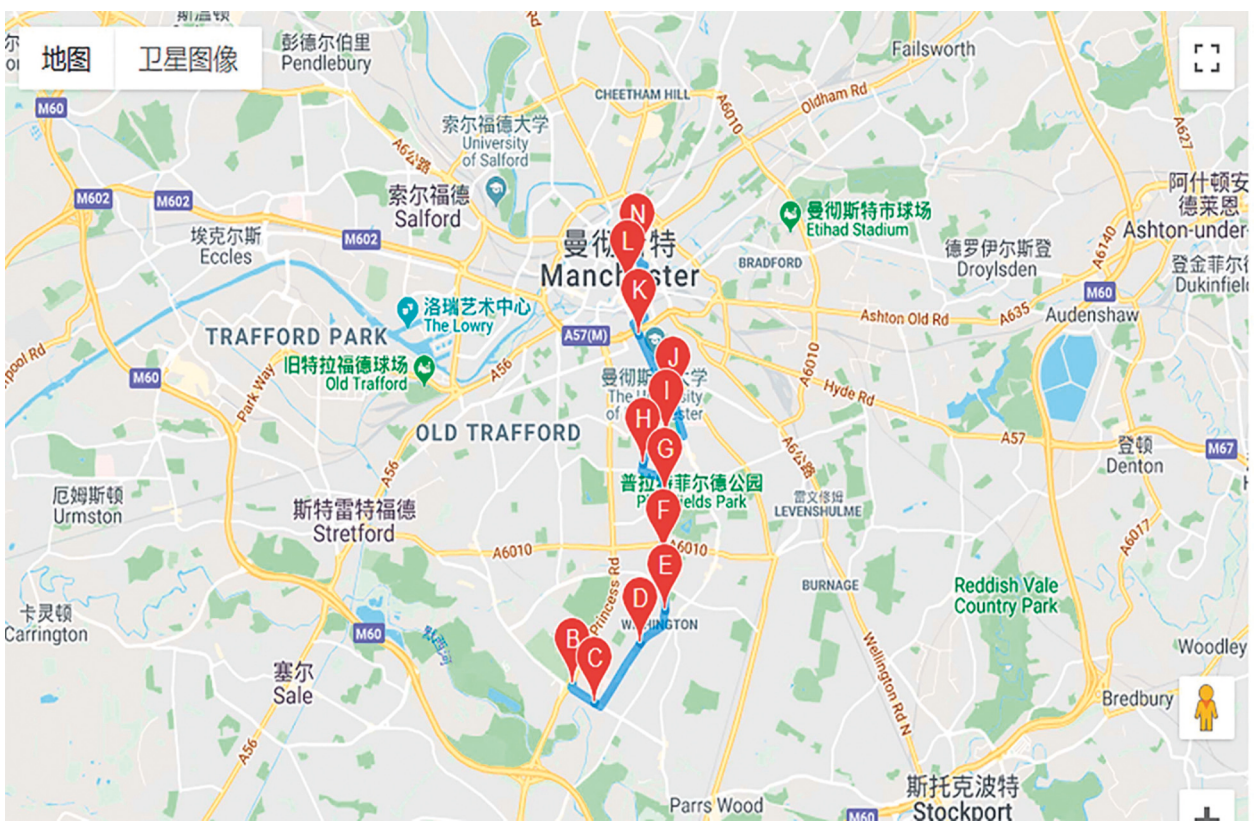

Figure 10: A bus route.

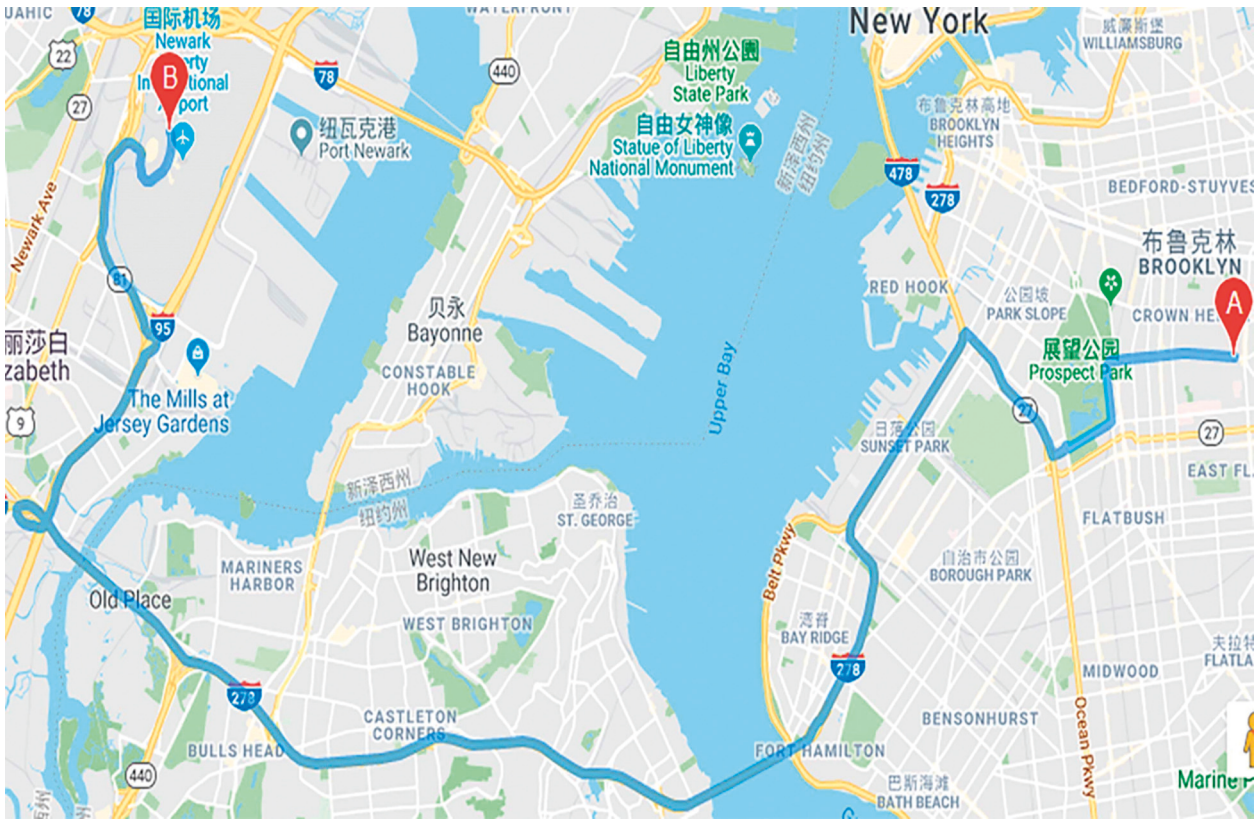

Figure 11: Uber route.

Broad Street	Old Portsmouth Portsmouth UK PO1 2JD
Guildhall Walk	Alec Rose Lane Portsmouth UK PO1 2BX
Isambard Brunel surface	Alec Rose Lane Portsmouth UK PO1 2BX
Seafront Canoe Lake	Southsea Esplanade Portsmouth UK PO4 0ST

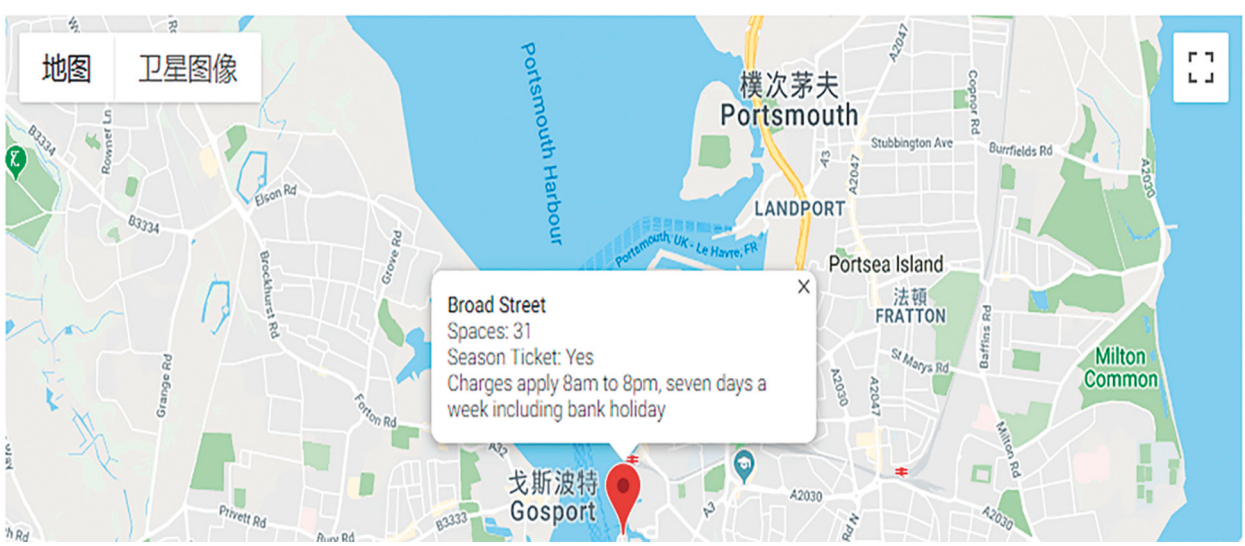

Figure 12: A car parking position.

Table 7: Comparison of testing data.

Testing data	Data source	Test status
Car parking data	Car parking system	PASS
Uber data	Uber system	PASS
National bus data	National Express system	PASS

Table 8: Functional testing results.

No	Description	Results
1	Search route based on leaving date and depart time and starting position and destination	No
2	Display the diverse routes which include different vehicles and detailed stop stations	Yes
3	Display the traffic accident of searching routes	No
4	Display the traffic jam of searching routes	No
5	Suggest an appropriate route based on user needs	Yes
6	Search car parking based on parking date and parking close to where user needs it through users' position	Yes
7	Create account and sign in, find an appropriate route based on user needs, and book it	Yes
8	Save favorite routes and recent searching routes	Yes
9	Help and FAQ	Yes
10	Social media including Twitter, Instagram, and Facebook	Yes
11	Suggest an appropriate route to go to car parking	Yes
12	The system can restrict different levels of users so only authorized users can do what they ought to do	Yes

Usability Testing. There are many guidelines and criteria that were built during usability testing, but the developer could not entirely depend on these guidelines [38]. When following these guidelines and criteria and during the development of the website, it is necessary for users to easily use the website [39]. In terms of the website completed in this paper, it is easy for users to visit and use. Therefore, the website meets the usability requirements.

Security Testing. The most necessary criterion for a web application is probably security. This involves regulating the retrieval of data, certifying user authorities, and storing and protecting system data.

Compatibility Testing. The compatibility of the website is a crucial aspect. The website has better compatibility with various available main browsers, including Google Chrome, Firefox, Safari, and Internet Explorer. Additionally, the website can be visited by the Linux and Windows operating systems, which shows that the website also has operating system compatibility.

Performance Testing. The entire web page loads in less than 5 s in the testing environment. However, as the Solid server and web server were built on the local computer, the test performance in the testing environment is uncertain. Therefore, performance testing needs to be further verified on a remote server.

Extensibility Testing. As the RDF data model was used on the website, it is easy to integrate other new public transportation data, which demonstrates that the website provides good extensibility.

Availability Testing. According to the test local Solid server, it is obvious that the website supplies good availability through the Solid platform.

6.3. Experiment Summary. In total, approximately 80 typical test cases were executed and presented in this paper. Each test case is designed to produce useful data. These test cases were chosen to develop data conversion, data storage, data retrieval, and visualization. Additionally, it is necessary to verify the user requirements and non-functional requirements of these test cases. In this section, some typical examples of these tests are presented, such as converting a heterogeneous data source into uniform RDF data, storing RDF data in the pod server to retrieve data through SPARQL, and finally displaying data on the web page based on Google Maps, CSS, and JavaScript. The test results demonstrate that the new website can meet user requirements.

Furthermore, applications are implemented as client-side web, which reads and writes data directly from the pods in this website in terms of a Solid platform. Multiple applications can also reuse the same data on pod servers. In addition, the new website system sustained the view that sharing public transportation data services could be improved through semantic web and Solid technologies. The website was also developed that is free and provides several protocols, for example, SPARQL. It is efficient for developing applications through Solid platforms.

In addition, the new system is a well-established standard for publishing and managing unstructured or structured data on the web, gathering and bridging knowledge from different data sources. C2RMF algorithm was developed to convert CSV into RDF, and also its performance test was verified.

6.4. Experiment Analysis. Figure 7 shows the comparison of the execution time of the C2RMF algorithm and the csv2rdf on different datasets. Figure 8 shows the comparison of the execution time of the C2RMF algorithm and the csv2rdf based on the different number of rows. In terms of Figures 7 and 8, we can make the following observations:

(i) The C2RMF algorithm and csv2rdf had the highest conversion execution time for the test dataset, Metro_Interstate_Traffic_dataset, 2768 kb, while another test dataset, bike-sharing-day-dataset, with 56 kb, had the least running time, as the execution time usually depends on the properties of the datasets.

(ii) The execution time of both the C2RMF algorithm and the csv2rdf exhibits approximately a linear growth rate as the number of dataset rows. As shown, when the number of dataset rows is low, then the execution time is less; it gradually increases based on the properties and sizes of the datasets.

(iii) The traditional method such as csv2rdf performs well on bike-sharing-day-dataset for converting CSV to RDF, but it is not sufficient to handle a larger number of CSV rows.

(iv) The C2RMF algorithm achieves approximately higher performance based on Figures 6 and 7, and these results demonstrate the effectiveness of the C2RMF algorithm compared with the traditional method because our method optimizes the processing flow and efficiency during the process of converting CSV files to RDF files. Therefore, the C2RMF algorithm can not only convert the original CSV data into RDF data without changing the data but also has high integration and extensibility.

On the other hand, Figure 9 shows the alternative bus route list to arrive at the destination based on this CSV file of the National bus system, which aims to provide the best alternative routes to arrive at the destination in urban areas according to open CSV data. Figure 10 shows a further test case; according to Figure 9, it retrieved each bus station of the selected bus route through SPARQL and finally displayed them on the website through the Solid platform. Figure 11 shows a test case from the CSV file of the Uber system. It suggests that these alternative routes arrive at the destination. The processing flow is similar to that in Figure 10, and the route is also shown on the website with Google Maps. Figure 12 shows the test case from a car parking CSV file, which suggests suitable car parking locations for a car based on its location and is shown on the web page with Google Maps.

However, there are some limitations:

(i) The data source is a single type file: among the different data sources, only the CSV file was selected and converted into an FDF file through our developed converting algorithm during the testing process. In a real environment, other data source files must be selected and converted.

(ii) History data source: the different open data sources were history data and not real-time data. It is helpful to provide online data in a real environment.

(iii) Lack of SPARQL interface: website developers need to be experienced with diverse data schemas and query evaluations to solve effective SPARQL queries.

7. Conclusion and Recommendations

In this paper, we proposed a novel approach that mainly included the proposed data processing method, the new C2RMF algorithm, the proposed system framework, and the web-based data-sharing system. The approach can achieve to integrate and share heterogeneous public transportation data to provide personalized sharing of these data between different users. The research results on the publicly available datasets demonstrate the significance of the approach from two aspects. (1) The proposed data processing method involves the management process of the full life cycle of data including data collected, data integrated and generated, data stored, data searched, and data shared. (2) The proposed approach provided a unified data operation mode for information storage and retrieval of heterogeneous public transportation data. It is useful to manage these data.

In future work, it would be very interesting to do the following. (1) We plan to convert other data types of public transportation including structured data into RDF data through our C2RMF algorithm. (2) We will try to forecast short-term traffic flow based on these public transportation data.

Data Availability

No data were used to support this study.

Conflicts of Interest

The authors declare that they have no conflicts of interest.

Acknowledgments

This study was supported by Major Public Welfare Projects of Henan Province (201300210500).

References

[1] T. M. O'Brien, "Vivek Kundra: federal cio in his own words," 2011, http://radar.oreilly.com/2009/03/vivek-kundra-federal-cio-in-hi.html,2011.

[2] M. Maksimovic, "The role of green internet of things (G-IoT) and big data in making cities smarter, safer and more sustainable," *International Journal of Computing and Digital Systemss*, vol. 6, no. 4, pp. 175–184, 2017.

[3] X. Ma, K. Zhang, L. Zhang et al., "Data-Driven niching differential evolution with adaptive parameters control for history matching and uncertainty quantification," *SPE Journal*, vol. 26, no. 02, pp. 993–1010, 2021.

[4] G. Sun, C. Li, and L. Deng, "An adaptive regeneration framework based on search space adjustment for differential evolution," *Neural Computing & Applications*, vol. 33, no. 15, pp. 9503–9519, 2021.

[5] L. Ding, S. Li, H. Gao, Y. J. Liu, L. Huang, and Z. Deng, "Adaptive neural network-based finite-time online optimal tracking control of the nonlinear system with dead zone," *IEEE Transactions on Cybernetics*, vol. 51, no. 1, pp. 382–392, 2021.

[6] J. Yang, M. Xi, B. Jiang, J. Man, Q. Meng, and B. Li, "FADN: fully connected attitude detection network based on industrial video," *IEEE Transactions on Industrial Informatics*, vol. 17, no. 3, pp. 2011–2020, 2021.

[7] S. Wang, W. A. Higashino, M. A. Hayes, and M. A. M. Capretz, "Service evolution patterns," in *Proceedings of the 2014 IEEE International Conference on Web Services, ICWS, 2014*, pp. 201–208, Anchorage, AK, USA, June 2014.

[8] T. Espinha, A. Zaidman, and H. G. Gross, "Web API growing pains: loosely coupled yet strongly tied," *Journal of Systems and Software*, vol. 100, pp. 27–43, 2015.

[9] J. Samuel and C. Rey, "Challenges in integrating multiple heterogeneous and autonomous web services using mediation approach," in *Proceedings of the 2016 Eleventh International Conference on Digital Information Management (ICDIM)*, pp. 185–190, IEEE, Porto, Portugal, September 2017.

[10] R. Tan, R. Chirkova, V. Gadepally et al., "Enabling query processing across heterogeneous data models: a survey," in *Proceedings of the 2017 IEEE Int'l Conf. on Big Data (Big Data)*, pp. 3211–3220, IEEE, Boston, MA, USA, December 2017.

[11] J. Domingue, D. Fensel, and J. A. Hendler, "Introduction to the semantic web technologies," in *Handbook of Semantic Web Technologies*, D. John, F. Dieter, and J. A. Hendler, Eds., pp. 3–41, Springer-Verlag, Berlin, Heidelberg, 2011.

[12] C. Bizer, T. Heath, and T. Berners-Lee, "Linked da+ta - the story so far," *International Journal on Semantic Web and Information Systems*, vol. 5, no. 3, pp. 1–22, 2009.

[13] Z. Wei, *Web-based Data Sharing System for Public+ Transportation, Unpublished Master's Thesis*, University of Portsmouth, ProQuest Dissertations and Theses Global, Portsmouth, England, 2019.

[14] "RDF vocabulary description language 1.0: RDF schema," 5 November 2007, http://www.w3.org/TR/2004/REC-rdf-schema-20040210.

[15] T. Berners-Lee and E. Miller, "The semantic web," 2002, http://www.w3.org/2002/Talks/01-sweb/.

[16] M. Dean, D. Connolly, F. van Harmelen et al., "OWL web ontology language 1.0 Reference," July 2002, http://www.w3.org/TR/owl-ref/.

[17] "Optimizations over decentralized RDF graphs," in *Proceedings of the IEEE International Conference on Data Engineering, IEEE Computer Society*, pp. 139–142, San Diego, CA, USA, April 2017.

[18] E. Mansour, A. Vlad Sambra, S. Hawke et al., "A demonstration of the solid platform for social web application," in *Proceedings of the 25th International Conference Companion on World Wide Web*, pp. 223–226, Montréal, Canada, April 2016.

[19] J. Borras, A. Moreno, and A. Valls, "Intelligent tourism recommender systems: a survey," *Expert Systems with Applications*, vol. 41, no. 16, pp. 7370–7389, 2014.

[20] D. Leffingwell and W. Don, *Managing Software Requirements: A Use Case Approach*, pp. 978–0321122476, Addison Wesley, Boston, MA, USA, 2003.

[21] E. Guzman and W. Maalej, "How do users like this feature? a fine grained sentiment analysis of app reviews," in *Proceedings of the 2014 IEEE 22nd International Requirements Engineering Conference (RE)*, pp. 153–162, IEEE, Karlskrona, Sweden, August 2014.

[22] M. Gohar, M. Muzammal, A. U. Rahman, and T. S. S. Smart, "Smart tss: defining transportation system behavior using big data analytics in smart cities," *Sustainable Cities and Society*, vol. 41, pp. 114–119, 2018.

[23] "How linked data is transforming eGovernment," January 2013, https://www.slideshare.net/nlout/d432-case-studydataintegrationv015.

[24] "Uber Pickups in NYC, dataset by data-society," 2015, https://data.world/data-society/uber-pickups-in-ny.

[25] "National express data," 2019, http://www.basemap.co.uk/data/NCSD/NCSC.ZIP.

[26] "Council car parks, data.gov.uk," 2019, https://data.gov.uk/dataset/f72d1bf7-44fb-4d69-b7df- 424589d42769/council-car-parks.

[27] R. Uceda-Sosa, B. Srivastava, and R. J. Schloss, "Building a highly consumable semantic model for smarter cities," in *Proceedings of the AI for an Intelligent Planet*, pp. 1–8, Barcelona Spain, July 2011.

[28] S.-C. Necula, "A semantic web solution for E-government educational services," *Informatica Economica*, vol. 19, no. 4/2015, pp. 43–54, 2015.

[29] S. Speicher, J. Arwe, and A. Malhotra, "Linked Data Platform 1.0, W3C Recommendation 26 February 2015. W3C Recommendation, World Wide Web Consortium (W3C)," 2015, http://www. w3. Org/TR/2015/REC-ldp-20150226.

[30] M. Baker and R. Boakes, "Slogger: a profiling and analysis system based on Semantic Web technologies," *Scientific Programming*, vol. 16, no. 2-3, pp. 183–204, 2008.

[31] S. M. H. Mahmud, M. A. Hossin, H. Jahan et al., "CSV2RDF: generating rdf data from CSV file using semantic web technologies," *Journal of Theoretical and Applied Information Technology*, vol. 96, no. 20, 2018.

[32] J. Tandy, I. Herman, and G. Kellogg, Eds., Generating RDF from tabular data on the web, w3c recommendation, 17 December 2015, https://www.w3.org/TR/csv2rdf/.

[33] M. P. Peterson, "International perspectives on maps and the internet: an introduction," in *International Perspectives on Maps and the Internet*, pp. 3–10, Springer, Berlin, Germany, 2008.

[34] J. Udell, *Beginning Google Maps Mashups with Mapplets, KML, and GeoRSS: From Novice to Professional*, Apress, New York, NY, USA, 2009.

[35] "csv2rdf," 2017, https://github.com/anuzzolese/csv2rdf.

[36] D. Dua and C. Graff, "UCI machine learning repository," Sept 2021, http://archive.ics.uci.edu/ml.

[37] S. Nidhra, "Black box and white box testing techniques - a literature review," *International Journal of Embedded Systems and Applications*, vol. 2, no. 2, pp. 2029–50, 2012.

[38] R. S. Pressman, *Software Engineering: A Practitioner's Approach*, Palgrave macmillan, London, UK, 2015.

[39] M. S. Hussain, A. Ali, and J. Shaf, "Enhance websites testing via functional and non-functional approach: case study," *International Journal of Application or Innovation in Engineering & Management*, vol. 2, no. 5, pp. 66–72, 2013.

Hindawi
Journal of Advanced Transportation
Volume 2022, Article ID 2006978, 8 pages
https://doi.org/10.1155/2022/2006978

Research Article

Optimization of the Reversible Lane considering the Relationship between Traffic Capacity and Number of Lanes

Jianrong Cai,[1] Jianhui Wu,[2] Zhixue Li,[1] Qiong Long,[1] Zhaoming Zhou,[1] Jie Yu,[1] and Xiangjun Jiang[3]

[1]*School of Civil Engineering, Hunan City University, Yiyang, Hunan 413000, China*
[2]*School of Information Science and Technology, Hunan Institute of Science and Technology, Yueyang 414006, China*
[3]*Department of Traffic Management, Hunan Police Academy, Changsha, Hunan 410000, China*

Correspondence should be addressed to Jianhui Wu; wjh_hnist@163.com

Received 11 March 2022; Revised 10 April 2022; Accepted 15 April 2022; Published 28 April 2022

Academic Editor: Elżbieta Macioszek

Copyright © 2022 Jianrong Cai et al. This is an open access article distributed under the Creative Commons Attribution License, which permits unrestricted use, distribution, and reproduction in any medium, provided the original work is properly cited.

To make full use of road resources, improve the operation efficiency of the road network system, and alleviate the coexistence between traffic congestion and road resources idle caused by the traffic tidal phenomenon, the impact of the number of lanes on traffic capacity is examined, and the mixed-integer bilevel programming model for reversible lane optimization is established with the aim to minimalize the total travel time of the system. Taking a test road network as an example, the influence of the reversible lane optimization on characteristic values of sections, the route travel time between OD pairs, and the total time of the system are analyzed. The results indicate that the reversible lane optimization can make full use of the idle road resources and make the road network structure match the travel demands better, and the system index after the reversible lane optimization is obviously better than the original system index.

1. Introduction

Urban traffic flow has two typical characteristics. One is temporal asymmetry on some roads and another is spacial asymmetry on some roads. As more and more urban residents choose to work in the city center and live in the suburbs, urban traffic has obvious tidal characteristics. During the peak hours, the flow in one direction of the lanes is greater than the capacity resulting in congestion, while the lanes in the other direction are not fully utilized resulting in the idleness of road resources, and the traffic system is in a state of congestion and inefficient operation.

There have been a large number of theoretical and simulation studies of traffic systems in order to solve the problem of congestion and achieve high traffic efficiency (e.g., Li et al. [1]). And the implementation of reversible lanes which adjusts the road resources in the light traffic flow direction to the heavy traffic flow direction is an effective measure to solve the problem of tidal traffic congestion and improve the operation efficiency of the whole road network system greatly, without changing the road structure, control facilities, or traffic infrastructure (e.g., Wong et al. [2], Jiang et al. [3], Yu et al. [4], Wolshon et al. [5], and Golub et al. [6]).

Zhang et al. [7] established the network reserve capacity model and demonstrated that reversible lane can greatly improve the reserve capacity of the road network. In the study of Li et al. [8], in order to make the periodic flow direction of the reversible traffic system change more smoothly, a reversible lane adjustment method suitable for urban trunk roads from off-peak time to peak time is proposed. Hausknecht et al. [9] pointed out that the reversible lane system can increase the capacity of congested sections, effectively reduce traffic congestion in peak hours, and facilitate the emergency evacuation of travel users. Wolshon et al. [10] analyzed the problems that can be solved by the setting of reversible lanes and believed that the cost, advantages, and disadvantages of various design schemes and the long-term benefits of the whole transportation system should be comprehensively considered when

planning reversible lanes. Waleczek et al. [11] studied the effectiveness, feasibility, and safety issues of reversible lanes and considered that the reversible lane system is a practical and safe intelligent traffic management tool.

Yue et al. [12] demonstrated the necessity and feasibility of implementing reversible lane during the Shanghai World Expo and preliminarily discussed the specific implementation scheme. Wang et al. [13] developed an optimization model to decide the number and scheduling rules of the reversible lanes of container gates under the constraints of limited spaces and imbalanced traffic volumes. Sheu et al. [14] analyzed the potential of applying lane reversal techniques to alleviate temporary congestion caused by traffic incidents and formulated a discrete-time nonlinear stochastic model with the estimation of lane-changing fractions for real-time incident management. Xiao et al. [15] focused on disseminating messages under global traffic information and studied the cooperative bargain for the separation of traffic flows in smart reversible lanes so as to make consistent movements when separating the flows. Mao et al. [16] proposed a real-time dynamic reversible lane scheme in the Intelligent Cooperative Vehicle Infrastructure System (CVIS) which was applied to determine the number of lanes and the timing of lane changes.

Bilevel programming model is increasingly used in the field of reversible lane optimization, typically the upper-level decides on the lanes, changing their performance depending on the lower-level travelers' routing decisions (e.g., Magnanti et al. [17]). Shi et al. [18] established a master-slave bilevel programming model with the goal of reducing the total travel cost in the peak period of the urban transportation network and reducing the management cost of reversible lane setting. Gao et al. [19] and Zhang et al. [20] constructed a bilevel programming model of reversible lane optimization with the goal of minimizing the total impedance of the road network, in which the upper level is the reversible lane setting scheme of the traffic management department and the lower level is the user optimal allocation of travel users according to the set scheme. Lu theoretically analyzed the behaviors of the players involved in the leader-follower strategic game and established a bilevel programming model considering the game equilibrium between road users and traffic controllers (e.g., Lu et al. [21]).

Di defines a coupling measure to quantify the relationship between network structure and demand structure, with the aim to maximize the coupling measure, and a nonlinear bilevel mixed-integer programming model is established to find the optimal lane combination strategy in the considered network from the viewpoint of systematology (e.g., Di et al. [22]). When the goal of the upper level is the same as the lower level, the problem can be formulated as a single-level programming model (e.g., Conceio et al. [23] and Cai et al. [24]).

The abovementioned studies on reversible lanes are based on the ideal assumption that the capacity of the road section is absolutely proportional to the number of lanes. But, in fact, with the increase in the number of lanes, the average capacity of each lane decreases accordingly. When the number of lanes is more than 4, the average capacity of each lane even decreases by more than 16%. Ignoring this practical impact may lead to a large deviation between the model and the actual situation (e.g., Yang et al. [25]). Therefore, this paper takes maintaining the normal traffic in the direction of light traffic flow during the implementation of reversible lanes as the basic premise, considers the reduction impact of the number of lanes on the traffic capacity of the road section, and studies the optimal setting scheme of the reversible lanes from the perspective of system optimization in order to ensure the effectiveness of the whole transportation system and alleviate the coexistence of traffic congestion and idle road resources.

This manuscript is structured as follows. After the introduction, Section 2 is the analysis of the relationship between road capacity and the number of lanes. In Section 3, the bilevel programming model for reversible lane optimization is established. In Section 4, the feasibility of this optimization model and its solution algorithm is verified. In Section 5, the calculations and analysis of numerical example are given. In Section 6, the conclusions of this research are drawn.

2. Analysis of the Relationship between Traffic Capacity and Number of Lanes

The capacity of the road section increases with the increase of the number of lanes, but with the increase of the number of lanes, the opportunity for vehicle lane-changing increases accordingly, the mutual interference between vehicles increases, and the increase of the actual traffic capacity of the road section decreases marginally with the increase of the number of lanes.

Understanding the effect of lane-changing on traffic is an important topic in designing optimal traffic control systems (e.g., Li et al. [26]). According to Xiaobao Yang et al.'s [27] research results, if the average capacity per lane of 2 lane section is c_2 and the lane-changing frequency is $a_2\,(a_2 = -0.224)$, the average capacity per lane of n lane section is c_n.

$$c_n = c_2 e^{a_2(n-2)/n}, \quad n \geq 2. \tag{1}$$

In specific planning, the lane number correction coefficient of single-lane section is 1, and the lane number correction coefficient of 2 lane section is 1.87 (e.g., Wang et al. [28]). If the traffic capacity of 1 lane is set as c_1, average capacity per lane of 2 lane section is c_2.

$$c_2 = \frac{1.87 c_1}{2} = 0.935 c_1. \tag{2}$$

The average capacity per lane of n lane section is c_n.

$$c_n = \begin{cases} 0.935 c_1 e^{a_2(n-2)/n}, & n \geq 2 \\ c_1 & n = 1 \end{cases}. \tag{3}$$

Take the unit impulse sequence as

$$\delta(n-1) = \begin{cases} 1, & n = 1 \\ 0, & \text{others} \end{cases}. \tag{4}$$

Table 1: Average capacity per lane.

Number of lanes	1	2	3	4	5	6	7	n
Average capacity per lane	c_a	0.935 c_a	0.8678 c_a	0.8359 c_a	0.8174 c_a	0.8053 c_a	0.7967 c_a	0.935 $e^{a_2(n-2)/n}c_a$

Take the unit step sequence as

$$u(n-2) = \begin{cases} 1, & n \geq 2 \\ 0, & \text{others} \end{cases}. \tag{5}$$

Then, the average capacity per lane of the n lane section can be obtained as

$$c_n = \delta(n-1)c_1 + u(n-2)0.935c_1 e^{a_2(n-2)/n}. \tag{6}$$

3. Bilevel Programming Model for Reversible Lane Optimization

Note that the node set of the whole road network is N, the road section set is A, and the OD (origin destination) pair set is w. Assuming that section $a \in A$ has a corresponding reverse section $\overline{a}$, note that the two-way section $\ddot{a}$ is composed of section a and section $\overline{a}$. x_a represents the flow of section a, l_a represents the number of lanes of section a, C_a represents the capacity of section a, and c_a represents the capacity of a single lane of section a. Note that the free travel time of section a is t_a^0, the travel time of each section is $t_a(x_a, l_a)$, and its functional form adopts BPR formula:

$$t_a(x_a, l_a) = t_a^0\left[1 + \alpha\left(\frac{x_a}{C_a}\right)^{\beta}\right], \quad a \in A, \tag{7}$$

where α and β are undetermined parameters and C_a can be obtained as

$$C_a = l_a \cdot c_n, \quad a \in A. \tag{8}$$

According to formula (6), the average capacity per lane of n lane section can be obtained as shown in Table 1.

It is assumed that all travelers have the decision to select the path with the minimum travel time, and the road network reaches the user equilibrium state. For the reversible lane system, the traffic management department can optimize the allocation of road resources through the adjustment of the number of lanes so that the road network structure can match the travel needs of urban residents better. Aiming at minimizing the total travel time of the whole road network, a mixed-integer bilevel programming model for the reversible lane optimization is constructed as follows:

Upper level:

$$\min Z = \sum_{a \in A} t_a(x_a, l_a) \cdot x_a. \tag{9}$$

$$\text{s.t. } 1 \leq l_a \leq l_{\ddot{a}} - 1 \quad \forall a \in A. \tag{10}$$

$$l_a + l_{\overline{a}} = l_{\ddot{a}}, \quad \forall a \in A, \overline{a} \in A. \tag{11}$$

Lower level:

$$\min \sum_{a \in A} \int_0^{x_a} t_a(\omega, l_a) \mathrm{d}\omega. \tag{12}$$

$$\text{s.t. } \sum_k f_k^{rs} = d_{rs}, \quad \forall (r,s) \in w. \tag{13}$$

$$f_k^{rs} \geq 0, \quad \forall (r,s) \in w. \tag{14}$$

$$x_a = \sum_r \sum_s \sum_k f_k^{rs} \delta_{a,k}^{rs}, \quad \forall a \in A, \tag{15}$$

where ω is the integral variable symbol, f_k^{rs} is the flow on the path k between OD pairs (r,s), d_{rs} is the travel demand between OD pairs (r,s), $\delta_{a,k}^{rs}$ is the correlation coefficient between the path and the section, when the path k passes through the section a, $\delta_{a,k}^{rs} = 1$, otherwise, $\delta_{a,k}^{rs} = 0$; formula (10) shows that the adjustment range of the number of lanes in the section a is $[1, l_{\ddot{a}} - 1]$; formula (11) is the conservation constraint of the number of lanes in the section; formula (13) is the conservation constraint of traffic flow; formula (14) is nonnegative constraint of path flow.

4. Model Solution

Considering the complexity of the solution process for the optimization model of nonlinear mixed-integer bilevel programming problem which includes NP-hard optimization problems (e.g., Karshenas et al. [29], Wang et al. [30], Zhou et al. [31], and Shi et al. [32]), we propose a chaotic particle swarm optimization algorithm, which is a parallel algorithm, starts from the random solution, and finds the optimal solution through iteration. The detailed steps are described as follows:

Step 1. Initialization. Let the number of iterations be η, the maximum allowable number of iterations be $\eta_{\max}$, the particle swarm size be m, the reduction coefficients be z_1 and z_2, respectively, the dynamic delay period be ξ, the maximum speed be $v_{a,\max}$, the inertia weight factor be κ, and the acceleration coefficients be γ_1 and γ_2, respectively. The position $(\cdots, \varphi_{a,\eta}^i, \cdots)$ of the ηth iteration of the $i(i = 1, 2 \cdots m)$th particle corresponds to the state $(\cdots, l_{a,\eta}^i, \cdots)$ of the ηth iteration of the ith reversible lane optimization scheme, the maximum particle position of section a is $\varphi_{a,\max}$, corresponding to the maximum number of lane settings $l_{\ddot{a}} - 1$ of section a, and the travel demand is d_{rs}; each feasible particle initial position $\varphi_{a,0}^i$ and initial speed $v_{a,0}^i$ are randomly generated, the chaotic parameter is μ, and the maximum number of iterations is $\psi_{\max}$.

Step 2. Calculate fitness. For each feasible particle, solve the lower user equilibrium traffic allocation model and then

solve the upper objective function value according to the section flow, that is, the fitness of the particle.

Step 3. Organize the particles in the swarm and update the fitness of the particles in the swarm. Particles are processed subchaotic iteratively $\psi_{\max}$ times using logistic maps. Assuming that the search space element of the same dimension as $(\cdots, \varphi^i_{a,\eta}, \cdots)$ is $Y = (\cdots, y_i, \cdots)$, y_i is the ith component of the vector Y, $y_i \in [0,1]$, and iteration is performed by $y_i^{k+1} = \mu y_i^k (1 - y_i^k)$, when the number of iterations is reached at $\psi_{\max}$, the chaotic sequence $\left\{y_i^j | j = 1, 2, \cdots, k\right\}$ of the ith component $y_i (i = 1, 2, \cdots)$ of the vector Y is obtained. When $\mu = 4$, the chaotic sequence obtained by the logistic maps is in a completely chaotic state, and when $\psi_{\max}$ large enough, the chaotic sequence is able to traverse all the values of the search space.

Step 4. Update the historical optimal location of individuals and groups. For the $i\,(i = 1, 2 \cdots m)$th particle, the individual extremum $pbest^i_{a,\eta}$ is updated with the position corresponding to the current optimal fitness. For particle swarm optimization, the optimal position of all $pbest_{a,\eta}$ is used to update the population extremum $gbest_{a,\eta}$. If $\text{gbest}_{a,\eta}$ does not improve after ξ successive iterations, make $\kappa = z_1 \kappa$, $v_{a,\max} = z_2 v_{a,\max}$.

Step 5. Update the particle velocity according to $v^i_{a,\eta+1} = \kappa v^i_{a,\eta} + \gamma_1 R_1 (pbest^i_{a,\eta} - \varphi^i_{a,\eta}) + \gamma_2 R_2 (gbest_{a,\eta} - \varphi^i_{a,\eta})$, where $v^i_{a,\eta}$ is the velocity of the ηth iteration of the $i\,(i = 1, 2 \cdots m)$th particle, R_1 and R_2 are random numbers between $(0, 1)$, and the velocity of each particle shall be rounded to an integer. If $v^i_{a,\eta+1} > v_{a,\max}$, order $v^i_{a,\eta+1} = v_{a,\max}$.

Step 6. Update the particle position based on $\varphi^i_{a,\eta+1} = \varphi^i_{a,\eta} + v^i_{a,\eta}$. If $\varphi^i_{a,\eta+1}$ does not meet the constraint condition $1 \le \varphi^i_{a,\eta+1} \le \varphi_{a,\max}$, it is discarded and the position of the ith particle is not updated. If the constraint conditions are met, judge the ith particle. If the particle makes no path connection between an OD pair, discard the new position and do not update the position of the ith particle, otherwise update the ith particle to the new position.

Step 7. Terminate the inspection. If the termination condition is satisfied, the iteration is stopped and $gbest_{a,\eta}$ is output as the optimal adjustment scheme. Otherwise, let $\eta = \eta + 1$ and return to Step 1.

5. Calculations and Analysis of Numerical Example

The test road network is shown in Figure 1, which is composed of four nodes and five two-way sections. It is assumed that there are four OD pairs, and the travel demand is $d_{14} = 4560$pcu/h, $d_{41} = 910$pcu/h, $d_{23} = 780$pcu/h, and $d_{32} = 1130$pcu/h. The parameter value of the BPR function is $\alpha = 0.15$ and $\beta = 4$. The characteristic parameters of each section, including free travel time, single-lane capacity, and number of lanes, are shown in Table 2.

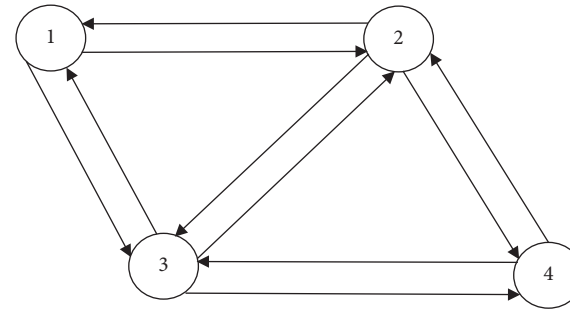

Figure 1: Test road network.

Table 2: Characteristic parameters of each section.

Section	Free travel time (s)	Single-lane capacity (pcu ·h^{-1})	Number of lanes
1–2	95	650	4
2–1	95	650	4
3–1	55	700	3
1–3	55	700	3
2–3	41	700	3
3–2	41	700	3
4–2	55	650	4
2–4	55	650	4
4–3	95	700	3
3–4	95	700	3

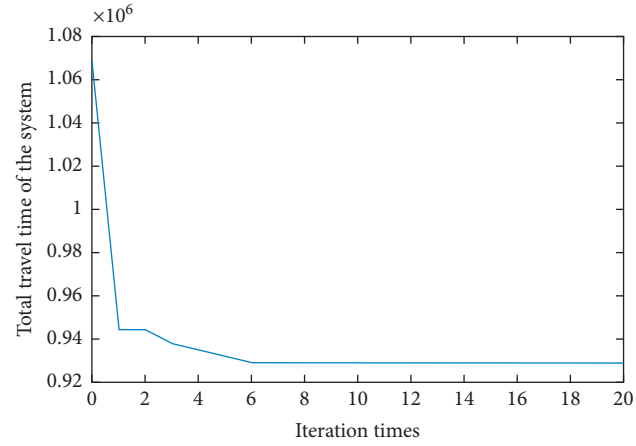

Figure 2: Total travel time of the system changes with iteration times.

For the number of lanes in each section in the example, set $\varphi_{1-2,\max} = 7$, $\varphi_{2-4,\max} = 7$, $\varphi_{1-3,\max} = 5$, $\varphi_{2-3,\max} = 5$, $\varphi_{3-4,\max} = 5$, $v_{1-2,\max} = 7$, $v_{2-4,\max} = 7$, $v_{1-3,\max} = 5$, $v_{2-3,\max} = 5$, and $v_{3-4,\max} = 5$. At the same time, in order to improve the convergence speed of particle swarm optimization algorithm and ensure its effective convergence, set $m = 20$, $z_1 = 0.9$, $z_2 = 0.9$, $\gamma_1 = 1.8$, $\gamma_2 = 1.8$, $\xi = 6$, $\kappa = 1.3$, $\eta_{\max} = 20$, $\mu = 4$, and $\psi_{\max} = 20$. The total travel time of the system under the reversible lane optimization scheme changes with iteration times as shown in Figure 2.

The comparison of characteristic values such as lane number, capacity, flow, and travel time of each section before and after reversible lane optimization is shown in

Table 3: Characteristic values of sections before and after optimization.

Section	Number of lanes		Capacity (pcu ·h^{-1})		Flow (pcu ·h^{-1})		Travel time (s)	
	Before	After	Before	After	Before	After	Before	After
1–2	4	7	2173	3625	2368	2537	115.10	98.42
2–1	4	1	2173	650	495	438	95.04	97.94
3–1	3	1	1822	700	415	472	55.02	56.70
1–3	3	5	1822	2861	2192	2023	72.28	57.06
2–3	3	2	1822	1309	780	780	41.21	41.78
3–2	3	4	1822	2341	1351	1151	42.86	41.36
4–2	4	1	2173	650	495	438	55.02	56.70
2–4	4	7	2173	3625	2590	2559	71.65	57.05
4–3	3	1	1822	700	415	472	95.04	97.94
3–4	3	5	1822	2861	1970	2001	114.48	98.41

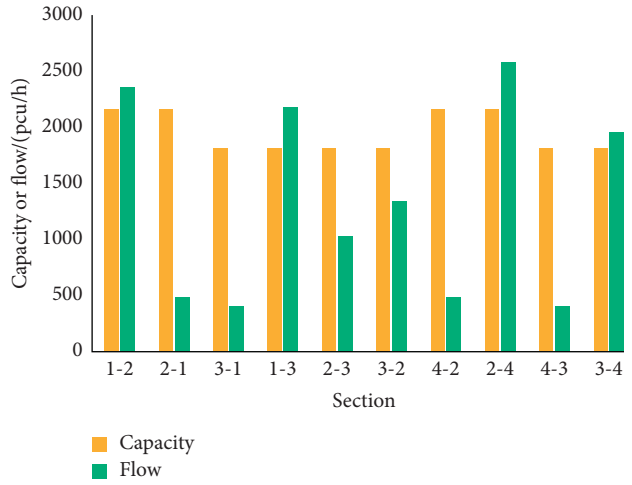

Figure 3: The capacity and flow of each section before reversible lane optimization.

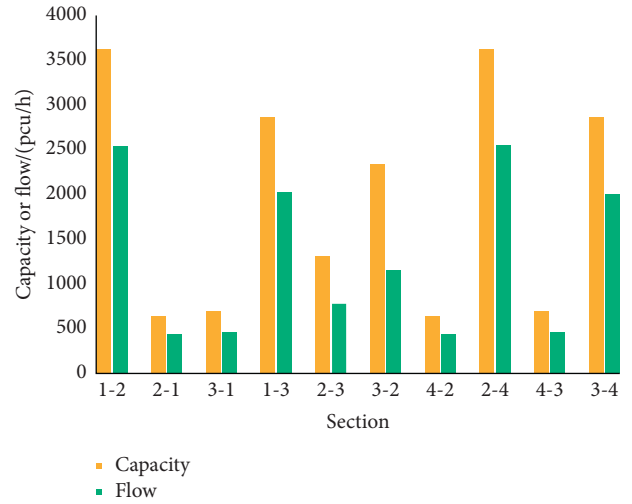

Figure 4: The capacity and flow of each section after reversible lane optimization.

Table 3. For comparison, the capacity and flow of each section before reversible lane optimization are shown in Figure 3. The capacity and flow of each section after reversible lane optimization are shown in Figure 4. The

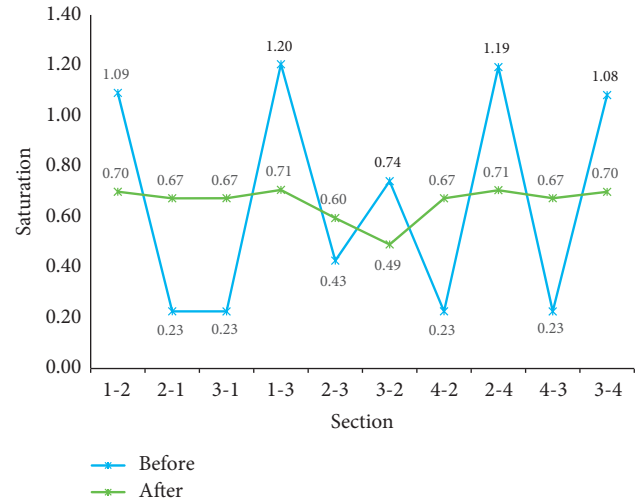

Figure 5: Saturation of sections before and after optimization.

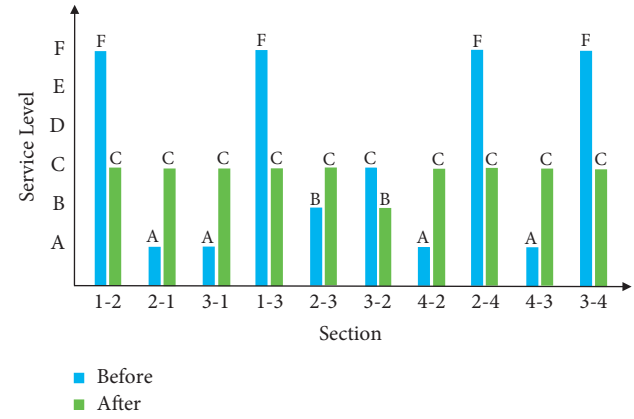

Figure 6: Service level of sections before and after optimization.

saturation comparison of each section before and after the optimal setting of reversible lane is shown in Figure 5. The service level of each section before and after the optimal setting of reversible lane is shown in Figure 6.

Before the optimal setting of reversible lanes, the traffic flow of sections 1–2, 2–4, 1–3, and 3–4 in heavy traffic flow direction is larger than the capacity, and the saturation exceeds 1, which is F service level, and the sections are very

Table 4: Route travel time before and after optimization.

OD pair	Route/in node order	Route travel time/s			Total time/s		
		Before	After	Difference	Before	After	Difference
(1,4)	1–2–4	186.8	155.5	−31.3	851808	709080	−142728
	1–2–3–4	270.8	238.6	−32.2			
	1–3–4	186.8	155.5	−31.3			
	1–3–2–4	186.8	155.5	−31.3			
(4,1)	4–2–1	150.1	154.6	4.5	136591	140686	4095
	4–2–3–1	151.3	155.2	3.9			
	4–3–1	150.1	154.6	4.5			
	4–3–2–1	232.9	237.2	4.3			
(2,3)	2–3	41.2	41.8	0.6	32136	32604	468
	2–4–3	166.7	155.0	−11.7			
	2–1–3	167.3	155.0	−12.3			
(3,2)	3–2	42.9	41.4	−1.5	48477	46782	−1695
	3–1–2	150.1	154.6	4.5			
	3–4–2	169.5	155.1	−14.4			

congested. The flow of sections 2–1, 4–2, 3–1, and 4–3 in the light traffic flow direction is much more smaller than the capacity, and the saturation is less than 0.25, which is A service level, and the road resources are not fully utilized. The traffic tide phenomenon in 2-way sections is obvious, and the problems of traffic congestion and idle road resources are prominent.

After the optimal setting of reversible lanes, the number of lanes of the section in the heavy traffic flow direction increases, the section's capacity increases accordingly, and the travel time decreases significantly, while the number of lanes of the section in the light traffic flow direction decreases, the section's capacity decreases accordingly, and the travel time increases slightly. The saturation of each section is between 0.45 and 0.75, with the variance decreased from 0.175 to 0.004, the saturation is more balanced, the sections are all at the service level of B or C, and there is neither excessive congestion nor idle road resources.

It shows that the reversible lane optimization scheme can make full use of the idle road resources in the light traffic flow direction to improve the capacity of the section in the heavy traffic flow direction, adjust the distribution of flow on the road network, reduce the travel time of sections in the heavy traffic flow direction significantly, balance the saturation and service level of sections, and alleviate the coexistence of traffic congestion and idle road resources caused by traffic tide phenomenon effectively.

The route travel time between OD pairs before and after reversible lane optimization is shown in Table 4. The total travel time of the system and between OD pairs before and after reversible lane optimization is shown in Figure 7.

From the perspective of equilibrium travel time between OD pairs, although the travel time between OD pairs (4,1) with smaller demand increased from 150.1s to 154.6s, and the travel time between OD pairs (2,3) also increased from 41.2s to 41.8s, the travel time between OD pairs (1,4) with larger demand decreased from 186.8s to 155.5s, and the travel time between OD pairs (3,2) also decreased from 42.9s to 41.4s. It shows that reversible lane optimization can adjust more road resources to travelers between OD pairs with larger demand and make the road network structure better match the travel demand.

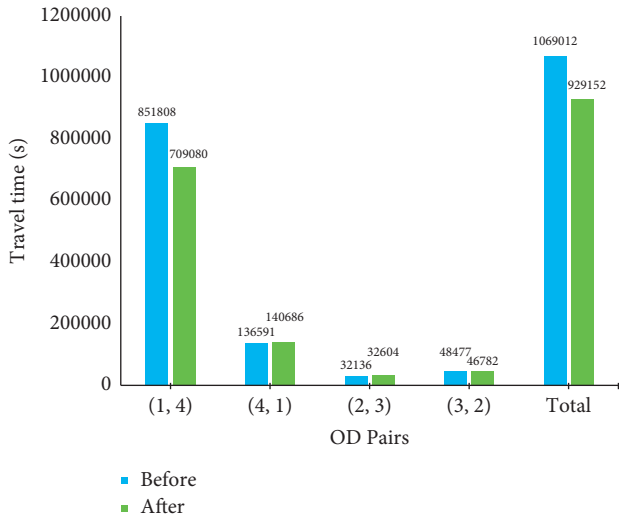

Figure 7: Total travel time of the system and between OD pairs before and after optimization.

From the perspective of the total travel time between OD pairs, although the total travel time between OD pairs (4,1) with smaller demand increased from 136591s to 140686s, and the total travel time between OD pairs (2,3) also increased from 32136s to 32604s, the travel time between OD pairs (1,4) with larger demand decreased from 851808s to 709080s, and the travel time between OD pairs (3,2) also decreased from 48477s to 46782s. The increase of total travel time between OD pairs with smaller demand is smaller, and the decrease of total travel time between OD pairs with larger demand is larger. Finally, the total travel time of the system decreases from 1069012s to 929152s, with a decrease of 13.08%, indicating that the effect of reversible lane optimization on reducing the total travel time of the system is obvious.

6. Conclusions

This manuscript established a mixed-integer bilevel programming model for reversible lane optimization, considering the influence of vehicle lane-changing on traffic

capacity which enhances the accuracy of the model, and proposed a chaotic particle swarm optimization algorithm for this model. Numerical examples verified the effectiveness of the proposed optimization scheme and its solution algorithm and showed the influences of reversible lane optimization on capacity, flow, travel time, saturation and service level of sections, route travel time between OD pairs, and total time of the system. The results showed that the reversible lane optimization can make the road network structure better match the travel demand, adjust the distribution of flow on the road network, reduce the travel time of sections in the heavy traffic flow direction, balance the saturation and service level of sections, and reduce the total travel time of the system obviously.

Beyond the above preliminary research, there are many interesting avenues for further study such as a couple of ablation studies may be added to evaluate the effects of the key parameters of the proposed method on the performance, the setting of the signal light may significantly affect the effect of the reversible lane optimization scheme, and an ongoing extension of this study is to integrate the signal control into our proposed model.

Data Availability

The data used to support the findings of this study are available from the corresponding author upon request.

Conflicts of Interest

The authors declare that there are no conflicts of interest regarding the publication of this paper.

Acknowledgments

This research work was supported by the Hunan Provincial Natural Science Foundation of China (Grant nos. 2021JJ40025 and 2019JJ50210) and Scientific Research Foundation of Hunan Provincial Education Department (Grant nos. 20A093 and 18C0859).

References

[1] X. Li and J.-Q. Sun, "Signal multiobjective optimization for urban traffic network," *IEEE Transactions on Intelligent Transportation Systems*, vol. 19, no. 11, pp. 3529–3537, 2018.

[2] C. K. Wong and S. C. Wong, "Lane-based optimization of signal timings for isolated junctions," *Transportation Research Part B: Methodological*, vol. 37, no. 1, pp. 63–84, 2003.

[3] Y. H. Jiang and L. X. Bao, "Study on setting of reversible lanes near intersection between one-way and two-way traffic," *Journal of Shanghai Jiaotong University*, vol. 45, no. 10, pp. 1562–1566, 2011.

[4] Q. Yu and R. Tian, "Research on reversal lane application method of urban road network based on the bi-level programming," *Advances in Intelligent Systems and Computing*, vol. 279, pp. 983–992, 2014.

[5] B. Wolshon and L. Lambert, *Convertible roadways and lanes: a synthesis of highway practice*, Vol. 340, Transportation Research Board National Research Council, , Washington, DC, USA, 2004.

[6] A. Golub, "Perceived costs and benefifits of reversible lanes in Phoenix, Arizona," *ITE Journal*, vol. 82, no. 2, pp. 38–42, 2012.

[7] P. Zhang, W. Li, and Y. Chang, "Reserve capacity model for urban road network with reversible lanes," *Journal of Southwest Jiaotong University*, vol. 45, no. 2, pp. 255–260, 2010.

[8] X. Li, J. Chen, and H. Wang, "Study on flow direction changing method of reversible lanes on urban arterial roadways in China," *Procedia - Social and Behavioral Sciences*, vol. 96, pp. 807–816, 2013.

[9] M. Hausknecht, T. C. Au, P. Stone, D. Fajardo, and T. Waller, "Dynamic lane reversal in traffic management," in *Proceedings of the 2011 14th International IEEE Conference on Intelligent Transportation Systems (ITSC)*, pp. 1929–1934, IEEE, Washington, DC, USA, October 2011.

[10] B. Wolshon and L. Lambert, "Reversible lane systems: synthesis of practice," *Journal Of Transportation Engineering*, vol. 132, no. 12, pp. 933–944, 2006.

[11] H. Waleczek, J. Geistefeldt, D. Cindric-Middendorf, and G. Riegelhuth, "Traffic flow at a freeway work zone with reversible median lane," *Transportation Research Procedia*, vol. 15, pp. 257–266, 2016.

[12] L. Yue, T. D. Xu, H. P. Xia, and Y. C. Du, "Reversible lane design for Shanghai world expo 2010," *Urban Transport of China*, vol. 8, no. 2, pp. 25–30, 2010.

[13] W. Y. Wang, Y. Jiang, Y. Peng, Y. Zhou, and Q. Tian, "Simheuristic method for the reversible lanes allocation and scheduling problem at smart container terminal gate," *Journal of Advanced Transportation*, vol. 2018, Article ID 1768536, 14 pages, 2018.

[14] J.-B. Sheu and S. G. Ritchie, "Stochastic modeling and real-time prediction of vehicular lane-changing behavior," *Transportation Research Part B: Methodological*, vol. 35, no. 7, pp. 695–716, 2001.

[15] G. Xiao, H. Zhang, N. Sun, Y. Chen, J. Shi, and Y. Zhang, "Cooperative Bargain for the Autonomous Separation of Trafic Flows in Smart Reversible Lanes," *Complexity*, vol. 2019, Article ID 2893732, 12 pages, 2019.

[16] L. Mao, W. Li, and P. Hu, "Design of real-time dynamic reversible lane in intelligent cooperative vehicle infrastructure system," *Journal of Advanced Transportation*, vol. 2020, Article ID 8838896, 8 pages, 2020.

[17] T. L. Magnanti and R. T. Wong, "Network design and transportation planning: models and algorithms," *Transportation Science*, vol. 18, no. 1, pp. 1–55, 1984.

[18] F. Shi, H. Y. Su, and X. Wang, "Design of reversible lanes with tidal flow on road network," *Journal of Transportation Systems Engineering and Information Technology*, vol. 15, no. 4, pp. 57–62, 2015.

[19] Z. Y. Gao, H. Z. Zhang, and H. J. Sun, "Bi-level programming models, approaches and applications in urban transportation network design problems," *Journal of Transportation Systems Engineering and Information Technology*, vol. 4, no. 1, pp. 35–44, 2004.

[20] H. Z. Zhang and Z. Y. Gao, "Optimization approach for traffic road network design problem," *Chinese Journal of Management Science*, vol. 15, no. 2, pp. 86–91, 2004.

[21] T. Lu, Z. Yang, D. Ma, and S. Jin, "Bi-level programming model for dynamic reversible lane assignment," *IEEE Access*, vol. 6, pp. 71592–71601, 2018.

[22] Z. Di and L. X. Yang, "Reversible lane network design for maximizing the coupling measure between demand structure and network structure," *Transportation Research Part E: Logistics and Transportation Review*, vol. 141, p. 102021, 2020.

[23] L. Conceio, G. Correia, and J. P. Tavares, "The reversible lane network design problem (RL-NDP) for smart cities with automated traffic," *Sustainability*, vol. 12, no. 3, p. 1226, 2020.
[24] J. R. Cai, Z. X. Huang, and L. X. Wu, "Optimization of reversible lane based on autonomous vehicles," *Journal of Highway and Transportation Research and Development*, vol. 35, no. 7, pp. 136–150, 2018.
[25] X. B. Yang, N. Zhang, and Y. Guan, "Behavior based analysis of the relationship between expressway capacity and number of lanes," *China Civil Engineering Journal*, vol. 43, no. 10, pp. 104–110, 2009.
[26] X. Li and J.-Q. Sun, "Studies of vehicle lane-changing dynamics and its effect on traffic efficiency, safety and environmental impact," *Physica A: Statistical Mechanics and Its Applications*, vol. 467, no. 1, pp. 41–58, 2017.
[27] X. B. Yang and N. Zhang, "Mathematical analysis of effects of lanes' number on expressway capacity," *Journal of Wuhan University of Technology*, vol. 32, no. 4, pp. 603–606, 2008.
[28] W. Wang and X. C. Guo, *Traffic engineering*, Vol. 156, Southeast University Press, Nanjing, China, 2009.
[29] H. Karshenas, R. Santana, C. Bielza, and P. Larranaga, "Multiobjective estimation of distribution algorithm based on joint modeling of objectives and variables," *IEEE Transactions on Evolutionary Computation*, vol. 18, no. 4, pp. 519–542, 2014.
[30] S.-Y. Wang and L. Wang, "An estimation of distribution algorithm-based memetic algorithm for the distributed assembly permutation flow-shop scheduling problem," *IEEE Transactions on Systems, Man, and Cybernetics: Systems*, vol. 46, no. 1, pp. 139–149, 2016.
[31] F. Zhou, J. H. Wu, Y. Xu, and C. Yi, "Optimization scheme of tradable credits and bus departure quantity for travelers' travel mode choice guidance," *Journal of Advanced Transportation*, vol. 2020, Article ID 6665161, 8 pages, 2020.
[32] W. Shi, W.-N. Chen, Y. Lin, T. Gu, S. Kwong, and J. Zhang, "An adaptive estimation of distribution algorithm for multipolicy insurance investment planning," *IEEE Transactions on Evolutionary Computation*, vol. 23, no. 1, pp. 1–14, 2019.

Hindawi
Journal of Advanced Transportation
Volume 2022, Article ID 1604303, 17 pages
https://doi.org/10.1155/2022/1604303

Research Article

Vehicle Routing Simulation for Prediction of Commuter's Behaviour

Przemysław Szufel[1], **Bartosz Pankratz**[1], **Anna Szczurek**[1], **Bogumił Kamiński**[1] and **Paweł Prałat**[2]

[1]*SGH Warsaw School of Economics, Warsaw, Poland*
[2]*Ryerson University, Toronto, Canada*

Correspondence should be addressed to Przemysław Szufel; pszufe@sgh.waw.pl

Received 13 January 2022; Revised 26 February 2022; Accepted 31 March 2022; Published 25 April 2022

Academic Editor: Elżbieta Macioszek

Copyright © 2022 Przemysław Szufel et al. This is an open access article distributed under the Creative Commons Attribution License, which permits unrestricted use, distribution, and reproduction in any medium, provided the original work is properly cited.

We propose a multiagent, large-scale, vehicle routing modeling framework for the simulation of transportation system. The goal of this paper is twofold. Firstly, we investigate how individual and social knowledge interact and ultimately influence the effectiveness of resulting traffic flow. Secondly, we evaluate how different discrete-event simulation designs (delays vs. queuing) affect conclusions within the model. We present a new agent-based model that combines the efficient discrete-event approach to modeling with the intelligent drivers who are capable to learn about their environment in the long-term perspective from both, individual experience, and widely available social knowledge. The approach is illustrated as practical application to modeling commuter behavior in the city of Winnipeg, Manitoba, Canada. All simulations in the paper are fully reproducible as they have been carried out by utilizing a set of opensource libraries and tools that we have developed for the Julia programming language and that are openly available on GitHub.

1. Introduction

Traffic flow and congestion models have been researched since '30s (eg., by Greenshields [1]). Nowadays, they can be classified by the level of detail considered into 4 groups: (1) macroscopic, (2) microscopic, (3) submicroscopic, and (4) mesoscopic [2–5].

Macroscopic traffic models concentrate on the relationships among traffic flow attributes such as flow, density, or speed [2, 6]. In those models, individual vehicles are not modelled but aggregated variables such as the average density or the average flow are analyzed [2]. The family of macroscopic models includes kinematic wave models [7] and ultidimensional fundamental d iagram [8, 9]. With macroscopic algorithms, it is difficult to compare the results from the model with real life data [10].

Microscopic traffic models simulate single vehicle-driver units focusing on the dynamic model variables representing microattributes such as the position or velocity of a single vehicle (e.g., basic cellular automaton Nagel and Schreckenberg [11] model). Perfect examples of microapproach are stimulus-response models [12], where driver is reacting (accelerating or decelerating) to three main stimuli: her own velocity, spacing, and relative velocity with respect to the leader. Microscopic models' calibration and validation can be challenging [10].

Submicroscopic traffic models include more details compared to microscopic ones: not only each vehicle is modelled individually but also functions inside the vehicle [3, 13], such as driver's psychological reactions (e.g., response to traffic lights) or vehicle performance (e.g., acceleration or braking curves). Submicroscopic approach can be problematic when it comes to model's effectiveness and the measurement and calibration of the thresholds (e.g., acceleration threshold) [13].

Mesoscopic model aggregation level is in between of those of microscopic and macroscopic models [14]. Classical mesoscopic approach describes aggregated vehicle behaviour

by a specific probability distribution function, while single vehicle behaviour rules are defined individually [2],e.g., gas-kinetic models [15, 16]. Finally, hybrid mesoscopic models appeared most recently: they combine microscopic and macroscopic approaches by modeling the traffic at different aggregation levels simultaneously [2]. Hybrid approach applies the microscopic model to areas of specific interest resulting in more detailed outcome (e.g., city centre), while simulating its surrounding network with macroscopic model guarantees fast results [10].

Naturally, there are some limitations concerning traffic flow models. According to Daiheng [17], they can be classified into four categories: (1) lack of model consistency, (2) lack of model flexibility to include driver heterogeneity, (3) lack of model capability to foresee near future, and (4) lack of model expandability beyond one-dimensional traffic. The first limitation describes the inconsistency between model outcome and observed traffic which may arise, e.g., in macroscopic models not taking into consideration individual drivers' behaviour [10, 17]. The next limitation focuses on driver heterogeneity such as different decision factors or different decision rules. Then, there is a "look-ahead" drivers' capability which affects decision- making process concerning near future. Finally, there are lots of successful one-dimensional traffic models, but still there is a gap left for an integrated traffic flow model incorporating a few traffic dimensions at once, such as car following, lane changing, and gap acceptance. All these limitations along with some improvements are widely discussed in Daiheng [17]. Drivers' heterogeneity in terms of agents' knowledge is the limitation that can be addressed by the model introduced in this paper.

An important long-term determinant of behaviour of drivers who are capable of planning their travels is based on what they learn from their previous experience and beliefs about the traffic density. On the microlevel of traffic network, modeling the question is how the information's spread might improve the effectiveness of traffic flow by increasing its smoothness, by optimizing the car speed in platoon, giving opportunity for the cars to avoid traffic congestion [18, 19], or how to design and implement the vehicle-to-vehicle communication system for the intelligent cars [20, 21] in order to optimize their behaviour in the traffic network. On the other hand, the problem of the macroscopic and long-term relations between knowledge and the structure of traffic flows might be crucial to better understand how individual decisions of drivers (or autonomous vehicles) contribute to the emergence of traffic congestion and how to optimize such systems. For example, by knowing how drivers react to changes in traffic network and how fast they adapt to new conditions, better solutions for planning the roadworks might be provided.

The subject of learning and adaptive behavior itself is a well-known concept in social sciences [22]. The idea of the modes of learning, individual and social one, was used to explain such different phenomena as pricing on the markets with asymmetric information and uncertainty [23, 24], organizational learning, and trade-off between the exploration of new possibilities and the exploitation of old certainties [25], or even more widely, the evolution of the culture and development of new inventions [26–28]. The problem of social learning is the most interesting part of those research studies. It appears to be more advantageous in comparison with individual one, because it allows to avoid the costs of trial-and-error learning and also reduces the uncertainty of the explored problem, but it turns out that the outcome of the social learning depends strictly on the learned subject. In cases when agents learn about the objects, which are independent and not varying in time, such as the quality of the good they are interested in buying in Izquierdo and Izquierdo [24] model, social learning turns out to be extremely effective. Using it decreases uncertainty, and in the extreme case, it might reduce the problem to the market with the perfect information case. However, when the environment is changing and nonuniform, relying on social knowledge is prone to error and may lead individuals to learn inappropriate or outdated information (Rogers, 1988; [28]).

The aim of this paper is twofold. Firstly, we investigate how individual and social knowledge of intelligent drivers interact and ultimately influence the effectiveness of resulting traffic flow. Secondly, we evaluate how different discrete-event simulation designs (delays vs. queuing) affect conclusions within the model. We present a new agent-based model that combines the efficient discrete-event approach to modeling with the intelligent drivers who are capable to learn about their environment in the long-term perspective from both, individual experience and widely available social knowledge.

Traffic congestion has been an issue in many cities around the world; hence, traffic flow modeling and prediction is one of the science's challenges. Moreover, infrastructure improvements tend to be very expensive; thus, it is crucial to evaluate its impact on the traffic flow beforehand. This paper introduces a computer simulation model as it proves to be exceptionally useful and a low-cost method which enables in-deep traffic flow analysis. Our model is composed of intelligent agents reflecting personalized behaviour of real drivers. A concept of "intelligent drivers" has already been investigated in several papers (e.g., Kesting et al. [29]; Camponogara and Kraus [30], or Ehlert and Rothkrantz [31]) with the adaptive cruise control (ACC) model as the first driver assistance system having the potential to impact real traffic flow environment [29] by automatically adapting car acceleration to different traffic conditions. Treiber et al. [32] proposed a simple microscopic ACC model of intelligent drivers that despite its simplicity (the model uses only a few intuitive parameters) yields realistic traffic flow collective dynamics along with drivers' acceleration and deceleration behaviour. We proposed a model composed of intelligent drivers as it helps to capture real traffic flow characteristics by taking into consideration human reflexes and behaviour with such parameters as drivers' acceleration strategy, breaking reactions, line changing decisions, or agents' heterogeneity represented by individual sets of parameters for each driver (Kesting, Treiber, and Helbing [33]; Kesting et al. [29]; Kesting, Treiber, and Helbing [34].

In real world, drivers' behaviour characteristics could fluctuate in time as drivers are able to learn and adapt to changing traffic environment due to human ability to process and analyze the available information. Automatic learning techniques seem to be very promising in boosting traffic models efficiency [30]. Indeed, a number of traffic flow models incorporating reinforcement learning have already been introduced, such as Camponogara and Kraus [30]; Wiering [35]; Balaji, German, and Srinivasan [36]; Ehlert and Rothkrantz [31]; or Logi and Ritchie [37]. Model proposed by this paper also uses reinforcement-learning algorithms since knowledge-based approach proves that personal and social knowledge highly influence traffic flow environment as agents make their traffic-decisions based on the information they have. Adaptive and flexible intelligent agents could incorporate into a model various types of personalized driving styles causing the simulated vehicles behaviour to be realistic which in turn makes it possible to investigate the interactions between drivers in the traffic flow ecosystem [31]. In this paper, we analyze how individual and social knowledge interact and influence the traffic flow model. Both types of information has already been researched but in another context: e.g., Camponogara and Kraus [30] studied personal knowledge by developing a traffic network model as a distributed, stochastic game in which agents solve reinforcement-learning problems;each driver seeks a policy maximizing his reward. Then, Wiering [35] analyzed both personal and social knowledge by introducing "co-learning": in their model, there are two types of intelligent agents: vehicles and traffic lights, both using reinforcement-learning in order to optimize their behaviour by minimizing the same value function. Finally, Balaji, German, and Srinivasan [36] proposed a traffic signal control model with reinforcement-learning agents capable of interacting with each other in order to not only reduce the overall travel time delay but also to increase vehicles' mean speed. Their model proved that agents' adaptability and information exchange resulted in higher drivers' ability to foresee as well as a reduced congestion. On the other hand, the model introduced in this paper in terms of knowledge strictly focuses on the impact of various levels of agents' ability to learn, both personal and social, on the overall model outcome.

We investigated two types of discrete-events simulation designs: model with queuing and model with delays. Each road segment can be described by two main parameters: its physical capacity and the flow rate [38]. As the capacity of each route segment is limited, it is crucial to decide what happens when agents are not able to enter a specific route when it reaches its maximum capacity level. In such situations, we considered two scenarios: in a queue-based approach, an agent must wait on its current edge until there is some space for its vehicle on a congested route segment. In a delay-based approach, it is always allowed to enter a congested road segment but with minimum possible vehicle speed. The first scenario reflects authentic traffic flow network, but it is very computationally expensive while the second one is simplified thus less realistic. This paper answers the question whether it is possible to replace an accurate queuing model with a less complicated delay-based approach, without losing model's generality. Both above approaches are discussed in more details in section 2. In order to compare those scenarios, we have implemented a computational framework for simulation of real-world transportation systems. The model as well as the simulation framework have been released as Open Source on GitHub1. Our implementation makes it possible to compare the discrete-event queuing mechanism as well as a simpler (and hence faster to run) queuing version.

The remainder of this paper is organized as follows. In Section 2, a description of the model is provided. In particular, the network representation, drivers' characteristics, and the mechanisms of capturing the traffic dynamics in both perspectives are presented. Additionally, we discuss the software architecture used to build this model and compare it to other options. Section 3.1 describes the conditions of the application of OpenStreetMapXDES.jl on a realistic traffic network (the model is calibrated for Winnipeg, Canada, but it can be used for other cities). In Section 3.2, results of the simulations are provided. Agents' behaviour is explained, and also two architectures described above are compared in terms of the execution speed as well as the quality of produced outcome. Finally, Section 4 concludes and presents the directions of future development of our model.

2. Traffic Modeling and Simulation on Networks

2.1. Simulation Environment and Behaviour of Agents. We consider a population of N agents living in a city represented by a weighted, directed graph $G = (V, E)$. Each node $n \in V$ in this graph serves as a depiction of a single intersection in the city road network and each (directed) edge $e^{(i)} = (a^{(i)}, b^{(i)}) \in E, i \in \{1, 2, \ldots, |E|\}$ represents a road segment from intersection $a^{(i)} \in V$ to intersection $b^{(i)} \in V$, $a^{(i)} \neq b^{(i)}$. Edge $e^{(i)}$, $i \in [|E|] = \{1, 2, \ldots, |E|\}$ is described by the following four parameters:

(1) $d^{(i)}$ – segment *length* expressed in meters

(2) $v_{\max}^{(i)}$ – *speed limit* on this particular segment expressed in meters per second

(3) $\rho_{\max}^{(i)}$ – segment *maximum density*, that is, the maximum number of cars capable to travel through the specific segment at the same time calculated as follows:

$$\rho_{\max}^{(i)} = \frac{d^{(i)} c^{(i)}}{\ell}, \tag{1}$$

where $c^{(i)}$ is a number of lanes available on this particular segment and ℓ is some fixed parameter representing the average length of the car.

(4) $\tau_0^{(i)}$ – *driving time* corresponding to the optimal situation when agents are able to travel with a velocity equal to the speed limit on this particular segment; that is, $\tau_0^{(i)} = d^{(i)}/v_{\max}^{(i)}$.

The main goal of this model is to study the repetitive, everyday behaviour of citizens of a large city that are

commuting to and from work and its impact on traffic on the network of roads. The way how the agents are defined emerges from this assumption. Three basic parameters that are used to describe them are $n_{\text{home}} \in V$ and $n_{\text{work}} \in V$ which are the nodes in graph G associated with home and work, respectively, workplace of the particular agent, and route of k edges

$$s = \left\{e^{(1)}, e^{(2)}, \ldots, e^{(k)}\right\}, \tag{2}$$

which is a sequence of incident edges visited during the agent's trip between n_{home} and n_{work}. (It is noted that s, n_{home}, and n_{work} are specific for each agent but in order to keep the notation simple we do not include it).

In order to simplify the model, we assume that agents are travelling only in one direction (from home to work) and that they are not driving through any additional points of interest associated with other daily activities such as driving their children to school or going shopping. Hence, we are essentially modeling the morning traffic. However, an analogous approach can be used to model the afternoon traffic. If we take the assumption that people work during fixed hours (e.g., 9am–5pm), the main difference between the morning and afternoon traffic is that in the morning many people try to arrive to work at the same time, and in the afternoon traffic, people depart at roughly the same time. Assuming homogeneous depart times and no side activities, the afternoon traffic would be symmetric to the morning traffic. However, we note that the framework described in this paper allows to easily extend the discussed model by depart time heterogeneity and after-work activities. In this paper, we focus only on the morning traffic which is more condensed.

As mentioned previously, we are interested in studying a long-term traffic dynamics. Hence, agents must be able to change their behaviour during the simulation's span. In every iteration t (representing one workday), $t \in [T]$, they adjust their routes to find the most efficient ones. In the model, we assume that the agent is interested in covering the route from n_{home} to n_{work} as fast as possible. However, the times of driving by route segments are affected by choices made by the other agents. The relationship between the number of cars on a given segment $e^{(i)}$ and the speed of a new car entering this particular part of the road is calculated by (the variant of) the Lighthill–Whitham–Richards equation (Lighthill and Whitham, 1955; [9]):

$$v^{(i)} = \left(v_{\max}^{(i)} - v_{\min}\right) \cdot \max\left(\frac{1 - \rho^{(i)}}{\rho_{\max}^{(i)}}, 0\right) + v_{\min}, \tag{3}$$

where $v_{\min}$ is a fixed, the lowest possible velocity equal to 1 mps, and $\rho^{(i)}$ is the traffic density on edge $e^{(i)}$. The relation between traffic congestion and velocity calculation mechanism will be further described in the following section focused on implementations of discrete-event simulations in OpenStreetMapXDES.jl framework. In particular, this approach will be compared against the queuing-based approach.

Agents are internalizing the differences between the expected driving time and the true current driving time on the particular road segment by using a simple temporal difference learning mechanism [39, 40]. Their beliefs about the expected driving times are based on the previous experience and are represented for the day t by $\widehat{\tau}_t^{(i)}$ for each $e^{(i)} \in E$. After visiting a particular edge $e^{(i)}$ and observing the actual travelling time $\tau_t^{(i)}$, they update their expectations as follows:

$$\widehat{\tau}_{t+1}^{(i)} = \left(1 - \lambda_{\text{ind}}\right)\widehat{\tau}_t^{(i)} + \lambda_{\text{ind}}\tau_t^{(i)} = \widehat{\tau}_t^{(i)} + \lambda_{\text{ind}}\left(\tau_t^{(i)} - \widehat{\tau}_t^{(i)}\right), \tag{4}$$

where $\lambda_{\text{ind}} \in [0, 1]$ is a parameter describing agent's learning rate on the individual level that controls the way how experience influences agent's behavior (it is noted that we consider only a single global λ_{ind}; however, our approach could be further extended by considering heterogeneity of λ_{ind} across the population). In particular, if $\lambda_{\text{ind}} = 0$, then agents do not learn at all which means that they will expect to drive a given segment of road in the time $\tau_0^{(i)}$ that does not include their experience with the traffic. On the other hand, if $\lambda_{\text{ind}} = 1$, then agents will be extremely myopic and consider only the most recent information about the driving time. In the model, the initial belief values are set to $\tau_0^{(i)}$; that is, travel times correspond to the situation where the is no congestion.

In real life situations, people make their decisions and assumptions about the surrounding world not only based on their experience but also from external sources such as various media, Internet, and communication with other people. Knowledge accumulated from all these sources will undoubtedly influence their decisions that, in turn, affect the commuting behaviour.

These mechanisms are implemented in the model in a rather simple but an effective way. For each edge, information about the driving times is collected during the simulation span. At the end of each day, the average driving times are calculated for all edges in graph $\tau_0^{(i)}$. Then, all agents are again adjust their expectations:

$$\widehat{\tau}_{t+1}^{(i)} = \widehat{\tau}_t^{(i)} + \lambda_{\text{soc}}\left(r\overline{\tau}_t^{(i)} - \widehat{\tau}_t^{(i)}\right), \tag{5}$$

where $\overline{\tau}_t^{(i)}$ is the average driving time on edge $e^{(i)}$ in day t, $\lambda_{\text{soc}} \in [0, 1]$ is a social learning rate, and r is a perturbation parameter, randomly selected with the expected value equal to 1. Hence, the expected driving time is a linear combination of what the agent observed and the population wide (perturbed) value. For simplicity, in our model, we assume no perturbation, that is, $r = 1$.

The social learning rate controls how much the information from the environment influences agents. If $\lambda_{\text{soc}} = 0$, then agents do not use their knowledge from outside sources at all. On the other hand, if $\lambda_{\text{soc}} = 1$, then agents only use the most recent information when planning their departure trip and time for the next day. Finally, let us point out that people are usually not able to obtain perfect information about their surroundings, and almost always it is somehow disrupted; random parameter r is a way of implementing and controlling this behavior.

The agent's belief update mechanism presented in (4) and (5) can be further combined to include a single model, both the individual and societal learning capabilities:

$$\widehat{\tau}_{t+1}^{(i)} = \widehat{\tau}_{t}^{(i)} + \lambda_{\text{ind}}\left(\tau_{t}^{(i)} - \widehat{\tau}_{t}^{(i)}\right) + \lambda_{\text{soc}}\left(r\overline{\tau}_{t}^{(i)} - \widehat{\tau}_{t}^{(i)}\right). \quad (6)$$

At the end of the day, when all agents have finished their trips and have updated their beliefs, they need to plan the next day. They possibly update their routes by choosing the fastest route (based on their current, adjusted expectations about driving times): $(e^{(1)}, e^{(2)}, \ldots, e^{(m)})$ (m is the is the number of edges in the route). Then, they also need to choose a proper departure time. For a given agent j, her departure time $D_{t+1}^{(j)}$ in iteration t is equal to

$$\tau_{t+1}^{(j)} = 0 - \sum_{l=1}^{m} \widehat{\tau}_{t}^{(l)}. \quad (7)$$

That is, we assume that all agents start their workday on the same hour, e.g., 9 a.m., which is represented in the model as "time-zero." Again, this assumption can be easily lifted within the analyzed framework by assigning heterogeneous work start times to the agents. However, in order to focus on the information flow within the travelling agent population, in this paper, we only consider a single cohort of agents.

Once all parameters are updated, single iteration ends and the model moves to the next day. In the next section, we provide more details about the routing algorithm and the discrete-event simulation mechanism that controls the flow of agents during a single day.

We note that the above (7) combined with (6) actually means that at the end of each day, agents make a decision on their departure time plans on the base of their experience and the available social knowledge (for example from an online maps routing application). This scenario happens in everyday life—people need to decide in the evening at what time to get up in the morning to arrive to work on time. Our simulation model aims to answer the question how the individual and societal knowledge affects the optimality of agents' decisions.

2.2. Vehicle Routing Mechanisms. Once the agents have their beliefs about the travel times, the actual vehicle movement is simulated. Following the solutions presented in Thulasidasan and Eidenbenz [38], we based our routing mechanism on the implementation of A^* search algorithm [41]. We consider two scenarios:

(i) discrete-event-simulator with vehicle queues at the graph edges

(ii) discrete-event-simulator with variable time delays at the graph edges

Both scenarios are discussed below.

2.2.1. Discrete-Event Model with Queuing. An essential part of building a discrete-event simulation model is defining proper events; if they are too specific, then the system updates too often and the model starts to resemble the continuous time simulation where the model is efficient but at the expense of loss of the accuracy. A single event in time $\mathbb{T}$ represents the moment of transition between two edges, segments of the route between two intersections. The agent cannot change the direction of the trip while it is driving on such defined part of the road, it can only drive forward. It means that all important decision regarding agent's trip must be made when it approaches the intersection.

Another important question regarding such traffic model is how to implement the mechanism of the creation of traffic congestion. The capacity of the route segments is finite and when it reaches its maximum level new agents that cannot enter such edge. In this scenario, traffic flow will be disturbed and congestion will propagate on the preceding edges. In this section, we describe the basic form of the traffic congestion diffusion in the queuing version of the model. Later, insection 2.2.2, we show a simplified version of this mechanism where queuing is replaced with reducing speed on the congested segment of the road.

We take a standard approach in discrete-event simulation models where the control flow is based on the simulation clock, which stores the time of the next event (here approaching the next intersection) for all agents in the model [42]. When the event at the time $\mathbb{T}$ is triggered and proper agent is brought forth, it tries to enter the next segment $e^{(i)}$ of its predefined route. When the current density on this edge $\rho_t^{(i)}$ is smaller than its maximal possible density $\rho_{\max}^{(i)}$, the agent is able to enter this segment. Otherwise, the agent must wait on its current edge $e^{(i-1)}$ until the traffic on $e^{(i)}$ declines or the agent changes its plans and travel by another edge $e^{(j)}$ reachable from the intersection the agent currently waits at.

An agent makes her choice by randomly selecting between $e^{(i)}$ and all the edges available from the particular intersection with densities smaller than their corresponding maximums; the decision is changed by an agent only when a new route can be entered immediately. When an agent needs to wait, it will do it on the segment that has previously selected as the part of the fastest route, and it will be added to the waiting list of edge $e^{(i)}$ with a priority corresponding to the current event time $\mathbb{T}$.

The process of crossing an intersection by an agent triggers the following chain of events. Firstly, the agent moves from edge $e^{(i-1)}$, so if there is another driver waiting to enter $e^{(i-1)}$ on her waiting list, it is permitted to do so. Then, if the density on $e^{(i-1)}$ allows another driver waiting in line to enter it, it will also enter $e^{(i-1)}$. Otherwise, the agent will randomly select the next edge in the same manner as described above. The procedure will continue until the first of the waiting agents will decide to stay in the queue or all of them will be removed from the waiting list of $e^{(i-1)}$.

During the update of the queue associated with $e^{(i-1)}$, the same procedure is employed on edges preceding it and then on their predecessors and so on. In a single event, all segments in the traffic network might be recursively updated, either propagating or reducing the traffic congestion in a model, depending on decisions of agents in previous links of the chain.

In a case when an agent is able to travel by some segment, its driving time $\tau^{(i)}$ is calculated according to (3). Then, the agent updates her beliefs according to (4), adjusting it to the time it spends in the queue: $\tau^{(i)} = \tau^{(i)} + \tau_{\text{waiting}}$. Finally, the internal simulation clock is updated to the next event,

indicating the moment when the agent ends driving by newly entered edge. Algorithm 1 describes the behaviour of the agent.

2.2.2. Discrete-Event Model with Delays. Mechanism presented in the previous section was designed to resemble the way how the traffic congestion behaves in the real life situations. However, capturing the full queuing mechanism is very computationally expensive,especially where one wants to perform population modeling in a 1 : 1 scale. One of the questions stated in this paper is whether it is possible to replace the discussed queuing model with a simplified approach, without losing model's generality. In this section, we focused on describing such alternative way of modeling traffic on a large scale.

Basic behaviour of this routing algorithm is similar to the previous one. The whole simulation is controlled by the clock with values of next event for all agents in the population. However, this time when agent is called and tries to enter a new edge $e^{(i)}$, there are no additional conditions for entering the edge, that is, she can always do it. Subsequently, agents' driving time $\tau^{(i)}$ is calculated according to (3) and when the density $\rho_t^{(i)}$ exceeds $\rho_{\max}^{(i)}$, then the speed of the agent on this segment of the route is reduced to $v_{\min}$. Algorithm 2 explains the way the model works. Finally, let us note that $v_{\min}$ is the smallest possible speed in the network and it is designed to correspond with the expected velocity in a heavy traffic jam.

2.3. Implementation Notes. The code presented in this paper is based on Julia programming language [43]. The discrete-event-simulation engine is available at OpenStreetMap XDES.jl3 library. We have implemented the routing mechanism in the OpenStreetMapX.jl library.4 For ad-hoc data visualization, a compatible Julia library OpenStreetMap XPlot.jl5 has been developed. All the software is Open Source and freely available at GitHub.

There are other vehicle simulation frameworks that support different traffic simulation models with main simulators including MATSim, FastTrans [38], SUMO [44], or TRANSIMS [45]. MATSim (Multi-Agent Transport Simulation) is a framework for implementing large-scale transport simulation, considering different modules such as demand, supply, or control of traffic systems which all can be combined or used standalone (Allan and Farid [46]. SUMO (Simulation of Urban Mobility) vehicles can move freely (vehicle behavior is taken into consideration, e.g., lane changes), and the collisions between them along with traffic accidents are simulated by Saidallah and El Fergougui and Elbelrhiti [47]. Finally, TRANSIMS (Transportation Analysis and Simulation System) is an integrated tool based on a cellular automaton concept that allows to conduct transportation analysis, simulation, and dynamic traffic assignment within an integrated development environment Saidallah and El Fergougui and Elbelrhiti [47].

However, the existing solutions have a few drawbacks from our point of view. Firstly, they are written in verbose programming languages with sharp learning curve: Java (MATSim) or *C++* (SUMO and TRANSIMS). On the other hand, Julia allows the code to have around 4 times less lines of code6 (compared to *C++* or Java) while maintaining similar execution speed what makes it specially useful for the numerical computing. Secondly, our Julia based-framework takes a more loose-coupled generic approach (rather than rely on some routing batch files like existing frameworks do) and makes it possible to fully control and program the behavior of each individual car in the model. This makes it possible to simulate in real time the adaptation of agents to the changing environment. Thirdly, the Julia language has an in-built support for distributed computing, and hence, a Julia simulation can be easily run on a large cluster or supercomputer without using external tools and libraries (such as Spark framework for Java or MPI for *C++*). Last but not least, it should be noted that the numerical performance of the discussed solution is very high—finding a customized route for a single agent can take as little as around 200 ns on a single CPU core on a modern machine.

3. Experiments and Results

3.1. Experiment Design. As a sample data set for our use cases, we have selected Winnipeg Metropolitan Area (WMA) in Canada having a total population of around 840,000 people. This region is isolated from other large cities in Canada with Regina (SK) over 500 km away as its closest neighbour (assuming cities with a population of at least 200,000). In Winnipeg, there are no freeways in the city but there is a 90 km beltway called Perimeter Highway around Winnipeg which reduces traffic volumes within the city by offering an alternate route for those who do not need to stop in the centre. These features classify Winnipeg as a city dominated by inner-city traffic (residents, commuters) and almost no transit traffic. Lack of freeways within the center of Winnipeg makes it also more difficult for commuting drivers in the city center to escape from traffic into a beltway. Since the only way to commute around Winnipeg area is a car and there is no transit traffic, a very significant portion of traffic in Winnipeg on workdays is home-to-work-to-home daily commute. This makes it possible to use census data along with business locations to estimate commute for a synthetic population of commuters. However, a similar approach could be used for other cities.

The WMA census data are available for 1,229 dissemination areas (DA, presented at Figure 1), small geographic regions in Canada, each comprising of around 1, 000 citizens.

Three datasets were used in the simulation experiment: (1) *Demographic data* (Canadian statistical office): socio-economic and demographic data of commuters aggregated to dissemination areas levels (data per each DA), (2) *Home-work flow matrix*: that represents an estimated number of people living in a given Winnipeg DA who are employed at a location outside their DA, and (3) *DA centroids*: geographic coordinates of centroid of each DA. The data sources include Winnipeg Open Data Portal (https://data.winnipeg.ca/), and data provided thanks to the courtesy of the Environics Analytics, Canada.

The starting location for an agent is being selected at random with probability weighted by the working population

```
while event_schedule ≠∅ do
  𝕋 = min_𝕋 (event_schedule)
  randomly select an agent assigned to the event at the time 𝕋.
  if ρ_𝕋^(i) + 1 ≤ ρ_max^(i) then
    remove agent from its previous edge cars count: C(e^(i−1))←C(e^(i−1)) − 1.
    add agent to e^(i) cars count: C(e^(i))←C(e^(i)) + 1.
    calculate agent driving time τ^(i) from eq. 3
    update agent beliefs τ̂^(i) from eq. 6
    update e^(i−1) waiting list
    if e^(i) is agent final edge then
      delete event_schedule  agent .
    else
      event_schedule[agent] = 𝕋 + τ^(i).
    end if
  else
    available_edges ← []
    insert e^(i) into available_edges
    for e^(j) in edges reachable from e^(i−1) do
      if ρ_𝕋^(j) + 1 ≤ ρ_max^(j) then
        insert e^(j) into available_edges
      end if
    end for
    randomly select edge e* form available_edges
    if e* = e^(i) then
      add agent to e^(i) waiting list
    else
      start driving by edge e*.
    end if
  end if
end while
```

Algorithm 1: Routing with implemented queuing mechanism.

```
while event_schedule ≠∅ do
  𝕋 = min_𝕋 (event_schedule).
  select agent assigned to the event 𝕋.
  remove agent from its previous edge cars count: C(e^(i−1))←C(e^(i−1)) − 1.
  add agent to e^(i) cars count: C(e^(i))←C(e^(i)) + 1.
  calculate agent driving time τ^(i) from eq. 3
  update agent beliefs τ̂^(i) from eq. 6
  if e^(i) is agent final edge then
    delete event_schedule [agent].
  else
    event_schedule[agent] = 𝕋 + τ^(i).
  end if
end while
```

Algorithm 2: Routing with delayed driving time.

travel to work by car as driver size of a given dissemination area. Destination location is chosen using the probabilities calculated based on *Home-work flow matrix*. In both cases, selected point is the centroid of specific DA or the closest point on the boundary of study area (see Figure 2).

Table 1 presents values of fixed parameters in the experiment. In every simulation run, both λ_{ind} and λ_{soc} are selected by grid search from interval $[0, 1]$ with step 0.05. Then, the simulation is running twice, independently for both implemented queuing mechanisms. Each simulation run finishes by aggregating the statistics on the population level. The procedure is repeated 441 times for different pairs of λ_{ind} and λ_{soc}.

3.2. Results. In this section, we focus on describing the output of both types of simulation presented. At first, the comparison between model with implemented queuing and its counterpart

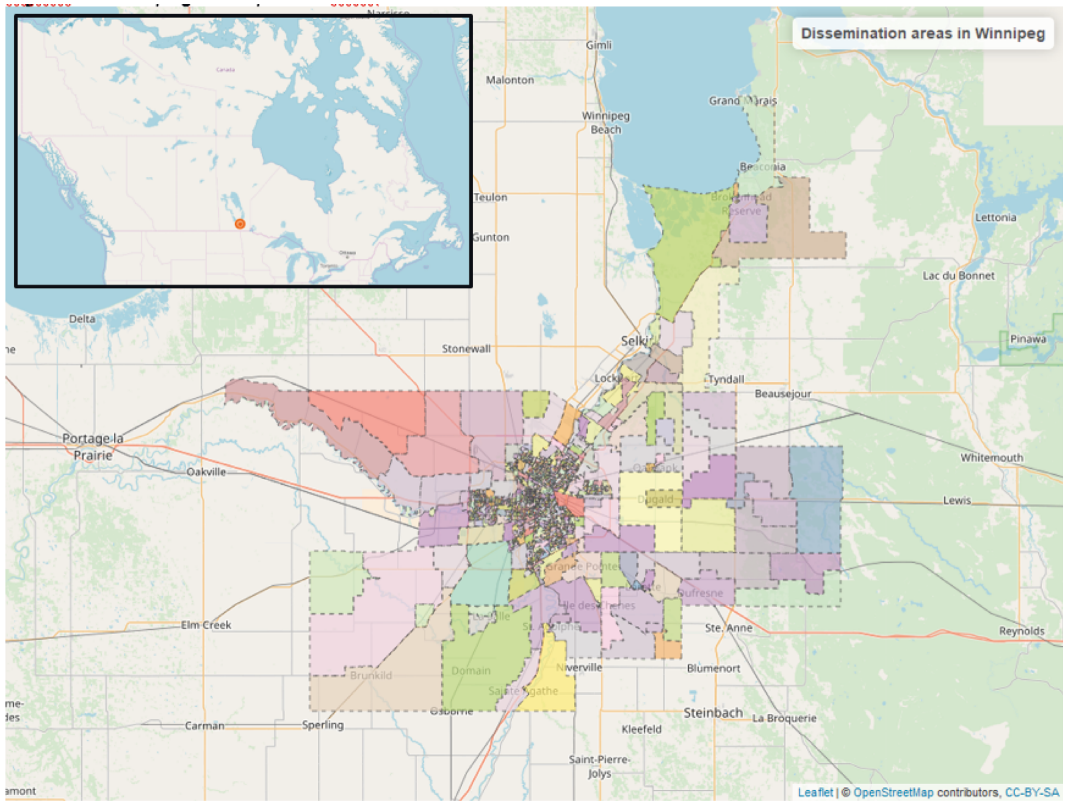

Figure 1: Winnipeg DAs spatial deployment.

Figure 2: Center of Winnipeg that has been used for simulation experiments (the size of the simulated area amounts to 104 square kilometers or 40 square miles).

method simplified by introducing delays of the driving time on clogged edges is provided. Then, we move to describing the obtained results based on provided statistics in order to better understand the implications of the implemented learning on the traffic system in a longer perspective.

Table 1: Values of fixed parameters in experiment.

Parameter	Description	Value
$\|V\|$	Number of vertices (nodes) in graph	5402
$\|E\|$	Number of edges in graph	8711
N	Size of agent's population	20000
T	Number of simulated days	100
ℓ	Average length of a car (in meters)	5

The analysis of the expected delays brings another important observation about the agent's behaviour. We can see from Figure 3 that agents are able to internalize the experience and knowledge about the traffic and adjust their departure times accordingly to increase the chance to arrive on time. On average, agents arrive at workplace significantly earlier than they are expected to, which shows that they not only start to travel at the proper time but also learn to keep a secure margin in case of ending in traffic jam. This result is in accordance with results of Cao et al. [48].

The most interesting findings come from the analysis of number of changed routes and expected driving times for different combinations of learning rates. At first glance, those results might be counter-intuitive; it turns out that the myopic behaviour of agents turns out to be a better solution in terms of the overall well being of the population (in a long-term) than a case when agents are able to use the signals from the environment in their decision processes. It is especially surprising in case when λ_{soc} is equal to 1. In such scenario, agent is basically relying on a navigation application (e.g. mobile phone app) to plan the trip and departure

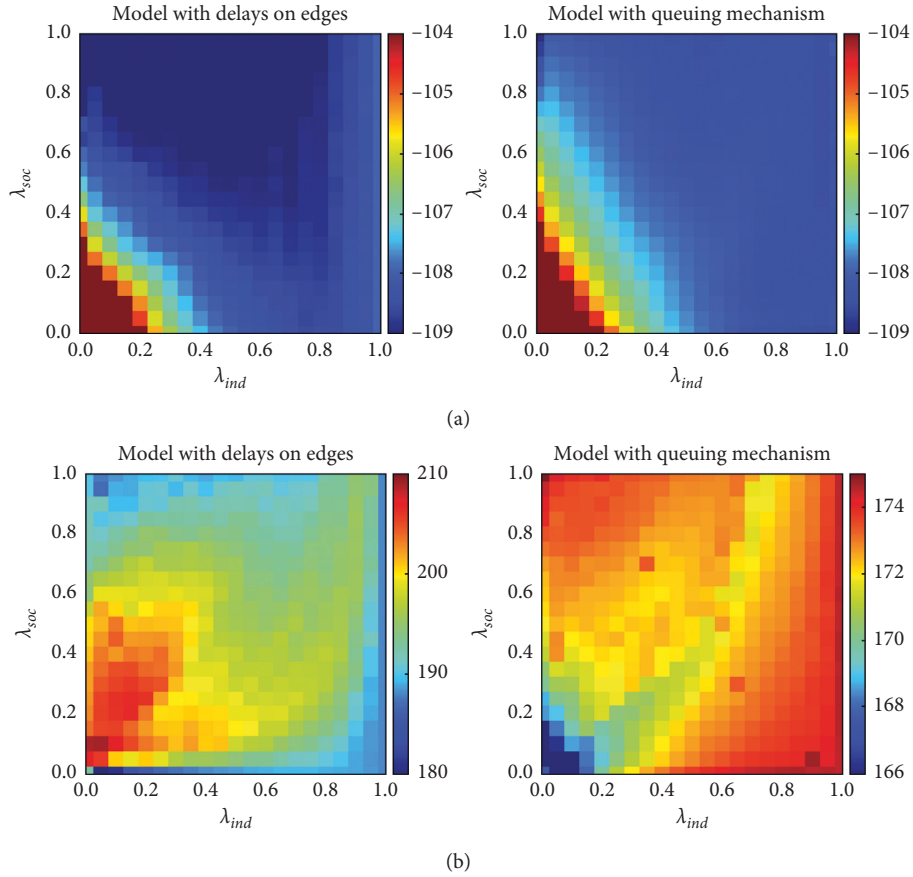

FIGURE 3: Aggregated results for expected arrival times. Each cell corresponds to single combination of λ_{ind} and λ_{soc} with value aggregated for all simulation's iterations which represents expected arrival time for all agents (a) and its standard deviation (b).

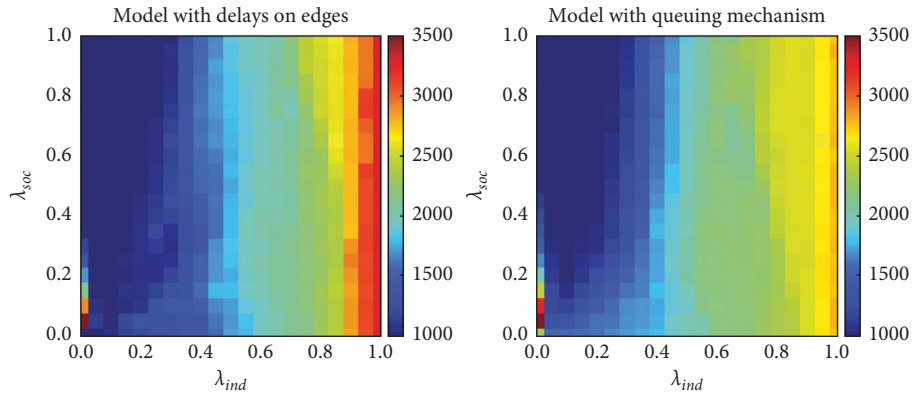

FIGURE 4: Aggregated results for number of routes changed during the simulation's run. Each cell corresponds to single combination of λ_{ind} and λ_{soc} with value aggregated for all simulation's iterations which represents average number of routes changed during this run.

time for the next day and one could expect that it should be most efficient solution, outperforming the naive and greedy route optimization attempts when agents are choosing the best routes based on their own past experience. However, after the more in-depth examinations, those results turn out to have logical explanation and their implications might be crucial in many different applications.

In order to better understand the situation, let us start with looking at the special structure of the traffic network presented in Figure 2. It is noted that primary roads are surrounded by smaller ones, which serve as a connection of minor streets to more major roads. Obviously, those types or roads differ in their parameters; usually, primary ones have more lanes, higher speed limits, interchange road junctions instead of the traditional intersections, and so on. Those differences implicate one important fact for drivers decision making process. The set of the attractive fastest routes is usually smaller than we might expect it to be; drivers tend to travel by primary roads instead of the less important ones. Even when the traffic density on such main road is huge, it is

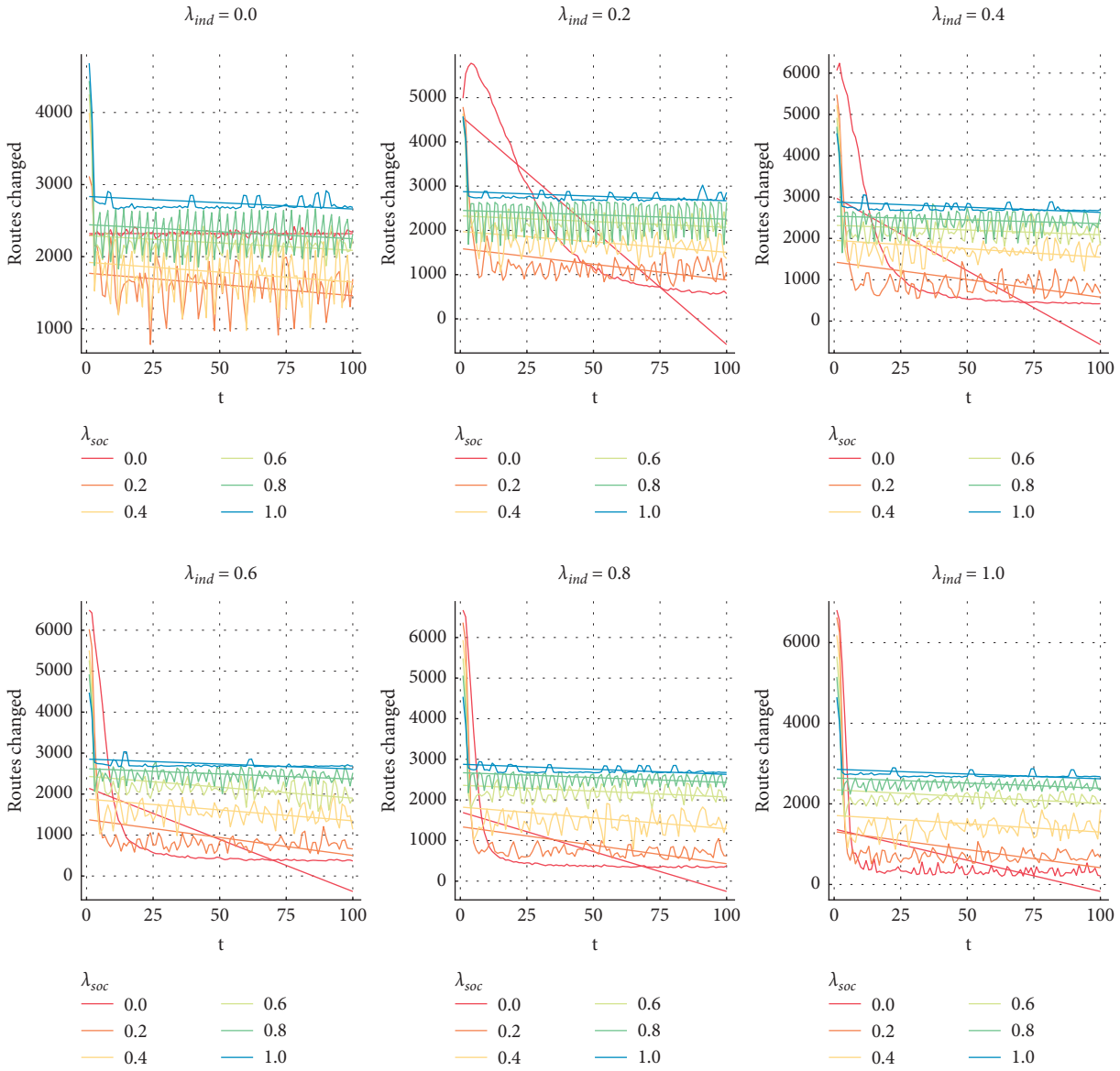

(a)

Figure 5: Continued.

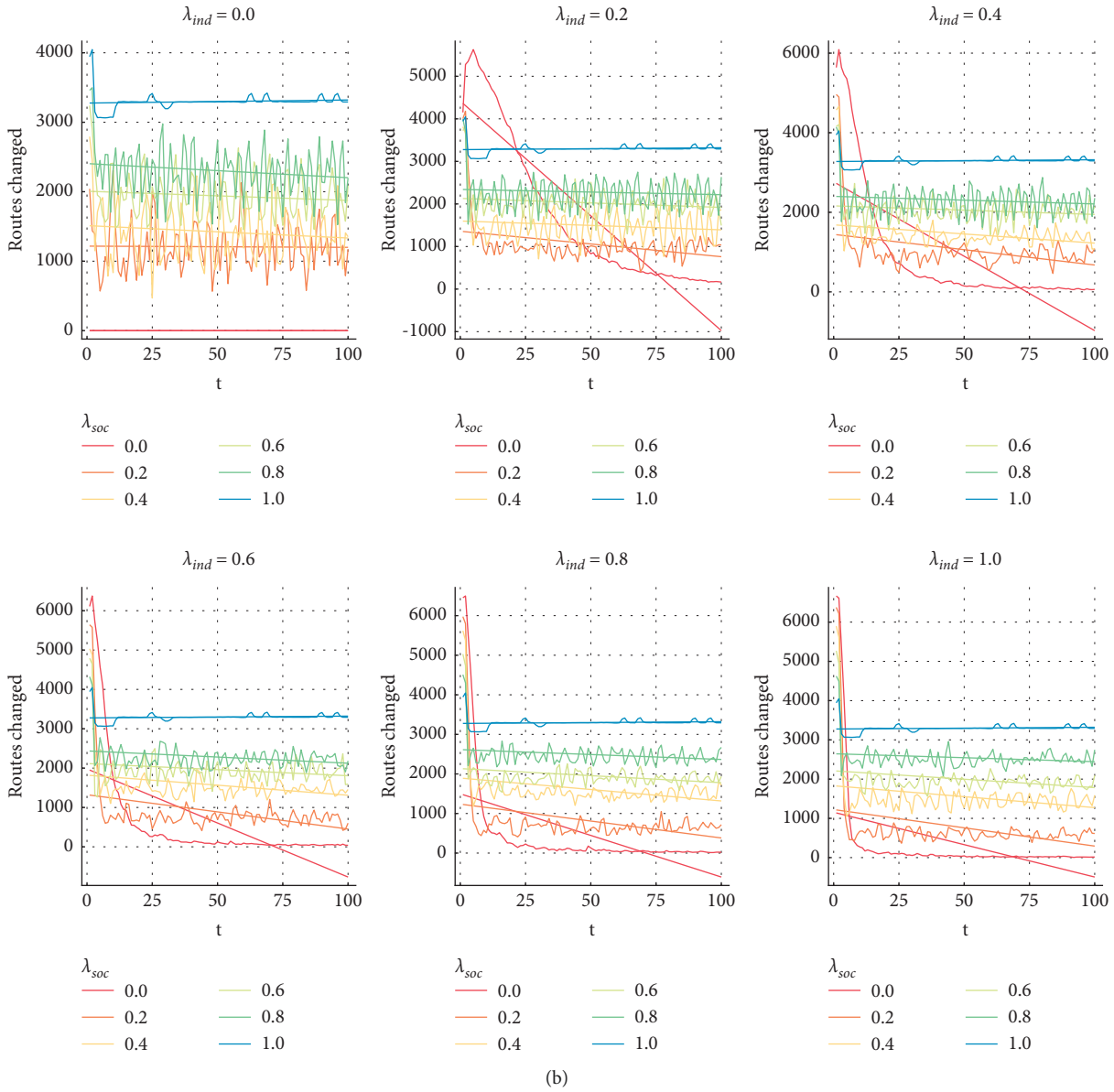

FIGURE 5: Results for number of routes changed during the simulation's run. Each subplot presents a different combinations of λ_{ind} and λ_{soc}. (a) Number of routes changed during the simulation for different combinations of lind and l_{soc} – model with queuing mechanism. (b) Number of routes changed during the simulation for different combinations of lind and l_{soc} – model with delays on edges.

usually still significantly faster to travel by than the surrounding residential streets.

How does it influence agents' behaviour? In Figures 4 and 5, we can observe that for large values of λ_{ind} number of drivers, changing their routes is in first few iterations of simulations is enormously high, significantly higher than for any other combinations of learning rates. At this stage of the simulation, agents are trying different solutions from their set of the best routes greedily choosing the best ones based on their beliefs. After a while, they are capable of finishing the exploration and they start to exploit the solution which is optimal based on their beliefs. Then, the number of changer routes plunges significantly and stays on a considerably low level for the rest of the simulation's run resulting in a stage of the quasiequilibrium, where majority of drivers are using the same route for the rest of the run and only a small number is changing their routes from iteration to iteration.

Obtained stability have a beneficial impact on the average driving times; when the traffic pattern is stable and predictable in a long term, it benefits the traffic flows by making them more smooth and fluent. As a result, expected driving time is higher than the best case scenario (driving with v_{max}) only by 8%.

When an agent starts to exploit its chosen route, it loses any track of the other possibilities; its knowledge about traffic is based on the situation the last time route was visited, somewhere at the beginning of the simulation. Obviously, when the current traffic on that routes is lower than during its last visit, the agent loses a great opportunity by sticking to its choice. The usage of the outside knowledge solves this

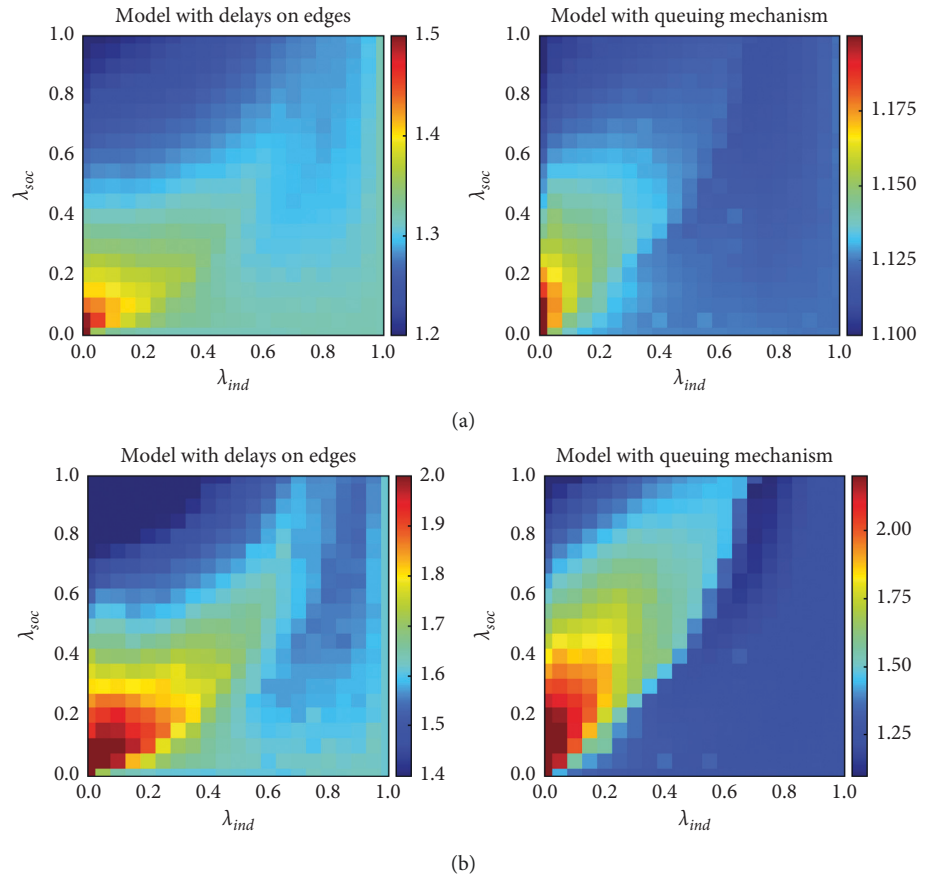

FIGURE 6: Aggregated results for expected driving times. Each cell corresponds to single combination of λ_{ind} and λ_{soc} with value aggregated for all simulation's iterations which represents percentage change in average driving time for all edges in traffic network compared to scenario where cars are driving with maximum velocity (a) and standard deviation of those changes (b).

problem, the agent tracks a traffic density on all routes, and the agent might choose a best solution in every iteration the without need of basing on own experience.

But in a long run, this results in the traffic network variation of the well-known tragedy of the commons [49]. Drivers who are independently selecting an optimal routes based on their self-interest as a result behave contrary to the common good of all users, which might be observed at Figure 6, where we can see that relying on the common knowledge of previous traffic increases expected driving time by 5 percentage points in comparison with acting only in accord to own past experience.

But how do we explain it? As it was stated before, social knowledge is an ex-ante estimation of the traffic flows based on the past experience. Agent still has no knowledge about the traffic on particular segment of the route right now when the agent start to drive by it. It chooses to do it believing that the situation on this segment will be exactly the same as in the past. However, other agents share this belief and they might also select this segment in order to improve their driving time, thus resulting in significant increase of the traffic density on that segment and decreasing the driving time for all of them.

It is visible on Figures 7, 8, and 5 where the traffic oscillations from iteration to iteration are clearly noticeable. For short periods of time, the traffic stabilizes (number of changed routes reaches its bottom in a cycle) and allocation of the drivers is relatively effective. But then, the information about better alternatives spreads around the population; thus, many agents decide to change their routes and system is again unbalanced, and as a result, even more agents change their routes. Perturbations last until the system again reaches a lowest point and cycle is repeating over and over again.

This situation resembles the classic game-theory problem of El Farol Bar [50, 51]. In its classic formulation, agents payoff depends on the behaviour of other players, if too many of them decided to go to the bar at the same moment and their utility will by lower than if they stayed at home. Moreover, all of them are obliged to decide at the same time whether they will go to the bar or not. Similarly, in the model described in this paper, driver's utility (measured as a speed of travelling by their routes) depends on the decisions of another users of the network, when the segment is clogged velocity of all drivers on this part of the route that is reduced; thus, their utility is lower than it might be. They are also planning their routes day before departure. Arthur [50] have proved that in such problem, no forecasting model can be employed by all individuals and be accurate at the same time. It basically means that if all drivers are using the same

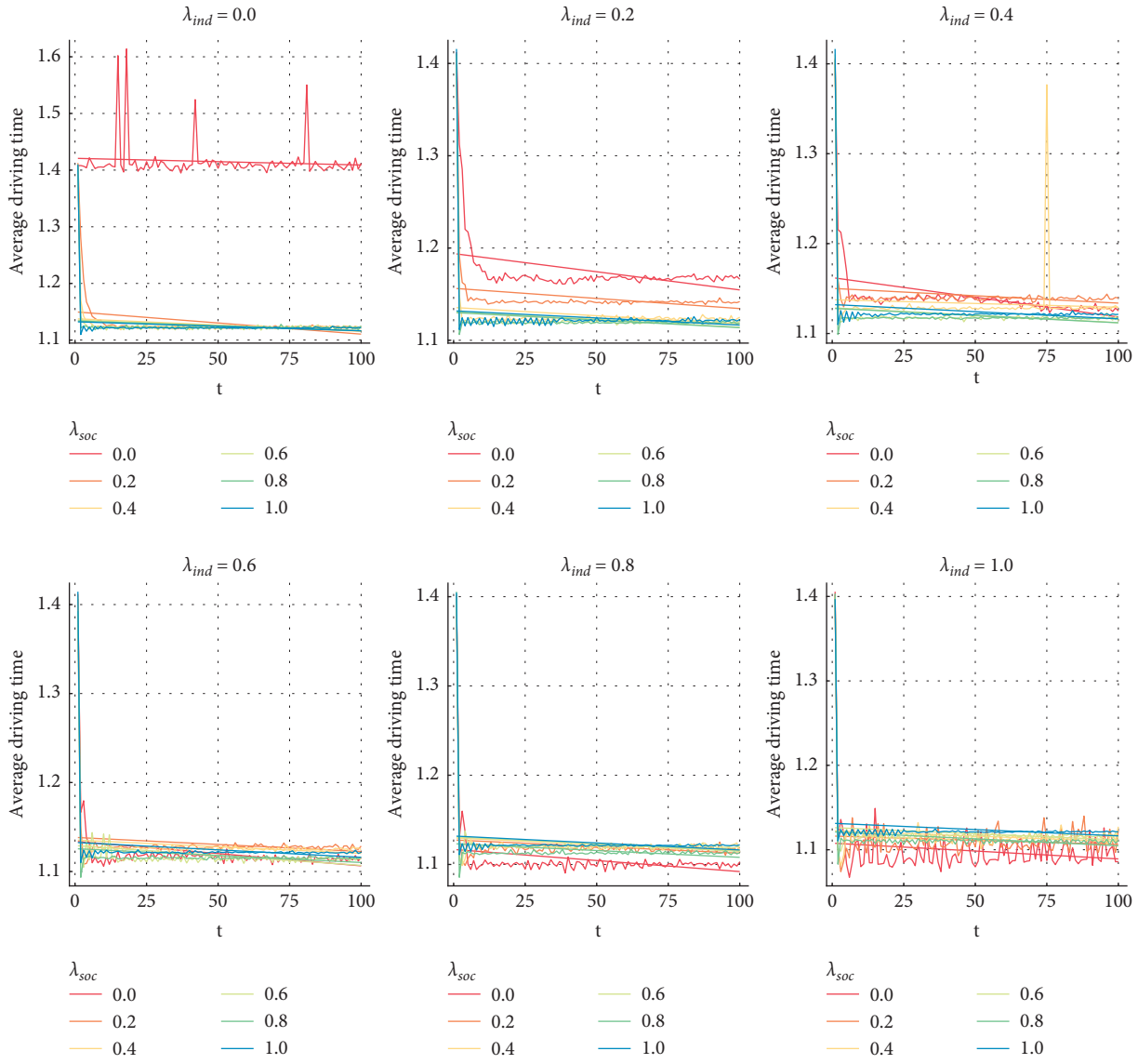

FIGURE 7: Changes of average driving times during the simulation for different combinations of λ_{ind} and λ_{soc} for the model with queuing mechanism.

strategy, in this case, the knowledge from the same source, it will not be effective, guarantying that the density on routes will be significantly higher than it could be.

Moreover, this kind of the global knowledge is averaged for all agents in the simulation, despite the fact that their departure time is varying. It means that those drivers who departure earlier, when the traffic density is lower, inherit the knowledge from ones who start their trip later when the density might be significantly higher. In such case, their decisions will be suboptimal, because their expectations about the densities on the edges will be significantly overestimated. Obviously, this mechanism will also work in a very similar manner for the agents who are starting their trip later, but this time, they will underestimate driving times.

As a result, when the knowledge is distributed in a manner described in this paper, it is not an effective method of selecting the routes, especially in comparison with the own experiences of the agents, which are adjusted to their usual departure time and are the proper way of estimating the driving time on segments of the agent routes. It follows the intuitions of Rogers [27]; learning based mostly on the social knowledge is more prone to exploiting the past experiences, incoherent with actual state of the system. One of the possible ways to avoid these errors is using the selective social learning as it is proposed by Enquist et al. [26].

In comparison with the previous literature on the subject of the autonomous [18–21] vehicles, this paper gives insights on the more general level of designing traffic system based on such vehicles. It turns out that the most effective approach to build the autonomous car transportation network is to schedule all of them with the fixed routes in a train-like manner. In such scenario, the system will be perfectly stable and, as a result, most efficient.

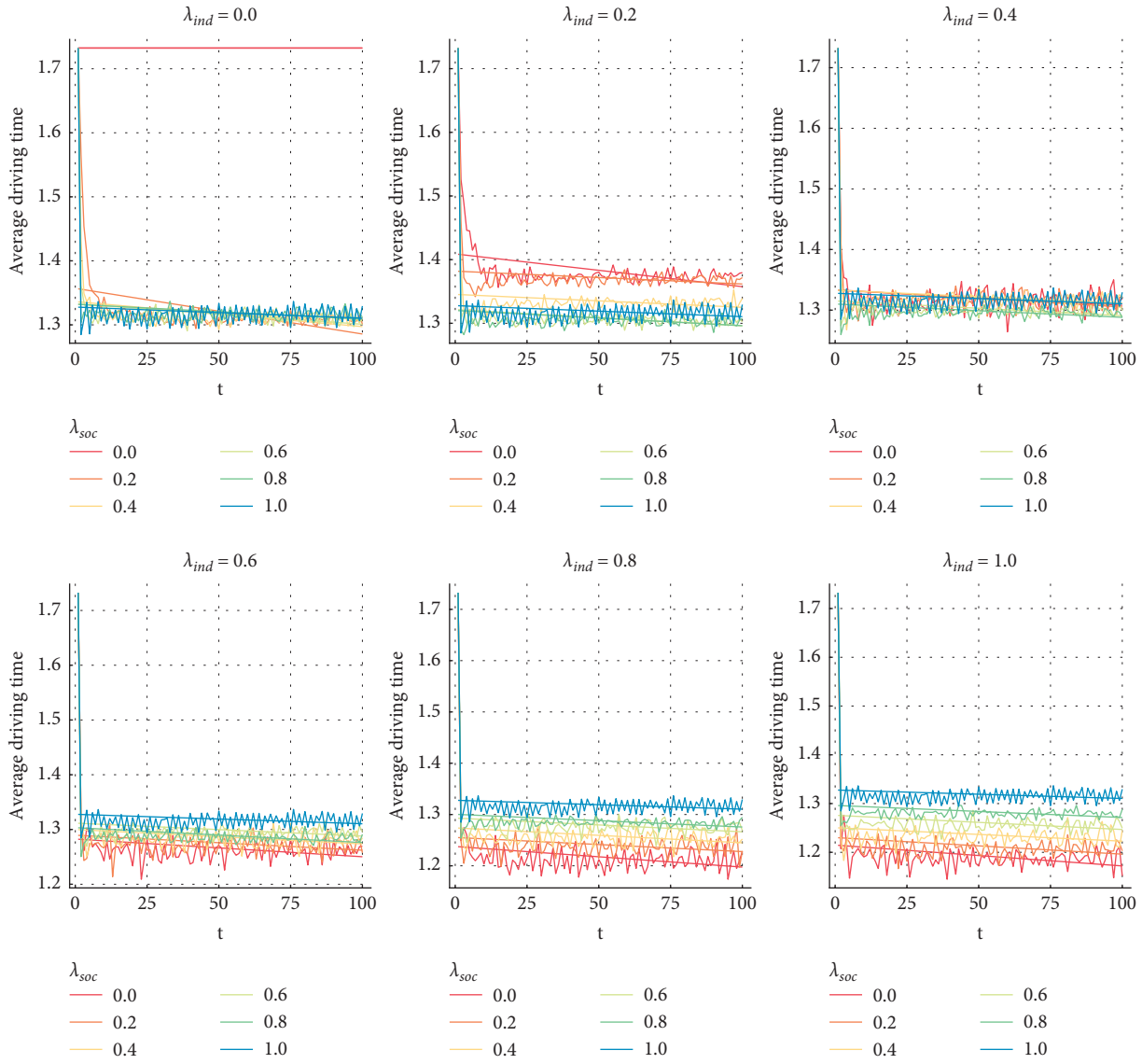

FIGURE 8: Changes of average driving times during the simulation for different combinations of λ_{ind} and λ_{soc} for the model with delays on edges.

4. Concluding Remarks

In this paper, we compare two scenarios for discrete-event-simulation modeling a transportation network, delay based and queuing based. The results show that the both the individual experience of the agents as well as exchange of information are important for city transportation system efficiency.

We show that the usage of the common knowledge can lead to a decrease of overall quality of the system by increasing variability and reducing effectiveness of utilization of the traffic network. The best scenarios are these ones where drivers select routes based on their previous experience and keep using them for the rest of the considered period of time. It results in situations when traffic flows are the most stable and efficient in terms of expected driving times, which is an important finding for the future research studies in traffic planning and management field.

Our model shows that microsimulations (and in particular agent-based simulation combined with discrete-event simulation) can bring a new level of detail for the analysis of real-word transportation systems. The developed simulation model and framework can be used to support policy making decisions in many ways. Firstly, it makes it possible to analyze outcomes to the changes in the transportation systems (such as a road closure), changes to transportation policy (that affects the number of cars), and the external effects of ongoing changes of attitude towards home working or car pooling. Since in the model we include experience of agents, it is also possible to analyze transition period to a new steady state after a change in the transportation system (not only long-term steady state). Finally, it is possible to use the proposed approach to optimize the global communication directed to the society if it can be assumed that the policy maker can influence the social learning component that we

use in our model (e.g., by broadcasting routing recommendations via the Internet).

We have created an Open Source transportation simulation framework in the Julia language consisting of three modules: OpenStreetMapX.jl for processing of spatial data and efficient vehicle routing, OpenStreetMapXPlot.jl for transportation system data visualization, and finally, OpenStreetMapXDES.jl for discrete-event simulation of transportation systems. The created frameworks offer great flexibility of model structure; it is possible to inject any type of behavior mechanism into the agents. This allows easy and convenient further extension of the presented research. All developed simulation code is available in the GitHub repository.

Constructed vehicle routing simulation framework applied to real-data of the city of Winnipeg in Canada proved to be useful in analyzing and predicting traffic size and commuter's behavior moving around the city. Model validation confirmed a good match between the artificial traffic returned by the simulation and the actual weekday traffic data for Winnipeg. Simulation results also proved to be very effective in predicting the demographic profiles of commuters across the city, which can be used in a number of practical applications. Simulation results allow to visualize and investigate city traffic size, spatial analysis of agents' demographic profiles, and single node investigation which includes the analysis of (1) network routes taken by all the agents passing by a node as well as (2) the distribution of agents' demographic profile attributes.

Indeed, the simulation framework can be applied to a wide range of real life problems based on spatial data, e.g. finding an optimal location of a school, restaurant, store or service, crowd control, fleet management, or out-of-home marketing. The study could be extended by introducing different framework modules (e.g. a new approach to the destination location selection or the expanded list of demographic profiles attributes). Validation outcome proves the overall potential of the presented framework.

The main limitation of this research is the set of simplifying assumption that have been made: (1) the model uses a discrete time rather than continues, (2) the model does not consider how intersections and street contribute to congestion (e.g. turning left vs turning right), (3) the impact of pedestrian traffic, bikes, and public transportation is not included, and (4) no model of actual vehicle acceleration. In the future research, we plan to address some of those limitations by including submicroscopic traffic modeling approach which would introduce driver's psychological reactions such as response time to traffic signal or brake lights of the preceding vehicle. Submicroscopic approach could also implement vehicle performance parameters, not only driver's reaction would be modelled but also car acceleration or breaking curves. In the next step, the third limitation could be also addressed by introducing pedestrian crossing traffic (e.g. pedestrians appearing on the crossing without traffic lights with some randomly distributed probabilities). Another possible extension of the model is the environmental pollution with regard to the traffic. Hence, a possible mechanism design question is how the market regulator should influence driver's decision in order to minimize the total congestion level. Since we model the time spent in traffic, this simulation can be also used as a part of simulation-optimization model for optimal out-of-home advertising locations.

Data Availability

We use the freely available data from the OpenStreetMap project - https://www.openstreetmap.org/Additionally, all codes and models are Open Source. The model and the framework can be reached at https://github.com/pszufe/OpenStreetMapXDES.jl, and https://github.com/pszufe/OpenStreetMapX.jl, respectively.

Conflicts of Interest

The authors declare that they have no conflicts of interest.

Acknowledgments

The initial version of simulation framework that was conducted in cooperation with Environics Analytics of Toronto within the research project entitled Agent-based simulation modelling of out-of-home advertising viewing opportunity was supported by the Ontario Centres of Excellence ("OCE") under Voucher for Innovation and Productivity (VIP) program, OCE Project Number: 30293.

References

[1] B. D. Greenshields, "The photographic method of studying traffic behavior," in *Proceedings of the 13th annual meeting of the highway research board*, pp. 382–399, Washington, D.C., USA, December 1934.

[2] F. Kessels, *Traffic Flow Modelling: Introduction to Traffic Flow Theory through a Genealogy of Models*, Springer, Berlin, Germany, 2019.

[3] P. A. Lopez, M. Behrisch, L. Bieker-Walz, J. Erdmann, and Y.-P. Flotterod, "Microscopic traffic simulation using sumo," in *Proceedings of the 21st international conference on intelligent transportation systems (ITSC)*, November 2018.

[4] M. Maciejewski, "A comparison of microscopic traffic flow simulation systems for an urban area," *Transport Problems*, vol. 5, no. 4, pp. 27–38, 2010.

[5] S. Maerivoet and B. De Moor, "Transportation planning and traffic flow models," 2005, https://arxiv.org/abs/physics/0507127.

[6] M. Di Francesco and M. D. Rosini, "Rigorous derivation of nonlinear scalar conservation laws from follow-the-leader type models via many particle limit," *Archive for Rational Mechanics and Analysis*, vol. 217, no. 3, pp. 831–871, 2015.

[7] J. Miller, "Basic concepts of kinematic-wave models," *U. S. Geological Survey Professional Paper*, vol. 5, no. 4, 1984.

[8] M. J. Lighthill and G. B. Whitham, "A theory of traffic flow on long crowded roads," *Proceedings of the Royal Society of London*, vol. 229, pp. 317–345, 1955.

[9] P. I. Richards, "Shock waves on the Highway," *Operations Research*, vol. 4, no. 1, pp. 42–51, 1956.

[10] W. Burghout, "Hybrid microscopic-mesoscopic traffic simulation," *Journal of the Transportation Research Board*, vol. 1934, 2004.

[11] K. Nagel and M. Schreckenberg, "A cellular automaton model for freeway traffic," *Journal dephysique I*, vol. 2, no. 12, pp. 2221–2229, 1992.

[12] M. Bando, K. Hasebe, K. Nakanishi, and A. Nakayama, "Analysis of optimal velocity model with explicit delay," *Physical Review*, vol. 58, no. 5, pp. 5429–5435, 1998.

[13] Z. Song and Z. Qin, "Review of the urban traffic modeling," *TELKOMNIKA Indonesian Journal of Electrical Engineering*, vol. 12, no. 11, pp. 7738–7757, 2014.

[14] F. V. Wageningen-Kessels, H. V. Lint, K. Vuik, and S. Hoogendoorn, "Genealogy of traffic flow models," *EURO Journal on Transportation and Logistics*, vol. 4, no. 4, pp. 445–473, 2015.

[15] S. P. Hoogendoorn and P. H. L. Bovy, "Generic gas-kinetic traffic systems modeling with applications to vehicular traffic flow," *Transportation Research B*, vol. 35, no. 4, pp. 317–336, 2001.

[16] S. L. Paveri–Fontana, "Boltzmann-Like treatments for traffic flow: a critical review of the basic model and an alternative proposal for dilute traffic analysis," *Transportation Research*, vol. 9, no. 9, pp. 225–235, 1975.

[17] D. Ni, "Limitations of current traffic models and strategies to address them," *Simulation Modelling Practice and Theory*, vol. 104, 2020.

[18] K. Hasebe, A. Nakayama, and Y. Sugiyama, "Dynamical model of a cooperative driving system for freeway traffic," *Physical review. E, Statistical, nonlinear, and soft matter physics*, vol. 68, no. 2, Article ID 026102, 2003.

[19] S. Ishikawa and S. Arai, "Evaluating advantage of sharing information among vehicles toward avoiding phantom traffic jam," in *Proceedings of the 2015 Winter Simulation Conference*, L. Yilmaz, W. K. V. Chan, I. Moon, T. M. K. Roeder, C. Macal, and M. D. Rossetti, Eds., pp. 300–311pp. 300–, Piscataway, New Jersey, NJ, USA, December 2015.

[20] D. Carlino, M. Depinet, P. Khandelwal, and P. Stone, "Approximately orchestrated routing and transportation analyzer: large-scale traffic simulation for autonomous vehicles," in *Proceedings of the Intelligent Transportation Systems Conference, 2012. ITSC'12*, September 2012.

[21] M. L. Sichitiu and M. Kihl, "Inter-vehicle communication systems: a survey," *IEEE Communications Surveys & Tutorials*, vol. 10, no. 2, 2008.

[22] N. J. Vriend, "An illustration of the essential difference between individual and social learning, and its consequences for computational analyses," *Journal of Economic Dynamics and Control*, vol. 24, pp. 1–19, 1998.

[23] D. Bergeman and J. Valimaki, "Learning and strategic pricing," *Econometrica*, vol. 64, no. 5, pp. 1125–1149, 1996.

[24] S. S. Izquierdo and L. R. Izquierdo, "The impact of quality uncertainty without asymmetric information on market efficiency," *Journal of Business Research*, vol. 60, no. 8, pp. 858–867, 2007.

[25] J. G. March, "Exploration and exploitation in organizational learning," *Organization Science*, vol. 2, no. 1, pp. 71–87, 1991.

[26] M. Enquist, K. Eriksson, and S. Ghirlanda, "Critical social learning: a solution to rogers's paradox of nonadaptive culture," *American Anthropologist*, vol. 109, no. 4, pp. 727–734, 2007.

[27] A. R. Rogers, "Does biology constrain culture?" *American Anthropologist*, vol. 90, no. 4, pp. 819–831, 1988.

[28] J. Y. Wakano, K. Aoki, and M. W Feldman, "Evolution of social learning: a mathematical analysis," *Theoretical Population Biology*, vol. 66, no. No. 3, pp. 249–258, 2004.

[29] A. Kesting, M. Treiber, M. Schönhof, and D. Helbing, "Adaptive cruise control design for active congestion avoidance," *Transportation Research Part C: Emerging Technologies*, vol. 16, no. 6, pp. 668–683, 2008.

[30] E. Camponogara and W. Kraus, "Distributed learning agents in urban traffic control, progress in artificial intelligence," in *Proceedings of the Distributed learning agents in urban traffic control. Portuguese Conference on Artificial Intelligence*, pp. 324–335, Springer, Beja, Portugal, December 2003.

[31] P. A. M. Ehlert and L. J. M. Rothkrantz, "A Microscopic traffic simulation with reactive driving agents," in *Proceedings of the Intelligent Transportation Systems Conference, 2001. ITSC'01*, pp. 1102–1107, IEEE, Oakland, CA, USA, August 2001.

[32] M. Treiber, A. Hennecke, and D. Helbing, "Congested traffic states in empirical observations and microscopic simulations," *Physical Review*, vol. 62, no. 2, pp. 1805–1824, 2000.

[33] A. Kesting, M. Treiber, and D. Helbing, "Agents for traffic simulation," *Multi-agent systems: Simulation and applications*, vol. 11, 2009.

[34] A. Kesting, M. Treiber, and D. Helbing, "Enhanced intelligent driver model to access the impact of driving strategies on traffic capacity," *Philosophical Transactions of the Royal Society A: Mathematical, Physical & Engineering Sciences*, vol. 368, no. 1928, pp. 4585–4605, 2010.

[35] M. A. Wiering, "Multi-agent reinforcement learning for traffic light control," in *Proceedings of the 17th International Conference on Machine Learning (ICML'2000)*, P. Langley, Ed., Stanford University, Stanford, CA, USA, pp. 1151–1158, 2000.

[36] P. G. Balaji, X. German, and D. Srisivasan, "Urban traffic signal control using reinforcement learning agents," *IET Intelligent Transport Systems*, vol. 4, no. 3, pp. 177–188, 2010.

[37] F. Logi and G. R. Stephen, "Development and evaluation of a knowledge-based system for traffic congestion management and control," *Transportation Research Part C: Emerging Technologies*, vol. 9, no. 2, pp. 433–459, 2001.

[38] S. Thulasidasan and S. Eidenbenz, "Accelerating traffic microsimulations: a parallel discrete-event queue-based approach for speed and scale," in *Proceedings of the 2009 Winter Simulation Conference*, M. D. Rossetti, R. R. Hill, B. Johansson, A. Dunkin, and R. G. Ingalls, Eds., pp. 2457–2466, Austin, Texas, USA, December 2009.

[39] R. S. Sutton and A. G. Barto, "Time-derivative models of Pavlovian reinforcement," in *Learning and Computational Neuroscience: Foundations of Adaptive Networks*, M. Gabriel and J. Moore, Eds., The MIT Press, Cambridge, MA, USA, 1990.

[40] G. Tesauro, "Temporal difference learning and TD-gammon," *Communications of the ACM*, vol. 38, no. 3, pp. 58–68, 1996.

[41] P. E. Hart, N. J. Nilsson, and B. Raphael, "A formal basis for the heuristic determination of minimum cost paths," *IEEE Transactions on Systems Science and Cybernetics SSC4*, vol. 4, no. 2, pp. 100–107, 1968.

[42] A. Law, *Simulation Modeling and Analysis*, McGraw-Hill, New York, NY, USA, 2007.

[43] J. Bezanson, A. Edelman, S. Karpinski, and V. B. Shah, "Julia: a fresh approach to numerical computing," *SIAM Review*, vol. 59, no. 1, pp. 65–98, 2017.

[44] D. Krajzewicz, J. Erdmann, M. Behrisch, and L. Bieker, "Recent development and applications of SUMO - simulation of urban MObility," *International Journal of Agile Systems and Management*, vol. 5, no. 3&4, pp. 128–138, 2012.

[45] L. R. Smith, D. Beckman, D. Anson, K. Nagel, and M. E. Williams, "TRANSIMS: transportation analysis and simulation system," in *Proceedings of the 5th National*

Conference on Transportation Planning Methods Application, Washington, D. C., USA, August 1995.

[46] D. F. Allan and A. M. Farid, "A benchmark analysis of open source transportation-electrification simulation tools,"pp. 1202–1208, IEEE 18th International Conference on Intelligent Transportation Systems, Gran Canaria, Spain, 2015, September.

[47] M. Saidallah, A. El Fergougui, and A. E. Elalaoui, "A comparative study of urban road traffic simulators," *MATEC Web of Conferences*, vol. 81, Article ID 05002, 2016.

[48] Z. Cao, H. Guo, J. Zhang, and U. Fastenrath, "Multi-agent–based route guidance for increasing the chance of arrival on time," in *Proceedings of the 30th AAAI Conference on Artificial Intelligence*, pp. 3814–3820, Phoenix, Arizona, AZ, USA, February 2016.

[49] G. Hardin, "The tragedy of the commons," *Science*, vol. 162, no. 3859, pp. 1243–1248, 1968.

[50] W. B. Arthur, "Inductive reasoning and bounded rationality," *The American Economic Review*, vol. 84, no. 2, pp. 406–411, 1994.

[51] D. Challet and Y.-C. Zhang, "Emergence of cooperation and organization in an evolutionary game," *Physica A*, vol. 246, no. No. 3 & 4, pp. 407–418, 1997.